Natural Zeolites and Plasma Surface Engineering for Innovating Biogas Purification and Advanced Adsorbents

by

Satriyo Krido Wahono

Principal Supervisor	**: Prof. Krasimir Vasilev**
Co-Supervisor	**: Prof. William Skinner**
Co-Supervisor	**: Prof. Jonas Addai-Mensah**
Co-Supervisor	**: Prof. Ajayan Vinu**

A Thesis submitted for the degree of

Doctor of Philosophy

Future Industries Institute – School of Engineering

Division of Information Technology, Engineering and the Environment

University of South Australia

December 2018

Contents

Contents ..... **ii**

List of Figures ..... **viii**

List of Tables ..... **xii**

List of Abbreviation ..... **xiv**

Summary ..... **xvii**

Acknowledgments ..... **xix**

Declarations ..... **xxi**

Publications and Presentations ..... **xxii**

Chapter 1 : Introduction **1**

1.1. Background 1

1.2. Research Aims and Objectives 4

1.3. Research Significance 4

1.4. Thesis Description 6

1.5. Structure of Thesis 7

References 9

Chapter 2 : Literature Review **12**

2.1. Introduction 12

2.2. Biogas 12

2.3. Biogas Utilisation 14

2.4. Biogas Purification 15

2.5. Molecular Sieve for CO_2 Removal 19

2.6. Indonesian Natural Zeolite 20

2.7. Chemical Treatment of Natural Zeolite 22

2.8. Calcination of Natural Zeolite 24

2.9. CO_2 Absorption and Adsorption by Amine 25

2.10. Plasma Polymerisation 27

2.11. Plasma Polymer Amine Deposition on Porous Material 28

2.12. Conclusions 30

References 31

Chapter 3 : Methodology 51

3.1. Source of Indonesian (Gunungkidul) Natural Zeolite 51

3.2. Physicochemical Modification of Indonesian Natural Zeolite 51

3.2.1. Dealumination 51

3.2.2. Calcination 52

3.2.3. Alkali impregnation 53

3.3. Plasma Polymerisation of Particulate Material for Environmental Application 54

3.3.1. Plasma polymer amine on porous, modified Indonesian natural zeolite for CO_2 adsorption 55

3.3.2. Air-plasma activation on porous material of Indonesian natural zeolite for water-vapour adsorption 57

3.3.3. Hydrophobic plasma polymer on nanoparticle of magnetic material for oil adsorption 57

3.4. Characterisation of Materials 59

3.4.1. Ellipsometry 59

3.4.2. Wettability test (analysis of water contact angle) 60

3.4.3. XPS 61

3.4.4. ToF-SIMS 62

3.4.5. SEM-EDX analysis 62

3.4.6. FTIR 63

3.4.7. ICP-MS 64

3.4.8. XRF 64

3.4.9. Nitrogen adsorption–desorption analysis 65

3.4.10. XRD 66

3.4.11. Sieve analysis (particle-size distribution) 67

3.4.12. pH measurement 67

3.4.13. CO_2 adsorption capacity 67

3.4.14. Water-vapour adsorption capacity 69

3.4.15. UV-Vis spectrophotometry 69

3.5. Conclusions 70

References 71

Chapter 4 : Carbon Dioxide Adsorption Enhancement of Natural Mordenite-Clinoptilolite Zeolite by Physicochemical Treatment 76

Abstract 76

4.1. Introduction 77

4.2. Results and Discussion 78

4.2.1. Characterisation of the pristine natural zeolite 78

4.2.2. Natural zeolite physiochemical treatment 81

4.2.2.1. Effect of acid concentration on dealumination 81

4.2.2.2. Calcination 86

4.2.3. CO_2 adsorption 90

4.2.4. Comparison with synthetic adsorbents 91

4.3. Conclusion 93

References 94

Chapter 5 : Natural Zeolite Transformation by Alkali Impregnation for Improving Carbon Dioxide Adsorption Capacity 100

Abstract 100

5.1. Introduction 101

5.2. Results and Discussion 102

5.2.1. Physicochemical characterisation of modified natural zeolites 102

5.2.2. Alkali impregnation 105

5.2.3. The CO_2 adsorption capacity of the natural zeolite after alkali impregnation 110

5.2.4. The comparison of alkali impregnation treatment for CO_2 adsorption capacity ... 112

5.3. Conclusion 113

References 115

Chapter 6 : Combination of Plasma Polymer Allylamine and Natural Zeolite as The Novel Carbon Dioxide Adsorbent 120

PART 1: Combination of Amine and Natural Zeolite as New Adsorbent Material for Carbon Dioxide Capture 120

Abstract 120

6.1. Introduction 121

6.2. Results and discussions 123

6.2.1. Characterisation of amine plasma deposition 123

6.2.2. CO_2 capture on natural zeolite and natural zeolite-amine plasma 125

6.2.3. Power variable of amine plasma deposition for CO_2 capture on Si wafer-amine 126

6.2.4. Controlling amine deposition thickness 128

6.3. Conclusions 130

References 131

PART 2: Novel Amine Plasma Polymer Facilitated Carbon Dioxide Adsorbents 135

Abstract 135

6.4. Introduction 136

6.5. Results and Discussions 138

6.5.1. Modified natural zeolite base material 138

6.5.2. Optimisation of plasma polymer deposition 139

6.5.3. Plasma polymer deposition on the A5 zeolite 141

6.5.4. Optimisation of the degassing temperature before CO_2 adsorption measurements 144

6.5.5. The CO_2 adsorption capacity 146

6.6. Conclusions 148

References 149

Chapter 7 : Plasma Activation on Natural Mordenite-Clinoptilolite Zeolite for Water-vapour Adsorption Enhancement 153

Abstract 153

7.1. Introduction 154

7.2. Results and Discussions 155

7.2.1. Characterisation and water-vapour adsorption capacity of physiochemically modified natural zeolites 155

7.2.2. Plasma activation 156

7.2.3. The water-vapour adsorption capacity of natural zeolite after plasma activation at 50 W and 1200 s 160

7.2.4. Effect of plasma power and time of treatment on the water adsorption of A5 zeolites 161

7.3. Conclusions 163

References 164

Chapter 8 : Plasma Polymer Facilitated Magnetic Technology for Removal of Oils from Contaminated Waters 168

Abstract 168

8.1. Introduction 169

8.2. Results and Discussion 170

8.2.1. Crude oils characteristics 170

8.2.2. Plasma polymer modification 171

8.2.3. Stability of the coatings in water 173

8.2.4. Chemical characterisation of coated magnetic nanoparticles 173

8.2.5. Oil recovery 175

8.2.5.1. Effect of Oil-Adsorbent Ratio 176

8.2.5.2. Effect of scale-up 178

8.2.6. Comparison of newly developed technology for oil recovery with literature 179

8.3. Conclusions 180

References 182

Chapter 9 : Conclusion and Future Work 186

9.1. Conclusion 186

9.2. Future Work 189

APPENDIX A: Copyrights and Permissions 191

APPENDIX B: Published Manuscripts 193

APPENDIX C: Supporting Information 212

List of Figures

Figure 1.1. Natural zeolite and biogas resources in Gunungkidul, Yogyakarta, Indonesia 2

Figure 1.2. Schematic of Indonesian Gunungkidul natural-zeolite structure modification and improvement for purifying biogas (CO_2 and H_2O removal)..... 3

Figure 1.3. Schematic of thesis structure of Indonesian natural zeolite and plasma polymerisation for biogas upgrading and other environmental applications..... 8

Figure 2.1. Biogas composition with methane as the primary gas and various gases impurities 13

Figure 2.2. Utilisation of biogas for supporting various activities: fertiliser production, farming activities, heat generation, electricity generation..... 15

Figure 2.3. Schematic of biogas purification for producing high purity of methane (biomethane) 17

Figure 2.4. Milestones of Indonesian (Gunungkidul) natural-zeolite use for biogas purification in Indonesia 22

Figure 2.5. Reaction between various types of amine and CO_2 26

Figure 2.6. Schematic of plasma polymerisation deposition on planar surface, particulate surface and porous material 28

Figure 3.1. Schematic of Indonesian natural-zeolite physicochemical modification: (a) dealumination study; (b) calcination study; (c) alkali-impregnation study..... 54

Figure 3.2. Schematic of plasma polymer reactor with agitation platform 55

Figure 3.3. Schematic of plasma polymer amine incorporation into the modified Indonesian natural zeolite for CO_2 adsorption..... 56

Figure 3.4. Schematic of CO_2 adsorption simple reactor for a preliminary study..... 56

Figure 3.5. Schematic of air-plasma activation on modified natural zeolite for water-vapour adsorption..... 57

Figure 3.6. Schematic of hydrophobic plasma polymer on nanomagnetic material for oil adsorption..... 59

Figure 3.7. Description of water contact angle results for hydrophobic–hydrophilic surface 61

Figure 4.1. Graphical abstract of CO_2 adsorption enhancement of natural mordenite-clinoptilolite zeolite by physicochemical treatment..... 76

Figure 4.2. The pristine natural mordenite-clinoptilolite zeolite used in this study: (a) SEM photomicrograph; and (b) XRD patterns. 80

Figure 4.3. Transformation of natural mordenite-clinoptilolite zeolite post various dealumination acid concentration and calcination at 400°C: (a) Si/Al ratio; (b) Surface element composition (XPS); (c) Bulk element composition (EDX); (d) Bulk element composition (XRF); and (e) Specific surface area..... 83

Figure 4.4. Characterisation of the natural mordenite-clinoptilolite zeolites post various dealumination acid concentration and calcination at 400°C: (a) SEM photomicrograph; and (b) Crystallinity and XRD patterns..... 85

Figure 4.5. Characterisation of the natural mordenite-clinoptilolite zeolites post 3 M HCl dealumination and various calcination temperatures: (a) Crystallinity and XRD patterns (b) SEM photomicrographs..... 88

Figure 4.6. (a) CO_2 isotherm adsorption capacity of A5 zeolite at 0, 10 and 25 ° C; and (b) Isosteric heat of adsorption of A5 zeolite..... 91

Figure 5.1. Graphical abstract of natural zeolite transformation by alkali impregnation for improving CO_2 adsorption capacity..... 100

Figure 5.2. Characterisation of A0 and C0 zeolite: (a) SEM photomicrograph, (b) XRD pattern, (c) Atomic percent element composition of XPS..... 104

Figure 5.3. Modified natural mordenite-clinoptilolite zeolite after NaOH impregnation: (a) XRD patterns; and (b) SEM photomicrograph. 108

Figure 5.4. Modified natural mordenite-clinoptilolite zeolite after KOH impregnation: (a) XRD patterns; and (b) SEM photomicrograph. 109

Figure 5.5. The CO_2 adsorption capacity of alkali impregnated modified natural mordenite-clinoptilolite zeolite: (a) NaOH impregnation; (b) NaOH impregnation isosteric heat; (c) KOH impregnation; (d) KOH impregnation isosteric heat..... 111

Figure 5.6. CO_2 adsorption comparison of alkali impregnated modified natural mordenite-clinoptilolite zeolite: (a) Capacity (mmol/g) at 25°C; (b) Normalised capacity (mmol/m^2) at 25°C; (c) Capacity (mmol/g) at 0°C; (d) Normalised capacity (mmol/m^2) at 0°C..... 113

Figure 6.1. (a) The thickness of allylamine deposition on various power and time; (b) N1s graph of allylamine deposition on natural zeolite 124

Figure 6.2. (a) C1s graph of CO_2 capture on natural zeolite and natural zeolite-amine plasma; (b) C1s graph of 10 W amine coat after CO_2 capture..... 126

Figure 6.3. (a) Colour transformation of high power amine coat after CO_2 capture; (b) Coat thickness increase on various condition after CO_2 capture..... 127

Figure 6.4. C1s and N1s graph of 50 W amine coat after CO_2 capture..... 128

Figure 6.5. SEM images of modified natural zeolite: (a) before deposition; (b) after long time deposition (300 s); (c) after short time deposition (30 s)..... 129

Figure 6.6. Thickness of allylamine short time deposition on various condition..... 130

Figure 6.7. Graphical abstract of novel amine plasma polymer facilitated CO_2 adsorbents..... 136

Figure 6.8. Characteristics of mordenite-clinoptilolite natural zeolite A0 and its modified product, A5 zeolite: (a) XRD spectra and crystal structure search-match analysis; (b) Surface morphology by SEM; (c) specific surface area with micro-mesopores distribution; and (d) elemental composition determined by XRF..... 139

Figure 6.9. Properties of allylamine based plasma polymer films deposited on silicon wafers. (a) Thickness growth as a function of deposition time and power; (b) water droplet spreading (c) thickness of films deposited for 10 s and 30 s at different pressure and power, and upon power pulsing. 141

Figure 6.10. (a) N1s high-resolution XPS spectra at various deposition times; (b) specific surface area of A5 zeolite before and after deposition of allylamine plasma polymer; (c) Nitrogen content measured by EDX; ToF-SIMS spectra of (d) A5 zeolite, and (e) A5-Am10W-10s. 143

Figure 6.11. Effect of degassing temperature on the chemical and structural properties of the untreated and plasma treated zeolites: (a) Evolution of the N1s high-resolution XPS spectra after degassing at different temperatures; (b) Specific surface area; and (c) Pores size distribution. 145

Figure 6.12. CO_2 adsorption of A5, A5-Am10s75, and A5-Am10s110 zeolite: (a) Bond strength profile of adsorbed CO_2; (b) CO_2 adsorption capacity (mmol CO_2/g); CO_2 adsorption affinity based on normalised specific surface area (mmol CO_2/m^2) 147

Figure 7.1. Graphical abstract of plasma activation on natural mordenite-clinoptilolite zeolite for water-vapour adsorption enhancement..... 153

Figure 7.2. Properties of zeolites before and after dealumination: (a) Si/Al ratio determined from EDX and XPS measurements; (b) Specific surface area; (c) water adsorption capacity..... 156

Figure 7.3. (a) XPS Survey spectra of A5 zeolite before and after plasma treatment; (b) Al 2p region zoom; (c) Oxygen percentage of A0, A1 and A5 zeolites as determined by XPS before and after plasma treatment; (d) FTIR spectra of A5 zeolite and; (e) SEM images of A5 zeolite before and after plasma treatment. 159

Figure 7.4. Water adsorption capacity before and after plasma activation for (a) A0 zeolite; (b) A1 zeolite; (c) A5 zeolite; and (d) water adsorption capacity normalised to the zeolites specific surface area. 161

Figure 7.5. The water adsorption capacity of A5 zeolite as a function of the conditions of plasma activation used: (a) duration of plasma activation and (b) plasma power. 162

Figure 8.1. Graphical abstract of plasma polymer facilitated magnetic technology for the removal of oils from contaminated waters 168

Figure 8.2. Coating thickness at four different deposition times before and after immersion in water: (a) Octadiene and (b) Perfluorooctane 173

Figure 8.3. The chemical composition of the nanoparticles surfaces determined by XPS before and after modification: (a) XPS survey spectra of Fe-Raw, Fe-Octadiene, and Fe-PFO; (b) Fe-1.7-octadiene; (c) Fe-perfluorooctane 174

Figure 8.4. ORE of magnetic nanoparticles: (a) coated with octadiene and perfluorooctane plasma polymers for different deposition times (Oil:Adsorbent ratio = 1:2); (b, c) plasma polymer coated and uncoated versus oil:adsorbent ratio for: (b) Crude oil 1; (c) Crude oil 2 176

Figure 8.5. The ORE of coated and uncoated magnetic adsorbents as a function of increasing water volume for 8:1 of oil:adsorbent ratio: (a) Crude oil 1; (b) Crude oil 2; and for 20:1 of oil:adsorbent ratio: (c) Crude oil 1; (d) Crude oil 2 178

Figure 9.1. Product prototype and application of Indonesian natural zeolite and plasma polymerisation modification 188

List of Tables

Table 2.1. Composition of biogas based on literature 14

Table 2.2. Comparison of biogas-purification technologies 18

Table 4.1. The composition of the pristine natural mordenite-clinoptilolite zeolite by different analytical techniques. 81

Table 4.2. Specific surface area and Si/Al ratio of natural mordenite-clinoptilolite zeolite post various dealumination acid concentration and calcination at 400°C 84

Table 4.3. The Search-Match analysis of natural mordenite-clinoptilolite zeolite crystal structure post various dealumination acid concentration and calcination at 400°C 86

Table 4.4. Specific surface area and Si/Al ratio of natural mordenite-clinoptilolite zeolite crystal and products structure post 3 M HCl dealumination and various calcination temperatures 87

Table 4.5. The Search-Match analysis of natural mordenite-clinoptilolite zeolite crystal and products structure post 3 M HCl dealumination and calcination at various temperatures 87

Table 4.6. The CO_2 adsorption capacity of various zeolite at 1 bar and 25°C 92

Table 4.7. The CO_2 adsorption capacity of various zeolite at 0°C 93

Table 5.1. Specific surface area and Si/Al ratio of modified natural mordenite-clinoptilolite zeolite after alkali impregnation 106

Table 5.2. Match Score of modified natural mordenite-clinoptilolite zeolite crystal structure from XRD analysis for different alkali impregnations 107

Table 6.1. The contact angle of 50 W allylamine deposition on different time 124

Table 6.2. The specific surface area of 10 W plasma polymer amine deposited on A5 zeolite in different duration and pulse 144

Table 6.3. The specific surface area of 10 W plasma polymer amine deposited on A5 zeolite in different degassing temperature 146

Table 7.1. Code of the natural zeolites in the various treatment of plasma activation 157

Table 7.2. O/Si ratio and specific surface area of the natural zeolites before and after plasma activation 158

Table 7.3. O/Si ratio, specific surface area, and adsorption affinity of the A5 zeolites after treatment using different plasma power and duration 162

Table 8.1. Density and viscosity of crude oil samples..... 171

Table 8.2. Thickness and surface wettability of plasma polymer films deposited on a silicon wafer..... 172

Table 8.3. Adsorption capacity and oil recovery for comparable materials published in the literature. 180

List of Abbreviation

AC	activated carbon
Al	aluminium
Al_2O_3	aluminium oxide
AMP	2-Amino-2-methyl propanol
At %	atomic percent
BOC	British Oxygen Company
BET	Brunauer–Emmett–Teller
BJH	Barrett-Joyner-Halenda
BSE	backscattered electrons
Ca	calcium
CaO	calcium oxide
$CaCO_3$	calcite/calcium carbonate
Cs	cesium
CH_4	methane
CO_2	carbon dioxide
CV	commanditaire vennootschap – dutch (limited partnership company)
DEA	di-ethanol amine
DGA	diglycolamine
DIPA	di-isopropanolamine
EDX	Energy-dispersive X-ray
EDXRF	Energy Dispersive X-Ray Fluorescence
Fe-EDTA	ferric ethylenediaminetetraacetic acid
FT-IR	Fourier Transform – Infra-Red
h	hour (time unit)
H_2	hydrogen
H_2S	hydrogen sulphide
H_2SO_4	sulphuric acid
H_2O	water
HCl	hydrochloric acid
HCN	hydrogen cyanide
HF	hydrogen fluoride
HNO_3	nitric acid

He	helium
ICP-MS	Inductively Coupled Plasma – Mass Spectrometry
IUPAC	International Union of Pure and Applied Chemistry
K	kalium/potassium
K_2CO_3	kalium/potassium carbonate
KBr	kalium/potassium bromide
KOH	kalium/potassium hydroxide
LMIG	liquid metal Au primary ion gun
M	Molar (concentration unit)
MEA	mono-ethanol amine
MDEA	methyl diethanolamine
Mg	magnesium
MOF	metal-organic framework
N_2	nitrogen
N_2O	nitrogen oxide
Na	natrium/sodium
NaOH	natrium/sodium hydroxide
NH_3	ammonia
O_2	oxygen
ORE	oil removal efficiency
PEG	polyethylene glycol
pH	potential of hydrogen
PIPA	piperazine
POME	palm oil mill effluent
ppm	part per million
PSA	pressure swing adsorption
PSD	particle size distribution
Q_{st}	isosteric heat of adsorption
Rb	rubidium
RF	radio frequency
s	Second (time unit)
SE	secondary electrons
SEM	Scanning Electron Microscopy
Si	silicon
SiO_2	silica/silicon dioxide

SO_2	sulphur dioxide
TCD	Thermal Conductivity Detector
TEG	triethylene glycol
ToF-SIMS	Time-of-Flight Secondary Ion Mass Spectrometry
TPD	Temperature-Programmed Desorption
UHV	ultra-high vacuum
UV-Vis	Ultraviolet-Visible
VASE	Variable Angle Spectroscopic Ellipsometer
W	Watt (power unit)
XPS	X-ray Photoelectron Spectroscopy
XRD	X-ray Diffraction
XRF	X-ray Fluorescence

Summary

Biogas is a renewable fuel source that contains approximately 40–75% methane by volume plus other impurities such as carbon dioxide (CO_2), hydrogen sulphide (H_2S), ammonia (NH_3) and water-vapour, depending on its origin. Methane concentration in biogas dictates its energy content, which is of vital importance in its application as a fuel source for various applications such as creating heat, electricity and gas fuel. Using natural zeolite as a biogas impurities adsorbent provides a prospective approach given its abundant availability and low cost. Natural zeolite (from Gunungkidul, Yogyakarta, Indonesia) has been used for biogas purification but performance needs to be improved. Thus, this thesis presents various treatments of natural zeolite to improve its adsorption capacity for biogas impurities, particularly CO_2 as the main impurity of biogas.

Preliminary characterisation of the pristine natural zeolite has confirmed that it involves natural calcite-rich mordenite–clinoptilolite zeolites. Both these zeolite structures suit gas adsorption. Some important factors in improving the CO_2 adsorption capacity of natural zeolite are ensuring a high specific surface area, high Si/Al ratio (representing hydrophobic surface), basicity presence, appropriate zeolite structure, and amine/nitrogen presence. For obtaining this condition, the folowing treatments were conducted in this study. Physicochemical treatment was performed by dealumination, calcination and alkali impregnation. The advanced treatment of plasma charging was applied as allylamine plasma polymerisation and air-plasma activation. In addition, using plasma polymerisation surface engineering of magnetic nanoparticles I also successfully created the efficient oil adsorbents.

Several types of modified Indonesian natural zeolite produced by different treatments for CO_2 adsorption include those created by thermal-acid treatment (A5-zeolite); NaOH impregnation (C2-zeolite), KOH impregnation (C4-zeolite), and the plasma polymer allylamine modified zeolite (A5-Am-10W-10s-75-zeolite). The A5-zeolite has the highest surface area of modified Indonesian natural zeolite, and offers the best physisorption mechanism of CO_2. The C2-zeolite provides the prospective adsorbent for the chemisorption mechanism of CO_2. The C4-zeolite shows the most effective surface for attracting CO_2 in physicochemical treatment. The plasma polymer allylamine modified zeolite (A5-Am-10W-10s-75) introduces a new facile technique for inducing the amine

functional group inside the micro–mesopores. This adsorbent also provides a more attracting surface for CO_2 by inducting the amine functional group inside the structure.

Another product of combining natural zeolite and plasma technology is air-plasma activation, which aims to improve water-vapour adsorption. The activated modified natural zeolite enhances the adsorption capacity and affinity of natural zeolite, particularly for the high Si/Al ratio zeolite, which was unsuitable as a water adsorbent before activation. Moreover, some additional advanced products were also created by the application of plasma polymerisation for surface engineering. Two types of nanoparticulate magnetic material that transform the hydrophobic surface by plasma polymer were also designed to be applied as oil-waste adsorbents.

All of the mentioned products are explored in detail in further chapters that have been published in peer reviewed articles (journals and proceedings) and a ready to be published draft as journal articles (Chapters 4 to 8). The investigation of the material characteristics in the various treatments also provides a great deal of valuable information for different future applications of natural zeolites and plasma technology. These investigations offer new horisons for application of Indonesian natural zeolite and plasma polymer for environmental purposes, and possibly provide new opportunities in other fields.

Acknowledgments

Thanks to ALLAH SWT

For all the countless gifts, guidance and miracle to accomplished this journey.

The first appreciation dedicates to my little family, lovely wife Happy Indah Kusumawati, attractively son Hapsa Cakra Dewantara Wahono, and the new cute baby girl Delisa Nidya Larasati Wahono. I also present this thesis for my parent (Bambang Susila Hadi-Hari Adiningsih) and my parent in law (Soedjito-Endang Pujiwati), then specialty my brother in law Anang Fitrianto, my cousin Eri Yanuar Ahmad and Elies Meilinawati; and all of my big family. All of you are my great inspiration and source of encouragement for the completion of this thesis.

It is a great pleasure to acknowledge my deepest thanks and gratitude to my best principal supervisor Prof. Krasimir Vasilev which has accepted me with all the shortcomings and limitations. The family man who is always caring to my family life and always come with meaningful encouragement, guidance, and patience. I also deliver very thankful for all supporting of my co-supervisors the Three Great Professors: Prof. William (Bill) Skinner, Prof. Jonas Addai-Mensah, and Prof. Ajayan Vinu. Thank you very much for providing necessary information, direction, and feedback for me to accomplish the thesis and project.

I want to thank the Vasilev Group: Dr. Melanie Ramiasa, Dr. Alex Cavallaro, Dr. Akash Bachuka, Dr. Neethu Ninan, Dr. Thomas Michl, Dr. Nirmal Goswami, Dr. Hanieh S Shirazi, Ms. Neelika Roy Chowdhury, Mr. Kola Ostrikov, Mr. Rahul M Visalakshan, Ms. Laura Gonzalez Garcia, Ms. Jo Chan, Mr. Hanif Haidari, and all other members. Also thanks to Dr. Andrew Michelmore, Dr. Bryan Coad, Mr. Andrew Robinson, Miss. Susie Ritch, Dr. John Denman, Dr. Rajesh Baskaran, Dr. Joseph Stalin, Dr. Kripal Singh, Dr. Gurwinder Singh, Dr. Kim In Young, Dr. Devaraju M Kempaiah, other students, and staff who are training me to operate the analysis equipment and laboratory induction in building V and building X. Also a lot of appreciation for technical and administration team of Mawson Institute, Future Industries Institute and School of Engineering, Division Information Technology, Engineering, and the Environment–University of South Australia for their kindness and helpfulness.

I would also like to thank the Chemical Processing Technology and Environmental Group of Research Unit for Natural Product Technology–Indonesian Institute of Sciences (BPTBA-LIPI) and Research Centre for Chemistry (P2K-LIPI) for supporting laboratory facilities and analysis equipment. Particularly, I deliver an excellent appreciation for research collaboration activity with Mr. Andri Suwanto, Mr. Tri Hadi Jatmiko, Mr. Dwi Joko Prasetyo, Mr. Hernawan, Ms. Diah Pratiwi, and Dr. Adep Adid Dwiatmoko. I would also like to deliver high gratitude for collaboration research opportunity with Dr. Agnieszka Mierczynska-Vasilev, Dr. Pawel Mierczynski, Dr. Pei Li and Prof. Jun Ma at the different field of research applications. Hopefully for all collaborators, we can continue this cooperation to create more attractive and valuable research activities. I would also like to thanks to Dr. Ardian Setiawan for reviewing my earlier academic paperwork and also for Elite Editing as my thesis editor for the valuable time in editing my draft.

I also gratefully acknowledge the Indonesian Government, particularly Ministry of Research and Technology and Higher Education, for the Research and Innovation in Science and Technology Project (RISET PRO) Scholarship with the full financial support to accomplishing this Ph.D. study. I also deliver the great appreciation to the Project Management Office (PMO) Team and Liaison Officer (LO) of LIPI for smoothly facilitating the scholarship procedure.

The last but not least, this is the FINISH line for another START.

Annual University of South Australia milestone account of Satriyo Krido Wahono:

Knowledge is an eternal treasure (1983-2015)

The discovery is not the end, but it’s a new way for other innovations (2015)

Knowledge is not about the journal only, but more importantly is the journey (2016)

Don’t be afraid of your future, since after it is present, it will be your past (2017)

The highest achievement is not a purpose without usefulness for others (2018)

Starting the journey with the novelty of knowledge, attitude, and wisdom (2019)

Declarations

This thesis presents work carried out by myself and does not incorporate without acknowledgment any material previously submitted for a degree or diploma in any university; to the best of my knowledge it does not contain any materials previously published or written by another person except where due reference is made in the text; and all substantive contributions by others to the work presented, including jointly authored publications, are clearly acknowledged.

Satriyo Krido Wahono



_____ on 10/12/2018

Publications and Presentations

List of Publications:

1. **Wahono, S. K.**, Skinner, W., Addai-Mensah, J., and Vasilev, K., 2016, *Preliminary study: Combination of amine and natural zeolite as new adsorbent material for CO2 capture*, Chemeca 2016: Chemical Engineering - Regeneration, Recovery and Reinvention, Engineers Australia, ISBN 9781922107831: p. 900-910. (Peer-reviewed Proceeding – **Chapter 6 Part 1**)

   https://search.informit.com.au/documentSummary;dn=411079056124005;res=IELENG

2. **Wahono, S. K.**, Cavallaro, A., Vasilev, K., and Mierczynska, A., 2018, *Plasma polymer facilitated magnetic technology for removal of oils from contaminated waters,* Environmental Pollution 240: p. 725-732. (Peer-reviewed Journal – **Chapter 8**)

   https://doi.org/10.1016/j.envpol.2018.05.023

3. **Wahono, S. K.**, Suwanto, A., Prasetyo, D. J., Hernawan, Jatmiko, T. H., and Vasilev, K., 2018, *Plasma Activation on Natural Mordenite-Clinoptilolite Zeolite for Water Vapour Adsorption Enhancement,* (under review in particular journal – **Chapter 7**)

4. **Wahono, S. K.**, Stalin, J., Vinu, A., Addai-Mensah, J., Skinner, W., and Vasilev, K., 2018, *Carbon Dioxide Adsorption Enhancement of Natural Mordenite-Clinoptilolite Zeolite by Physicochemical Treatment,* (in preparation to be submitted to particular journal – **Chapter 4**)

5. **Wahono, S. K.**, Stalin, J., Vinu, A., Addai-Mensah, J., Skinner, W., and Vasilev, K., 2018, *Natural Zeolite Transformation by Alkali Impregnation for Improving Carbon Dioxide Adsorption Capacity,* (in preparation to be submitted to particular journal – **Chapter 5**)

6. **Wahono, S. K.**, Dwiatmoko, A. A., Vinu, A., Addai-Mensah, J., Skinner, W., and Vasilev, K., 2018, *Novel Amine Plasma Polymer Facilitated Carbon Dioxide Adsorbents,* (in preparation to be submitted to particular journal – **Chapter 6 Part 2**)

List of Presentations:

1. **Wahono, S. K.**, Skinner, W., Addai-Mensah, J., and Vasilev, K., 2016, *Preliminary study: Combination of amine and natural zeolite as new adsorbent material for CO2 capture*, Chemeca 2016: Chemical Engineering - Regeneration, Recovery and Reinvention, Adelaide, SA Australia (Poster Presentation – Peer-reviewed Proceeding published at The Informit Engineering Collection, RMIT – Engineers Australia)

2. **Wahono, S. K.**, Prasetyo, D. J., Jatmiko T. H., Suwanto, A., Pratiwi, D., Hernawan, and Vasilev, K., 2018, Transformation of Mordenite-Clinoptilolite Natural Zeolite at Different

Calcination Temperatures, ICONPROBIOS 2018: The 2nd International Conference on Natural Products and Bioresource Sciences, Serpong, Indonesia (Oral Presentation – Peer-reviewed Proceeding, in press at the Institute of Physics – IOP Conference Proceeding)

3. **Wahono, S. K.**, Prasetyo, D. J., Jatmiko T. H., Pratiwi, D., Suwanto, A., Hernawan, and Vasilev, K., 2018, *Multi-Stage Dealumination for Characteristic Engineering of Mordenite-Clinoptilolite Natural Zeolite,* RCChE 2018: The Regional Conference on Chemical Engineering, Yogyakarta, Indonesia (Oral Presentation – Peer-reviewed Proceeding, in press at the American Institute of Physics – AIP Conference Proceeding)

Chapter 1 : Introduction

1.1. Background

The development of new and renewable-energy systems (e.g., biogas, solar and wind) is a common issue around the world. Many researchers have conducted studies, and published and applied new inventions and innovations related to this issue. Commonly, such studies anticipate a rapid increase in global energy demand due to economic reasons, technological development and population growth around the world [1-3]. Additionally, conventional fossil-fuel-based energy supplies such as crude oils, natural gases and coals are limited. The vast use of conventional energy supplies from such fossil fuels has also accelerated the effects of global warming due to the simultaneous generation of voluminous greenhouse gases. These outcomes are contrasted with the effects of renewable-energy technologies [4-8].

One of the renewable-energy sources is biogas produced from the anaerobic fermentation of biomass and other organic materials. The primary composition of biogas is methane (CH_4), constituting 40–75% volume. Most of the impure gases comprise carbon dioxide (CO_2), hydrogen sulphide (H_2S), water-vapour (H_2O), nitrogen (N_2), hydrogen (H_2) and oxygen (O_2) [9-14]. Biogas with methane content <60% is used as a cooking fuel and is very rarely used for generating electricity [15]. By increasing the concentration of methane in biogas or biomethane, it can be utilised for advanced applications such as electricity generation and fuel-cell technology [16]. Therefore, effective methods for significantly increasing the methane content in biogas by reducing its gas impurities are needed.

CO_2 gas removal is the priority action because it is the primary or main impurity of biogas. One of the methods commonly used to remove CO_2 from biogas is absorption using amine solutions [17, 18]. However, this method has some disadvantages given that it can lead to increased corrosive potential in a wet-process application involving an oxidising chemical compound. Further, the absorption process using amine solutions is expensive in relation to the capital and operating costs, the money investment to be made, and the challenges faced in amine-solution regeneration [19]. Therefore, a dry amine-based adsorption method of biogas purification that is more cost efective and has reduced corrosive amine potential is needed.

One of the potential solid adsorbents for the dry process of methane purification is a natural zeolite used as a micro–mesoporous material. In Indonesia, the deposit of natural zeolite is large and has a relatively high concentration of silica content (approximately 60%), particularly Gunungkidul natural zeolite, which has a high Si/Al ratio of approximately 5 [20] and abundant availability of 55,000,000 m^3 [21, 22]. Gunungkidul natural zeolite appears to be an appropriate material for improving biogas purification, and may be applied directly to the installation of biogas in areas that have a high population of cattle as prospective biogas resources by utilizing its manure. The prospective collaboration of natural zeolite and biogas resources in Gunungkidul, Yogyakarta, Indonesia is presented in Figure 1.1.

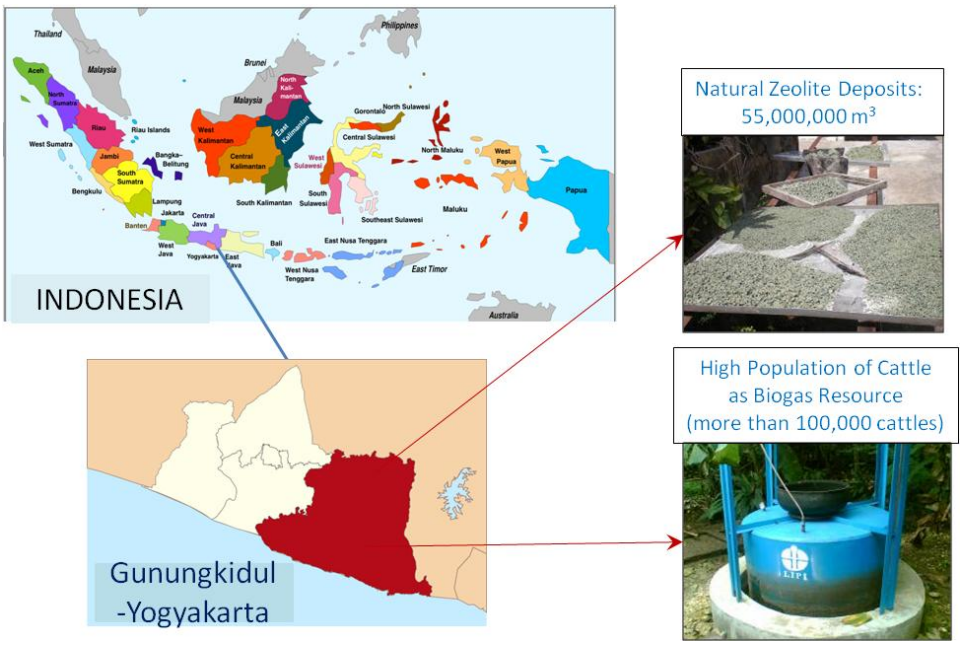

Figure 1.1. Natural zeolite and biogas resources in Gunungkidul, Yogyakarta, Indonesia

Indonesian Gunungkidul natural zeolites have the ability to enrich the methane content of biogas up to 20%, have good selectivity for biogas composition, remove bad odours and decrease corrosion potential [21, 23-26]. However, there remains room for improvement in modification given that previous studies have applied limited physical and chemical treatment [27], in which optimisation of physicochemical conditions was not performed. Further knowledge and new findings for improving the CO_2 adsorption characteristics of Indonesian natural zeolites via physicochemical treatment optimisation and structure modification and improvement are needed to engender diverse applications these zeolites.

Further, the introduction of new treatments and technologies provides further possibilites for improving the CO_2 adsorption characteristics of Indonesian natural zeolites. Combining zeolite with amine functional groups on solid sorbent is a possibility for enhancing the capability of biogas purification. This combination also overcomes the disadvantages of each method. Utilisation of plasma polymerisation technology for collaborating amine and natural zeolite is also a possible new technique for CO_2 adsorbent improvement. Natural zeolite can be inducted with an amine using plasma polymerisation technology, which means it can increase natural zeolite's ability to capture CO_2. In previous research, plasma polymer has been utilised for coating the membrane of gas-permselective composite, particularly for O_2/N_2 selectivity [28]. Moreover, the plasma polymer deposition on porous material can be successfully controlled on mesoporous [29, 30] and macroporous material [31-36]. However, plasma polymer induction on porous adsorbent materials for capturing CO_2 has not yet been developed. Therefore, the amine functional group coated by plasma polymer will be a newly designed adsorption material. The improvements and modifications of natural zeolite by different physicochemical treatments and plasma treatments are shown in Figure 1.2.

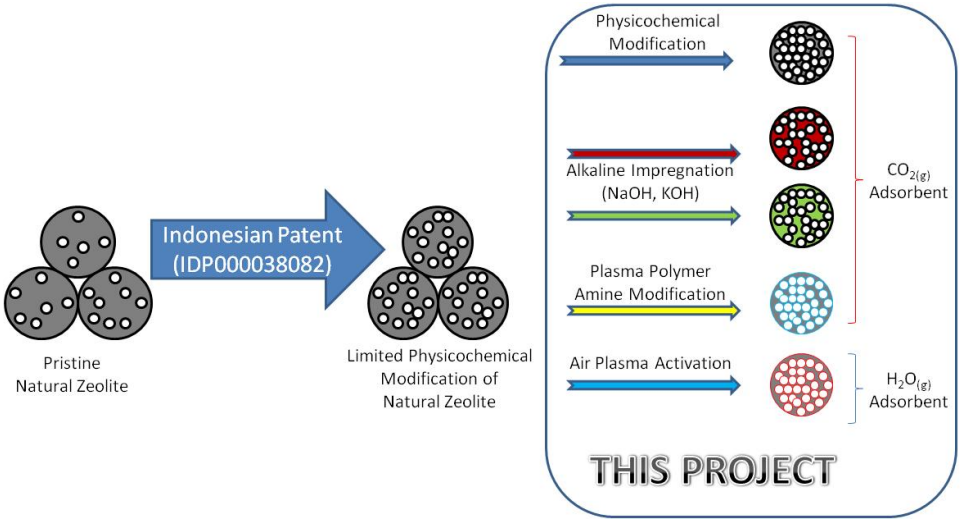

Figure 1.2. Schematic of Indonesian Gunungkidul natural-zeolite structure modification and improvement for purifying biogas (CO_2 and H_2O removal).

1.2. Research Aims and Objectives

The overarching aim of this thesis is to improve the Indonesian Gunungkidul natural zeolites capability in advanced combination with plasma surface engineering for innovating advanced adsorbents, particularly in biogas purification. Specifically, this research was conducted to improve the properties of natural zeolite, particularly the specific surface area, basicity and amine/nitrogen incorporation using physicochemical treatments and plasma polymerisation technology to create the best adsorbent of CO_2. Another application of natural-zeolite surface engineering for improved water-vapour adsorption is explored via air-plasma activation. Further, the introduction of plasma polymer technology together with improvements of particulate-material surface engineering for environmental applications, particularly for oil-contaminant removal from water, is also investigated. The objectives of this study are outlined as follows:

- increasing surface area of Indonesian natural zeolite by physicochemical treatment to improve CO_2 adsorption capacity
- controlling Indonesian natural zeolites basicity property by impregnation of alkali compound for enhanced CO_2 affinity
- introducing amine functional groups into the Indonesian natural-zeolite channel by plasma polymerisation technology for improving CO_2 affinity
- activating Indonesian natural zeolite by air-plasma treatment for improving capacity of water-vapour adsorption
- fabricating hydrophobic properties on the particulate-material surface using plasma polymerisation for environmental applications (application and optimisation of the nanomagnetic-hydrophobic surface for oil capture).

1.3. Research Significance

The presence of CO_2 as the most prevalent greenhouse gas in the world encourages many studies on CO_2 capture in liquid absorption and solid adsorption. As a micro–mesoporous material, Indonesian natural zeolite offers a prospective material for CO_2 adsorption, particularly in biogas purification given its multiadsorption capability with gases. While previous studies have applied limited physicochemical treatments, they have created a biogas-purification capability of zeolite that can continue to be improved through various

treatments. Further, plasma polymerisation technology also offers a facile technique for material improvement, particularly for surface engineering. This technology provides a new perspective of collaboration material by conducting plasma charging on the surface of Indonesian natural zeolite using appropriate precursors for plasma polymerisation application and using air-plasma activation for increasing surface reactivity. While the plasma polymer amine produces a hydrophilic surface after deposition, a hydrophobic surface can also be created by plasma polymer using different monomers. Therefore, particulate-material coating is also conducted for fabricating a hydrophobic surface to be used as a new oil-adsorbent material. Further, plasma charging activates the natural-zeolite surface for improving water-vapour adsorption, which is also related to biogas purification.

The output of this research will provide a significant contribution to knowledge related to the utilisation and improved performance of Indonesian natural zeolite as an adsorbent, particularly in the biogas-purification process. It can be applied to natural gas purification for large-scale applications because biogas has similar characteristics and gas composition to natural gas but with lower capacity and lower methane content. Moreover, the prospective product related to the particulate surface engineering of plasma polymerisation will create various possible applications in environmental fields.

For industry, biogas-purification technology will promote biogas as an attractive alternative energy source, particularly in industries that have the potential to create biomass residue. This new adsorbent technology will improve the purity of biogas and reduce the corrosion potential of equipment such as boilers. Improvement of biogas quality will help industries reduce their reliance on external electrical-energy sources. Further, this new adsorption material can be utilised as an adsorbent for reducing air pollutants, which are also generated by such industries.

From an economic perspective, the increased utilisation of biomass wastes should be encouraged. Currently, in Indonesia, biomass wastes are used mainly as materials to produce organic fertilisers that are applied in many organic farms as new farming products. Conversion of these wastes into electricity will result in a significantly higher economic value. Moreover, the advanced processing of the new zeolite products and applications will increase the economic value of Indonesian natural-zeolite products by creating a new mining industry.

For the community, new adsorbent technology will create another alternative utilisation of biogas, which is currently used mainly for cooking. Communities living in marginal areas that produce abundant biomass wastes and are remote from the power grid will be the primary beneficiaries of this technology. In addition, sustainable energy production in a particular area enhances the community's quality of life and social interaction [15, 25].

1.4. Thesis Description

The following chapters present detailed descriptions, new findings, and further opportunities and challenges for the modification of Indonesian natural zeolite and explore the different wettability possibilities of plasma polymer coating in environmental applications. All the thesis outcomes were accomplished from 2015 to 2018, with some of the results having already been published in refereed scientific journals, and others being ready for submission to such journals. The thesis was conducted in the following five major stages:

1. physicochemical modification of Indonesian natural zeolite:
   a. dealumination using strong acid in a various concentrations
   b. calcination at various high temperatures
   c. CO_2 adsorption capacity measurement of selected material
2. alkali impregnation of Indonesian natural zeolite:
   a. alkali impregnation using strong base in various concentrations
   b. characterisation of alkali impregnated natural zeolite
   c. CO_2 adsorption capacity measurement of the selected material
3. amine functional group induction into Indonesian natural zeolite by plasma polymerisation:
   a. determination of the appropriate condition of plasma polymer amine
   b. control of plasma polymer amine deposition on micro–mesoporous natural zeolite
   c. determination of the proper degassing preparation of natural zeolite modified by plasma polymer amine
   d. CO_2 adsorption capacity measurement of the selected material.
4. air-plasma activation on modified Indonesian natural zeolite of high Si/Al ratio
   a. determination of water-vapour adsorption capacity of modified natural zeolite without air-plasma activation

b. characterisation of modified natural zeolite activated by air plasma
c. determination of water-vapour adsorption capacity of modified natural zeolite after air-plasma activation

5. hydrophobic surface engineering on nanomagnetic material by plasma polymerisation:
   a. characterisation of hydrophobic plasma polymer deposition
   b. characterisation of coated nanomagnetic particles by hydrophobic plasma polymer
   c. application and optimisation of nanomagnetic-hydrophobic surface for oil capture.

1.5. Structure of Thesis

This PhD thesis contains published and unpublished research in compliance with the Academic Regulations for Higher Degrees by Research (section 16.1.1.b) of the University of South Australia. The thesis comprises nine chapters: an introduction, literature review, general methodology, five chapters presenting the main results and discussions, overall conclusions and recommendations.

Chapter 1 provides a description of the background, problem statement, research aims and objectives related to biogas purification using Indonesian natural zeolite and further improvement of plasma polymerisation technology. Chapter 2 presents a review of recent literature that provides information related to issues and conditions of biogas purification, CO_2 adsorption, natural zeolite, amine adsorbent and plasma polymerisation. Chapter 3 describes the stages of the thesis, methodology and characterisation techniques used in this thesis. Chapters 4, 5, 6, 7 and 8 present the results and discussions of results for the various modifications performed on the structure of Indonesian natural zeolite and the plasma polymer surface engineering on particulate material and CO_2 adsorption investigations (see Figure 1.3). The headings of these chapters is presented below:

- Chapter 4: CO_2 Adsorption Enhancement of Natural Mordenite–Clinoptilolite Zeolite by Physicochemical Treatment
- Chapter 5: Indonesian Natural Zeolite Transformation by Alkali Impregnation for Improving CO_2 Adsorption
- Chapter 6:
  - Part 1: Preliminary Study: Combination of Amine and Natural Zeolite as New Adsorbent Material for CO_2 Capture

- Part 2: Novel Prospective CO_2 Adsorbent of Plasma Polymer Allylamine Deposition on Natural Mordenite–Clinoptilolite Zeolite

- Chapter 7: Plasma Activation on Natural Mordenite–Clinoptilolite Zeolite for Water-vapour Adsorption Enhancement
- Chapter 8: Plasma polymer facilitated magnetic technology for the removal of oils from contaminated waters

Chapter 9 presents the general findings and conclusions of the research, as well as prospective future research directions for further improving the properties of Indonesian natural zeolite and enhancing the plasma polymerisation technique. The appendices provide additional information such as copyright permissions, published manuscript and supplementary information.

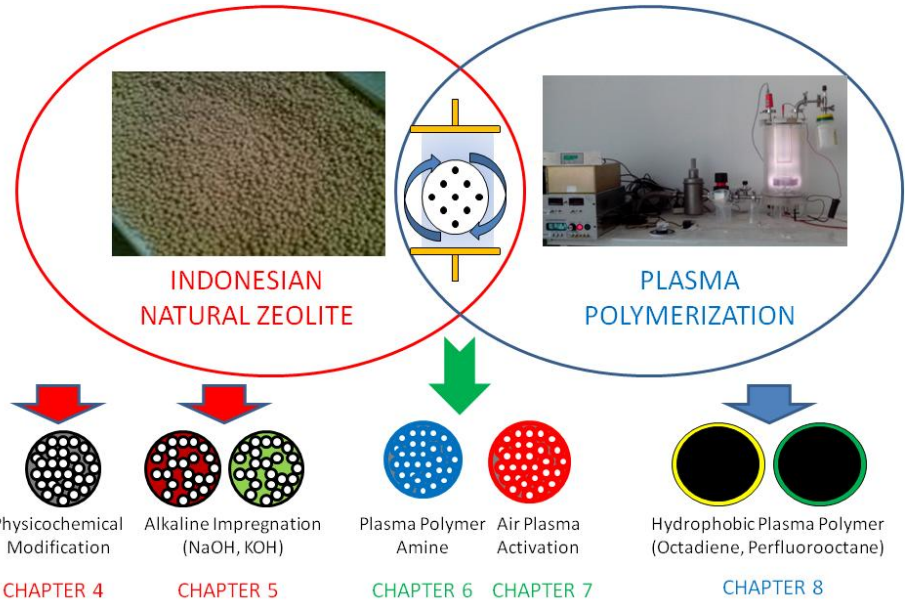

Figure 1.3. Schematic of thesis structure of Indonesian natural zeolite and plasma polymerisation for biogas upgrading and other environmental applications

References

1. Ferguson, R., W. Wilkinson, and R. Hill, *Electricity Use and Economic Development.* Energy Policy, 2000. **28**(13): p. 923-934.

2. Roberts, L., *Energy Production*, in *The Global Environment*. 2008, Wiley-VCH Verlag GmbH. p. 290-302.

3. Wahono, S.K. and P.I. Pudjiono, *Bioenergi dan Industri Manufaktur [Bioenergy and Manufacturing Industries]*, in *National Seminar on Technology–State Polytechnic of Semarang*. 2007: Semarang–Indonesia.

4. Abbasi, T., S.M. Tauseef, and S.A. Abbasi, *Biogas and Global Warming*, in *Biogas Energy*. 2012, Springer New York. p. 25-34.

5. Chand, M.B., B.P. Upadhyay, and R. Maskey, *Biogas: Option for Mitigating and Adaptation of Climate Change: Climate Change Adaptation and Mitigation In Kanchanpur District of Nepal*. 2012: Lap Lambert Academic Publishing GmbH KG.

6. Khoiyangbam, R.S., S. Kumar, and M.C. Jain, *Methane Losses from Floating Gasholder Type Biogas Plants in Relation to Global Warming.* Journal of scientific and industrial research : JSIR, 2004. **63**(4): p. 344-347.

7. Mahat, S., P. Lamichhane, and U.K. Thapa, *Global Warming Mitigation Potential of Biogas Technology in Security Institutions of Kathmandu Valley, Central Nepal.* International Research Journal of Environment Sciences, 2014. **3**(10): p. 68-74.

8. Pathak, H., et al., *Global Warming Mitigation Potential of Biogas Plants in India.* Environmental Monitoring and Assessment, 2009. **157**(1-4): p. 407-418.

9. Rasi, S., A. Veijanen, and J. Rintala, *Trace compounds of Biogas from Different Biogas Production Plants.* Energy, 2007. **32**(8): p. 1375-1380.

10. Arifin, R., F.F.P. Perdana, and S.R. Juliastuti, *Pengaruh Enzim α-Amilase dan EM-4 terhadap Pembentukan Biogas dari Limbah Padat Tapioka [Effect of α-Amylase Enzyme and EM-4 for Biogas Production from Solid Waste of Starchy]*, in *National Seminar on Chemical Engineering and Processes*. 2008, Chemical Engineering Department, Diponegoro University: Semarang–Indonesia. p. D107 1-8.

11. Hambali, E., et al., *Teknologi Bioenergi [Technology of Bioenergy]*. 2007: Agro Media Pustaka.

12. Monnet, F., *An Introduction to Anaerobic Digestion of Organic Wastes*. 2003, Remade Scotland.

13. Muryanto, J.S., K. Ekaningtyas, and Sudadiyono, *Biogas, Energi Alternatif Ramah Lingkungan [Biogas, Green Alternative Energy]*. 2006, Semarang–Indonesia: Institute for Agricultural Technology (BPTP), Central Java.

14. Lastella, G., et al., *Anaerobic Digestion of Semi-Solid Organic Waste: Biogas Production and Its Purification.* Energy Conversion and Management, 2002. **43**(1): p. 63-75.

15. Febrisiantosa, A. and H. Julendra, *Konversi Limbah Ternak Sapi Bali Bos javanicus Menjadi Biogas di UPT Kapitan Meo Kabupaten Belu Nusa Tenggara Timur [Bali Cattle Boss javanicus Waste Convertion to Biogas in UPT Kapitan Meo Belu East Nusa Tenggara]*, in *National Seminar on Chemical Engineering and Processes*. 2008, Chemical Engineering Department, Diponegoro University: Semarang–Indonesia. p. J045 1-5.

16. Wahono, S.K., *Kajian: Alternatif Optimasi dan Penyimpanan Energi Secara Aman pada Sistem Instalasi Biogas [Review: Optimization for The Safe Energy Storage of Biogas Installation System]*, in *Proceeding Call For Paper–Kontribusi Insinyur Muda untuk Indonesia, Temu Insinyur Jogja*. 2007: Yogyakarta–Indonesia.

17. Álvarez-Gutiérrez, N., et al., *Towards Bio-Upgrading of Biogas: Biomass Waste-Based Adsorbents.* Energy Procedia, 2014. **63**: p. 6527-6533.

18. Rochelle, G.T., *Amine Scrubbing for CO_2 Capture.* Science, 2009. **325**(5948): p. 1652-1654.

19. Shao, R. and A. Stangeland, *Amines Used in CO_2 Capture*, in *Bellona Report*. 2009, The Bellona Foundation.

20. Widayat, et al., *Pengaruh Konsentrasi HCl dan Jenis Reaktan dalam Pembuatan Katalis Zeolit untuk Proses Dehidrasi dari Zeolit Alam [Effect of HCl Concentration and Reactant Type in The Zeolite Catalysts Production for Dehydration Process of Natural Zeolite]*, in *National Seminar on Chemical Engineering and Processes*. 2008, Chemical Engineering Department, Diponegoro University: Semarang–Indonesia. p. H091 1-9.

21. Wahono, S.K. and W.A. Rizal, *Biogas Filter Based on Local Natural Zeolite Materials.* International Journal of Renewable Energy Development, 2014. **3**(1): p. 1-5.

22. Idrus, A., et al., *Geology, Characterization, Quality Improvement and Recommended Utilization of Natural Zeolite (Zeolitic Tuff) Deposits from Gunungkidul, Yogyakarta Special Teritory, Indonesia.*, in *"2nd IASME / WSEAS International Conference on Geology and Seismology (GES'08)*. 2008, ISSN 1790-2769; ISBN 978-960-6766-39-8: Cambridge, UK. p. 21-25.

23. Wahono, S.K., R. Maryana, and M. Kismurtono, *Biogas Purification Process to Increase Gen—Set Efficiency.* AIP Conference Proceedings, 2009. **1169**(1): p. 185-189.

24. Wahono, S.K., *Kajian: Pemanfaatan Zeolit Lokal Gunungkidul–Yogyakarta untuk Optimasi Sistem Biogas [Review : Utilization of Gunungkidul Local Zeolite for Biogas System optimization]*, in *National Seminar on Chemical Engineering Fundamentals and Applications*. 2008, Chemical Engineering Departement of Institute of Technology Sepuluh November Surabaya: Surabaya–Indonesia. p. E14.

25. Wahono, S.K., H. Julendra, and A. Febrisiantosa, *Peningkatan Performa Biogas Melalui Teknologi Pemurnian Metana di UPT Kapitan Meo, Kabupaten Belu–Nusa Tenggara Timur [Performance Enhancement of Biogas Using Purification Technology of Methane at UPT Kapitan Meo, District Belu–East Nusa Tenggara]*, in *National Seminar on Technology Development Based on Local Materials*. 2009: Yogyakarta–Indonesia. p. 505-508.

26. Wahono, S.K., et al., *Modifikasi Zeolit Lokal Gunungkidul sebagai Upaya Peningkatan Performa Biogas untuk Pembangkit Listrik [Modification as an Effort Local Zeolite–Gunungkidul Performance Improvement for Biogas Electricity Generation]*, in *National Seminar on Chemical Engineering and Processes*. 2010: Semarang–Indonesia. p. D-11.

27. Wahono, S.K., et al., *Metoda dan Alat untuk Meningkatkan Kadar Methana dalam Biogas [Methods and Tools for Increasing Methane Contents of Biogas]*. Patent, 2010. IDP000038082: Indonesia.

28. Nomura, H., *Gas Permselective Composite Membrane Prepared by Plasma Polymerization Coating Techniques*. 1989, Google Patents.

29. McInnes, S.J.P., et al., *Combination of iCVD and Porous Silicon for The Development of a Controlled Drug Delivery System.* ACS Applied Materials & Interfaces, 2012. **4**(7): p. 3566-3574.

30. Dusan, L., et al., *Surface Modification of Nanoporous Alumina Membranes by Plasma Polymerization.* Nanotechnology, 2008. **19**(24): p. 245704.

31. Hamerli, P., et al., *Surface Properties of and Cell Adhesion onto Allylamine-Plasma-coated Polyethylenterephtalat Membranes.* Biomaterials, 2003. **24**(22): p. 3989-3999.

32. Simovic, S., D. Losic, and K. Vasilev, *Controlled Drug Release from Porous Materials by Plasma Polymer Deposition.* Chemical Communications, 2010. **46**(8): p. 1317-1319.

33. Rebl, H., et al., *Accelerated Cell-surface Interlocking on Plasma Polymer-Modified Porous Ceramics.* Materials Science and Engineering: C, 2016. **69**: p. 1116-1124.

34. Bergemann, C., et al., *Continuous Cellularization of Calcium Phosphate Hybrid Scaffolds Induced by Plasma Polymer Activation.* Materials Science and Engineering: C, 2016. **59**: p. 514-523.

35. Vasilev, K., et al., *Tailoring The Surface Functionalities of Titania Nanotube Arrays.* Biomaterials, 2010. **31**(3): p. 532-540.

36. Andrew, M., et al., *Versatile Gradients of Chemistry, Bound Ligands and Nanoparticles on Alumina Nanopore Arrays.* Nanotechnology, 2011. **22**(41): p. 415601.

Chapter 2 : Literature Review

2.1. Introduction

This chapter explores the literature related to biogas purification using Indonesian natural zeolite from the Gunungkidul area as the base adsorbent material focusing on CO_2 removal. The chapter explains applications of biogas and further applications for which it can be used after impure gases other than methane have been removed. The literature review also examines biogas-purification technology, particularly the possibilities provided by Indonesian natural zeolite and its various physicochemical treatments for improving its CO_2 adsorption capacity. The new technique of plasma polymerisation is explored as a prospective novel technology of solid amine induction in CO_2 adsorption, which this new technique collaborates well with the capacity of Indonesian natural zeolite. Moreover, air-plasma activation on natural zeolite for water-vapour adsorption and hydrophobic surface of plasma polymerisation are also observed in their capacity for application as materials in environmental uses. This literature review provides detailed information about recent technologies to provide an introduction to the concepts and techniques presented in subsequent chapters.

2.2. Biogas

Biogas is gas produced by the organic decomposition of microorganisms in anaerobic conditions. Anaerobic-digestion technology as a producer of biogas is a highly prospective technology with great potential. Biogas has been suggested as the most efficient conversion of biomass [1-4]. The World Bank categorises biogas as a modern cooking fuel [5].

Biogas technologies have been developed in many of countries (e.g., Denmark since the 1970s and China and India since the 1980s) [6]. In Europe and many other parts of the world, biogas production in the agricultural sector has been increasing. In Indonesia, there are more than 9500 units of biogas digesters for domestic utilisation [7].

It has been projected that at least 25% of all bioenergy originating from biogas is produced by fermentation of wet organic materials such as animal manure, whole crop silages, wet food and feed wastes [8]. The quality and quantity of biogas production depends on several parameters that influence the fermentation process. These are anaerobic conditions, pH, temperature, water and solids ratio, C/N ratio, toxic materials, mixing, type of substrate, and time of fermentation in the digester [9-12]. The purity of the biogas produced by the biodigester is not optimal, with the primary gas composition in the form of methane at levels between 40 and 75% (shown in Figure 2.1; detailed in Table 2.1).

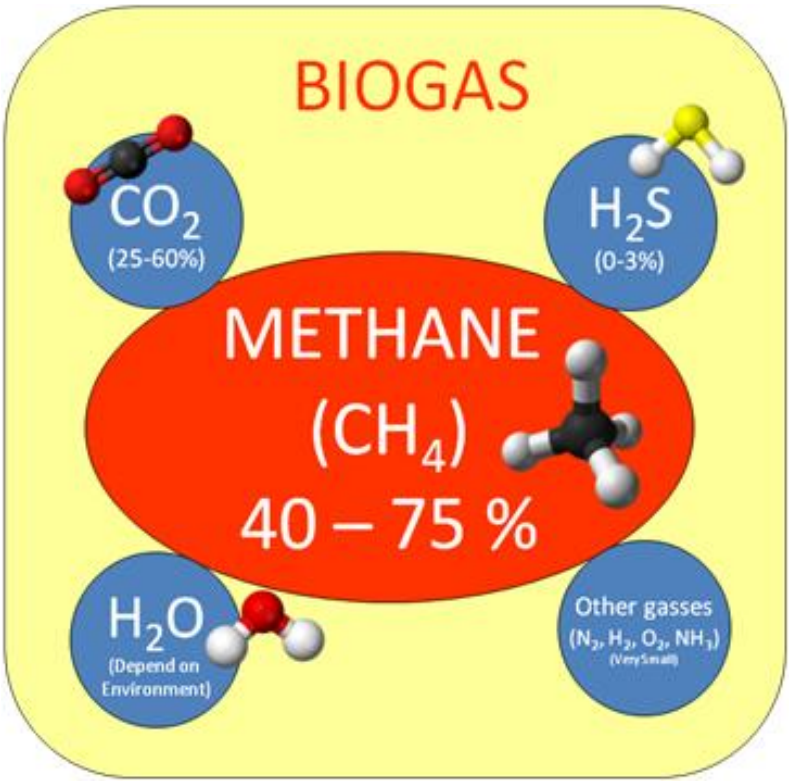

Figure 2.1. Biogas composition with methane as the primary gas and various gases impurities

Table 2.1. Composition of biogas based on literature

No.	Gas	Unit	Composition					
			(a)	(b)	(c)	(d)	(e)	(f)
1	CH_4	%	47–65	55–65	50–75	55–70	40–70	60–68
2	CO_2	%	36–41	35–45	25–40	30–45	30–60	32–40
3	H_2S	Ppm	<169	0–1	<2	<500	0–3	<1000
4	N_2	%	1–2	0–3	<2	0–2	–	–
5	H_2	%	–	0–1	<1	–	0–1	–
6	O_2	Ppm	<1	–	<2	–	–	–

References: (a) [13]; (b) [14]; (c) [15]; (d) [16]; (e) [17]; (f) [18]

2.3. Biogas Utilisation

Biogas, which includes multifunctional energy technologies due to its side products, can also be used as a high-quality organic fertiliser, vegetable media growth, livestock feed and fishpond water [19]. The utilisation of methane in biogas is environmentally friendly because without the methane utilisation, methane will decompose naturally as separated waste and pollute the atmosphere as a greenhouse gas [20]. The utilisation of biogas methane and sludge for supporting various activities is presented in Figure 2.2.

Biogas can be used for heat or electricity generation, injected into the gas-piping system, converted into other chemicals, used as a hydrogen source, or utilised as vehicle fuel [3, 9, 21]. In commercial and industrial sectors, the biogas unit system is built on a large scale to generate electricity (e.g., in electric power plants; in palm oil mills, which use palm oil mill effluent [POME] to produce electricity) [7]. Biogas offers economic value as an alternative to fossil fuels [9].

Biogas conversion into electricity is undertaken because methane as the main component of biogas cannot be compressed into liquid form at room temperature in a pressurised tank [22]. Biogas energy is more comfortable for distribution and utilisation once it has been converted into electricity [3, 23]. A higher content of methane, in gas which is termed ‘biomethane’ can

be produced by the purification of biogas using various technologies (pressure swing adsorption, water scrubber, membrane, cryogenic method, chemical absorption, biological process, and molecular sieve). Methane upgrading of biogas also improves the performance of the gas generator as the increased heating value and maintain the durability of the engine generator because it reduces the possibility of corrosion in the engine [24, 25].



Figure 2.2. Utilisation of biogas for supporting various activities: fertiliser production, farming activities, heat generation, electricity generation

2.4. Biogas Purification

Apart from methane as a fuel gas, biogas contains various other gas impurities. Thus, methane purification in biogas is needed to optimise the energy biogas can produce. In general, biogas purification can refer to CO_2 (as the main impure gas of biogas) removal. Other gases that need to be reduced or removed from biogas are H_2O and H_2S. These impure gases need to be removed because their presence creates disadvantages such as decreasing the

heating value, accelerating corrosion, and emitting bad odours [25-27]. The schematic of biogas purification for producing a high purity of methane is presented in Figure 2.3.

Purification procedures may consist of simple dehydration to the perfect separation of H_2O, H_2S, CO_2 and CH_4. Separation using solid and liquid absorbent materials can be either chemical or physical [28]. Gas-separation technology to separate CO_2 from a gas stream has been developed. The various purification technologies developed can be classified into seven categories based on the type of technology used (see Table 2.2). Biogas-purification processes can also be classified into seven categories: (1) pressure swing adsorption; (2) water scrubber; (3) chemical absorption; (4) membrane separation; (5) cryogenic separation; (6) biological processes; (7) molecular sieves [26, 29-32].

Several CO_2 absorption methods using chemical solutions have been developed and applied on an industrial scale. CO_2 absorption using NaOH for biogas can absorb gas with a degree of absorption up to more than 70% of the purity of CH_4 [33]. In the ammonia plant, CO_2 is dissolved in an absorbent solution such as NaOH, KOH and K_2CO_3, accompanied by a chemical reaction [20, 33]. Amine utilisation as the liquid absorbent is the most readily applicable in industry for capturing CO_2, and can remove 85–90% of CO_2 and other impurities. However, this technology is complex, costly, and creates environmental and human-health problems [30, 34].

The water-vapour content in biogas usually varies between 5 and 100% (saturation with water vapour); the water-vapour can be separated partly through gravity separation using in-line gravity outflow, the triethylene glycol (TEG) system, molecular sieves, filtering, heating, and cooling air or refrigeration [35]. Excessive water vapour in the installation pipe will disrupt the distribution of biogas. Additionally, corrosion occurs then destructs a metal pipe and equipment, which means extra costs for maintenance. Silica gel is a commonly utilised material for water-vapour adsorption given its ability to drain air by absorbing liquid from the air passing through silica gel [36, 37]. Another prospective material is Indonesian natural zeolite, which has been applied for removing water vapour in bioethanol dehydration [38, 39]. Meanwhile, the metal–organic framework (MOF) is considered a water-adsorption material given the stable structure in a gas or liquid environment [40, 41].

The separation processes of H_2S (including biogas) can be accomplished in physics, biology, and chemistry [42]. In physics, it is accomplished using water absorption, adsorption with a membrane or activated carbon, impregnated activated carbon, zeolite, iron oxide, and zinc oxide [43-45]. Biogas purification of H_2S content can also be accomplished using a biological process by which bacteria decompose H_2S into sulphate [46, 47]. Both methods are rarely applied because they are financially expensive. Biogas purification of H_2S is often achieved chemically by using absorbent solutions [42, 48]. One of the absorbents widely used in the industry is monoethanolamine (MEA); other absorbents include nitrite solution, alkali salts, the slurry of iron oxide or zinc oxide and solution chelated iron [42]. The purification of biogas from H_2S using solution chelated iron (Fe-EDTA) provides many advantages such as regenerating absorbent, separating sulphur into solid form, having high effectiveness of adsorption, and producing residue that is more environmentally friendly [48].

Besides having CO_2, water vapour and H_2S as disruptive main impurities, biogas also contains other impure gases in low quantities (e.g., NH_3, H_2, N_2 and O_2). These impurities can be ignored because they do not have a calorific-value impact or are separated by the primary-impurity gas-separation process of biogas. Moreover, given the small content of H_2S in biogas, H_2S removal can be ignored for a small or household scale biogas digester because H_2S is commonly capturing through the process of CO_2 or water-vapour purification.

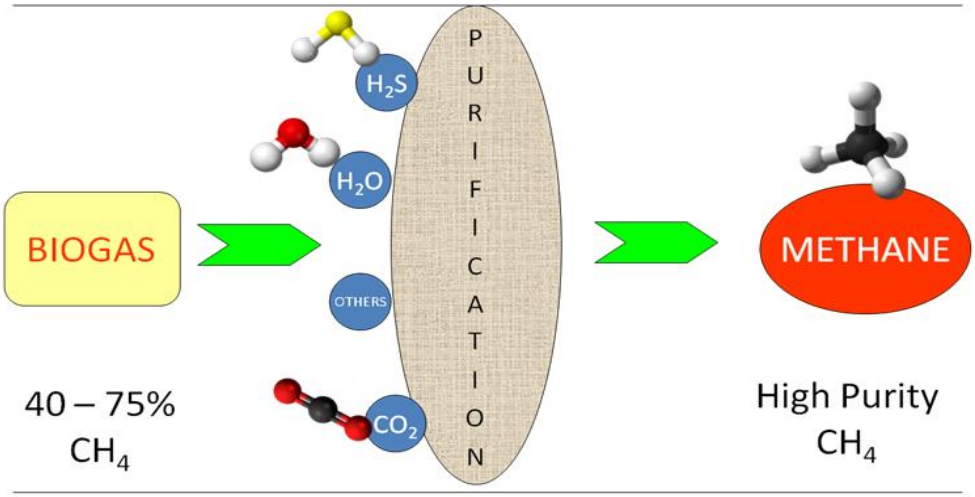

Figure 2.3. Schematic of biogas purification for producing high purity of methane (biomethane)

Table 2.2. Comparison of biogas-purification technologies

No	Technology	Removed Gas Impurities					Variable				
		CO_2	H_2O	H_2S	CH_4	Others	Investment	Operation	Regeneration	Energy	Others
1	PSA	v	v	v	95–98%	O_2, N_2	expensive	expensive	–	dynamic pressure	tight control
2	Water scrubber	v	–	v	>97%		expensive	expensive; easy	Possible	pressure	low flexibility
3	Chemical absorption (e.g., amine, alkali, PEG)	v	v	v	>99%	NH_3, HCN	expensive	expensive (PEG); cheap (amine)	difficult heat	pressure; high temperature; regeneration	corrosion
4	Membrane separation	v	v	v	>96%	-	cheap	cheap; simple	fouling membranes	high pressure	low selectivity; high price
5	Cryogenic separation	v	v	v	90–98%	Except CH_4	expensive	expensive	–	high pressure; low temperature	tight control
6	Biological processes	v	–	v	enriching	–	–	extra nutrient	possible	ambient pressure (1 atm)	experimental; add microbe
7	Molecular sieve (e.g., zeolite, carbon active, MOF)	v	v	v	up to 93%	–	cheap	cheap	possible	ambient pressure-temperature (1 atm, 25°C)	needs pre-treatment

Notes. PSA = Pressure swing adsorption; PEG = polyethylene glycol; MOF = metal–organic framework; CO_2 = carbon dioxide; H_2O = water; H_2S = hydrogen sulphide; CH_4 = methane; O_2 = oxygen; N_2 = nitrogen; NH_3 = ammonia; HCN = hydrogen cyanide

2.5. Molecular Sieve for CO_2 Removal

One of the common methods for biogas purification is the adsorption process using the molecular sieve. Adsorption is usually applied to enhance the heating value of fuels by removing N_2, CO_2, H_2O and eliminating undesirable impurities such as H_2S and mercaptans [49]. As the main impure gas of biogas, CO_2 is the priority for removal. There are many types of solid adsorbents developed for CO_2 capture, for example, activated carbon [50-54], silica gel [54-56], zeolite [57-61], metal–organic frameworks (MOF) [62-64] and synthetic resins [65, 66]. These adsorbents are usually solid particles with high porosity and sized 12 μm to 120 μm passive to the wanted product [67].

Several molecular sieves with microporous materials (e.g., activated carbon, zeolite and MOFs) have been studied for CO_2 capture by physical adsorption [68-72]. Some studies have applied activated carbons for CO_2 adsorption of CO_2-CH_4 mixtures [73-80]. The utilisation of a silica framework combined with another purification technology [81] or another adsorbent [82] has also improved methane concentration of CO_2-CH_4 mixtures. Ferro-organic frameworks (Fe-EDTA), effective for H_2S removal, are also able to reduce CO_2 with high efficiency from CO_2-CH_4 mixtures [83-85].

The adsorption method using a molecular sieve can be conducted through physical or chemical processes. In the physical process, the adsorbent surfaces bind the molecules, which go through the adsorbents because of the attraction forces of the surface molecules; this process is referred to as physisorption. In the chemical process, the molecules are able to be captured because of the chemical reaction between the molecules and adsorbent surfaces; this process is referred to as chemisorption. The adsorption process condition affects the isosteric heat of adsorption value, and chemisorption has a higher isosteric heat value than physisorption. Some studies provide the value of 50 kJ/mol as the line between chemisorption and physisorption [86-88]. The isosteric heat value also has consequences for the regeneration process. Physisorption with lower isosteric heat value is easier for regeneration than chemisorption because the value indicates lower energy for desorption as the regeneration action [88].

2.6. Indonesian Natural Zeolite

Zeolites are a member of the group of aluminium silicate minerals that have a microporous structure of crystalline solids and a similar basic tetrahedral structure of $Al_XSi_YO_Z$. Aluminium, silicone and oxygen atoms in zeolites are commonly found in the form of $[SiO_4]^{4-}$ and $[AlO_4]^{5-}$ compounds [89]. Based on the pore-size classification of the International Union of Pure and Applied Chemistry (IUPAC) [90], zeolites can be microporous (<2 nm), mesoporous (2– 50 nm), and even macroporous (>50 nm) [91], although only the microporous and mesoporous function as adsorption sites [92]. Natural zeolite has a skeletal structure, containing blank spaces that are occupied by cations of Na^+, K^+, Ca^{2+}, Mg^{2+} (alkali group) and free water molecules to allow ion exchange and absorption of chemical compounds [93].

Zeolites form naturally by reaction of volcanic ash and alkali groundwater, then by being deposited for thousands to millions of years. However, synthetic zeolites have been produced on a large scale from manufacturing a silica and alumina combination. There are many types of zeolite depending on the environment of formation and the source of materials [94-99]. At December 2017, there were 235 unique structures of zeolites in the worldwide [100], and 57 are confirmed as natural-zeolite structures [101].

The synthetic production of zeolite offers phase purity and uniform structure, but has the disadvantages of high production cost, complex processing and waste production. However, natural zeolite is available in abundant quantity and can be found in many locations around the world (e.g., China, Jordan, Korea, Japan, Turkey, USA, Slovakia, and Indonesia) [102-104]. Although the adsorption capacity of natural zeolite (raw or modified) cannot be compared that of with synthetic materials, this is compensated by the low production cost and bulk availability [105]. Some studies have investigated the gas-adsorption and separation capability of natural zeolite from various areas (e.g., helium [106], hydrogen [107], CO_2 [108], H_2S [109], water-vapour [110], and biogas [111-113]).

Indonesia is one of the largest producers of natural zeolite in the world, and is where most of the product utilised for pozzolanic cement manufacture is mined [104, 114]. Natural zeolite in Indonesia has high purity and a silica concentration of approximately 60%, and is found in the following areas: South Lampung, Bajah, Cikembar, Cipatujah, West Java

Nangapada, Ende, Nusa Tenggara Timur, Malang and Gunungkidul [20, 115, 116]. There are two types of natural zeolite commonly found in Indonesia: clinoptilolite [$(Na, K, Ca)_{2-3}Al_3(Al, Si)_2Si_{13}O_{36}\cdot 12H_2O$] and mordenite [$(Ca, Na_2, K_2)Al_2Si_{10}O_{24}\cdot 7H_2O$] [104, 116-118]. Both of these types of natural zeolite have been found by previous studies to be suitable zeolite types for gas adsorption [119]. However, the utilisation of Indonesian natural zeolite for gas adsorption has been limited since common studies are conducted for catalyst and liquid adsorbent.

Indonesian natural zeolite, particularly the zeolite found in Gunungkidul, has the potential to be used as an adsorbent for improving the performance of biogas through purification. Not only does Gunungkidul's zeolite have a suitable crystal type for gas adsorption, but it also has reasonably extensive deposits (55,000,000 m^3) [25, 120], as well as a silica content of approximately 60% [115]. Activated and modified natural zeolite (dealumination and calcination) from Gunungkidul is of good quality because it produces a relatively high SiO_2/Al_2O_3 ratio [115]. Activation of this zeolite also changes some of its material characteristics (e.g., surface area, crystallinity, functional groups) [38, 39], thus providing a prospective material for various applications. The Gunungkidul natural zeolite has been studied for various applications (e.g., catalyst [121-124], drug delivery [125], radioactive waste treatment [126, 127], wastewater treatment [128-131], bioethanol dehydration [38, 39, 132], and biogas purification [24, 25, 133, 134]).

Particularly for biogas, which is a mixed gas composition, zeolite can increase purity because it can absorb all the main impure gases such as water vapour, CO_2 and H_2S, but it does not adsorb CH_4 which is the main purified gas [20]. The zeolite ability is also supported by other studies that confirm that zeolite's structure can perform adsorption of the compounds H_2O, CO_2, SO_2 and H_2S [135], with an adsorption ability of up to 25% [136]. Further, zeolite can control gases that are the leading cause of greenhouse effects (e.g., CO_2 and N_2O), with the exception that CH_4 that is not absorbed [137]. The milestones of the use of Indonesian (Gunungkidul) natural zeolite in biogas purification are presented in Figure 2.4.

Specifically in relation to gas, previous studies have found that natural zeolite has an excellent ability to capture water vapour from the air or can by used for dehydration purposes [38, 39, 93, 110] such as adsorbing the water vapour in the biogas. Moreover,

zeolite has high selectivity to CO_2, allowing it to be utilised for methane purification of natural gas or biogas [60]. The CO_2 adsorption selectivity is also supported by the transformation of the properties of Indonesian (Gunungkidul) natural zeolite after dealumination and calcination, particularly the Si/Al ratio is more appropriate than in previous processes [115]. Thus, activated and modified Indonesian natural zeolite is appropriate for use as a biogas adsorbent.

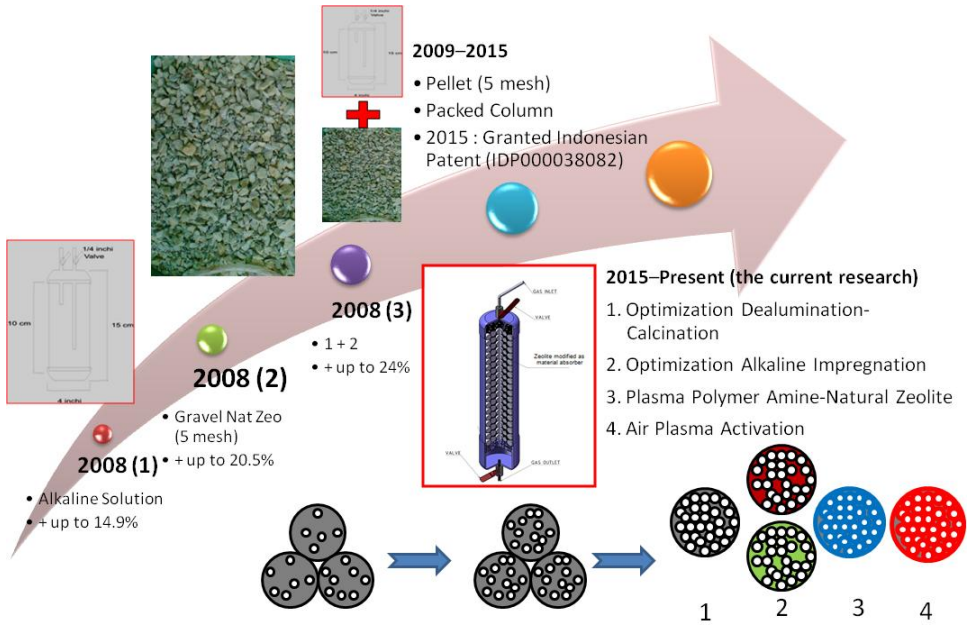

Figure 2.4. Milestones of Indonesian (Gunungkidul) natural-zeolite use for biogas purification in Indonesia

2.7. Chemical Treatment of Natural Zeolite

Natural zeolite is one of the materials used for gas multiadsorption. The selectivity of zeolite adsorption depends on several factors based on the material's characteristics; one of these factors is the Si/Al ratio. The ratio determines the tendency to water on zeolite with hydrophobic zeolite as the best option for gas adsorption. A higher Si/Al ratio indicates a lower alumina content inside the structure of zeolite, which increases the hydrophobic nature of zeolite. Hydrophobic zeolite is zeolite with an Si/Al ratio more than 5 [138-141], and is appropriate for gas adsorption, while zeolite with a Si/Al ratio under 5 (or

hydrophilic zeolite) is more appropriate for water-vapour adsorption [139] and H_2S adsorption [142]. There are two types of chemical treatments that are usually used for controlling the Si/Al ratio of zeolite: acid-solution treatment and alkaline-solution treatment. The acid-solution treatment, which is referred to as dealumination, is applied more frequently than to alkaline-solution treatment to zeolites. The acid-solution treatment (dealumination) is conducted to reduce the Al compound in zeolite, thus increasing the Si/Al ratio. When the alkaline-solution treatment is conducted, it reduces the Si compound in zeolite, thus producing the opposite effect.

Dealumination is the release process of Al from inside the Al framework to outside the Al framework [143, 144]. Several studies on zeolite dealumination have been conducted to improve the quality of natural zeolite by increasing the surface area and pore volume, reducing the mean pore size, increasing the Si/Al ratio, controlling selectivity and acidity, optimising Al composition for high-temperature stability, and enhancing adsorption capacity [115, 143-150]. This process is commonly conducted by reacting zeolite with a strong acid solution such as HCl, HNO_3, H_2SO_4, and HF (low concentration). The H^+ ions resulting from ionisation of acid will break the bond of Al in the zeolite framework and are attacked by oxygen atoms bonded to Si and Al. H^+ ions are more likely to break the Al-O bond than the Si-O bond because the dissociation energy of the Al-O bond (116 kcal/mol) is lower than that of the Si-O bond (190 kcal/mol) [135, 151]. Dealumination also removes other cations such as the alkali element (Ca, Na, K, and Mg) and metal cations because of anion–acid attraction. Further, dealumination can be conducted by flowing high-temperature water vapour into the zeolite, which is referred to as a hydrothermal process [144, 152-154].

Several researchers have also conducted alkaline-solution treatment in zeolite activation [155-164]. These studies have used NaOH and KOH to clean the surface pore, remove the impure compounds and increase adsorption capacity because increasing basicity attracts CO_2 [165]. Alkali impregnation also provides the possibility of cation exchange. The alkaline metal-cations group 1A has the highest priority ion exchange order of zeolite, and is higher than alkaline earth and other metal cations that are arranged as $Cs^+ > Rb^+ > K^+ > Na^+ > Ca^{2+} > Al^{3+} > Mg^{2+}$ [155, 165-167]. The higher priority indicates that it is relatively convenient to exchange other elements in the structure. However, the ion exchange is also

affected by the cation size, where in a small size, it is easy to penetrate the channel and interact with other elements in the structure [155, 165].

Further, an alkaline solution dissolves SiO_2 better than water because silica reacts with alkali [155, 158]. This process is appropriate for reducing the Si/Al ratio because it removes SiO_2 from the framework (referred to as desilication) [168-171], particularly in high-temperature alkaline-solution treatments [155]. Another method for desilication is treatment using high concentration HF or combination HF with another compound [171-174].

2.8. Calcination of Natural Zeolite

The adsorption capacity of natural zeolite can be improved by physical treatment using high-temperature heating (referred to as calcination). Calcination aims to evaporate water that is trapped in pores crystal (dehydration) and to remove all impure trapped gases. Calcination is conducted at high temperatures of more than 100°C because the minimal purpose is material dehydration. This action increases the surface area and porosity, enhances crystallinity, decomposes organic compounds and controls acidity characteristics [127, 175-179]. However, calcination does not commonly affect the type of mineral composition and the fixed structure of zeolite because the Si/Al ratio and measurement analysis results are relatively similar during the treatment [180, 181].

Commonly, calcination does not change the structure of most types of zeolite (e.g., chabazite, clinoptilolite, erionite and mordenite). However, several studies indicate that some types of zeolite (e.g., scolecite and natrolite) run into transformation during calcination [182-185]. At more than 500°C, the zeolite changes into siliceous phases, such as quartz or cristobalite, or a compact aluminosilicate phase such as labradorite [91, 182, 186-188], and even changes to amorphous crystal at temperatures over 1000°C [189]. The high temperature of calcination can change the function of the surface and destruct the pore, which produces lower adsorption capacity [177, 179].

The calcination process is also applied to the regeneration procedure of zeolite or other materials. Some researchers have conducted calcination for regeneration, particularly on

adsorbent materials of organic compounds, such as adsorbed gases, organic dyes, and organic guest molecules [177, 180, 190, 191]. Calcination is conducted because it decomposes organic compounds or breaks the chemical bond, which releases gases but does not destruct the structure of zeolites. Nevertheless, regeneration does not restore zeolite performance into its original state because zeolite activation is not performed through the calcination process only.

2.9. CO_2 Absorption and Adsorption by Amine

Amines are derivatives of ammonia in which alkyl or aryl groups change the hydrogen atoms. Based on the number of hydrogen atoms changing, amines are divided into three groups: primary, secondary and tertiary. Amine compounds, which are commonly utilised for CO_2 absorption, are MEA, diethanolamine (DEA), methyldiethanolamine (MDEA), diglycolamine (DGA), 2-Amino-2-methyl propanol (AMP), diisopropanolamine (DIPA), and piperazine (PIPA) [34].

The utilisation of amine solution for CO_2 absorption is the most practical in industry, for example, for natural gas treatment, filtering flue gas of food industry, landfill upgrading, and filtering flue gas of power plants [30, 192]. Amine solution can absorb the highest CO_2 content of the gases (85–90%), other impure gases (NO_x and SO_2), and particles (ashes). The amine-absorption process has a low operational cost, low energy requirement, low liquid waste and low amine release into the atmosphere. However, this method has several problems that need to be solved, namely high investment cost, difficult regeneration, high corrosive potential, and gaps in environmental and human-health risks [34]. Therefore, research focusing on alternatives to amine absorption requires continuing improvement. One possible improvement is to change amine solutions into amine solids so that amine will develop as a dry-absorption process.

Several studies on solid amines have increased the capacity of CO_2 capture. These have used solid materials as amine carriers of an amine functional group, such as carbon fly-ash–silica, polymethylmethacrylate–silica, polyethylenimine–silica, and magnesium tetraphenylporphyrin [193-197]. The solid-functionalised amine adsorbents have

demonstrated improvements in CO_2 adsorption selectivity [198]. The solid amine adsorbent performance is not affected by the appearance of water vapour [199]. This condition is caused by the establishment of carbamate from the reaction between primary or secondary amines and CO_2, which accelerate in the water presence [200, 201]. The reaction between the various types of amines and CO_2 is presented in Figure 2.5.

Solid amine materials have a high capacity to capture CO_2, mainly through their adsorption selectivity. However, CO_2 hardly penetrates the material because the pores are filled by amine-functional-group attachment; solid amine material is also difficult in the regeneration process [202]. Further, solid amine material is commonly produced by the conventional technique of wet chemical reaction that occurs in complex reactions, is highly substrate dependent and produces toxic waste [203, 204]. Therefore, there is a great deal of room for improvement in applying solid amine materials for CO_2 capture, particularly for increasing CO_2 adsorption capacity by controlling amine-functional-group induction and changing the induction technique to ensure a smooth and ecofriendly process.

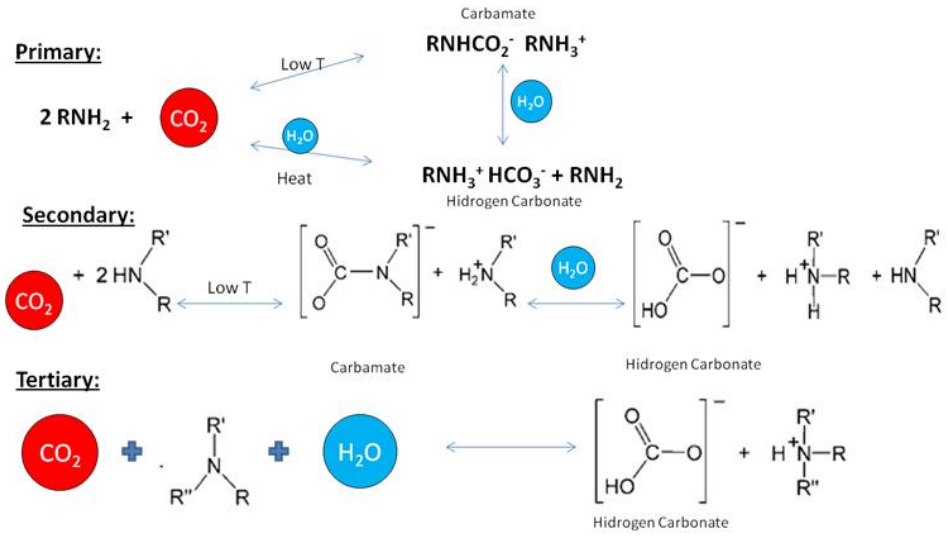

Figure 2.5. Reaction between various types of amine and CO_2

2.10. Plasma Polymerisation

Plasma polymerisation is a surface-modification technology that coats surfaces with ultrathin layers of monomers for various purposes. This process provides a polymer-like deposition and a highly crosslinked coating of organic precursor vapour [205-208]. Plasma polymer can create wettability properties simply by using appropriate monomers on the surface. The appropriate monomer candidates for creating hydrophobic surfaces are octadiene, hexamethyl-disiloxane and fluorocarbon groups [209-214]. In contrast, hydrophilic surfaces are produced using other monomers such as acrylic acid, allylamine and tetra(ethylene glycol) dimethyl ether (tetraglyme) [210, 215-217].

The monomers form an ultrathin layer on the surface, coating the material. Time depositions of plasma polymerisation can control monomer deposition. When the deposition occurs continuously, it will produce greater thickness of monomer coating on materials. After several monomer layers have formed on the surface, the next layer becomes substrate independent on the outer surface. The outer layer of monomer is able to react with other compounds around the material [218]. The monomer layer produces a reactive surface to attract the appropriate particles or compounds that correlate to the independent substrate.

Plasma polymerisation is a substrate-independent, single-step procedure in which no solvent is needed and allows reliable deposits on various surface configurations. The substrate-independent characteristic produces conformable deposition on the surface of various materials by a similar process of plasma polymerisation [218, 219]. The plasma transforms and activates the monomers in single-step procedure, so the monomers are polymerised or deposited on the material surface, which constitutes a shorter and more effective process than wet-chemical method. This method is conducted in the dry process to react between monomers and the material surface. The absence of solvent means less waste is produced and fewer chemicals are involved in the process. The ability of deposition on various surfaces has been proven by attaching to solid material, including micromaterials and nanomaterials [214, 220-222] or porous material particularly on mesoporous [205, 223-227]. The schematic of plasma polymerisation deposition on various types of material is presented in Figure 2.6.

Further, plasma charging using gas or air (without a monomer precursor) also provides surface engineering to increase reactivity [228-230]. The plasma charging affects the wettability of a surface, particularly to create a hydrophilic property, as found in studies that demonstrate that air-plasma activation on the planar surface of silicon, silicon oxide, and glass reduces water contact angle [231, 232]. The plasma activation offers some advantages over wet chemical processes that provide the possibility of mimicking the surface-engineering effect of the wet chemical process effectively.

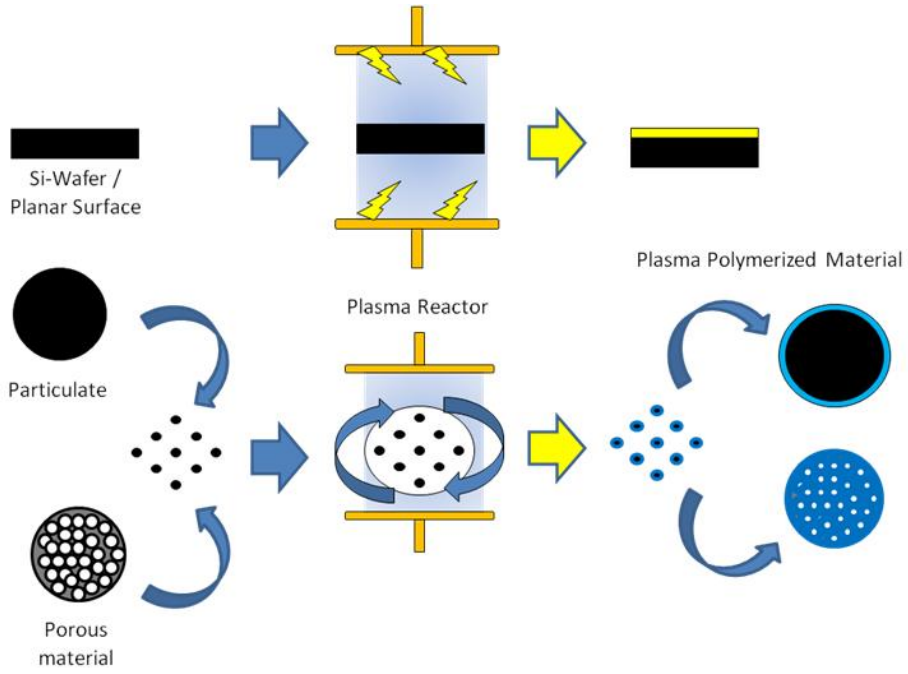

Figure 2.6. Schematic of plasma polymerisation deposition on planar surface, particulate surface and porous material

2.11. Plasma Polymer Amine Deposition on Porous Material

The independent substrates of plasma polymerisation can be utilised to improve CO_2 adsorption capacity. The prospective monomers that can react with CO_2 are amine monomers because amine-solution absorption is the most commonly applied technique for CO_2 absorption in industry. Amine monomers are deposited successfully by plasma polymer in various applications for surface modification. Previous studies are an

application of plasma polymer amine for thin material coating, thin films deposition, sensors, and membrane surface modification [205, 219, 233, 234].

There are many precursors able to produce amine monomers, for example, allylamine, propylamine, propargylamine, butylamine, heptylamine, diamino propane, ethylenediamine, and gas mixtures containing nitrogen [234-236]. However, allylamine was selected by several studies as the most applied precursor for creating plasma polymer amine given that it produces high-density amine, with a double and even triple bond of carbon–nitrogen [218, 237, 238]. Plasma polymer allylamine also has a more smooth surface deposition at a low thickness (2–3 nm) than heptylamine deposition (5–6 nm), and even produces similar chemical properties to saturated amine functional groups [205].

The induction of plasma polymer amine into a molecular sieve surface provides a new prospective solid amine material for CO_2 adsorption. This induction overcomes the drawbacks of the previous amine-induction technique that uses a wet-chemical technique. To support CO_2 adsorption application, it is necessary to control the plasma polymer deposition on particulate or powder, even on porous material. The porous material is appropriate with molecular sieve (adsorbent) material as the amine functional group carrier. Previous studies have applied plasma polymerisation successfully on particulate or powdered material surfaces using specific plasma reactor designs such as fluidised bed [239, 240], rotating chamber [241, 242] and agitation platform chamber [134, 243]

Particularly for porous material, the continuous deposition of the monomer is possible to clog the pores so that the pore function will disappear. However, the deposition duration of plasma polymerisation can limit the thickness of the monomer. The monomer deposition will not stop up the pores but reduce the diameter only, particularly for mesopore size [244]. Previous studies of plasma polymerisation treatment on the porous material have been able to control deposition on mesoporous [244, 245] and macroporous material [223-226, 246, 247]. These previous studies never applied plasma polymerisation deposition on a microporous material, thus providing prospective exploration of such a technique to find a more appropriate application of controlling plasma polymer amine deposition. Other than plasma polymerisation, air-plasma activation without monomer precursor also offers prospective improvement for application onto porous material particularly in high silica content [231, 232].

2.12. Conclusions

Biogas purification is a necessary technology for converting biogas into having a high purity of biomethane, so it can be applied to utilise as readily as natural gas. Further application of purified biogas is able to produce electricity by removing CO_2 as the primary impurity of biogas, as well as H_2O, H_2S and other contaminants. CO_2 adsorption is the primary concern in increasing biogas quality, and this has been achieved through various technologies. Indonesian natural zeolite is one of the prospective adsorbents for capturing CO_2, and has been discovered as a biogas purifier that has the advantages of abundant availability and low production cost. However, this natural zeolite still has a great deal of room for improvement through optimisation of or additions to previous processes. Chemical and physical or physicochemical treatments (e.g., improving surface area, Si/Al ratio, crystallinity and basicity) can be explored to improve the capacity of natural zeolite to adsorb CO_2.

Further, the possibility of other appropriate applications of natural zeolite can be discovered based on the unique characterisation of natural zeolite after the treatment given that the various applications of Indonesian natural zeolite have been explored in advance studies. Another procedure for increasing CO_2 adsorption capacity is induction of amine into micro–mesopores of Indonesian natural zeolite. This new technique of amine induction can be applied by plasma polymerisation because this is a more simple and ecofriendly method than previous methods. Allylamine can be selected as an amine-functional-group resource because it can create a high density of the amine functional group on the material surface. Particularly in its use for CO_2 adsorption technology, plasma polymer amine provides room for understanding and controlling the deposition of particulates and microporous material. In addition, air-plasma activation offers prospective surface engineering to utilise natural zeolite as a new adsorbent, particularly for water vapour since the hydrophilic effect after activation. These procedures can also be applied for creating other novel materials for various applications through surface-engineering modification using various monomer precursors or through using air-plasma activation without a monomer precursor.

References

1. Arumugam, S., et al., *Bio-fuels : Technology Status and Future Trends, Technology Assessment and Decision Support*. 2007: International Centre for Science and High Technology, United Nations Industrial Development Organization.

2. Salafudin, et al., *Biological Purification System: Integrated Biogas from Small Anaerobic Digestion and Natural Microalgae.* Procedia Chemistry, 2015. **14**(0): p. 387-393.

3. Pöschl, M., S. Ward, and P. Owende, *Evaluation of Energy Efficiency of Various Biogas Production and Utilization Pathways.* Applied Energy, 2010. **87**(11): p. 3305-3321.

4. Deublein, D. and A. Steinhauser, *Utilization of Gas to Generate Current and Heat*, in *Biogas from Waste and Renewable Resources*. 2010.

5. Burke, P.J., *One Goal, Two Paths: Achieving Universal Access to Modern Energy in East Asia and the Pacific–By World Bank.* Asian-Pacific Economic Literature, 2012. **26**(2): p. 167-168.

6. Raven, R.P.J.M. and K.H. Gregersen, *Biogas Plants in Denmark: Successes and Setbacks.* Renewable and Sustainable Energy Reviews, 2007. **11**(1): p. 116-132.

7. Kusdiana, D., *Existing and New Bio Energy Policies Needed and Implementation Target*. 2013, Indonesia EBTKE Conference and Exhibition 2013, Ministry of Energy and Mineral Resources of The Republic of Indonesia: Jakarta–Indonesia.

8. Holm-Nielsen, J.B., T. Al Seadi, and P. Oleskowicz-Popiel, *The Future of Anaerobic Digestion and Biogas Utilization.* Bioresource Technology, 2009. **100**(22): p. 5478-5484.

9. Weiland, P., *Biogas Production: Current State and Perspectives.* Applied Microbiology and Biotechnology, 2010. **85**(4): p. 849-860.

10. Zhang, C., et al., *Reviewing The Anaerobic Digestion of Food Waste for Biogas Production.* Renewable and Sustainable Energy Reviews, 2014. **38**: p. 383-392.

11. Hughes, W.L., et al., *Supplement, Energy for Rural Development: Renewable Resources and Alternative Technologies for Developing Countries*. 1981: National Academy Press.

12. Thahir, R. and Mustafa, *Pemanfatan Limbah Sayur untuk Dijadikan Biogas sebagai Energi Alternatif yang Dapat Diperbaharui [The Vegetable Waste was Converted into Biogas as Renewable Alternative Energy]*, in *National Seminar on Chemical Engineering Fundamentals and Applications*. 2007, Chemical Engineering Departement of Institute of Technology Sepuluh November Surabaya: Surabaya–Indonesia. p. E2 1-6.

13. Rasi, S., A. Veijanen, and J. Rintala, *Trace Compounds of Biogas from Different Biogas Production Plants.* Energy, 2007. **32**(8): p. 1375-1380.

14. Arifin, R., F.F.P. Perdana, and S.R. Juliastuti, *Pengaruh Enzim α-Amilase dan EM-4 terhadap Pembentukan Biogas dari Limbah Padat Tapioka [Effect of α-Amylase Enzyme and EM-4 for Biogas Production from Solid Waste of Starchy]*, in *National Seminar on Chemical Engineering and Processes*. 2008, Chemical Engineering Department, Diponegoro University: Semarang–Indonesia. p. D107 1-8.

15. Hambali, E., et al., *Teknologi Bioenergi [Technology of Bioenergy]*. 2007: Agro Media Pustaka.

16. Monnet, F., *An Introduction to Anaerobic Digestion of Organic Wastes*. 2003, Remade Scotland.

17. Muryanto, J.S., K. Ekaningtyas, and Sudadiyono, *Biogas, Energi Alternatif Ramah Lingkungan [Biogas, Green Alternative Energy]*. 2006, Semarang–Indonesia: Institute for Agricultural Technology (BPTP), Central Java.

18. Lastella, G., et al., *Anaerobic Digestion of Semi-Solid Organic Waste: Biogas Production and Its Purification.* Energy Conversion and Management, 2002. **43**(1): p. 63-75.

19. Hendroko, S.R., et al., *The Study of Optimization Hydrolysis Substrate Retention Time and Augmentation as an Effort to Increasing Biogas Productivity from Jatropha Curcas Linn. Capsule Husk at Two Stage Digestion.* Energy Procedia, 2014. **47**(0): p. 255-262.

20. Wahono, S.K., *Kajian: Pemanfaatan Zeolit Lokal Gunungkidul–Yogyakarta untuk Optimasi Sistem Biogas [Review: Utilization of Gunungkidul Local Zeolite for Biogas System optimization]*, in *National Seminar on Chemical Engineering Fundamentals and Applications*. 2008, Chemical Engineering Departement of Institute of Technology Sepuluh November Surabaya: Surabaya–Indonesia. p. E14.

21. Kangmin, L. and M.-W. Ho, *Biogas China*. 2006, Institute of Science in Society

22. Wahono, S.K. and P.I. Pudjiono, *Bioenergi dan Industri Manufaktur [Bioenergy and Manufacturing Industry]*, in *National Seminar on Technology–State Polytechnic of Semarang*. 2007: Semarang–Indonesia.

23. Wahono, S.K., *Kajian: Alternatif Optimasi dan Penyimpanan Energi Secara Aman pada Sistem Instalasi Biogas [Review: Optimization for The Safe Energy Storage of Biogas Installation System]*, in *Proceeding Call For Paper–Kontribusi Insinyur Muda untuk Indonesia, Temu Insinyur Jogja*. 2007: Yogyakarta–Indonesia.

24. Wahono, S.K., R. Maryana, and M. Kismurtono, *Biogas Purification Process to Increase Gen—Set Efficiency.* AIP Conference Proceedings, 2009. **1169**(1): p. 185-189.

25. Wahono, S.K. and W.A. Rizal, *Biogas Filter Based on Local Natural Zeolite Materials.* International Journal of Renewable Energy Development, 2014. **3**(1): p. 1-5.

26. Ryckebosch, E., M. Drouillon, and H. Vervaeren, *Techniques for Transformation of Biogas to Biomethane.* Biomass and Bioenergy, 2011. **35**(5): p. 1633-1645.

27. Wahono, S.K., H. Julendra, and A. Febrisiantosa, *Peningkatan Performa Biogas Melalui Teknologi Pemurnian Metana di UPT Kapitan Meo, Kabupaten Belu–Nusa Tenggara Timur [Performance Enhancement of Biogas Using Purification Technology of Methane at UPT Kapitan Meo, District Belu–East Nusa Tenggara]*, in *National Seminar on Technology Development Based on Local Materials*. 2009: Yogyakarta–Indonesia. p. 505-508.

28. Sarkar, S.C. and A. Bose, *Role of Activated Carbon Pellets in Carbon Dioxide Removal.* Energy Conversion and Management, 1997. **38, Supplement**(0): p. S105-S110.

29. Abatzoglou, N. and S. Boivin, *A Review of Biogas Purification Processes.* Biofuels, Bioproducts and Biorefining, 2009. **3**(1): p. 42-71.

30. Álvarez-Gutiérrez, N., et al., *Towards Bio-Upgrading of Biogas: Biomass Waste-Based Adsorbents.* Energy Procedia, 2014. **63**: p. 6527-6533.

31. Andriani, D., et al., *A Review on Optimization Production and Upgrading Biogas Through CO_2 Removal Using Various Techniques.* Applied Biochemistry and Biotechnology, 2014. **172**(4): p. 1909-1928.

32. Kohl, A.L. and R. Nielsen, *Gas Purification*. 1997: Elsevier Science.

33. Hargono, *Pembuatan Biogas serta Pemurniannya Melalui Absorbsi Gas Karbondioksida (CO_2) dengan Menggunakan Larutan NaOH (Suatu Upaya Sosialisasi Pembuatan dan Penggunaan Biogas Kepada Kelompok Peternak Sapi) [Biogas Production and Its Purification by CO_2 Absorbtion using NaOH Solution (Sosialitation of Biogas Manufacture and Utilization for Cattle Farmers Group)]*, in *National Seminar on Chemical Engineering and Processes*. 2008, Chemical Engineering Department, Diponegoro University: Semarang–Indonesia. p. D119 1-6.

34. Shao, R. and A. Stangeland, *Amines Used in CO_2 Capture*, in *Bellona Report*. 2009, The Bellona Foundation.

35. Budiyono, I.N. Widiasa, and Sunarso, *Perkembangan Teknologi Pemisahan untuk Pemurnian Biogas [Separation Technology Development for Biogas Purification]*, in *National Seminar on Chemical Engineering and Processes*. 2008, Chemical Engineering Department, Diponegoro University: Semarang–Indonesia. p. E129 1-10.

36. Ng, K.C., et al., *Experimental Investigation of The Silica Gel–Water Adsorption Isotherm Characteristics.* Applied Thermal Engineering, 2001. **21**(16): p. 1631-1642.

37. Wang, D., et al., *Progress in Silica Gel–Water Adsorption Refrigeration Technology.* Renewable and Sustainable Energy Reviews, 2014. **30**: p. 85-104.

38. Wahono, S.K., et al., *Characterization and Utilization of Gunungkidul Natural Zeolite for Bioethanol Dehydration.* Energy Procedia, 2014. **47**: p. 263-267.

39. Hernawan, et al., *Modification of Gunungkidul Natural Zeolite as Bioethanol Dehydrating Agents.* Energy Procedia, 2015. **65**: p. 116-120.

40. Canivet, J., et al., *Water Adsorption in MOFs: Fundamentals and Applications.* Chemical Society Reviews, 2014. **43**(16): p. 5594-5617.

41. Kim, H., et al., *Water Harvesting from Air with Metal-Organic Frameworks Powered by Natural Sunlight.* Science, 2017. **356**(6336): p. 430-434.

42. Zicari, S.M., *Removal of Hydrogen Sulfide from Biogas Using Cow-manure Compost*, in *Faculty of the Graduate School*. 2003, Cornell University: New York, USA.

43. Minier-Matar, J., et al., *Application of Membrane Contactors to Remove Hydrogen Sulfide from Sour Water.* Journal of Membrane Science, 2017. **541**: p. 378-385.

44. Tilahun, E., E. Sahinkaya, and B. Çalli, *A Hybrid Membrane Gas Absorption and Bio-Oxidation Process for The Removal of Hydrogen Sulfide from Biogas.* International Biodeterioration & Biodegradation, 2018. **127**: p. 69-76.

45. Yamamoto, T., M. Tayakout-Fayolle, and C. Geantet, *Gas-Phase Removal of Hydrogen Sulfide Using Iron Oxyhydroxide at Low Temperature: Measurement of Breakthrough Curve and Modeling of Sulfidation Mechanism.* Chemical Engineering Journal, 2015. **262**: p. 702-709.

46. Rattanapan, C., P. Boonsawang, and D. Kantachote, *Removal of H_2S in Down-Flow Gac Biofiltration Using Sulfide Oxidizing Bacteria from Concentrated Latex Wastewater.* Bioresource Technology, 2009. **100**(1): p. 125-130.

47. Mahmood, Q., et al., *Sources of Sulfide in Waste Streams and Current Biotechnologies for Its Removal.* Journal of Zhejiang University-SCIENCE A, 2007. **8**(7): p. 1126-1140.

48. Kwartiningsih, E. and A. Jumari, *Pemurnian Biogas dari Kandungan H_2S dengan Menggunakan Larutan Absorben Fe-EDTA [Biogas Purification for H_2S Content Reduction by Fe-EDTA as Absorbent Solution]*, in *National Seminar on Chemical Engineering and Processes*. 2007, Chemical Engineering Department, Diponegoro University: Semarang–Indonesia. p. E14 1-4.

49. Ackley, M.W., S.U. Rege, and H. Saxena, *Application of Natural Zeolites in The Purification and Separation of Gases.* Microporous and Mesoporous Materials, 2003. **61**(1–3): p. 25-42.

50. Wickramaratne, N.P. and M. Jaroniec, *Activated Carbon Spheres for CO_2 Adsorption.* ACS Applied Materials & Interfaces, 2013. **5**(5): p. 1849-1855.

51. Singh, G., et al., *Highly Efficient Method for The Synthesis of Activated Mesoporous Biocarbons with Extremely High Surface Area for High-Pressure CO_2 Adsorption.* ACS Applied Materials & Interfaces, 2017. **9**(35): p. 29782-29793.

52. Caglayan, B.S. and A.E. Aksoylu, *CO_2 Adsorption on Chemically Modified Activated Carbon.* Journal of Hazardous Materials, 2013. **252**(Supplement C): p. 19-28.

53. Hao, W., et al., *High-Performance Magnetic Activated Carbon from Solid Waste from Lignin Conversion Processes. 1. Their Use As Adsorbents for CO_2.* ACS Sustainable Chemistry & Engineering, 2017. **5**(4): p. 3087-3095.

54. Wang, X., Q. Guo, and T. Kong, *Tetraethylenepentamine-Modified MCM-41/Silica Gel with Hierarchical Mesoporous Structure for CO_2 Capture.* Chemical Engineering Journal, 2015. **273**(Supplement C): p. 472-480.

55. Lee, C.H., et al., *Effect of Surfactant on CO_2 Adsorption of APS-Grafted Silica Gel by One-Pot Process.* Bulletin of the Chemical Society of Japan, 2016. **89**(7): p. 823-832.

56. Tahari, A., et al., *XRD and CO_2 Adsorption Studies of Modified Silica Gel with Octadecylamine*, in *Materials Science Forum*. 2017, Trans Tech Publ. p. 529-533.

57. Siriwardane, R.V., et al., *Adsorption of CO_2 on Zeolites at Moderate Temperatures.* Energy & Fuels, 2005. **19**(3): p. 1153-1159.

58. Hudson, M.R., et al., *Unconventional, Highly Selective CO_2 Adsorption in Zeolite SSZ-13.* Journal of the American Chemical Society, 2012. **134**(4): p. 1970-1973.

59. Xia, Y., et al., *Superior CO_2 Adsorption Capacity on N-doped, High-Surface-Area, Microporous Carbons Templated from Zeolite.* Advanced Energy Materials, 2011. **1**(4): p. 678-683.

60. Cavenati, S., C.A. Grande, and A.E. Rodrigues, *Adsorption Equilibrium of Methane, Carbon Dioxide, and Nitrogen on Zeolite 13X at High Pressures.* Journal of Chemical & Engineering Data, 2004. **49**(4): p. 1095-1101.

61. Stevens, R.W., R.V. Siriwardane, and J. Logan, *In Situ Fourier Transform Infrared (FTIR) Investigation of CO_2 Adsorption onto Zeolite Materials.* Energy & Fuels, 2008. **22**(5): p. 3070-3079.

62. Yazaydın, A.Ö., et al., *Enhanced CO_2 Adsorption in Metal-Organic Frameworks via Occupation of Open-Metal Sites by Coordinated Water Molecules.* Chemistry of Materials, 2009. **21**(8): p. 1425-1430.

63. Li, J.-R., et al., *Carbon Dioxide Capture-Related Gas Adsorption and Separation in Metal-Organic Frameworks.* Coordination Chemistry Reviews, 2011. **255**(15): p. 1791-1823.

64. Millward, A.R. and O.M. Yaghi, *Metal−Organic Frameworks with Exceptionally High Capacity for Storage of Carbon Dioxide at Room Temperature.* Journal of the American Chemical Society, 2005. **127**(51): p. 17998-17999.

65. Liu, F., et al., *CO_2 Adsorption Behavior and Kinetics on Polyethylenimine Modified Porous Phenolic Resin.* Journal of Porous Materials, 2017. **24**(5): p. 1335-1342.

66. Chen, Z., et al., *Polyethylenimine-Impregnated Resin for High CO_2 Adsorption: An Efficient Adsorbent for CO_2 Capture from Simulated Flue Gas and Ambient Air.* ACS Applied Materials & Interfaces, 2013. **5**(15): p. 6937-6945.

67. Huertas, J., N. Giraldo, and S. Izquierdo, *Removal of H_2S and CO_2 from Biogas by Amine Absorption*. 2011: INTECH Open Access Publisher.

68. Bae, Y.-S., et al., *Separation of CO_2 from CH_4 Using Mixed-Ligand Metal-Organic Frameworks.* Langmuir, 2008. **24**(16): p. 8592-8598.

69. Belmabkhout, Y. and A. Sayari, *Adsorption of CO_2 from Dry Gases on MCM-41 Silica at Ambient Temperature and High Pressure. 2: Adsorption of CO_2/N_2, CO_2/CH_4 and CO_2/H_2 Binary Mixtures.* Chemical Engineering Science, 2009. **64**(17): p. 3729-3735.

70. Belmabkhout, Y., R. Serna-Guerrero, and A. Sayari, *Adsorption of CO_2 from Dry Gases on MCM-41 Silica at Ambient Temperature and High Pressure. 1: Pure Adsorption.* Chemical Engineering Science, 2009. **64**(17): p. 3721-3728.

71. Dantas, T.L.P., et al., *Modeling of The Fixed-Bed Adsorption of Carbon Dioxide and a Carbon Dioxide-Nitrogen Mixture on Zeolite 13X.* Brazilian Journal of Chemical Engineering, 2011. **28**(3): p. 533.

72. Singh, G., et al., *Single Step Synthesis of Activated Bio-Carbons with a High Surface Area and Their Excellent CO_2 Adsorption Capacity.* Carbon, 2017. **116**: p. 448-455.

73. Rios, R.B., et al., *Studies on The Adsorption Behavior of CO_2-CH_4 Mixtures Using Activated Carbon.* Brazilian Journal of Chemical Engineering, 2013. **30**(4): p. 939-951.

74. Bazan, R.E., et al., *Adsorption Equilibria of Natural Gas Components on Activated Carbon: Pure and Mixed Gas Isotherms.* Adsorption Science & Technology, 2008. **26**(5): p. 323-332.

75. Goetz, V., O. Pupier, and A. Guillot, *Carbon Dioxide-Methane Mixture Adsorption on Activated Carbon.* Adsorption, 2006. **12**(1): p. 55-63.

76. Van Der Vaart, R., et al., *Single and Mixed Gas Adsorption Equilibria of Carbon Dioxide/Methane on Activated Carbon.* Adsorption, 2000. **6**(4): p. 311-323.

77. Qiao, S., K. Wang, and X. Hu, *Using Local IAST with Micropore Size Distribution to Predict Multicomponent Adsorption Equilibrium of Gases in Activated Carbon.* Langmuir, 2000. **16**(3): p. 1292-1298.

78. Ahmadpour, A., K. Wang, and D.D. Do, *Comparison of Models on The Prediction of Binary Equilibrium Data of Activated Carbons.* AIChE Journal, 1998. **44**(3): p. 740-752.

79. Buss, E., *Gravimetric Measurement of Binary Gas Adsorption Equilibria of Methane-Carbon Dioxide Mixtures on Activated Carbon.* Gas Separation & Purification, 1995. **9**(3): p. 189-197.

80. Dreisbach, F., R. Staudt, and J.U. Keller, *High Pressure Adsorption Data of Methane, Nitrogen, Carbon Dioxide and Their Binary and Ternary Mixtures on Activated Carbon.* Adsorption, 1999. **5**(3): p. 215-227.

81. Delgado, J., et al., *Fixed-Bed Adsorption of Carbon Dioxide/Methane Mixtures on Silicalite Pellets.* Adsorption, 2006. **12**(1): p. 5-18.

82. Chege, J.M., et al., *Studies on Adsorption Biogas Purification Reactor for Domestic Sized Digesters in Kenya.* International Journal of Innovative Scientific & Engineering Technologies Research, 2014. **2**(2): p. 1-9.

83. Maia, D.C.S., et al., *Purification of Biogas for Energy Use.* Chemical Engineering Transactions, 2014. **37**: p. 643-648.

84. Magomnang, A.-A.S.M. and E.P. Villanueva, *Removal of Hydrogen Sulfide from Biogas Using Dry Desulfurization Systems*, in *International Conference on Agricultural, Environmental and Biological Sciences (AEBS-2014)*. 2014: Phuket (Thailand).

85. Horikawa, M.S., et al., *Chemical Absorption of H_2S for Biogas Purification.* Brazilian Journal of Chemical Engineering, 2004. **21**(3): p. 415.

86. Chowdhury, S., et al., *Adsorption Thermodynamics, Kinetics and Isosteric Heat of Adsorption of Malachite Green onto Chemically Modified Rice Husk.* Desalination, 2011. **265**(1): p. 159-168.

87. Doğan, M. and M. Alkan, *Removal of Methyl Violet from Aqueous Solution by Perlite.* Journal of Colloid and Interface Science, 2003. **267**(1): p. 32-41.

88. Pham, T.-H., B.-K. Lee, and J. Kim, *Novel Improvement of CO_2 Adsorption Capacity and Selectivity by Ethylenediamine-Modified Nano Zeolite.* Journal of the Taiwan Institute of Chemical Engineers, 2016. **66**: p. 239-248.

89. Jha, B. and D.N. Singh, *Basics of Zeolites*, in *Fly Ash Zeolites: Innovations, Applications, and Directions*. 2016, Springer Singapore: Singapore. p. 5-31.

90. Rouquerol, J., et al., *Recommendations for The Characterization of Porous Solids (Technical Report)*, in *Pure and Applied Chemistry*. 1994. p. 1739.

91. Breck, D.W., *Zeolite Molecular Sieves: Structure, Chemistry, and Use*. 1984: R.E. Krieger.

92. Inglezakis, V. and A. Zorpas, *Natural Zeolites Structure and Porosity*, in *Handbook of natural zeolites. Inglezakis, VJ and A. Zorpas (Eds.). Bentham Science Publisher. Sharjah UAE*, V.J. Inglezakis and A.A. Zorpas, Editors. 2012. p. 133-146.

93. Anggoro, D.D., et al., *Pemanfaatan Zeolit Alam dalam Proses Pengeringan Daun Tembakau [Natural Zeolites Utilization for Drying of Tobacco Leaf]*, in *National Seminar on Chemical Engineering Fundamentals and Applications*. 2005, Chemical Engineering Departement of Institute of Technology Sepuluh November Surabaya: Surabaya–Indonesia. p. DP8 1-5.

94. Fernández, N., et al., *Real Evidence About Zeolite as Microorganisms Immobilizer in Anaerobic Fluidized Bed Reactors.* Process Biochemistry, 2007. **42**(4): p. 721-728.

95. Hansson, A., *Mechanism of Zeolite Activity in Biogas Co-Digestion*, in *Department of Physics, Chemistry and Biology*. 2011, Linköping University: Linköping, Sweden.

96. Hedström, A., *Ion Exchange of Ammonium in Zeolites: A Literature Review.* Journal of Environmental Engineering, 2001. **127**(8): p. 673-681.

97. Li, Z., et al., *Long-Term Chemical and Biological Stability of Surfactant-Modified Zeolite.* Environmental Science & Technology, 1998. **32**(17): p. 2628-2632.

98. Mumpton, F.A., *La roca magica: Uses of Natural Zeolites in Agriculture and Industry.* Proceedings of the National Academy of Sciences of the United States of America, 1999. **96**(7): p. 3463-3470.

99. Venuto, P.B., *Organic Catalysis Over Zeolites: A Perspective on Reaction Paths within Micropores.* Microporous Materials, 1994. **2**(5): p. 297-411.

100. Baerlocher, C. and L. McCusker, *Database of Zeolite Structures: http://www. iza-structure. org/databases*, 2017.

101. Colella, C., *Natural Zeolites.* Stud Surf Sci Catal, 2005. **157**: p. 13-40.

102. Wang, S. and Y. Peng, *Natural Zeolites as Effective Adsorbents in Water and Wastewater Treatment.* Chemical Engineering Journal, 2010. **156**(1): p. 11-24.

103. Ozaydin, S., G. Kocer, and A. Hepbasli, *Natural Zeolites in Energy Applications.* Energy Sources, Part A: Recovery, Utilization, and Environmental Effects, 2006. **28**(15): p. 1425-1431.

104. Marantos, I., G.E. Christidis, and M. Ulmanu, *Zeolite Formation and Deposits*, in *Handbook of Natural Zeolites*, V.J. Inglezakis and A.A. Zorpas, Editors. 2012, Bentham Science Publishers. p. 28-51.

105. Misaelides, P., *Application of Natural Zeolites in Environmental Remediation: A Short Review.* Microporous and Mesoporous Materials, 2011. **144**(1–3): p. 15-18.

106. Arami-Niya, A., et al., *Gravimetric Adsorption Measurements of Helium on Natural Clinoptilolite and Synthetic Molecular Sieves at Pressures up to 3500 kPa.* Microporous and Mesoporous Materials, 2017. **244**(Supplement C): p. 218-225.

107. Farjoo, A., S.M. Kuznicki, and M. Sadrzadeh, *Hydrogen Separation by Natural Zeolite Composite Membranes: Single and Multicomponent Gas Transport.* Materials, 2017. **10**(10): p. 1159.

108. Karousos, D.S., et al., *A Study on Natural Clinoptilolite for CO_2/N_2 Gas Separation.* Separation Science and Technology, 2016. **51**(1): p. 83-95.

109. Yaşyerli, S., et al., *Removal of Hydrogen Sulfide by Clinoptilolite in a Fixed Bed Adsorber.* Chemical Engineering and Processing: Process Intensification, 2002. **41**(9): p. 785-792.

110. Favvas, E.P., et al., *Clinoptilolite, a Natural Zeolite Material: Structural Characterization and Performance Evaluation on Its Dehydration Properties of Hydrocarbon-Based Fuels.* Microporous and Mesoporous Materials, 2016. **225**(Supplement C): p. 385-391.

111. Alonso-Vicario, A., et al., *Purification and Upgrading of Biogas by Pressure Swing Adsorption on Synthetic and Natural Zeolites.* Microporous and Mesoporous Materials, 2010. **134**(1–3): p. 100-107.

112. Paolini, V., et al., *Biogas Cleaning and Upgrading with Natural Zeolites from Tuffs.* Environmental Technology, 2016. **37**(11): p. 1418-1427.

113. Sadchikov, A., et al., *Use of Natural Zeolite in Systems for Separation and Purification of Gas Mixtures Containing Methane*, in *Key Engineering Materials*. 2017, Trans Tech Publ. p. 179-182.

114. Flanagan, D.M., *2015 Minerals Yearbook: Zeolites (Advance Release)*, U.S.G.S. U.S. Department of the Interior, Editor. 2016.

115. Widayat, et al., *Pengaruh Konsentrasi HCl dan Jenis Reaktan dalam Pembuatan Katalis Zeolit untuk Proses Dehidrasi dari Zeolit Alam [Effect of HCl Concentration and Reactant Type in The Zeolite Catalysts Production for Dehydration Process of Natural Zeolite]*, in *National Seminar on Chemical Engineering and Processes*. 2008, Chemical Engineering Department, Diponegoro University: Semarang–Indonesia. p. H091 1-9.

116. Kusdarto, K., *Potency of Zeolite in Indonesia.* Jurnal Zeolit Indonesia, 2008. **7**(2): p. 78-87.

117. Kogel, J.E., *Industrial Minerals and Rocks: Commodities, Markets, and Uses*. 2006: SME.

118. Lestari, D.Y., *Kajian Modifikasi dan Karakterisasi Zeolit Alam dari Berbagai Negara [Review of Natural Zeolites Modification and Characterization from Various Countries]*, in *National Seminar of Chemistry and Education of Chemistry*. 2010, Education of Chemistry Department, Yogyakarta State University: Yogyakarta–Indonesia.

119. Wang, S., *Utilisation of Natural Zeolites for Air Separation and Pollution Control*, in *Handbook of Natural Zeolites*, V.J. Inglezakis and A.A. Zorpas, Editors. 2012, Bentham Science Publishers. p. 569-587.

120. Idrus, A., et al., *Geology, Characterization, Quality Improvement and Recommended Utilization of Natural Zeolite (Zeolitic Tuff) Deposits from Gunungkidul, Yogyakarta Special Teritory, Indonesia.*, in *"2nd IASME / WSEAS International Conference on Geology and Seismology (GES'08)*. 2008, ISSN 1790-2769; ISBN 978-960-6766-39-8: Cambridge, UK. p. 21-25.

121. Widayat, W., R. Achmad, and R. Muhammad, *Diethyl Ether Production Process with Various Catalyst Type.* International Journal of Science and Engineering, 2013. **4**(1): p. 6-10.

122. Kristiani, A., et al., *Metal Supported on Natural Zeolite as Catalysts for Conversion of Ethanol to Gasoline.* MATEC Web Conf., 2017. **101**: p. 01001.

123. Widayat, W., H. Susanto, and H. Satriadi, *Optimization Process of H-Zeolite Catalyst Preparation with Surface Response Methods*, in *Green Chemistry Proceeding Of 9th Joint Conference on Chemistry*. 2014, Department of Chemistry Diponegoro University. p. 124-129.

124. Widayat, A. Roesyadi, and M. Rachimoellah, *The Effect of Time Dealumination and Solvent Concentration in Synthesis of Zeolite Catalyst and Catalytic Test for DiEthyl Ether Production Process.* AIP Conference Proceedings, 2009. **1169**(1): p. 106-112.

125. Ainurofiq, A. and S. Choiri, *Drug Release Mechanism of Slightly Soluble Drug from Nanocomposite Matrix Formulated with Zeolite/Hydrotalcite as Drug Carrier.* Tropical Journal of Pharmaceutical Research, 2015. **14**(7): p. 1129-1135.

126. Rosita, W., A.W.Y.P. Ferdiansjah, and T.J. Prihatin, *Indonesia's Local Material Effect in Clay-Based Ceramic Filter Fabrication as an Alternative for Liquid Radioactive Waste Processing Material.* Materials Sciences and Applications, 2016. **7**(07): p. 371.

127. Subagiono, R. and D. Biyantoro, *Kinetika Reaksi Proses Adsorpsi Campuran Uranium dan Molibdenum dalam Zeolit [Reaction Kinetics of The Sorption Process*

of Uranium and Molibdenum Mixture in The Zeolite], in *Conference and Science Presentation of Basic Research and Technology of Nuclear*. 2006, National Atomic Energy Agency of Indonesia: Yogyakarta, Indonesia. p. 219-225.

128. Kok, T., *Characterization of Natural Zeolite from Gunungkidul, Yogyakarta, Indonesia and Its Modification, and Its Use to Reduce the Contamination of Zinc in Waste Water.* Journal of Materials Science and Engineering, 2010. **4**(1): p. 64-68.

129. Pich, B., et al., *Modified Natural Zeolite and Bentonite as Adsorbents of Heavy Metal Ions from Polluted Groundwater in Yogyakarta Urban Area, Indonesia.* 2015, 2015. **2**(1).

130. Retnaningrum, E. and W. Wilopo, *Removal of Sulphate and Manganese on Synthetic Wastewater in Sulphate Reducing Bioreactor Using Indonesian Natural Zeolite.* 2017, 2017. **17**(2).

131. Wilopo, W., et al., *Copper (Cu2+) Removal from Water Using Natural Zeolite from Gedangsari, Gunungkidul, Yogyakarta.* Journal of Applied Geology, 2010. **2**(2).

132. Laksmono, J., et al., *Development of Porous Structured Polyvinyl Alcohol/Zeolite/Carbon Composites as Adsorbent*, in *IOP Conference Series: Materials Science and Engineering*. 2017, IOP Publishing. p. 012006.

133. Kismurtono, M., et al., *Development of a New Phase Change Biogas for Renewable Energy Storage System.* 2015, 2015: p. 4.

134. Wahono, S.K., et al., *Preliminary study: Combination of Amine and Natural Zeolite as New Adsorbent Material for CO_2 Capture*, in *Chemeca 2016: Chemical Engineering-Regeneration, Recovery and Reinvention*. 2016. p. 900-910.

135. Weitkamp, J. and L. Puppe, *Catalysis and Zeolites Fundamentals and Applications*. Springer Archives. 1999, Berlin, Heidelberg: Springer Berlin Heidelberg : Imprint: Springer.

136. Sutarti, M. and M. Rachmawati, *Zeolit Tinjauan Literatur [Zeolite Literature Review]*. 1994, Scientific Information and Documentation Centre, Indonesian Institute of Sciences: Jakarta.

137. Delahay, G. and B. Coq, *Pollution Abatement Using Zeolites: State of The Art and Further Needs*, In *Zeolites for Cleaner Technologies*. 2002, Published by imperial college press and distributed by world scientific publishing co. p. 345-374.

138. Shirazi, L., E. Jamshidi, and M.R. Ghasemi, *The Effect of Si/Al Ratio of ZSM-5 Zeolite on Its Morphology, Acidity and Crystal Size.* Crystal Research and Technology, 2008. **43**(12): p. 1300-1306.

139. Ramesh, K. and D.D. Reddy, *Chapter Four - Zeolites and Their Potential Uses in Agriculture*, in *Advances in Agronomy*, D.L. Sparks, Editor. 2011, Academic Press. p. 219-241.

140. Sriatun, S. and A. Darmawan, *Dealuminasi Zeolit Alam Cipatujah Melalui Penambahan Asam dan Oksidator [Dealumination of Cipatujah Natural Zeolites by Acid and Oxidants Addition]*. Kimia Sains dan Aplikasi, 2005. **8**(2).

141. Mandasari, W., B. Sitorus, and D.R. Jati, *Pembuatan dan Karakterisasi Adsorben Gas H_2S dari Zeolit Alam [Preparation and Characterization of Natural Zeolite as H_2S Adsorbents]*. Jurnal Kimia Khatulistiwa, 2014. **3**(2): p. 56-63.

142. Cosoli, P., et al., *Hydrogen Sulphide Removal from Biogas by Zeolite Adsorption: Part I. GCMC Molecular Simulations.* Chemical Engineering Journal, 2008. **145**(1): p. 86-92.

143. Dziedzicka, A., B. Sulikowski, and M. Ruggiero-Mikołajczyk, *Catalytic and Physicochemical Properties of Modified Natural Clinoptilolite.* Catalysis Today, 2016. **259**: p. 50-58.

144. Wahyuni, S., *Preparasi dan Karakterisasi Katalis Ni-Zeolit Alam Terdealuminasi dengan Metode Perlakuan Asam [Preparation and Characterization of Dealumnated Ni-Natural Zeolite Catalyst by Acid Treatment Method]*, in *National Seminar Chemistry and Education of Chemistry*. 2006, Semarang State University: Semarang–Indonesia.

145. Boveri, M., et al., *Steam and Acid Dealumination of Mordenite: Characterization and Influence on The Catalytic Performance in Linear Alkylbenzene Synthesis.* Catalysis Today, 2006. **114**(2–3): p. 217-225.

146. Korkuna, O., et al., *Structural and Physicochemical Properties of Natural Zeolites: Clinoptilolite and Mordenite.* Microporous and Mesoporous Materials, 2006. **87**(3): p. 243-254.

147. Chal, R., et al., *Overview and Industrial Assessment of Synthesis Strategies Towards Zeolites with Mesopores.* ChemCatChem, 2011. **3**(1): p. 67-81.

148. Li, K., J. Valla, and J. Garcia-Martinez, *Realizing the Commercial Potential of Hierarchical Zeolites: New Opportunities in Catalytic Cracking.* ChemCatChem, 2014. **6**(1): p. 46-66.

149. Handoko, D.S.P., *Pengaruh Perlakuan Asam, Hidrotermal dan Impregnasi Logam Kromium Pada Zeolit Alam dalam Preparasi Katalis [The Effect of Acid, Hydrothermal and Support Chromium Treatments of Natural Zeolite in Catalyst Preparation]*. Jurnal Ilmu Dasar, 2002. **3**(2): p. 103-109.

150. Kesuma, R.F., B. Sitorus, and Adhitiyawarman, *Karakterisasi Pori Adsorben Berbahan Baku Kaolin Capkala dan Zeolit Dealuminasi [Pore Characterization of Adsorbent Made From Kaolin Capkala and zeolite dealumination]*. Jurnal Kimia Khatulistiwa, 2013. **2**(1).

151. Maleiva, L.T.N., B. Sitorus, and D.R. Jati, *Penurunan Konsentrasi Gas Karbon Monoksida dari Kendaraan Bermotor Menggunakan Adsorben Zeolit Alam*

[Decreased concentration of Carbon Monoxide Gas Vehicle Using Natural Zeolite Adsorbents]. Jurnal Kimia Khatulistiwa, 2015. **4**(1): p. 26-33.

152. Campbell, S.M., et al., *Dealumination of HZSM-5 Zeolites: I. Calcination and Hydrothermal Treatment.* Journal of Catalysis, 1996. **161**(1): p. 338-349.

153. Satrya, C.E.B., *Pengaruh Proses Dealuminasi Terhadap Keasaman Sampel Modernit [Dealumination Effect for Acidity of Modernite Sample]*, in *Mathematics and Sciences Faculty*. 2002, Gadjah Mada University: Yogyakarta - Indonesia.

154. Fleisch, T.H., et al., *Hydrothermal Dealumination of Faujasites.* Journal of Catalysis, 1986. **99**(1): p. 117-125.

155. Lin, H., et al., *Physicochemical Properties and Mechanism Study of Clinoptilolite Modified by NaOH.* Microporous and Mesoporous Materials, 2015. **218**: p. 174-179.

156. Masaru, O., et al., *Formation of Uniform Mesopores in ZSM-5 Zeolite Through Treatment in Alkaline Solution.* Chemistry Letters, 2000. **29**(8): p. 882-883.

157. Le Van Mao, R., et al., *Modification of The Micropore Characteristics of The Desilicated ZSM-5 Zeolite by Thermal Treatment.* Zeolites, 1997. **19**(4): p. 270-278.

158. Widyanuriawan, D. and Sugiarto, *Biogas Purification Using Natural Zeolite and NaOH.* Applied Mechanics and Materials, 2014. **664**: p. 415-418.

159. Dienullah, M., H.S. Tira, and Y.A. Padang, *Pemurnian Biogas dengan Sistem Berlapis Menggunakan Fe_2O_3, Zeolit Sintetik dan Zeolit Alam [Biogas Purification Using Multi-Layer System of Fe_2O_3, Synthetic Zeolite and Natural Zeolite]*. Jurnal Ilmiah Teknik Mesin, 2018. **15**(1): p. 1-8.

160. Hamidi, N., I.N. Gede Wardana, and D. Widhiyanuriyawan, *Peningkatan Kualitas Bahan Bakar Biogas Melalui Proses Pemurnian dengan Zeolit Alam [Quality Improvement of Biogas Fuel by Purification Using Natural Zeolites].* Rekayasa Mesin, 2012. **2**(3): p. 227-231.

161. Iruretagoyena, D., et al., *Influence of Alkali Metals (Na, K, and Cs) on CO_2 Adsorption by Layered Double Oxides Supported on Graphene Oxide.* Industrial & Engineering Chemistry Research, 2015. **54**(46): p. 11610-11618.

162. Kim, Y.K., G.M. Kim, and J.W. Lee, *Highly Porous N-Doped Carbons Impregnated with Sodium for Efficient CO_2 Capture.* Journal of Materials Chemistry A, 2015. **3**(20): p. 10919-10927.

163. Lee, K.-M., et al., *Adsorption of Low-Level CO_2 Using Modified Zeolites and Activated Carbon.* Industrial & Engineering Chemistry Research, 2012. **51**(3): p. 1355-1363.

164. Liu, X., et al., *Potassium and Zeolitic Structure Modified Ultra-Microporous Adsorbent Materials from a Renewable Feedstock with Favorable Surface Chemistry for CO_2 Capture.* ACS Applied Materials & Interfaces, 2017. **9**(32): p. 26826-26839.

165. Bonenfant, D., et al., *Advances in Principal Factors Influencing Carbon Dioxide Adsorption on Zeolites.* Science and Technology of Advanced Materials, 2008. **9**(1): p. 013007.

166. Arletti, R., et al., *Evidence for The Formation of Stable CO_2 Hydrates in Zeolite NaY: Structural Characterization by Synchrotron X-ray Powder Diffraction.* Microporous and Mesoporous Materials, 2016. **228**: p. 248-255.

167. Khulbe, K.C., et al., *Recent Development on The Effect of Water/Moisture on The Performance of Zeolite Membrane and MMMs Containing Zeolite for Gas Separation; Review.* RSC Advances, 2016. **6**(49): p. 42943-42961.

168. Chen, D.-s., et al., *Desilication from Titanium–Vanadium Slag by Alkaline Leaching.* Transactions of Nonferrous Metals Society of China, 2013. **23**(10): p. 3076-3082.

169. Groen, J.C., et al., *In Situ Monitoring of Desilication of MFI-Type Zeolites in Alkaline Medium.* Physical Chemistry Chemical Physics, 2007. **9**(34): p. 4822-4830.

170. Shen, B., et al., *Desilication by Alkaline Treatment and Increasing The Silica to Alumina Ratio of Zeolite Y.* Chinese Journal of Catalysis, 2012. **33**(1): p. 152-163.

171. Groen, J.C., J.A. Moulijn, and J. Perez-Ramirez, *Desilication: on The Controlled Generation of Mesoporosity in MFI Zeolites.* Journal of Materials Chemistry, 2006. **16**(22): p. 2121-2131.

172. Qin, Z., et al., *Chemical Equilibrium Controlled Etching of MFI-Type Zeolite and Its Influence on Zeolite Structure, Acidity, and Catalytic Activity.* Chemistry of Materials, 2013. **25**(14): p. 2759-2766.

173. Qin, Z., J.-P. Gilson, and V. Valtchev, *Mesoporous Zeolites by Fluoride Etching.* Current Opinion in Chemical Engineering, 2015. **8**: p. 1-6.

174. Spierings, G.A.C.M., *Wet Chemical Etching of Silicate Glasses in Hydrofluoric Acid Based Solutions.* Journal of Materials Science, 1993. **28**(23): p. 6261-6273.

175. Lu, J., et al., *Effects of Calcination Temperature on The Acidity and Catalytic Performances of HZSM-5 Zeolite Catalysts for The Catalytic Cracking of n-Butane.* Journal of Natural Gas Chemistry, 2005. **14**(4): p. 213–220.

176. Giudici, R., *Synthesis, Dealumination, and Adsorption Behavior of Mordenite Extrudates: diss. submitted for the degree of doctor of technical science*. 1999, Swiss Federal Institute of Technology Zurich: Zurich, Swiss.

177. Wang, S. and Z.H. Zhu, *Characterisation and Environmental Application of an Australian Natural Zeolite for Basic Dye Removal from Aqueous Solution.* Journal of Hazardous Materials, 2006. **136**(3): p. 946-952.

178. Widhiyanuriyawan, D. and N. Hamidi, *Variasi Temperatur Pemanasan Zeolite alam-NaOH Untuk Pemurnian Biogas [Heating Temperature Variation of Natural Zeolites-NaOH for Biogas Purification]*. Jurnal Energi Dan Manufaktur, 2013. **6**(1): p. 53-63.

179. Cobzaru, C., *Modified Zeolites: Modification of Natural Zeolites for Catalytic Applications*, in *Handbook of Natural Zeolites*, V.J. Inglezakis and A.A. Zorpas, Editors. 2012. p. 185-213.

180. Lemoine, G., *Comparison of Different Types of Zeolites Used as Solid Acid Catalysts in The Transesterification Reaction of Jatropha-Type Oil for Biodiesel Production*. 2013, Worcester Polytechnic Institute.

181. Windati, W., Y. Syah, and A.A. Widati, *Impregnasi Zeolit Alam dengan TiO_2 untuk Degradasi Jingga Metil secara Fotokatalitik [Natural Zeolites Impregnation by TiO_2 for Photocatalytic Degradation of Methyl Orange]*. Journal Universitas Airlangga, 2013. **1**(1).

182. Roque-Malherbe, R., *Applications of Natural Zeolites in Pollution Abatement and Industry*, in *Handbook of Surfaces and Interfaces of Materials*, H.S. Nalwa, Editor. 2001, Academic Press. p. 495-522.

183. Banon, C. and T.E. Suharto, *Adsorpsi Amoniak oleh Adsorben Zeolit Alam yang Diaktivasi dengan Larutan Amonium Nitrat [Ammonia Adsorption by Natural Zeolites Adsorbent which Activated by Ammonium Nitrate Solution]*. Jurnal Gradien, 2015. **4**(2).

184. Armbruster, T. and M.E. Gunter, *Stepwise Dehydration of Heulandite-Clinoptilolite from Succor Creelq Oregon, USA: A Single-Crystal X-Ray Study at 100 K.* American Mineralogist, 1991. **76**: p. 1872-1883.

185. Knowlton, G.D., T.R. White, and H.L. McKague, *Thermal Study of Types of Water Associated with Clinoptilolite.* Clays Clay Min, 1981. **29**: p. 403-411.

186. Roque-Malherbe, R., et al., *The State of Iron in Natural Zeolites: A Mössbauer Study.* Zeolites, 1990. **10**(7): p. 685-689.

187. Hernandez-Velez, M., et al., *New Materials Obtained from High Temperature Phase Transformations of Natural Zeolites.* Journal of Materials Science Letters, 1995. **14**(23): p. 1653-1656.

188. Arcoya, A., et al., *Role of The Countercations on The Molecular Sieve Properties of a Clinoptilolite.* Microporous Materials, 1996. **7**(1): p. 1-13.

189. Mimura, H. and T. Kanno, *Processing of Radioactive Waste Solution with Zeolites (I): Thermal-Transformations of Na, Cs and Sr Forms of Zeolites.* Science reports of the Research Institutes, Tohoku University. Ser. A, Physics, chemistry and metallurgy, 1980. **29**: p. 102-111.

190. Gualtieri, M., *Synthesis and Characterization of Zeolite Films and Membranes*, in *Department of Chemical Engineering and Geosciences, Division of Chemical Technology*. 2006, Luleå University of Technology: Luleå, Sweden.

191. Gualtieri, M.L., A.F. Gualtieri, and J. Hedlund, *The Influence of Heating Rate on Template Removal in Silicalite-1: An in Situ HT-XRPD Study.* Microporous and Mesoporous Materials, 2006. **89**(1–3): p. 1-8.

192. Rochelle, G.T., *Amine Scrubbing for CO_2 Capture.* Science, 2009. **325**(5948): p. 1652-1654.

193. Govar, A.A., *Development of a Pressure Swing Adsorption Process for CO_2 Capture from Flue Gas Using Solid Amine Sorbents*, in *Chemical Engineering, College of Engineering and Computing*. 2014, University of South Carolina: Columbia.

194. Gray, M.L., et al., *Capture of Carbon Dioxide by Solid Amine Sorbents.* International Journal of Environmental Technology and Management, 2004. **4**(1): p. 82-88.

195. Veneman, R., et al., *Continuous CO_2 Capture in a Circulating Fluidized Bed Using Supported Amine Sorbents.* Chemical Engineering Journal, 2012. **207–208**(0): p. 18-26.

196. Wang, D., et al., *Adsorption of Oils from Pure Liquid and Oil–Water Emulsion on Hydrophobic Silica Aerogels.* Separation and Purification Technology, 2012. **99**: p. 28-35.

197. Zhang, Z., et al., *Enhancing Sorption Performance of Solid Amine Sorbents for CO_2 Capture by Additives.* Energy Procedia, 2013. **37**(0): p. 205-210.

198. Chen, C., J. Kim, and W.-S. Ahn, *CO_2 Capture by Amine-Functionalized Nanoporous Materials: A Review.* Korean Journal of Chemical Engineering, 2014. **31**(11): p. 1919-1934.

199. Sayari, A. and Y. Belmabkhout, *Stabilization of Amine-Containing CO_2 Adsorbents: Dramatic Effect of Water Vapor.* Journal of the American Chemical Society, 2010. **132**(18): p. 6312-6314.

200. Ünveren, E.E., et al., *Solid Amine Sorbents for CO_2 Capture by Chemical Adsorption: A Review.* Petroleum, 2017. **3**(1): p. 37-50.

201. D'Alessandro, D.M., B. Smit, and J.R. Long, *Carbon Dioxide Capture: Prospects for New Materials.* Angewandte Chemie International Edition, 2010. **49**(35): p. 6058-6082.

202. Jiang, H., *Amine-Pillared Nanosheet Adsorbents for CO_2 Capture Applications*, in *Department of Chemical Engineering*. 2015, Northeastern University: Boston, Massachusetts.

203. Morent, R., et al., *Plasma Surface Modification of Biodegradable Polymers: A Review.* Plasma Processes and Polymers, 2011. **8**(3): p. 171-190.

204. Hernandez-Lopez, J.L., et al., *Functional Polymers as Nanoscopic Building Blocks.* Materials Science and Engineering: C, 2003. **23**(1): p. 267-274.

205. Vasilev, K., *Nanoengineered Plasma Polymer Films for Biomaterial Applications.* Plasma Chemistry and Plasma Processing, 2014. **34**(3): p. 545-558.

206. Yasuda, H. and Y. Matsuzawa, *Economical Advantages of Low-Pressure Plasma Polymerization Coating.* Plasma Processes and Polymers, 2005. **2**(6): p. 507-512.

207. Denes, F.S. and S. Manolache, *Macromolecular Plasma-Chemistry: An Emerging Field of Polymer Science.* Progress in Polymer Science, 2004. **29**(8): p. 815-885.

208. Biederman, H. and D. Slavínská, *Plasma Polymer Films and Their Future Prospects.* Surface and Coatings Technology, 2000. **125**(1): p. 371-376.

209. Michelmore, A., et al., *Role of Positive Ions in Determining The Deposition Rate and Film Chemistry of Continuous Wave Hexamethyl Disiloxane Plasmas.* Langmuir, 2011. **27**(19): p. 11943-11950.

210. Ramiasa-MacGregor, M., et al., *Tuning and predicting The Wetting of Nanoengineered Material Surface.* Nanoscale, 2016. **8**(8): p. 4635-4642.

211. Akhavan, B., K. Jarvis, and P. Majewski, *Evolution of Hydrophobicity in Plasma Polymerised 1,7-Octadiene Films.* Plasma Processes and Polymers, 2013. **10**(11): p. 1018-1029.

212. Vaswani, S., J. Koskinen, and D.W. Hess, *Surface Modification of Paper and Cellulose by Plasma-Assisted Deposition of Fluorocarbon Films.* Surface and Coatings Technology, 2005. **195**(2–3): p. 121-129.

213. Hegemann, D., H. Brunner, and C. Oehr, *Plasma Treatment of Polymers to Generate Stable, Hydrophobic Surfaces.* Plasmas and Polymers, 2001. **6**(4): p. 221-235.

214. Wahono, S.K., et al., *Plasma Polymer Facilitated Magnetic Technology for Removal of Oils from Contaminated Waters.* Environmental Pollution, 2018. **240**: p. 725-732.

215. Garcia-Torres, J., et al., *Surface Modification of Cellulosic Substrates via Atmospheric Pressure Plasma Polymerization of Acrylic Acid: Structure and Properties.* Applied Surface Science, 2014. **305**: p. 292-300.

216. Buxadera-Palomero, J., et al., *Antifouling Coatings for Dental Implants: Polyethylene Glycol-Like Coatings on Titanium by Plasma Polymerization.* Biointerphases, 2015. **10**(2): p. 029505.

217. Nisol, B., et al., *Atmospheric Plasma Synthesized PEG Coatings: Non-Fouling Biomaterials Showing Protein and Cell Repulsion.* Surface and Coatings Technology, 2014. **252**: p. 126-133.

218. Vasilev, K., et al., *Substrate Influence on The Initial Growth Phase of Plasma-Deposited Polymer Films.* Chemical Communications, 2009(24): p. 3600-3602.

219. Vasilev, K., et al., *Early Stages of Growth of Plasma Polymer Coatings Deposited from Nitrogen- and Oxygen-Containing Monomers.* Plasma Processes and Polymers, 2010. **7**(9-10): p. 824-835.

220. Manakhov, A., et al., *Deposition of Stable Amine Coating onto Polycaprolactone Nanofibers by Low Pressure Cyclopropylamine Plasma Polymerization.* Thin Solid Films, 2015. **581**: p. 7-13.

221. Duan, S., et al., *Plasma Surface Modification of Materials and Their Entrapment of Water Contaminant: A Review.* Plasma Processes and Polymers, 2017. **14**(9): p. 1600218.

222. Mierczynska-Vasilev, A., et al., *A Novel Technology for The Rapid, Selective, Magnetic Removal of Pathogenesis-Related Proteins from Wines.* Food Chemistry, 2017. **232**(Supplement C): p. 508-514.

223. Hamerli, P., et al., *Surface Properties of and Cell Adhesion onto Allylamine-Plasma-Coated Polyethylenterephtalat Membranes.* Biomaterials, 2003. **24**(22): p. 3989-3999.

224. Simovic, S., D. Losic, and K. Vasilev, *Controlled Drug Release from Porous Materials by Plasma Polymer Deposition.* Chemical Communications, 2010. **46**(8): p. 1317-1319.

225. Rebl, H., et al., *Accelerated Cell-Surface Interlocking on Plasma Polymer-Modified Porous Ceramics.* Materials Science and Engineering: C, 2016. **69**: p. 1116-1124.

226. Bergemann, C., et al., *Continuous Cellularization of Calcium Phosphate Hybrid Scaffolds Induced by Plasma Polymer Activation.* Materials Science and Engineering: C, 2016. **59**: p. 514-523.

227. Reis, R., et al., *Amine Enrichment of Thin-Film Composite Membranes via Low Pressure Plasma Polymerization for Antimicrobial Adhesion.* ACS Applied Materials & Interfaces, 2015. **7**(27): p. 14644-14653.

228. Pasquariello, D., C. Hedlund, and K. Hjort, *Oxidation and Induced Damage in Oxygen Plasma in Situ Wafer Bonding.* Journal of The Electrochemical Society, 2000. **147**(7): p. 2699-2703.

229. Kibria, M., et al., *Comprehensive Investigation of Sequential Plasma Activated Si/Si Bonded Interfaces for Nano-Integration on The Wafer Scale.* Nanotechnology, 2010. **21**(13): p. 134011.

230. Ma, X., et al., *Study of The Ge Wafer Surface Hydrophilicity after Low-Temperature Plasma Activation.* Journal of The Electrochemical Society, 2009. **156**(5): p. H307-H310.

231. Alam, A., M. Howlader, and M. Deen, *Oxygen Plasma and Humidity Dependent Surface Analysis of Silicon, Silicon Dioxide and Glass for Direct Wafer Bonding.* ECS Journal of Solid State Science and Technology, 2013. **2**(12): p. P515-P523.

232. Alam, A., M. Howlader, and M. Deen, *The Effects of Oxygen Plasma and Humidity on Surface Roughness, Water Contact Angle and Hardness of Silicon, Silicon Dioxide and Glass.* Journal of Micromechanics and Microengineering, 2014. **24**(3): p. 035010.

233. Choukourov, A., et al., *Properties of Amine-Containing Coatings Prepared by Plasma Polymerization.* Journal of Applied Polymer Science, 2004. **92**(2): p. 979-990.

234. Vasilev, K., et al., *Solvent-Induced Porosity in Ultrathin Amine Plasma Polymer Coatings.* The Journal of Physical Chemistry B, 2008. **112**(35): p. 10915-10921.

235. Daunton, C., et al., *Plasma Parameter Aspects in the Fabrication of Stable Amine Functionalized Plasma Polymer Films.* Plasma Processes and Polymers, 2015. **12**(8): p. 817-826.

236. Choukourov, A., et al., *Mechanistic Studies of Plasma Polymerization of Allylamine.* The Journal of Physical Chemistry B, 2005. **109**(48): p. 23086-23095.

237. Siow, K.S., et al., *Plasma Methods for The Generation of Chemically Reactive Surfaces for Biomolecule Immobilization and Cell Colonization - A Review.* Plasma Processes and Polymers, 2006. **3**(6-7): p. 392-418.

238. Liu, X., et al., *Surface Modification by Allylamine Plasma Polymerization Promotes Osteogenic Differentiation of Human Adipose-Derived Stem Cells.* ACS Applied Materials & Interfaces, 2014. **6**(12): p. 9733-9741.

239. Kim, J.W. and H.S. Choi, *Surface Crosslinking of High-Density Polyethylene Beads in a Modified Plasma Reactor.* Journal of Applied Polymer Science, 2002. **83**(13): p. 2921-2929.

240. Karches, M. and P.R. von Rohr, *Microwave Plasma Characteristics of a Circulating Fluidized Bed-Plasma Reactor for Coating of Powders.* Surface and Coatings Technology, 2001. **142–144**: p. 28-33.

241. Jarvis, K.L. and P. Majewski, *Plasma Polymerized Allylamine Coated Quartz Particles for Humic Acid Removal.* Journal of Colloid and Interface Science, 2012. **380**(1): p. 150-158.

242. De Vietro, N., R. d'Agostino, and F. Fracassi, *Introduction of Basic Functionalities on The Surface of Granular Adsorbers by Low Pressure Plasma Processes.* Plasma Processes and Polymers, 2012. **9**(9): p. 911-918.

243. Cavallaro, A. and K. Vasilev, *Controlled and Sustained Release of Pharmaceuticals via Single Step Solvent-Free Encapsulation.* Chemical Communications, 2015. **51**(10): p. 1838-1841.

244. Dusan, L., et al., *Surface Modification of Nanoporous Alumina Membranes by Plasma Polymerization.* Nanotechnology, 2008. **19**(24): p. 245704.

245. McInnes, S.J.P., et al., *Combination of iCVD and Porous Silicon for the Development of a Controlled Drug Delivery System.* ACS Applied Materials & Interfaces, 2012. **4**(7): p. 3566-3574.

246. Vasilev, K., et al., *Tailoring The Surface Functionalities of Titania Nanotube Arrays.* Biomaterials, 2010. **31**(3): p. 532-540.

247. Andrew, M., et al., *Versatile Gradients of Chemistry, Bound Ligands and Nanoparticles on Alumina Nanopore Arrays.* Nanotechnology, 2011. **22**(41): p. 415601.

Chapter 3 : Methodology

3.1. Source of Indonesian (Gunungkidul) Natural Zeolite

Indonesia is a major world producer of natural zeolite, with deposits found in various areas of the country [1, 2]. The common mining areas of natural zeolite in Indonesia are South Lampung, Bajah, Cikembar, Cipatujah, West Java Nangapada, Ende, Nusa Tenggara Timur, Malang, and Gunungkidul [3, 4]. This research selected natural zeolite from Gunungkidul, Yogyakarta in Indonesia as the adsorbent material of interest for value addition and improvement to purify biogas. The natural zeolite was supplied in powder of less than 425 μm (40 mesh) by the local mining-supply company CV Mountain Stone. In its pristine form, the Gunungkidul natural zeolite is referred to as A0 zeolite. The crystallo-chemical characteristics and properties of the pristine sample (e.g., its mineralogical and elemental composition, Si/Al ratio, particle size, surface area, porosity, crystallinity and morphology) were determined in this research using appropriate analytical equipment and techniques.

3.2. Physicochemical Modification of Indonesian Natural Zeolite

In this study, the applied physicochemical treatments were dealumination, calcination and alkali impregnation. The methods were conducted in combination to obtain various unique characteristics that are appropriate for application in biogas purification, particularly for CO_2 removal and water-vapour adsorption. The pre-treatment and structure modifications were selected for investigating CO_2 gas-adsorption capacity using Quanta Chrome Isorb HP1 and the isosteric heat of adsorption as the additional data.

3.2.1. Dealumination

Dealumination is a process for removing aluminium from the zeolite structure [5, 6]. There are various techniques for the dealumination of zeolite; these include the use of chemical reagents (e.g., acid, complexing agents, gaseous halogen compounds), the hydrothermal process, and silicon framework substitution (e.g., silicon tetrachloride, silicon halides,

ammonium hexafluorosilicate) [7]. Dealumination using chemical agents, was selected as the appropriate dealumination process of the zeolite, particularly acid dealumination using HCl. HCl dealumination leads to an increase in the surface area and in the Si/Al ratio by reducing Al in the natural zeolite [3]. HCl was supplied by Merck in the concentration of 37–38%.

In the dealumination experiments, known volumes of natural-zeolite samples were dispersed in HCl solution at specific concentrations (1, 3, 5, 9, 12 M) for 24 h with a similar zeolite to HCl solution volume ratio. As a modification procedure of previous studies, the addition of an acid-neutralisation step by aquadest washing was included [8, 9]. To study the dealumination effect, the neutralised zeolite was treated at a similar calcination temperature of 400°C, and the resulting calcined products were referred to as A1, A2, A3, A4 and A5, where the numbers 1, 2, 3, 4 and 5 indicate the different HCl concentrations, respectively. The schematic of the different dealumination acid-concentration processes is presented in Figure 3.1(a). Each material was characterised to determine its mineralogical and element composition, Si/Al ratio, crystallinity, porosity, specific surface area and morphology using appropriate techniques.

3.2.2. Calcination

Calcination was conducted at a high temperature (more than 100°C) to remove water vapour and other impurities inside the channels of porous material. This action also affects the surface area and crystallinity of zeolite, except in particular types of zeolite (e.g., mordenite and 13-X zeolite) [10, 11]. To study the effect of calcination temperature, a constant HCl concentration (3 M) for dealumination and aquadest washing procedures was applied to the pristine natural zeolite, followed by heating at elevated temperatures (400, 450, 500 and 550°C).

In this experiment, A2 zeolite (3 M HCl dealumination) was selected as the base material. It was heated to temperatures of 400, 450, 500 and 550°C for 3 h in a modified furnace [8, 9]. They resulting products were referred to as A2/D0, D1, D2 and D3 zeolite. The schematic of the different calcination temperature processes is presented in Figure 3.1(b).

The properties of the Si/Al ratio, surface area, crystallinity and morphology were determined using appropriate equipment and techniques.

3.2.3. Alkali impregnation

Alkali impregnation involves incorporation of alkali elements from alkaline solution into the natural-zeolite structure. This action can increase the zeolite's basicity for CO_2 adsorption enhancement [12]. Further, this action may also lead to the removal of impurities from the channels and possibly cause a desilication effect on the material, particularly for treatment at high concentration and high temperature [13].

In this experiment, the A2 zeolite (3 M HCl dealumination) sample was selected as the base material. The alkali-impregnation step was inserted between the dealumination and calcination process in different concentrations and alkaline solutions. After aquadest washing and ambient drying, the material was submerged in different concentrations (1, 3, and 5 M) of NaOH or KOH for 24 h. The post-impregnation material was washed and oven dried overnight, followed by calcination at 400°C for 3 h. The resulting products were referred to as A2/C0 for non-impregnated; C1, C2, C3 for concentration sequence of NaOH impregnation; and C4, C5, C6 for concentration sequence of KOH impregnation. The schematic of the different alkali-impregnation types and concentration processes is presented in Figure 3.1(c).

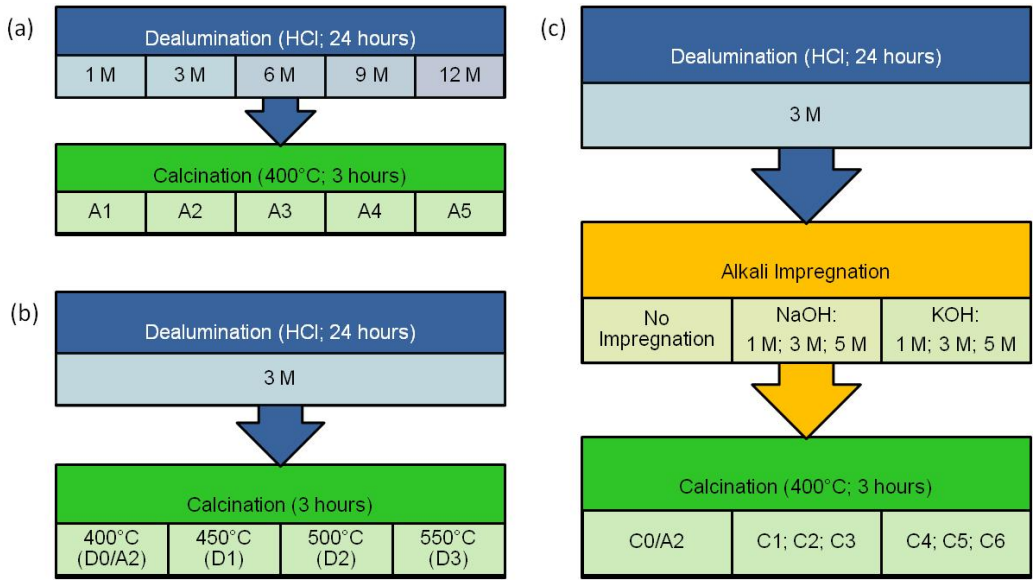

Figure 3.1. Schematic of Indonesian natural-zeolite physicochemical modification: (a) dealumination study; (b) calcination study; (c) alkali-impregnation study

3.3. Plasma Polymerisation of Particulate Material for Environmental Application

Plasma polymerisation has the ability to coat the material surface with ultrathin layers of monomers as polymer-like depositions with a highly crosslinked coating [14-17]. For the preliminary study and technique development, plasma polymerisation was implemented on the planar surface of a 1 cm^2 silicon wafer. The main focus was to determine the properties (e.g., coating or polymer film thickness, wettability and stability) related to the monomers' deposition as a guide for similar deposition on other surfaces.

In other studies, polymer films produced by plasma polymerisation have been deposited successfully on particulate or powdered material surfaces using plasma reactors such as fluidised bed [18, 19], rotating chamber [20, 21] and agitation platform chamber [22-25]. In this experiment, the plasma deposition was conducted in a custom built, cylindrical plasma reactor with two electrodes, and a U-shape at the upper side and a round shape at the bottom side (see Figure 3.2). The plasma was powered by a 13.56 MHz plasma generator, and equipped with pulse equipment regulator and a temporary agitation platform attached to the bottom electrode for shaking the particulate or powder material [22-25].

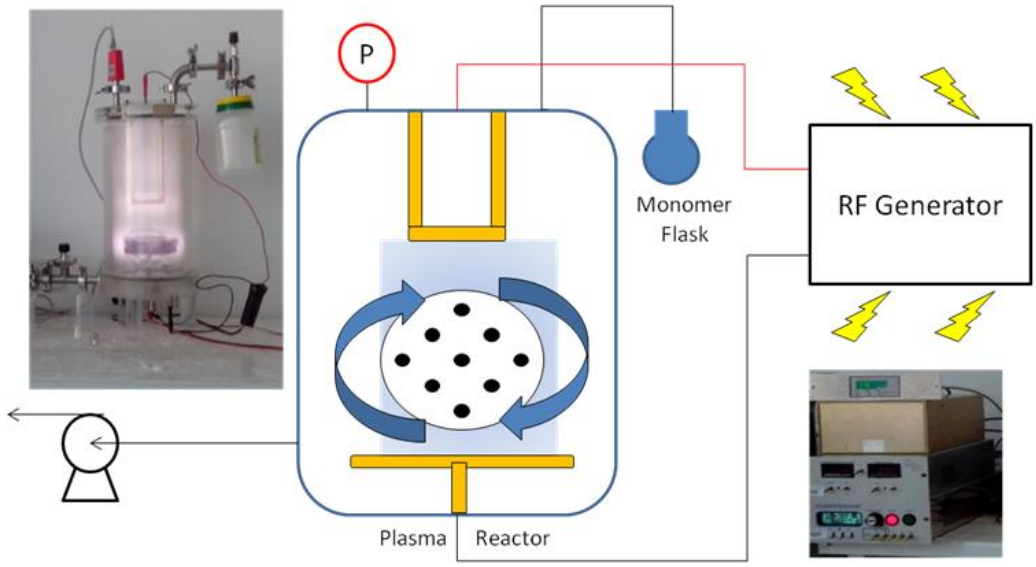

Figure 3.2. Schematic of plasma polymer reactor with agitation platform

3.3.1. Plasma polymer amine on porous, modified Indonesian natural zeolite for CO_2 adsorption

Allylamine (C_3H_7N) was selected as the precursor for creating an amine-rich surface deposition [26-28], while amine is the prospective monomer for CO_2 adsorption. Allylamine was obtained from Sigma-Aldrich at 98% purity, and was used as received. Allylamine deposition was conducted at various pressures of 4, 10, and 16 Pa (mostly), Radio Frequency (RF) plasma powers of 10 (mostly), 40, 50, 60 W, time range of 5–1800 s and pulse technique (on/off: 90 ms/10 ms). The schematic of natural-zeolite modification by plasma polymer amine for CO_2 adsorption is shown in Figure 3.3.

For preliminary characterisation, the plasma polymer was deposited on the planar surface of the silicon wafer to determine its thickness, wettability and surface composition, which were characterised using ellipsometry, the sessile drop technique, and X-ray photoelectron spectroscopy (XPS), respectively. The selected conditions and properties were optimised for the low blockage of the pores, maintaining high porosity to adsorb the impure gas. The modified zeolite with deposited amine material was characterised to examine the surface area, morphology, composition and surface-chemistry profile by the isotherm nitrogen

adsorption–desorption, scanning electron microscopy (SEM), energy-dispersive X-ray (EDX), XPS, and time-of-flight secondary ion mass spectrometry (ToF-SIMS), respectively.

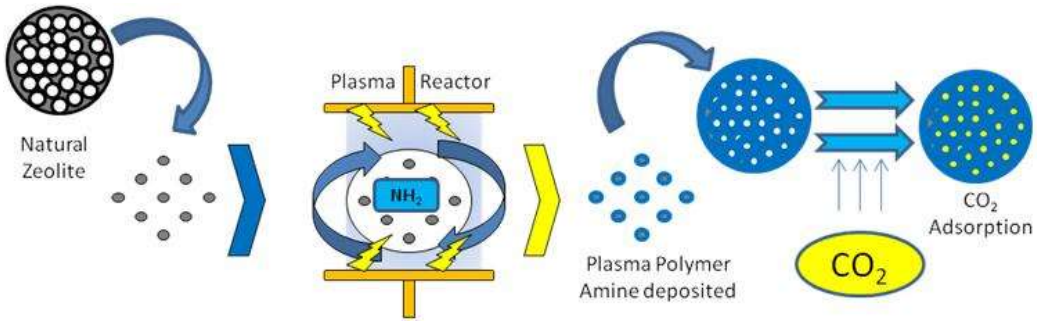

Figure 3.3. Schematic of plasma polymer amine incorporation into the modified Indonesian natural zeolite for CO_2 adsorption

For the preliminary study of CO_2 adsorption, the experiment was conducted in the reactor (see Figure 3.4). The simulation gas of CO_2 was supplied by BOC Australia (supplier gas company) on D size cylinder. The deposited amine material on both the silicon wafer and zeolite were placed in the reactor for 2 h with a new exposure of CO_2 per hour for creating a high concentration of CO_2. For water-vapour presence, hot water was provided inside the reactor with the similar refreshment of CO_2. After the adsorption, the material was observed during the transformation of surface composition using XPS. For advanced measurement of CO_2 adsorption capacity, the plasma polymer amine–natural zeolites were examined using temperature-programmed desorption (TPD) of CO_2 (i.e., TPD of CO_2) by Micromeritics Autochem II.

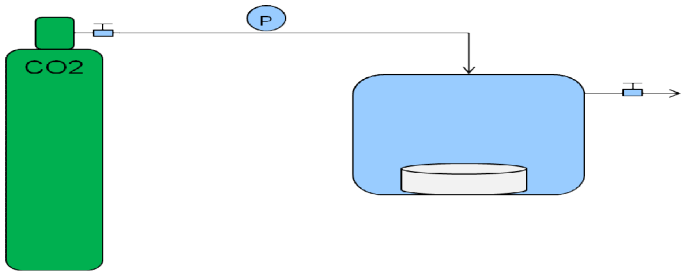

Figure 3.4. Schematic of CO_2 adsorption simple reactor for a preliminary study

3.3.2. Air-plasma activation on porous material of Indonesian natural zeolite for water-vapour adsorption

Air-plasma activation was conducted on the A0, A1, and A5 zeolites at 16 Pa, 50 W and 1200 s. Further investigation was conducted with the selected natural zeolite of A5 zeolite, which was varied at three different plasma powers of 10, 30, and 50 W; and plasma time activation range of 300–1200 s. Some characterisations were conducted on some parameters for pre-plasma and post-plasma activation. These were morphology, Si/Al ratio (composition), specific surface area and porosity, and type of bonding. The gravimetric method was applied to determine water-vapour adsorption capacity by weighing the zeolite during the adsorption in the desiccator. The schematic of natural-zeolite modification by air-plasma activation for water-vapour adsorption is presented in Figure 3.5.

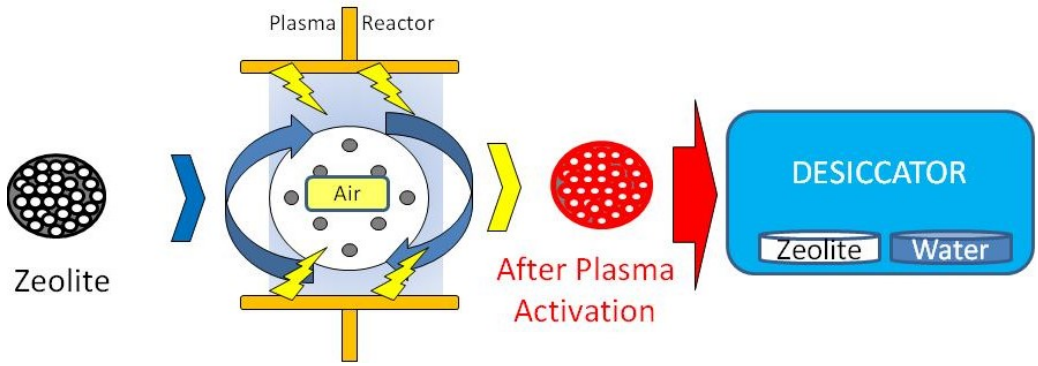

Figure 3.5. Schematic of air-plasma activation on modified natural zeolite for water-vapour adsorption

3.3.3. Hydrophobic plasma polymer on nanoparticle of magnetic material for oil adsorption

Two crude-oil samples were collected from the waste store of the University of South Australia to be used as model oils whose density and viscosity were measured to determine the type. The black powder of nanomagnetic material of 316L stainless steel was supplied by Hongwu International Group, Guangzhou, China with a purity of 99.99% and size of 70 nm. Then, 1.7-octadiene (C_8H_{14}) and perfluorooctane (octadecafluorooctane-C_8F_{18})

(Sigma-Aldrich) were selected as hydrophobic plasma precursors, and were used as received. The plasma polymerisation of octadiene and perfluorooctane was conducted on the planar surface of the silicon wafer and the particulate surface of the nanomagnetic material at the pressures of 16 and 23 Pa, respectively; RF power of 50 W; and range deposition time between 600 and 2400 s.

The planar surface deposition on the silicon wafer was conducted to investigate polymer film thickness, wettability (contact angle), and stability. The thickness and wettability were determined using ellipsometry measurement and sessile drop technique, respectively. Analysis of thickness loss was examined in a polymer film stability test after a predetermined period soaking in ultrapure water, a technique developed in previous studies [25, 29, 30]. The selected procedure of plasma polymer deposition was applied to nanomagnetic material. The surface composition and morphology of particulate deposition was characterised using XPS and SEM, respectively.

For the oil-capture experiment, mixtures of water and crude oil of 20,000 ppm were prepared in 20 mL volume. The coated nanomagnetic materials were applied in a different weight ratio of oil to adsorbent (between 8 and 1200 mg). The adsorbent was mixed into the mixture samples then stirred for 30 s and rested for 600 s. The various variables of plasma treatment were conducted in this experiment, for example, plasma-deposition time between 0 and 2400 s; ratio of oil to adsorbent between 1:3 and 50:1; and scale up in three different volumes of water: 50, 100 and 250 mL. The adsorbent was collected by a magnet, while the rest of the solution was mixed with n-hexane to determine oil residue by ultraviolet-visible (UV-Vis) measurement. The schematic of nanomagnetic material modification by hydrophobic plasma polymer for oil adsorption is prsented in Figure 3.6. The oil-residue measurement was utilised to calculate the oil-removal efficiency (ORE) which following this equation:

$$\mathrm{ORE} = \frac{\text{initial oil concentration} - \text{residual oil concentration}}{\text{initial oil concentration}}\, x\, 100\%$$

(Equation 3.1)

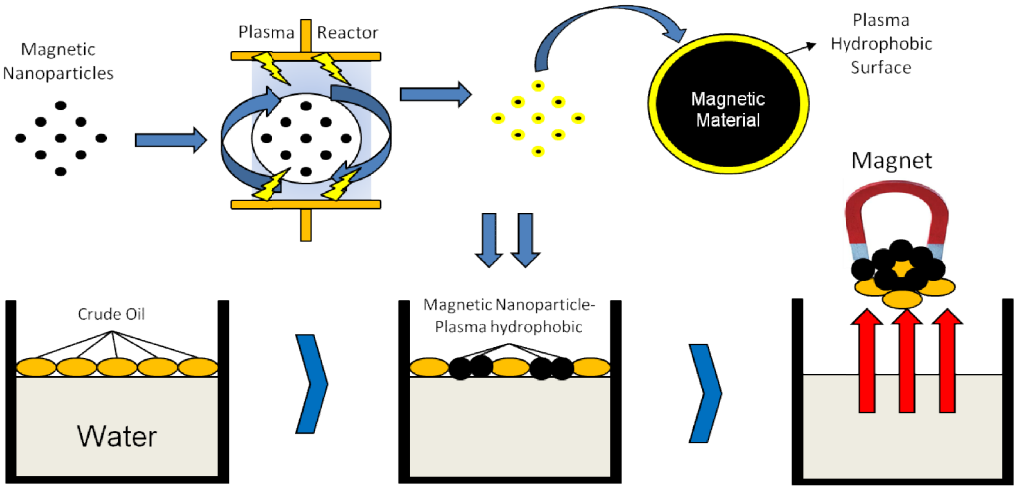

Figure 3.6. Schematic of hydrophobic plasma polymer on nanomagnetic material for oil adsorption

3.4. Characterisation of Materials

Material characterisation in this research was conducted to investigate the surface and bulk properties of the material, and to evaluate material performance in the application. Composition, surface area, chemical bonding, structure, morphology and size distribution are the essential properties for investigation, while thickness and wettability are other particular features must be observed for plasma polymerised materials. After material preparation, the performance of the new materials must be evaluated according to their applications. CO_2 adsorption capacity was measured by Quanta Chrome Isorb HP1 or Micromeritics Autochem II. For the other environmental applications, water-vapour adsorption performance was determined using the gravimetric method and oil-adsorption performance was determined using UV-Vis spectrophotometry.

3.4.1. Ellipsometry

Ellipsometry is an accurate and straightforward technique for surface property measurement based on polarisation transform over light reflectance or transmission [31,

32]. The transformation of the reflected light correlates to the optical properties that can measure film thickness accurately from less than one nanometre up to several micrometres. The light source radiates polarised light through a polariser, then is directed to the sample at various angles. The multiple angles of reflected light are captured by the analyser and detector to determine the shape and orientation of the ellipse, thus the measurement device is called an ellipsometer [33]. This measurement technique was utilised to assess the thicknesses of the plasma polymer deposition [33, 34].

In these studies, the thickness of the plasma polymer depositions was measured using Variable Angle Spectroscopic Ellipsometer (VASE) ellipsometer (JA Woollam Co., Inc., United States), and all data were analysed with WVASE32 software. Silicon wafer coated polymers were attached to the ellipsometer by the vacuum suction mechanism, then measured at various angles. The plain silicon wafers were measured as the non-coated plasma reference and for calibration purposes.

3.4.2. Wettability test (analysis of water contact angle)

Wettability is a property of a surface that determines whether the surface is hydrophobic or hydrophilic. Wettability is determined by the measurement of the water contact angle with the surface and is connected to the surface's chemical properties given that water has sensitivity to small surface physicochemical transformation [35-37].

The sessile drop technique is a wettability measurement method that can be applied smoothly. This technique uses a high-resolution camera to capture the interaction between a water drop and the surface; the picture of the water contact angle is then analysed by software. A hydrophobic surface is indicated by a contact angle of above 90°; a lower contact angle implies increasingly hydrophilic surface behaviour until 0° for complete wetting of the surface. The description of the water contact angle for a hydrophobic–hydrophilic surface is presented in Figure 3.7. The different contact angles reveal the different water-surface interactions, wherein weak interaction indicates hydrophobicity and strong interaction indicates hydrophilicity.

In these studies, the sessile drop method was applied using a Logitec digital camera to capture the image, then the static water contact angle was determined by Drop-Snake (v2.1) ImageJ plug-in [38].

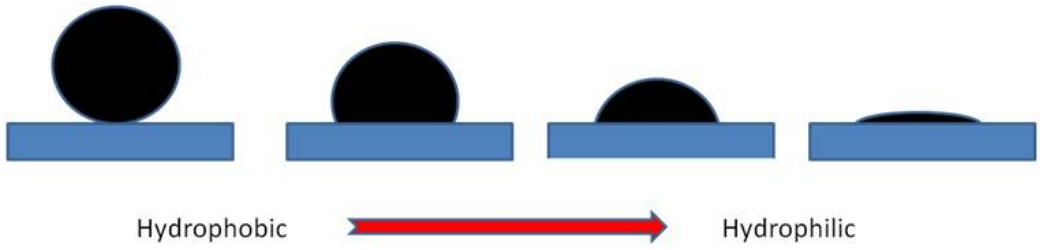

Figure 3.7. Description of water contact angle results for hydrophobic–hydrophilic surface

3.4.3. XPS

XPS is a surface-characterisation technique that works on surface thickness up to 10 nm based on the spectroscopic method for measuring the photoelectric effect. The monochromatic X-rays of 10–15 keV, which are emitted by a magnesium or aluminium anode (Mg Kα or Al Kα), discharge the sample under ultrahigh vacuum (UHV) ($P<10^{-7}$ Pa) condition to eliminate surface contamination. The electron energy is transferred to a core electron of an atom in the substrate, then the excess core electron is emitted from the surface; this is a photoelectron. The calculation of kinetic energy and the number of electron escapes from the surface create the XPS spectrum of the survey and the high-resolution atom.

The XPS technique is commonly used to determine quantitative atomic composition at survey scanning, and atomic bond characteristic at a specific atom high-resolution scanning for the plasma-deposited films [39]. Moreover, it is utilised to determine surface contamination, empirical formula, binding energy, and density of electronic states [40]. However, binding-energy calibration is needed to analyse the XPS spectrum, which is rectified based on C-C bond at 285.0 eV [41] given that there is a presence of adventitious carbon contamination from the atmosphere on surface thickness of 1–2 nm.

In these studies, XPS spectra of the flat surface sample and powder sample were obtained on SPECS Sage XPS (SPECS GmbH, Germany) (which was equipped with a Mg Kα radiation source [hν 1253.6 eV]) and the hemispherical analyser Phoibos 150 (which was equipped with an MCD-9 detector). Survey spectra were recorded over the energy range 0–1000 eV using 120 eV pass and 0.5 eV resolution; then, high-resolution spectra were obtained using 20 eV pass and 0.1 eV resolution. The processing and fitting of XPS spectra were analysed using CasaXPS V2.3.14 (Casa Software Ltd).

3.4.4. ToF-SIMS

ToF-SIMS is a surface and thin-film analytical technique that involves sputtering the surface with a bombarding primary ion beam. The ejected secondary ion is collected and analysed by a time-of-flight detector to determine the surface composition profile of elements, isotopes and molecules and their fragments to the depth of 1 to 2 nm [42]. This analysis is the most sensitive surface observation, particularly in qualitative studies. It is possible to conduct quantitative analysis by using standards for comparison.

ToF-SIMS analysis was carried out using the PHI TRIFT V nanoTOF instrument (Physical Electronics Inc., United States) to characterise the adsorbent surface profile in high sensitivity, particularly on amine-deposition exploration. Samples were prepared by attaching it on a low background adhesive. A pulsed liquid metal Au primary ion gun (LMIG) was operated in this analysis at 30 kV in ‘unbunched’ mode under a vacuum of 5×10^{-6} Pa. The raw data were obtained as the interesting chemical maps of species, which were retrospectively produced. WincadenceN software (Physical Electronics Inc., United States) was utilised for further processing and investigation of the sample spectra and images.

3.4.5. SEM-EDX analysis

SEM analysis was used to determine particle morphology and the surface structure of the material. This procedure involves electrons beams that interact with the material surface

and create morphology, topography, composition and other property images of the surface. Conventional SEM performs observation in a high-vacuum condition, but the new technology environmental SEM can perform in a normal-environment condition [43].

Several essential combination factors of capturing image control are voltage acceleration, spot intensity, image focusing, contrast, brightness and magnification. Further, they must be a conductive sample, so the low conductivity sample must be coated by an electrically conductive material such as gold, platinum, chromium, osmium or carbon [44, 45].

For creating an image on SEM analysis, backscattered electrons (BSE) and secondary electrons (SE) are applied as the main signal. Another signal commonly used as characteristic X-ray is EDX spectroscopy to determine the chemical-element composition of the surface sample [44, 46]. The X-rays penetrate up to 0.5–2 μm, depending on the selected voltage acceleration, and determine the composition at that depth.

In these studies, scanning electron microscopy – energy-dispersive X-ray (SEM-EDX) analysis was performed on powder material using the Hitachi SU3500 (Hitachi, Japan); equipped with EDX analyser by EDAX Element. The sample was dried before analysis, then a small quantity of powder sample was splashed on carbon tape surface as preparation before analysis. For EDX analysis, the minimum voltage acceleration was selected at 3 kV, then increase based on the material conductivity.

3.4.6. FTIR

Fourier-transform infrared (FTIR) spectroscopy is an analytical technique used to determine chemical functional groups and compounds by emission or absorption of the infrared spectrum [47]. Infrared absorption is detected because of the molecule dipole moment transformation and the sufficient transition energy of the infrared photon [48, 49]. Commonly, the sample is prepared in two different ways for powder and liquid measurements. The powder sample is mixed with potassium bromide (KBr), then pressed by force and vacuum into a disk or deposited in liquid paraffin (Nujol). However, some FTIR equipment can analyse the powder sample directly without preparation. The spectra

are compared with the spectra reported in the literature to identify the appropriate structures [47].

In this study, the FTIR spectra were observed using Thermo Nicolet Magna 750 FTIR equipped with an MTEC model 300 photoacoustic detector (GMI, United States) and supported by Omnic software for the experimental procedure. The powder samples were put directly into the aluminium pan as the sample holder, then loaded directly to the instrument for analysis. The measurement was operated using the mirror velocity of 0.1581 cm/s, which is appropriate with a sampling depth of 22.4 μm. The observation was conducted at a resolution of 8 with the default setting of 256 scans on the range of 4000–400 cm^{-1}.

3.4.7. ICP-MS

Inductively coupled plasma mass spectrometry (ICP-MS) is used to determine the concentrations of mineral species in multielement sample solutions simultaneously [50, 51]. Two general step procedures work in this technique: converting the sample into an ion by inductively coupled plasma; and separating and calculating the ions by the mass spectrometer. In these studies, ICP-MS (Agilent 8800 Triple Quadrupole, United States) is performed to determine the bulk-composition analysis of natural zeolite. For sample preparation, the powder sample is mixed with a mixture of nitric acid and hydrochloric acid then digested using microwave before analysis.

3.4.8. XRF

X-ray fluorescence (XRF) is an analytical tool used to determine the bulk elemental composition of mineral samples by measuring the fluorescent or secondary X-ray emission from the material after discharge by primary radiation of high-energy X-rays. The unique characteristic fluorescent X-rays of each element provide a specific identification and produce an excellent qualitative and quantitative elemental-composition analysis. Particularly for zeolite, XRF is one of the leading observation techniques for effectively

determining bulk-composition analysis [52], particularly the Si/Al ratio [53]. In these studies, XRF was conducted to determine the bulk-composition analysis of natural zeolite as the reference for the surface composition analysis. XRF analysis was conducted using quantitative S2 Ranger, Energy Dispersive XRF (EDXRF) (Bruker AXS, Germany).

3.4.9. Nitrogen adsorption–desorption analysis

Nitrogen adsorption–desorption analysis was conducted to determine surface area, pore volume and pore-size distribution of porous material. These were measured using the Micromeritics ASAP 2420 analysis software. The analysis was conducted through isotherm nitrogen adsorption–desorption at –196°C. For preparation, samples were degassed at a particular time and temperature based on the condition and limitation of the material to remove water and other impurities [54, 55]. The degassing procedure for each material was as follows: natural zeolite at 24 h and 120°C; physicochemical and alkali impregnation of modified natural zeolite at 24 h and 350°C; natural zeolite inducted plasma polymer allylamine after degassing optimisation at 72 h and 75°C.

The Brunauer–Emmett–Teller (BET) model and Barrett–Joyner–Halenda (BJH) model were calculated by supporting software of Micromeritics ASAP 2420 analyser for determination of further properties. The specific surface area was determined using the standard BET model [55, 56]. The BET equation is expressed as follows:

$$\frac{\mathrm{p/p^0}}{\mathrm{n(1-p/p^0)}} = \frac{1}{\mathrm{n_m C}} + \frac{\mathrm{C-1}}{\mathrm{n_m C}}\left(\frac{\mathrm{p}}{\mathrm{p^0}}\right)$$

(Equation 3.2)

where p/p^0 is relative pressure; n is specific amount adsorbed at a relative pressure; n_m is the particular monolayer capacity; and C is BET constant. Porosity was determined from the standard BJH model as modified from the Kelvin equation [57]. The BJH equation is expressed as follows:

$$V_{pn} = \frac{r_{pn}^2}{(r_{kn} + \Delta t_n)^2}\,\Delta V_n - \frac{r_{pn}^2}{(r_{kn} + \Delta t_n)^2}\,\Delta t_n \sum_{j=1}^{n-1} \frac{r_{pj} - t_j}{r_{pj}}\,\frac{2V_{pj}}{r_{pj}}$$

(Equation 3.3)

Then the r_k is calculated by the Kelvin equation:

$$r_k = \frac{-4.14}{lo\,g(p/p^0)}$$

(Equation 3.4)

where V is desorbed volume; r is radius; t is thickness; and p/p^0 is relative pressure.

3.4.10. XRD

X-ray diffraction (XRD) is an analysis technique used to determine material mineralogy and crystallinity based on the specific diffraction of X-rays in many directions. The diffraction data constructs a three-dimensional design, which is addressed to the particular crystal [58]. XRD is commonly performed to determine specific and disordered material dimensions, quantify percent crystallinity, and measure sample purity.

In these studies, XRD was conducted for natural zeolite because it is one of the leading observations to determine crystallinity [52]. The crystal structure analysis was observed by PANalytical Empyrean XRD (PANalytical Empyrean, United Kingdom). The analysis was performed at high-angle powder XRD, with a scan rate of 0.02°/sec on high-angle measurement (5–80°). The measurement was operated by Cu Kα radiation with wavelength 1.5406 Å, generating at 40 kV and 40 mA. The HighScore Plus software was used to determine the crystal type and semi-quantitative measurement based on the search–match method. For further analysis of semi-quantitative measurements, the reference data were obtained from a web mineral database.

3.4.11. Sieve analysis (particle-size distribution)

Sieve analysis or gradation analysis is a simple technique for particle sizing to determine the particle-size distribution of granular or powder material [59]. The various grade sieve screens with standard sieve sizes are used to separate the particles into different size intervals by a mechanical shaker. The screens are arranged in sequence with the coarsest screen opening at the highest and the finest screen opening at the lowest level (above the base pan), then the sieves set column are shaken for a certain time. After shaking is completed, the samples retained on every sieve are weighed to calculate the various masses for each size.

In these studies, the particle-size distribution was conducted to determine the size composition of natural zeolite using Sieve Shaker of Retsch AS 200 (Retsch, Germany). In preparation, the zeolite rock was destructed using size-reduction equipment until the size of 425 microns by a local mining-supply company. The sieve screen arranged the screen size in sequences from small to big, with sizes of 53, 106, 212, 300 and 425 microns.

3.4.12. pH measurement

The potential of hydrogen (pH) is a grade number that indicates acidity or basicity of a solution. It is determined precisely using a pH meter, which involves an indicating unit (monitor display) and a detecting unit (glass-electrode probe) [60]. The pH meter was calibrated at three pH points of 4.00, 7.00, and 10.00 using buffer solutions. For quick pH determination, pH litmus-paper indicator/universal indicator is also commonly used. A visual comparison between the paper indicator's color after measurement and the standard color of the paper indicator provide the proper pH near the round number.

3.4.13. CO_2 adsorption capacity

CO_2 adsorption capacity was measured using Quanta Chrome Isorb HP1 (particularly for physicochemically modified natural zeolite) equipped with a temperature-controlled

circulator to maintain isotherm condition. It was operated at three different analysis temperatures of 0, 10 and 25°C, with multilevel pressure up to 30 bar. For preparation, the samples were degassed for a specific time and temperature (as noted in the discussion of nitrogen adsorption–desorption analysis, section 3.4.9) based on the material condition and limitation clean up the channel [54, 55].

As supporting data, the Clausius–Clapeyron equation was used to calculate the isosteric heat of adsorption as the critical thermodynamic properties for further application of practical design [61]. The isosteric heat of adsorption value can be used to determine the adsorption mechanism of chemisorption or physisorption [62-64]. The Clausius–Clapeyron equation is expressed as follows:

$$\mathrm{Ln}\left(\frac{P_2}{P_1}\right) = -\frac{Q_{st}}{R}\left(\frac{1}{T_2}-\frac{1}{T_1}\right)$$

(Equation 3.5)

Where P is the partial pressure (Pa); T is the absolute temperature (K); R is universal gas constant (8.314 J mol^{-1} K^{-1}); and Q_{st} is the isosteric heat of adsorption.

Further, CO_2 adsorption was determined by TPD of CO_2 using Micromeritics Autochem II (particularly for plasma polymerised allylamine natural zeolite), which was equipped with a microreactor. The samples were pre-treated under 5% O_2/He (volume %) flow (20 mL min-1) at the optimum certain degassing temperature for 2 h (over 300°C) or 6 h (under 300°C), depending on the material type.

CO_2 adsorption was conducted at room temperature for 1 h (20 mL min-1). TPD of CO_2 was also conducted heating the sample at 5 K/min up to a certain degassing temperature, under helium flow (20 mL min-1), while the Thermal Conductivity Detector (TCD) detector captured the signal. The desorption profiles were deconvoluted using Gaussian curves to understand the strong adsorption bond on the surface. CO_2 adsorption capacity was determined by normalised signal intensity of the adsorbent weight, then by calculating

the curve area as the adsorption capacity, and calibrating the signal intensity to the standard graph of CO_2 adsorption volume.

3.4.14. Water-vapour adsorption capacity

For the preparation of material, various treatment zeolites by plasma activation were dried in the oven at 105°C overnight. One gram of zeolite placed in an open container was stored in the desiccator containing water and stored at room temperature. The following measurement process was replicated three times. The amount of water vapour adsorbed by zeolite was measured by weighing the zeolite at certain time intervals. Weighing was conducted until the zeolite weight was stable. Further, the normalised specific surface area of water-vapour adsorption capacity of the various natural zeolites was also calculated to determine the water-adsorption affinity.

3.4.15. UV-Vis spectrophotometry

UV-Vis spectrophotometry works on the absorption or reflection of an UV-Vis light range. It measures the transformation of light intensity before and after through the sample at a specific wavelength. UV-Vis spectrophotometry is applied widely in chemical analysis as a simple analytical technique [65, 66]. Commonly, the reference curve of a specific compound is created before sample analysis is conducted, with the high correlation coefficient ($R>0.99$) obtained for standard linear curves, then the least squares approach is applied for further calculation.

In these studies, UV-Vis spectrophotometry was utilised to measure the oil-residue content by Varian Carry 50 Bio UV-VIS (Agilent, United States) [67]. For the calibration curve, exploration was conducted in the wavelength range of 250–350 nm, finding the appropriate wavelengths of 255 nm and 256 nm to determine oil concentration. The sample was diluted to n-hexane as a preparation sample before analysis, and n-hexane was used as the blank sample.

3.5. Conclusions

The modification of Indonesian natural zeolite by physicochemical treatment (particularly increasing surface area) is the first step in improving the capacity of this zeolite's CO_2 adsorption. Improving CO_2 adsorption capacity by enhancing basicity and introducing amine on the selected material was achieved to provide a new perspective of CO_2 adsorption capacity. A new technique of material preparation was presented in this research, particularly in amine introduction using plasma polymerisation. The natural-zeolite properties for each treatment were also investigated to select the appropriate modified natural zeolite. The selected material was evaluated to determine CO_2 adsorption capacity as the final evaluation. Air-plasma activation was also applied to the modified natural zeolite of high silica content to improve water-vapour adsorption capacity. As an additional experiment of surface engineering by plasma polymerisation, the hydrophobic surface layer was also deposited on the nanomagnetic material surface using octadiene and perfluorooctane as the precursors. The new product was evaluated in relation to oil-adsorption performance in contaminated water. These experiments modifying the structure of natural zeolites and engineering plasma polymer surface were conducted successfully and are reported in Chapters 4 to 9.

References

1. Marantos, I., G.E. Christidis, and M. Ulmanu, *Zeolite Formation and Deposits*, in *Handbook of Natural Zeolites*, V.J. Inglezakis and A.A. Zorpas, Editors. 2012, Bentham Science Publishers. p. 28-51.

2. Flanagan, D.M., *2015 Minerals Yearbook: Zeolites (Advance Release)*, U.S.G.S. U.S. Department of the Interior, Editor. 2016.

3. Widayat, et al., *Pengaruh Konsentrasi HCl dan Jenis Reaktan dalam Pembuatan Katalis Zeolit untuk Proses Dehidrasi dari Zeolit Alam [Effect of HCl Concentration and Reactant Type in The Zeolite Catalysts Production for Dehydration Process of Natural Zeolite]*, in *National Seminar on Chemical Engineering and Processes*. 2008, Chemical Engineering Department, Diponegoro University: Semarang–Indonesia. p. H091 1-9.

4. Wahono, S.K., *Kajian: Pemanfaatan Zeolit Lokal Gunungkidul–Yogyakarta untuk Optimasi Sistem Biogas [Review : Utilization of Gunungkidul Local Zeolite for Biogas System optimization]*, in *National Seminar on Chemical Engineering Fundamentals and Applications*. 2008, Chemical Engineering Departement of Institute of Technology Sepuluh November Surabaya: Surabaya–Indonesia. p. E14.

5. Dziedzicka, A., B. Sulikowski, and M. Ruggiero-Mikołajczyk, *Catalytic and Physicochemical Properties of Modified Natural Clinoptilolite.* Catalysis Today, 2016. **259**: p. 50-58.

6. Wahyuni, S., *Preparasi dan Karakterisasi Katalis Ni-Zeolit Alam Terdealuminasi dengan Metode Perlakuan Asam [Preparation and Characterization of Dealumnated Ni-Natural Zeolite Catalyst by Acid Treatment Method]*, in *National Seminar Chemistry and Education of Chemistry*. 2006, Semarang State University: Semarang–Indonesia.

7. Beyer, H.K., *Dealumination Techniques for Zeolites*, in *Post-Synthesis Modification I*. 2002, Springer Berlin Heidelberg: Berlin, Heidelberg. p. 203-255.

8. Wahono, S.K., et al., *Metoda dan Alat untuk Meningkatkan Kadar Methana dalam Biogas [Methods and Tools for Increasing Methane Contents of Biogas]*. Patent, 2010. IDP000038082: Indonesia.

9. Wahono, S.K. and W.A. Rizal, *Biogas Filter Based on Local Natural Zeolite Materials.* International Journal of Renewable Energy Development, 2014. **3**(1): p. 1-5.

10. Lemoine, G., *Comparison of Different Types of Zeolites Used as Solid Acid Catalysts in The Transesterification Reaction of Jatropha-Type Oil for Biodiesel Production*. 2013, Worcester Polytechnic Institute.

11. Windati, W., Y. Syah, and A.A. Widati, *Impregnasi Zeolit Alam dengan TiO_2 untuk Degradasi Jingga Metil Secara Fotokatalitik [Natural Zeolites Impregnation by TiO_2 for Photocatalytic Degradation of Methyl Orange]*. Journal Universitas Airlangga, 2013. **1**(1).

12. Bonenfant, D., et al., *Advances in Principal Factors Influencing Carbon Dioxide Adsorption on Zeolites.* Science and Technology of Advanced Materials, 2008. **9**(1): p. 013007.

13. Lin, H., et al., *Physicochemical Properties and Mechanism Study of Clinoptilolite Modified by NaOH.* Microporous and Mesoporous Materials, 2015. **218**: p. 174-179.

14. Vasilev, K., *Nanoengineered Plasma Polymer Films for Biomaterial Applications.* Plasma Chemistry and Plasma Processing, 2014. **34**(3): p. 545-558.

15. Yasuda, H. and Y. Matsuzawa, *Economical Advantages of Low-Pressure Plasma Polymerization Coating.* Plasma Processes and Polymers, 2005. **2**(6): p. 507-512.

16. Denes, F.S. and S. Manolache, *Macromolecular Plasma-Chemistry: An Emerging Field of Polymer Science.* Progress in Polymer Science, 2004. **29**(8): p. 815-885.

17. Biederman, H. and D. Slavínská, *Plasma Polymer Films and Their Future Prospects.* Surface and Coatings Technology, 2000. **125**(1): p. 371-376.

18. Kim, J.W. and H.S. Choi, *Surface Crosslinking of High-Density Polyethylene Beads in a Modified Plasma Reactor.* Journal of Applied Polymer Science, 2002. **83**(13): p. 2921-2929.

19. Karches, M. and P.R. von Rohr, *Microwave Plasma Characteristics of a Circulating Fluidized Bed-Plasma Reactor for Coating of Powders.* Surface and Coatings Technology, 2001. **142–144**: p. 28-33.

20. Jarvis, K.L. and P. Majewski, *Plasma Polymerized Allylamine Coated Quartz Particles for Humic Acid Removal.* Journal of Colloid and Interface Science, 2012. **380**(1): p. 150-158.

21. De Vietro, N., R. d'Agostino, and F. Fracassi, *Introduction of Basic Functionalities on The Surface of Granular Adsorbers by Low Pressure Plasma Processes.* Plasma Processes and Polymers, 2012. **9**(9): p. 911-918.

22. Wahono, S.K., et al., *Preliminary Study: Combination of Amine and Natural Zeolite as New Adsorbent Material for CO_2 Capture*, in *Chemeca 2016: Chemical Engineering-Regeneration, Recovery and Reinvention*. 2016. p. 900-910.

23. Cavallaro, A. and K. Vasilev, *Controlled and Sustained Release of Pharmaceuticals via Single Step Solvent-Free Encapsulation.* Chemical Communications, 2015. **51**(10): p. 1838-1841.

24. Mierczynska-Vasilev, A., et al., *A Novel Technology for The Rapid, Selective, Magnetic Removal of Pathogenesis-Related Proteins from Wines.* Food Chemistry, 2017. **232**(Supplement C): p. 508-514.

25. Wahono, S.K., et al., *Plasma Polymer Facilitated Magnetic Technology for Removal of Oils from Contaminated Waters.* Environmental Pollution, 2018. **240**: p. 725-732.

26. Siow, K.S., et al., *Plasma Methods for The Generation of Chemically Reactive Surfaces for Biomolecule Immobilization and Cell Colonization - A Review.* Plasma Processes and Polymers, 2006. **3**(6-7): p. 392-418.

27. Liu, X., et al., *Surface Modification by Allylamine Plasma Polymerization Promotes Osteogenic Differentiation of Human Adipose-Derived Stem Cells.* ACS Applied Materials & Interfaces, 2014. **6**(12): p. 9733-9741.

28. Vasilev, K., et al., *Substrate Influence on The Initial Growth Phase of Plasma-Deposited Polymer Films.* Chemical Communications, 2009(24): p. 3600-3602.

29. Macgregor-Ramiasa, M.N., A.A. Cavallaro, and K. Vasilev, *Properties and Reactivity of Polyoxazoline Plasma Polymer Films.* Journal of Materials Chemistry B, 2015. **3**(30): p. 6327-6337.

30. Vasilev, K., et al., *Solvent-Induced Porosity in Ultrathin Amine Plasma Polymer Coatings.* The Journal of Physical Chemistry B, 2008. **112**(35): p. 10915-10921.

31. McCrackin, F.L., et al., *Measurement of The Thickness and Refractive Index of Very Thin Films and The Optical Properties of Surfaces by Ellipsometry.* 1963.

32. Ulman, A., *An Introduction to Ultrathin Organic Films: From Langmuir--Blodgett to Self--Assembly*. 2013: Academic press.

33. Fujiwara, H., *Spectroscopic Ellipsometry: Principles and Applications*. 2007: John Wiley & Sons.

34. Tompkins, H. and E.A. Irene, *Handbook of Ellipsometry*. 2005: William Andrew.

35. Decker, E., et al., *Physics of Contact Angle Measurement.* Colloids and Surfaces A: Physicochemical and Engineering Aspects, 1999. **156**(1-3): p. 177-189.

36. Janssen, D., et al., *Static Solvent Contact Angle Measurements, Surface Free Energy and Wettability Determination of Various Self-Assembled Monolayers on Silicon Dioxide.* Thin Solid Films, 2006. **515**(4): p. 1433-1438.

37. De Gennes, P.-G., *Wetting: Statics and Dynamics.* Reviews of modern physics, 1985. **57**(3): p. 827.

38. Stalder, A.F., et al., *A Snake-Based Approach to Accurate Determination of Both Contact Points and Contact Angles.* Colloids and Surfaces A: Physicochemical and Engineering Aspects, 2006. **286**(1): p. 92-103.

39. Vandencasteele, N. and F. Reniers, *Plasma-Modified Polymer Surfaces: Characterization Using XPS.* Journal of Electron Spectroscopy and Related Phenomena, 2010. **178-179**: p. 394-408.

40. Ulman, A., *Characterization of Organic Thin Films.* 1995.

41. Oswald, S., M. Hoffmann, and M. Zier, *Peak Position Differences Observed During XPS Sputter Depth Profiling of The SEI on Lithiated and Delithiated Carbon-Based Anode Material for Li-Ion Batteries.* Applied Surface Science, 2017. **401**: p. 408-413.

42. Benninghoven, A., *Chemical Analysis of Inorganic and Organic Surfaces and Thin Films by Static Time-of-Flight Secondary Ion Mass Spectrometry (ToF-SIMS).* Angewandte Chemie International Edition in English, 1994. **33**(10): p. 1023-1043.

43. Stokes, D., *Principles and Practice of Variable Pressure: Environmental Scanning Electron Microscopy (VP-ESEM)*. 2008: John Wiley & Sons.

44. O'Connor, D.J., B.A. Sexton, and R.S. Smart, *Surface Analysis Methods in Materials Science*. Vol. 23. 2013: Springer Science & Business Media.

45. Suzuki, E., *High-Resolution Scanning Electron Microscopy of Immunogold-Labelled Cells by The Use of Thin Plasma Coating of Osmium.* Journal of microscopy, 2002. **208**(3): p. 153-157.

46. Goldstein, J.I., et al., *Scanning Electron Microscopy and X-Ray Microanalysis*. 2017: Springer.

47. Pavia, D.L., et al., *Introduction to Spectroscopy*. 2014: Cengage Learning.

48. Stuart, B., *Infrared Spectroscopy*, in *Kirk-Othmer Encyclopedia of Chemical Technology*. 2015.

49. Smith, B.C., *Fundamentals of Fourier Transform Infrared Spectroscopy*. 2011: CRC press.

50. Beauchemin, D., *Inductively Coupled Plasma Mass Spectrometry.* Analytical Chemistry, 2010. **82**(12): p. 4786-4810.

51. Montaser, A., *Inductively Coupled Plasma Mass Spectrometry*. 1998: John Wiley & Sons.

52. Stocker, K., et al., *Characterization and Utilization of Natural Zeolites in Technical Applications.* BHM Berg- und Hüttenmännische Monatshefte, 2017. **162**(4): p. 142-147.

53. Somerset, V.S., et al., *The Use of X-Ray Fluorescence (XRF) Analysis in Predicting The Alkaline Hydrothermal Conversion of Fly Ash Precipitates into Zeolites.* Talanta, 2004. **64**(1): p. 109-114.

54. Figini-Albisetti, A., et al., *Effect of Outgassing Temperature on The Performance of Porous Materials.* Applied Surface Science, 2010. **256**(17): p. 5182-5186.

55. Thommes, M., et al., *Physisorption of Gases, with Special Reference to The Evaluation of Surface Area and Pore Size Distribution (IUPAC Technical Report)*, in *Pure and Applied Chemistry*. 2015. p. 1051.

56. Brunauer, S., P.H. Emmett, and E. Teller, *Adsorption of Gases in Multimolecular Layers.* Journal of the American Chemical Society, 1938. **60**(2): p. 309-319.

57. Barrett, E.P., L.G. Joyner, and P.P. Halenda, *The Determination of Pore Volume and Area Distributions in Porous Substances. I. Computations from Nitrogen Isotherms.* Journal of the American Chemical Society, 1951. **73**(1): p. 373-380.

58. Authier, A., *Early Days of X-Ray Crystallography*. 2013: OUP Oxford.

59. McGlinchey, D., *Characterisation of Bulk Solids*. 2009: John Wiley & Sons.

60. Covington, A.K., R. Bates, and R. Durst, *Definition of pH Scales, Standard Reference Values, Measurement of pH and Related Terminology (Recommendations 1984).* Pure and Applied Chemistry, 1985. **57**(3): p. 531-542.

61. Sircar, S., et al., *Isosteric Heat of Adsorption: Theory and Experiment.* The Journal of Physical Chemistry B, 1999. **103**(31): p. 6539-6546.

62. Pham, T.-H., B.-K. Lee, and J. Kim, *Novel Improvement of CO_2 Adsorption Capacity and Selectivity by Ethylenediamine-Modified Nano Zeolite.* Journal of the Taiwan Institute of Chemical Engineers, 2016. **66**: p. 239-248.

63. Chowdhury, S., et al., *Adsorption Thermodynamics, Kinetics and Isosteric Heat of Adsorption of Malachite Green onto Chemically Modified Rice Husk.* Desalination, 2011. **265**(1): p. 159-168.

64. Doğan, M. and M. Alkan, *Removal of Methyl Violet from Aqueous Solution by Perlite.* Journal of Colloid and Interface Science, 2003. **267**(1): p. 32-41.

65. Skoog, D.A., F.J. Holler, and S.R. Crouch, *Principles of Instrumental Analysis*. 2017: Cengage learning.

66. Weckhuysen, B.M., *Ultraviolet—Visible Spectroscopy.* ChemInform, 2005. **36**(21).

67. Buck, V.E. and S.A. Barringer, *Comparison of Hexane and Petroleum Ether to Measure Surface Oil Content.* Journal of AOAC International, 2007. **90**(6): p. 1729-1730.

Chapter 4 : Carbon Dioxide Adsorption Enhancement of Natural Mordenite-Clinoptilolite Zeolite by Physicochemical Treatment

Abstract

Due to their low cost and abundant availability in many regions around the world, natural zeolites are attractive in many applications including adsorption of CO_2. However, to achieve optimal performance, certain modifications need to be carried out. In this work, we report on investigations involving physicochemical modification (calcination and dealumination) of natural Indonesian calcite-rich mordenite-clinoptilolite zeolites to improve their CO_2 adsorption capacity. The highest specific surface area of 179.44 m^2/g was obtained by dealumination with 12 M HCl and calcination at 400°C. This modification resulted in the highest CO_2 adsorption capacity of 5.218 mmol/g at 0°C and 30 bar; corresponding to the specific surface area normalised CO_2 adsorption capacity of 2.91 x 10^{-2} $mmol/m^2$. This promising result shows that prudent modification of the natural, low-cost zeolite led to excellent CO_2 adsorption affinity when compared with the more costly synthetic materials. This finding, thus, underscores the potential of the natural product to be developed and utilised as a cost-effective CO_2 adsorbent.

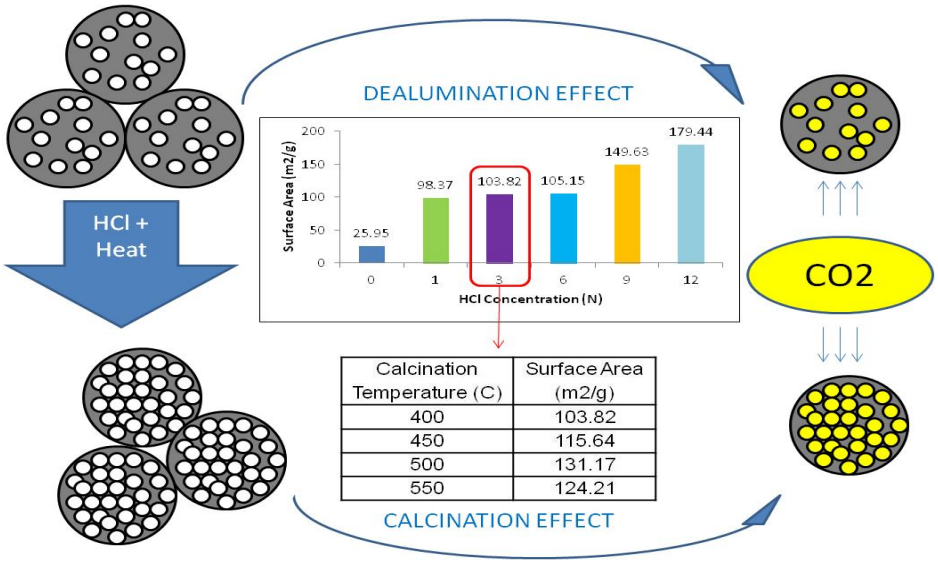

Figure 4.1. Graphical abstract of CO_2 adsorption enhancement of natural mordenite-clinoptilolite zeolite by physicochemical treatment

4.1. Introduction

CO_2 released into the atmosphere by anthropogenic or human activities such as industrial operations, transportation, and electricity generation has been recognised as the leading cause of global warming. CO_2 makes around 81% of greenhouse gasses composition, and its emission has escalated rapidly since the beginning of the last century [1]. CO_2 capture before its release into the atmosphere is one of the strategies to contain its detrimental effect on the global climate. The concept of CO_2 reduction through capture has been applied in the purification or upgrading gas fuels such as natural gas and landfill biogas [2] and producing chemical products [3, 4].

Various CO_2 capture methods have been proposed, one of them being the utilisation of microporous solid adsorbents. Zeolites are one of the prospective candidates in CO_2 adsorption technologies [5-9]. The most effective ones to date have proven to be the synthetic zeolite forms. However, the manufacture of these materials involves high capital expenditure and operating costs, complex processing, and unwanted waste management. Utilisation of natural zeolites as an alternative is desirable because of their abundant availability and low cost [10-12]. However, the adsorption capacity of this potentially valuable natural resource does not compete with their synthetic counterparts [13]. With the possibility of physiochemical enhancement of their gas adsorption capacities, there is a significant interest in adopting natural zeolites in many areas including adsorbing or separating various gases such as hydrogen [14], helium [15], H_2S [16], CO_2 [17], biogas [18-21], and water-vapour [22].

There are six types of natural zeolites which are suitable for gas adsorption and separation, namely clinoptilolite, chabazite, erionite, mordenite, phillipsite, and ferrierite. The three most favoured natural zeolites are clinoptilolite, chabazite, and mordenite [23]. Some of the natural zeolites are intricately structured as a combination of mordenite [$(\underline{Ca},\underline{Na_2},\underline{K_2})\underline{Al_2}\underline{Si_{10}}\underline{O_{24}}\cdot 7\underline{H_2O}$] and clinoptilolite [$(Na,K,Ca)_{2\text{-}3}Al_3(Al,Si)_2Si_{13}O_{36}\cdot 12H_2O$] phases, rather than a single phase zeolite structure. Clinoptilolite is the most common natural zeolite structure in the world having abundant availability. This material has been investigated in various adsorption studies [10], including for CO_2 adsorption. Clinoptilolite

was investigated for CO_2 adsorption from mixture of gases where it was activated or modified by cation exchange [24-26], calcined [17, 18, 27] and pellet bound [28]. For mordenite, CO_2 adsorption studies have been commonly conducted as a single or dominant natural zeolite phase activated by cation exchange [29], amine impregnation [30], and calcination [27].

To date, only a limited number of studies of the effect of zeolite dealumination on CO_2 adsorption have conducted [31, 32], despite the great potential to achieve dramatic increase in porosity and SI/Al ratio, both influence the CO_2 adsorption capacity [33]. This approach engenders a significant CO_2 adsorption efficacy enhancement prospect for mordenite-clinoptilolite natural zeolite. A previous study of biogas purification by CO_2 capture showed that promising results, with scope for further improvement, could be achieved via prudent modification of mordenite-clinoptilolite natural zeolite by chemical and physical treatment [31]. Therefore, the present study was undertaken to explore the possibility of achieving significant improvement in the CO_2 adsorption capacity of natural calcite ($CaCO_3$)-rich mordenite-clinoptilolite zeolite via modification and optimisation of selected physicochemical treatments involving calcination and dealumination.

4.2. Results and Discussion

4.2.1. Characterisation of the pristine natural zeolite

The natural zeolite was characterised in terms of the morphology, dominant mineral phases, elemental composition, crystallinity, and structure as shown below in Figure 4.2 and Table 4.1. The SEM images in Figure 4.2(a) show that the material consists of fine-grained, irregular shaped, polydispersed particles which display noticeable agglomeration propensity. The network of agglomerated particles reflected in BET specific surface area, pore volume and average pore size diameter of 25.95 m^2/g, 5.31 x 10^{-2} cm^3/g, and 8.18 nm, respectively. This observation is consistent with published studies of natural zeolite which report specific surface area range of 14-30 m^2/g [22, 34, 35]. In comparison with the studies by Korkuna et al. [36], this specific surface area was nearer to natural mordenite than natural clinoptilolite.

The XRD spectra in Figure 4.2(b) show that the material comprised natural mordenite and clinoptilolite zeolites and calcite crystals, as indicated by the two diffraction pattern groups at 5-32° and 30-60° 2θ, respectively. The A0 zeolite Match-Score (Table 4.3 and Table 4.5) (by High Score Plus Software) is consistent with the presence of both mordenite and clinoptilolite crystalline phases, with the Match-Score of the former (48) higher than that of the latter (31). Semi-quantitative of XRD analysis indicated that the sample composed of calcite (~50%), mordenite (23%) and clinoptilolite (27%). Although the mordenite phase present was less in semi-quantitative, it was dominant in the Match-Score peak intensity than the clinoptilolite phase. The findings are good agreement with a previous study of the classification of Indonesian (Gunungkidul area, Java Island) natural zeolite as mordenite-clinoptilolite zeolite type [12, 37-39].

The indication of a significant amount of calcite in the sample is also in agreement with recent studies [2] which reported that the material contains more calcium than other alkali metal elements. The concentration of detected elements appears to vary with different techniques.

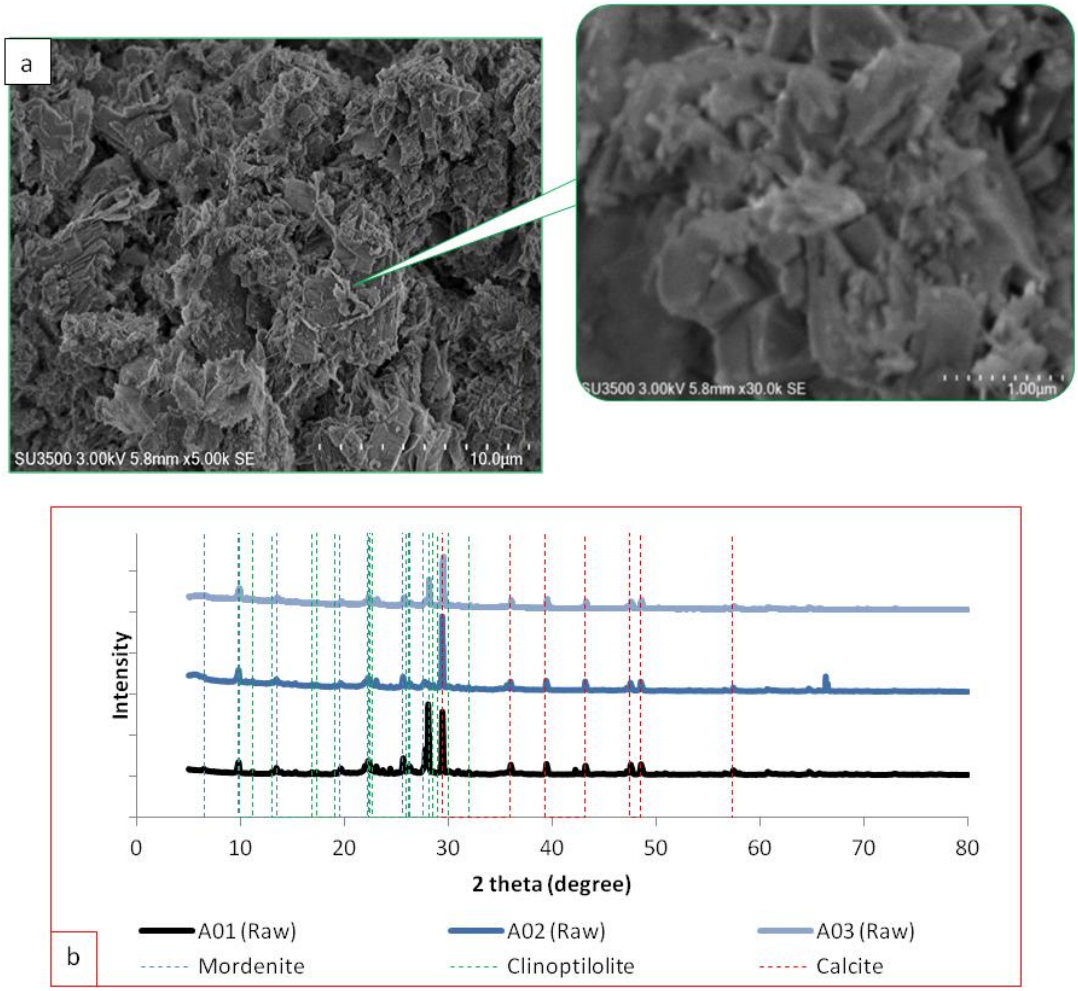

Figure 4.2. The pristine natural mordenite-clinoptilolite zeolite used in this study: (a) SEM photomicrograph; and (b) XRD patterns.

ICP-MS, XRF, and EDX provide information about the bulk structure whilst XPS examines the surface composition of the outermost 10 nm of the sample. Regardless, Table 4.1 reveals that the majority of the oxide composition of this natural zeolite is in the form of CaO, SiO_2, and Al_2O_3, consistent with calcite, mordenite-clinoptilolite dominated chemical compounds. This composition is different from that of other natural mordenite and clinoptilolite zeolites which displayed higher silica concentration [36].

The Si/Al ratio determined by different analytical methods used in the range of 3.5 – 6.1, which is a good start-up characteristic for utilisation in gas and water-vapour capture [40-

43]. In the following, we carry out specific treatment of the material to enhance the Si/Al ratio and with this its CO_2 adsorption characteristics.

Table 4.1. The composition of the pristine natural mordenite-clinoptilolite zeolite by different analytical techniques.

Element	XPS – surface (%)	Oxide Element	ICP-MS (%)	XRF (%)	EDX (%)
Ca	22.5	CaO	57.2	44.7	6.8
Mg	-	MgO	0.9	1.7	-
K	4.2	K_2O	1.1	1.0	1.1
Na	-	Na_2O	2.5	8.3	0.7
Fe	1.3	Fe_2O_3	1.9	5.9	15.2
Al	6.7	Al_2O_3	8.2	5.4	13.5
Si	22.7	SiO_2	28.4	33.1	62.7
C	13.9				
O	28.7				
Si/Al	3.9		3.5	6.1	4.6

4.2.2. Natural zeolite physiochemical treatment

The zeolite properties affecting CO_2 adsorption are the specific surface area, crystallinity, and Si/Al ratio. Dealumination (chemical treatment) and calcination (physical treatment) were selected to alter material properties and achieve enhanced CO_2 adsorption capacity.

4.2.2.1. Effect of acid concentration on dealumination

The acid treatment of natural zeolite decreases the aluminum (Al) concentration. The process also removes alkali cations such as Ca, Na, and K as well as other metals such as iron (Fe). The changes in the elemental composition, as well as the Si/Al ratio, are shown in Figure 4.3(a-d). The graphs show that the alkali metals' content decreased relative to Si concentration, indicating that the acid treatment had no noticeable impact on the Si or Si-O

bonds present in the structure. In the case of Al removal, the dissociation energy of the Al-O bond (116 kcal/mol) is lower than that of the Si-O bond (190 kcal/mol) [44, 45]. Consequently, the Si/Al ratio increased when treatment is carried out with a higher concentration of HCl, exceeding 10 when 12 M HCl is used which shown in Figure 4.3(a). The highest Si/Al ratio was obtained at A5 zeolite with the value of 11.9, 11.1, and 11.0 based on XPS, EDX, and XRF analysis, respectively.

In the process of dealumination, the acid anion attracts the metal ions which results in the formation of salt compounds. The salts were then removed from the structural channels by washing with water. These results increased the porosity of the material and produced a higher specific surface area. The specific surface area enhancement after dealumination treatment is shown in Figure 4.3(e). The highest specific surface area was achieved at A5 zeolite of 179.44 m^2/g. As expected, higher acid concentration led to the increased specific surface area as the metal ions are removed, and possibly some organic impurities. The compilation of specific surface area and the Si/Al ratio effect of various dealumination treatments is shown in Table 4.2.

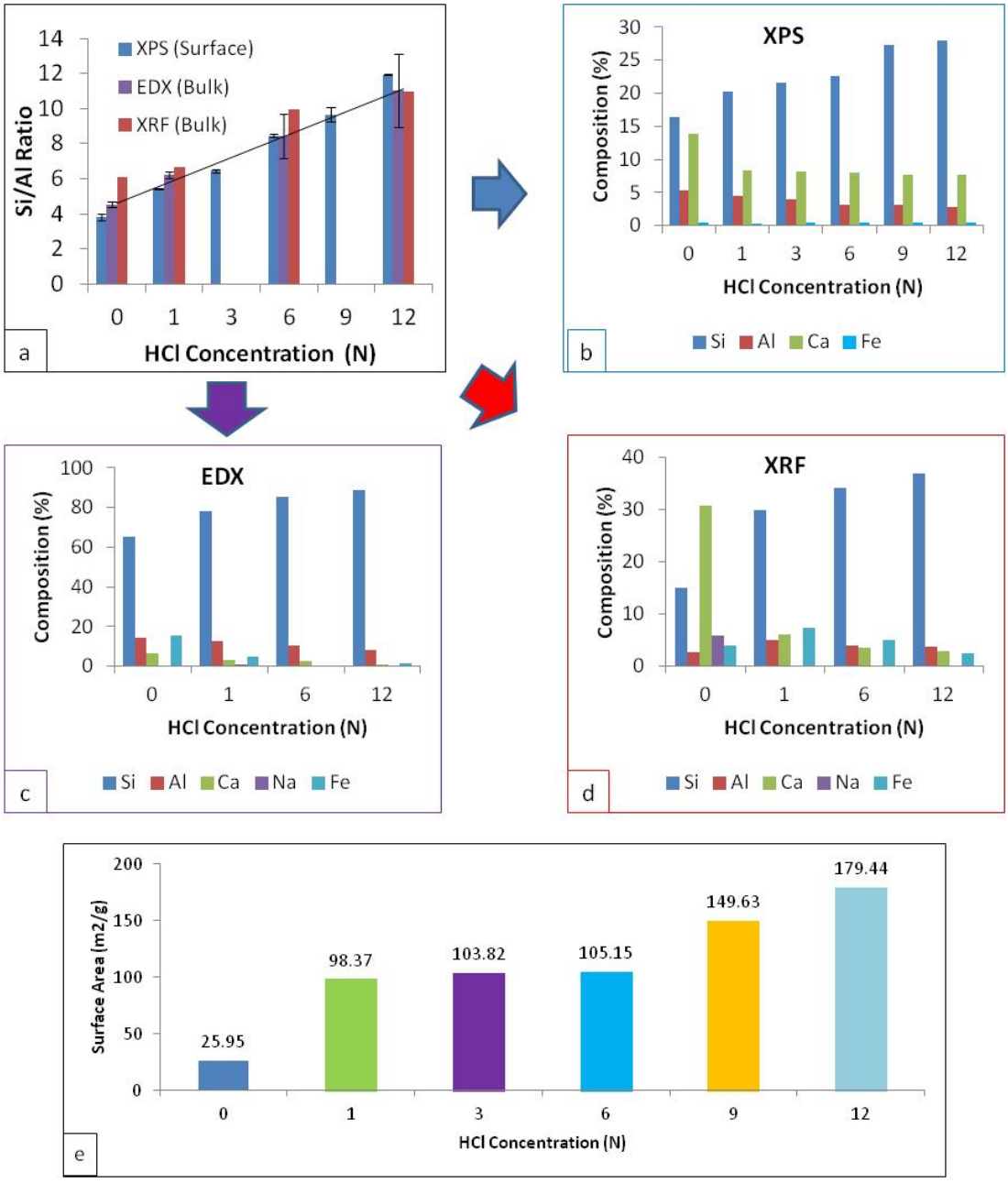

Figure 4.3. Transformation of natural mordenite-clinoptilolite zeolite post various dealumination acid concentration and calcination at 400°C: (a) Si/Al ratio; (b) Surface element composition (XPS); (c) Bulk element composition (EDX); (d) Bulk element composition (XRF); and (e) Specific surface area

Table 4.2. Specific surface area and Si/Al ratio of natural mordenite-clinoptilolite zeolite post various dealumination acid concentration and calcination at 400°C

Code	Calcination Temp. (°C)	HCl Concentration (M)	Specific surface area (m^2/g)	Si/Al ratio		
				XPS	EDX	XRF
A0	0	0	25.95	3.9	4.6	6.1
A1	400	1.0	98.37	5.4	6.2	6.7
A2		3.0	103.82	6.5	-	-
A3		6.0	105.15	8.5	8.4	10.0
A4		9.0	149.63	9.7	-	-
A5		12.0	179.44	11.9	11.1	11.0

The morphology of the particles after dealumination is shown in Figure 4.4(a). The SEM images reveal that the structure of the material does not significantly transform when compared with the pristine structure shown in Figure 4.2(a). The images show multilayers of irregular-shaped, agglomerated mass of colloidal size particles. XRD analyses, on the other hand, indicated the formation of new structures post-dealumination as shown in Figure 4.4(b); which also supported by the search-match analysis as shown in Table 4.3. Part of the zeolite alumina-silicate structure transformed into quartz (diffraction peaks at 21°, 27°, and 50° 2θ) due to aluminum removal. The presence of quartz is also indicated by the quartz Match-Score in Table 4.2 (A1-A5 zeolite).

The formation of a new calcium silicate crystal structure, anorthite, by reaction between calcite and silica with the disappearance of calcite, is indicated by the XRD data. This anorthite product also is also indicated to be effective for CO_2 removal, creating a better adsorptive structure than calcite [46-49]. Particularly for the zeolite structure, there was no transformation of mordenite-clinoptilolite zeolite crystal structure which shown the Match-Score for mordenite and clinoptilolite of 46-52 and 20-25, respectively.

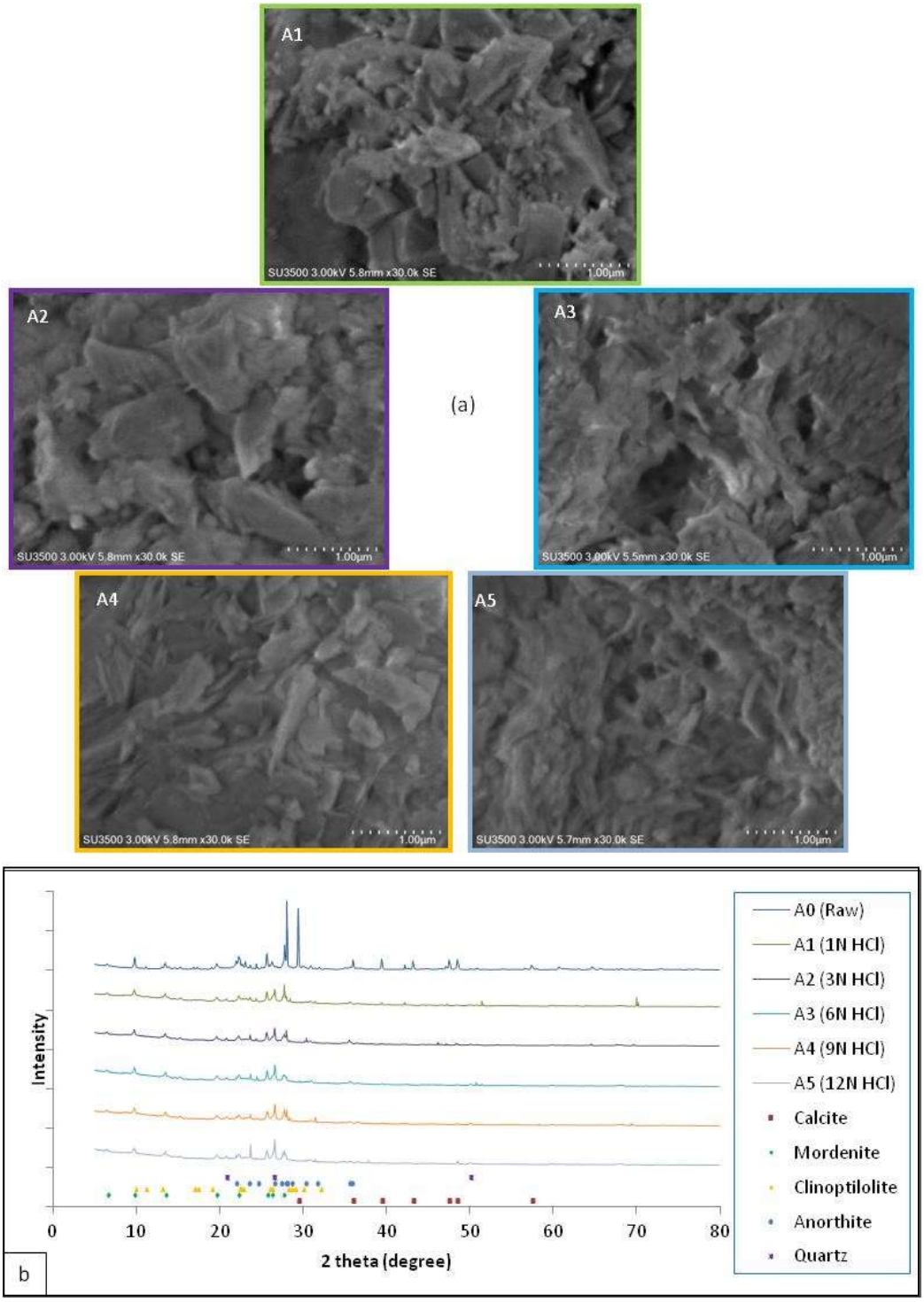

Figure 4.4. Characterisation of the natural mordenite-clinoptilolite zeolites post various dealumination acid concentration and calcination at 400°C: (a) SEM photomicrograph; and (b) Crystallinity and XRD patterns.

Table 4.3. The Search-Match analysis of natural mordenite-clinoptilolite zeolite crystal structure post various dealumination acid concentration and calcination at 400°C

Code	HCl Concentration (M)	Calcination Temp. (°C)	Crystal Structure Match Score				
			Calcite	Mordenite	Clinoptilolite	Anorthite	Quartz
A0	0	0	63	48	31	-	-
A1	1.0	400	-	51	24	35	43
A2	3.0		-	52	21	37	51
A3	6.0		-	52	23	31	53
A4	9.0		-	46	20	27	54
A5	12.0		-	52	21	29	51

4.2.2.2. Calcination

Another approach for optimising natural zeolite adsorption performance is calcination which conducted at high temperatures. Recent studies suggested calcination of zeolite at temperature > 350°C can remove gases trapped in the pores [50], while zeolite calcination well over 500°C transformed it into others structure of which the pores are destroyed [51, 52], typically as compact aluminosilicate, siliceous phase, or amorphous solids [53-58]. Therefore, calcination was conducted in the temperature range 400-550°C in this work to open the pores blocked by the organic compound and alter the specific surface area, the Si/Al ratio, crystallinity, and morphology as shown in Table 4.4, Table 4.5, and Figure 4.5.

A2 zeolite (3 M HCl dealumination) with a specific surface area of 103.82 m^2/g was selected as the reference material for the calcination temperature variation at a fixed Si/Al ratio (6.5). The Si/Al ratio of 6.5 (Table 4.2) indicates the hydrophobic surface which is more favourable for gas adsorption than water-vapour adsorption [41, 59]. Some published studies indicated the hydrophobic surface was provided by the Si/Al ratio value of over 5 [40, 43, 60, 61], so this ratio suits to the minimum requirement of hydrophobic surface.

Table 4.4. Specific surface area and Si/Al ratio of natural mordenite-clinoptilolite zeolite crystal and products structure post 3 M HCl dealumination and various calcination temperatures

Code	Calcination Temp. (°C)	HCl Concentration (M)	Specific Surf. Area (m^2/g)	Si/Al ratio
A0	0	0	25.95	3.9
A2-0	0	3.0	146.91	7.1
D0 = A2	400		103.82	6.5
D1	450		115.64	6.4
D2	500		131.17	6.5
D3	550		124.21	6.7

Table 4.5. The Search-Match analysis of natural mordenite-clinoptilolite zeolite crystal and products structure post 3 M HCl dealumination and calcination at various temperatures

Code	Calcination Temp. (°C)	HCl Concentration (M)	Crystal Structure Match Score				
			Calcite	Mordenite	Clinoptilolite	Anorthite	Quartz
A0	0	0	63	48	31	-	-
A2-0	0	3.0	56	51	26	-	41
D0	400		-	52	21	37	51
D1	450		-	51	24	27	37
D2	500		-	53	23	28	45
D3	550		-	52	22	30	44

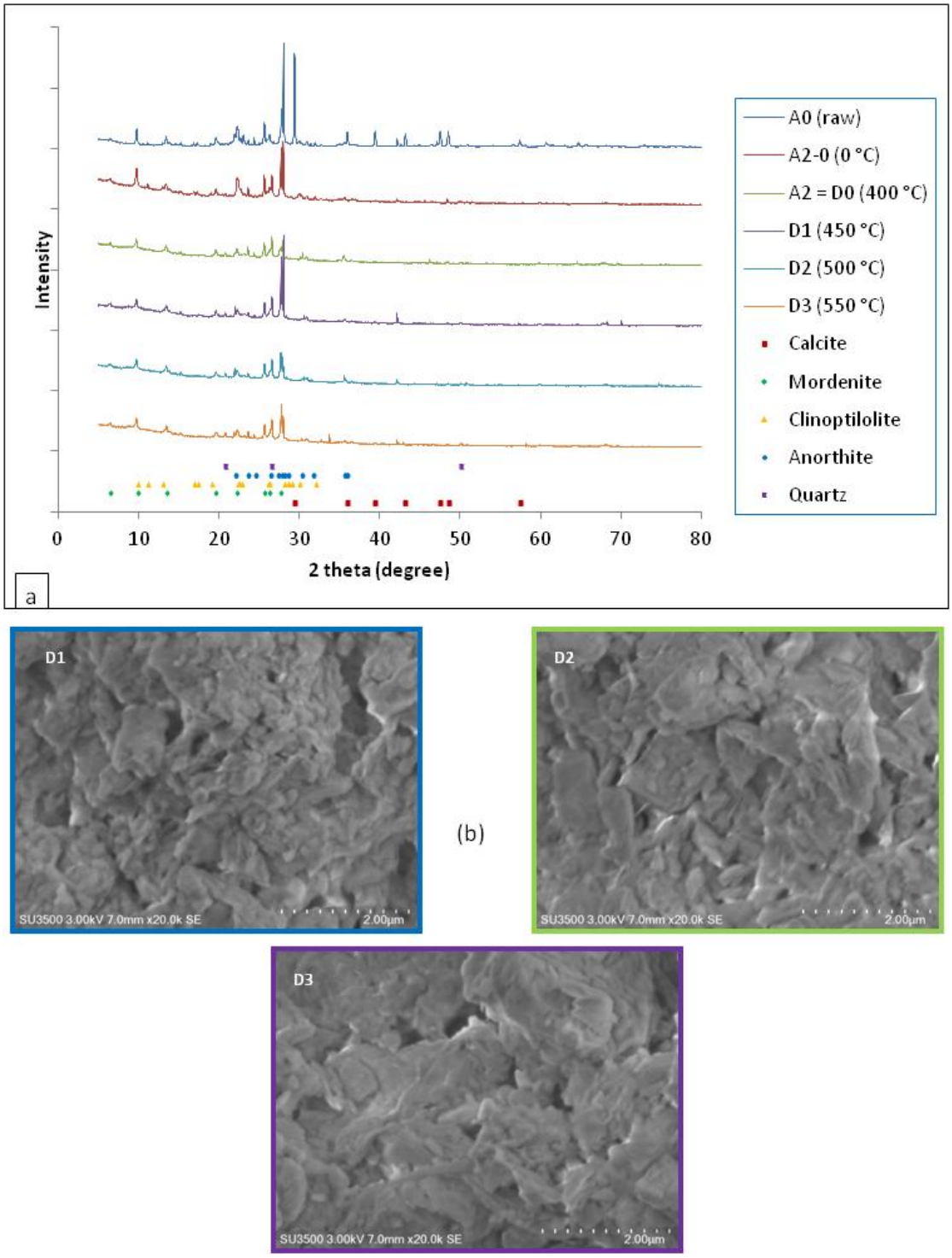

Figure 4.5. Characterisation of the natural mordenite-clinoptilolite zeolites post 3 M HCl dealumination and various calcination temperatures: (a) Crystallinity and XRD patterns (b) SEM photomicrographs.

Table 4.4 shows the specific surface area and the Si/Al ratio effect of the various calcination temperatures, including the dealumination treatment only or non-calcination treatment (A2-0 zeolite). Particularly for A2-0 zeolite, although it has the highest specific surface area, the crystal structure still contained calcite as shown in Table 4.5. The carbonate structure has to decompose for creating the adsorptive structure of CO_2 [46-49]. It also has the Si/Al ratio of 7.1 as the highest ratio than other calcination treatments, but this different value for natural material was considered a similar effect.

For the various calcination treatment (D0-D3 zeolite), the specific surface area increases gradually with increasing temperature from 400 ^{o}C to 500 ^{o}C but then decrease at 550 ^{o}C. As a natural material, the range of specific surface area was not changing considerably, so the appointed range of calcination temperature variable did not effect on this properties. The insignificant effect also happened on the Si/Al ratio, the interval of the ratio was between 6.4-6.7 for the temperature of 400-550 ^{o}C. It showed that the increasing temperature did not provide a significant change in the Si/Al ratio.

Figure 4.5(a) which supported by the Match-Score in Table 4.5 shows the crystal structure of natural zeolite on various calcination treatments. There are two or three types of structure for each material on this graph that are zeolite crystal type, calcium crystal type, and silica oxide. The calcination fostered the transformation of calcite into anorthite which indicated by the Match-Score analysis shown in Table 4.5. The overall results confirm that the calcination played a significant role in the structural modification of the sample. Particularly for D2 zeolite, the Match-Score analysis shows the highest intensity of mordenite than others, which indicates the optimum mordenite construction by calcination.

Figure 4.5(b) shows the morphological change of the sample at different calcination temperatures and relative to Figure 4.4(a)-A2 at the lowest temperature variable (400 ^{o}C). There is no significant change of morphology with temperature which is consistent with the similar properties of the specific surface area and the Si/Al ratio as mentioned in the previous part. However, the highest temperature of Figure 4.5(b)-D3 showed slightly different particle shape, reflecting some subtle structure change due to higher temperature effect [53-58] and specific surface area reduction [51, 52].

4.2.3. CO_2 adsorption

For CO_2 adsorption studies, the material with the highest specific surface area was selected for the best performance [28, 62], especially in high-pressure adsorption loading [33, 63]. Based on the nitrogen adsorption/ BET results in Table 4.2 and Table 4.4, the A5 zeolite was selected. The results of the CO_2 adsorption measurements for A5 zeolite are shown in Figure 4.6(a). These were determined under isotherm conditions at three different temperatures and were carried out at the pressures up to 30 bar.

At temperatures of 10 and 25°C, the adsorption capacity of the A5 zeolite showed a similar trend as a function of the pressure and reached maximum capacity at 30 bar of 2.427 and 2.326 mmol/g, respectively. The adsorption at both temperatures increased rapidly with pressure between 0-3 bar, then increased gradually up to 30 bar. After 3 bar, the adsorption capacity at 25°C was slightly greater than that at 10°C. The results indicate that at temperatures of 10 and 25°C the material performs well at the low-pressure condition, but reaches saturation when pressure increases. The highest adsorption capacity of 5.218 mmol/g was achieved at 0°C and 30 bar. The CO_2 adsorption proceeded rapidly in the pressure range of 0-3 bar, then gradually increases between 3-20 bar, which was followed by a rapid increase above 20 bar. The results suggest that the works well in low and high-pressure conditions at 0°C and agree with other studies which reported that CO_2 adsorption capacity is higher at the lower temperature [64, 65].

The isosteric heat of adsorption (Q_{st}), shown in Figure 4.6(b), was determined from the CO_2 adsorption isotherm data at 0, 10, 25°C employing the Clausius-Clapeyron equation. The initial isosteric heat adsorption value of the A5 zeolite was 35.857 kJ/mol. The isosteric value lower than 50 kJ/mol suggests physisorption mechanism as the dominant process in the interaction between CO_2 and adsorbent [66] and also indicates a reversible adsorption process, which may provide opportunities for regeneration.

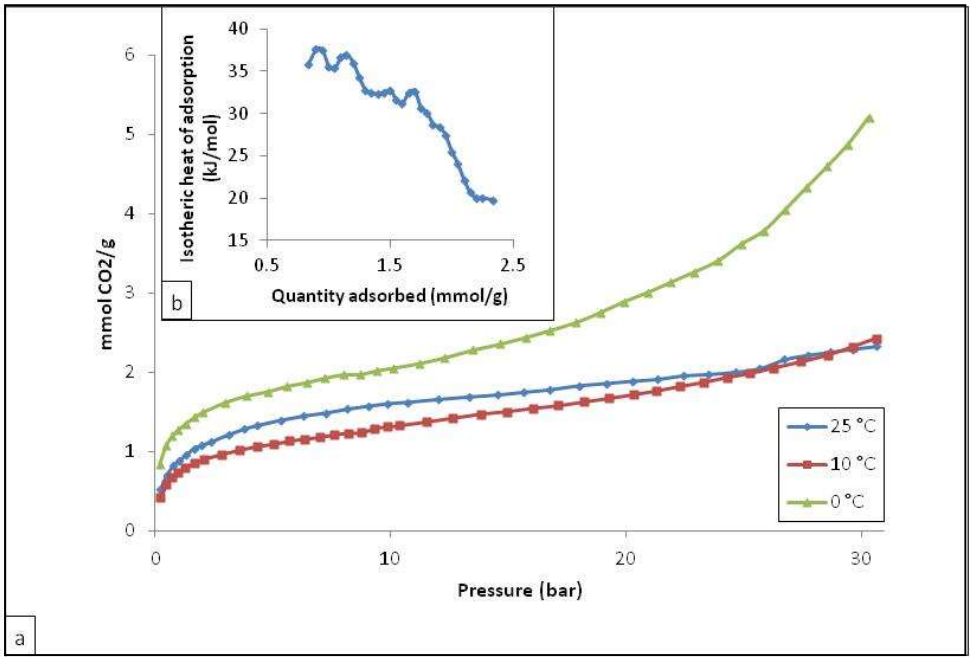

Figure 4.6. (a) CO_2 isotherm adsorption capacity of A5 zeolite at 0, 10 and 25 ° C; and (b) Isosteric heat of adsorption of A5 zeolite

4.2.4. Comparison with synthetic adsorbents

As a natural pores material, the mordenite-clinoptilolite natural zeolite had a lower specific surface area than the synthetic material developed for CO_2 adsorption, even after modification by dealumination. For making an adequate comparison with synthetic adsorbents, the parameter of the normalised specific surface area was applied as shown in Table 4.6 and 4.7.

Table 4.6 shows the specific surface area normalised CO_2 adsorption capacity at 1 bar and 25°C as the room temperature application for A5 zeolite developed in this work and best performing synthetic materials taken from the literature. The data shows that the normalised specific surface area CO_2 adsorption capacity of A5 is even higher than some synthetic material. For the highest CO_2 adsorption capacity results, the comparison at 0°C, 1 bar versus 30 bar is shown in Table 4.7. It is pertinent to note that although the adsorption capacity of A5 zeolite is lower than other synthetic adsorbents, the specific

surface area normalised CO_2 adsorption capacity is the highest. It means that the A5 zeolite has an excellent CO_2 adsorption surface affinity compare with others at 0°C adsorption.

The low cost and simple material properties optimisation and production encourage utilisation and development of the A5 zeolite for CO_2 adsorption. Furthermore, the significant enhancement the properties of the material (e.g., Si/Al ratio, micro-porosity/ surface area, and crystallinity) provides huge opportunities for use in other fields including catalysis, liquid component adsorption, water-vapour adsorption, dyes removal, and waste removal. The results of this study also encourage the study and application of other forms of natural mordenite-clinoptilolite zeolites which are abundant in many regions around the world.

Table 4.6. The CO_2 adsorption capacity of various zeolite at 1 bar and 25°C

Sample	Specific Surf. Area (m^2/g)	CO_2 uptake (mmol/g)	Norm. CO_2 Uptake ($x\ 10^{-3}$ mmol/m^2)	Reference
CEM 750	3360	4.38	1.304	[7]
NZ	681.86	4.89	7.172	[66]
Zeolite 13X	584	5.19	8.887	[67]
H-SSZ-13	764	3.98	5.209	[6]
K@RWY	716	4.98	6.955	[68]
NaX-Fau	500	3.9	7.800	[69]
Na-MOR	425	2.9	6.824	[69]
ZAPS	426	2.6	6.103	[27]
ZNT	266	1.1	4.135	[27]
A5 Zeolite	179.44	0.954	5.317	This study

Table 4.7. The CO_2 adsorption capacity of various zeolite at 0°C

Sample	Press. (bar)	Specific Surf. Area (m^2/g)	CO_2 Uptake (mmol/g)	Norm. CO_2 Uptake (x 10^{-3}mmol/m^2)	Reference
CEM 750	1	3360	6.92	2.060	[7]
KLB2		1122	6.3	5.615	[62]
CHA		572	3.5	6.119	[70]
Phloroglucinol-based POFs		917	4.2	4.580	[71]
A5 Zeolite		179.44	1.35	7.523	This study
SEW-MCN-1-130	30	655	15.4	23.511	[72]
KLB2		1122	15.4	13.725	[62]
AMB3-500		3298	30.2	9.157	[73]
Cu-SBA-15-100-5		861.5	17.1	19.849	[74]
A5 Zeolite		179.44	5.22	29.079	This study

4.3. Conclusion

In this work, we investigated the possibility to enhance the CO_2 adsorption capacity of natural, impure mordenite-clinoptilolite zeolite by dealumination and calcination. Characterisation of the pristine material showed that the mordenite and clinoptilolite structures are main zeolite crystal types with calcite as the main impurity. Dealumination increased the specific surface area from 26 to 179 m^2/g and the Si/Al ratio to 11-12 at the highest concentration of HCl of 12 M for 24 h and calcination at 400°C for 3 h. The modification leading to the highest specific surface area was investigated for its CO_2 adsorption capacity. The highest CO_2 adsorption capacity of 5.218 mmol/g was achieved at 0°C and pressure 30 bar. This result corresponds to a specific surface area normalised CO_2 adsorption capacity of 2.91 x 10^{-2} mmol/m^2 which compares well with synthetic analogs. The results of this work demonstrate that the potential of deployment of modified natural zeolites containing calcite impurity for application as a CO_2 adsorbent. Their low price, ease of modification and abundant availability make them attractive alternatives to synthetic adsorbents.

References

1. Delahay, G. and B. Coq, *Pollution Abatement Using Zeolites: State of The Art and Further Needs*, in *Zeolites for Cleaner Technologies*. 2002, Published by imperial college press and distributed by world scientific publishing co. p. 345-374.

2. Wahono, S.K., et al., *Preliminary Study: Combination of Amine and Natural Zeolite as New Adsorbent Material for CO_2 Capture*, in *Chemeca 2016: Chemical Engineering-Regeneration, Recovery and Reinvention*. 2016. p. 900-910.

3. Pan, S.-Y., et al., *An Innovative Approach to Integrated Carbon Mineralization and Waste Utilization: A Review.* Aerosol Air Qual Res, 2015. **15**: p. 1072-1091.

4. Li, P., et al., *Challenges and Perspectives on Carbon Fixation and Utilization Technologies: An Overview.* Aerosol Air Qual. Res, 2016. **16**: p. 1327-1344.

5. Siriwardane, R.V., et al., *Adsorption of CO_2 on Zeolites at Moderate Temperatures.* Energy & Fuels, 2005. **19**(3): p. 1153-1159.

6. Hudson, M.R., et al., *Unconventional, Highly Selective CO_2 Adsorption in Zeolite SSZ-13.* Journal of the American Chemical Society, 2012. **134**(4): p. 1970-1973.

7. Xia, Y., et al., *Superior CO_2 Adsorption Capacity on N-Doped, High-Surface-Area, Microporous Carbons Templated from Zeolite.* Advanced Energy Materials, 2011. **1**(4): p. 678-683.

8. Cavenati, S., C.A. Grande, and A.E. Rodrigues, *Adsorption Equilibrium of Methane, Carbon Dioxide, and Nitrogen on Zeolite 13X at High Pressures.* Journal of Chemical & Engineering Data, 2004. **49**(4): p. 1095-1101.

9. Stevens, R.W., R.V. Siriwardane, and J. Logan, *In Situ Fourier Transform Infrared (FTIR) Investigation of CO_2 Adsorption onto Zeolite Materials.* Energy & Fuels, 2008. **22**(5): p. 3070-3079.

10. Wang, S. and Y. Peng, *Natural Zeolites as Effective Adsorbents in Water and Wastewater Treatment.* Chemical Engineering Journal, 2010. **156**(1): p. 11-24.

11. Ozaydin, S., G. Kocer, and A. Hepbasli, *Natural Zeolites in Energy Applications.* Energy Sources, Part A: Recovery, Utilization, and Environmental Effects, 2006. **28**(15): p. 1425-1431.

12. Marantos, I., G.E. Christidis, and M. Ulmanu, *Zeolite Formation and Deposits*, in *Handbook of Natural Zeolites*, V.J. Inglezakis and A.A. Zorpas, Editors. 2012, Bentham Science Publishers. p. 28-51.

13. Misaelides, P., *Application of Natural Zeolites in Environmental Remediation: A Short Review.* Microporous and Mesoporous Materials, 2011. **144**(1–3): p. 15-18.

14. Farjoo, A., S.M. Kuznicki, and M. Sadrzadeh, *Hydrogen Separation by Natural Zeolite Composite Membranes: Single and Multicomponent Gas Transport.* Materials, 2017. **10**(10): p. 1159.

15. Arami-Niya, A., et al., *Gravimetric Adsorption Measurements of Helium on Natural Clinoptilolite and Synthetic Molecular Sieves at Pressures up to 3500 kPa.* Microporous and Mesoporous Materials, 2017. **244**(Supplement C): p. 218-225.

16. Yaşyerli, S., et al., *Removal of Hydrogen Sulfide by Clinoptilolite in a Fixed Bed Adsorber.* Chemical Engineering and Processing: Process Intensification, 2002. **41**(9): p. 785-792.

17. Karousos, D.S., et al., *A Study on Natural Clinoptilolite for CO_2/N_2 Gas Separation.* Separation Science and Technology, 2016. **51**(1): p. 83-95.

18. Alonso-Vicario, A., et al., *Purification and Upgrading of Biogas by Pressure Swing Adsorption on Synthetic and Natural Zeolites.* Microporous and Mesoporous Materials, 2010. **134**(1–3): p. 100-107.

19. Paolini, V., et al., *Biogas Cleaning and Upgrading with Natural Zeolites from Tuffs.* Environmental Technology, 2016. **37**(11): p. 1418-1427.

20. Sadchikov, A., et al., *Use of Natural Zeolite in Systems for Separation and Purification of Gas Mixtures Containing Methane*, in *Key Engineering Materials*. 2017, Trans Tech Publ. p. 179-182.

21. Wahono, S.K. and W.A. Rizal, *Biogas Filter Based on Local Natural Zeolite Materials.* International Journal of Renewable Energy Development, 2014. **3**(1): p. 1-5.

22. Favvas, E.P., et al., *Clinoptilolite, a Natural Zeolite Material: Structural Characterization and Performance Evaluation on Its Dehydration Properties of Hydrocarbon-Based Fuels.* Microporous and Mesoporous Materials, 2016. **225**(Supplement C): p. 385-391.

23. Wang, S., *Utilisation of Natural Zeolites for Air Separation and Pollution Control*, in *Handbook of Natural Zeolites*, V.J. Inglezakis and A.A. Zorpas, Editors. 2012, Bentham Science Publishers. p. 569-587.

24. Aguilar-Armenta, G., et al., *Adsorption Kinetics of CO_2, O_2, N_2, and CH_4 in Cation-Exchanged Clinoptilolite.* The Journal of Physical Chemistry B, 2001. **105**(7): p. 1313-1319.

25. Gargiulo, N., F. Pepe, and D. Caputo, *CO_2 Adsorption by Functionalized Nanoporous Materials: A Review.* Journal of nanoscience and nanotechnology, 2014. **14**(2): p. 1811-1822.

26. Sánchez-Ruíz, A., I. Robles-Gutiérrez, and F. Espejel-Ayala, *Preparation of Zeolitic Material Using Natural Clinoptilolite for CO_2 Capture.* Revista Mexicana de Ingeniería Química, 2018. **17**(2): p. 573-585.

27. Hernández-Huesca, R., L. Díaz, and G. Aguilar-Armenta, *Adsorption Equilibria and Kinetics of CO_2, CH_4 and N_2 in Natural Zeolites.* Separation and Purification Technology, 1999. **15**(2): p. 163-173.

28. Arefi Pour, A., et al., *Performance Evaluation of Clinoptilolite and 13X Zeolites in CO_2 Separation from CO_2/CH_4 Mixture.* Journal of Natural Gas Science and Engineering, 2015. **26**: p. 1246-1253.

29. Vansant, E.F. and R. Voets, *Adsorption of Binary Gas Mixtures in Ion-Exchanged Forms of Mordenite.* Journal of the Chemical Society, Faraday Transactions 1: Physical Chemistry in Condensed Phases, 1981. **77**(6): p. 1371-1380.

30. Su, F., et al., *Adsorption of CO_2 on Amine-Functionalized Y-Type Zeolites.* Energy & Fuels, 2010. **24**(2): p. 1441-1448.

31. Wahono, S.K., et al., *Metoda dan Alat untuk Meningkatkan Kadar Methana dalam Biogas [Methods and Tools for Increasing Methane Contents of Biogas]*. Patent, 2010. IDP000038082: Indonesia.

32. Kusrini, E., et al., *Biogas From Palm Oil Mill Effluent: Characterization and Removal of CO_2 Using Modified Clinoptilolite Zeolites in a Fixed-Bed Column.* International Journal of Technology, 2016. **4**: p. 625-634.

33. Bonenfant, D., et al., *Advances in Principal Factors Influencing Carbon Dioxide Adsorption on Zeolites.* Science and Technology of Advanced Materials, 2008. **9**(1): p. 013007.

34. Hernawan, et al., *Modification of Gunungkidul Natural Zeolite as Bioethanol Dehydrating Agents.* Energy Procedia, 2015. **65**: p. 116-120.

35. Dziedzicka, A., B. Sulikowski, and M. Ruggiero-Mikołajczyk, *Catalytic and Physicochemical Properties of Modified Natural Clinoptilolite.* Catalysis Today, 2016. **259**: p. 50-58.

36. Korkuna, O., et al., *Structural and Physicochemical Properties of Natural Zeolites: Clinoptilolite and Mordenite.* Microporous and Mesoporous Materials, 2006. **87**(3): p. 243-254.

37. Kogel, J.E., *Industrial Minerals and Rocks: Commodities, Markets, and Uses*. 2006: SME.

38. Lestari, D.Y., *Kajian Modifikasi dan Karakterisasi Zeolit Alam dari Berbagai Negara [Review of Natural Zeolites Modification and Characterization from Various Countries]*, in *National Seminar of Chemistry and Education of Chemistry*. 2010,

Education of Chemistry Department, Yogyakarta State University: Yogyakarta–Indonesia.

39. Kusdarto, K., *Potency of Zeolite in Indonesia.* Jurnal Zeolit Indonesia, 2008. **7**(2): p. 78-87.

40. Sriatun, S. and A. Darmawan, *Dealuminasi Zeolit Alam Cipatujah Melalui Penambahan Asam dan Oksidator [Dealumination of Cipatujah Natural Zeolites by Acid and Oxidants Addition]*. Kimia Sains dan Aplikasi, 2005. **8**(2).

41. Cosoli, P., et al., *Hydrogen Sulphide Removal from Biogas by Zeolite Adsorption: Part I. GCMC Molecular Simulations.* Chemical Engineering Journal, 2008. **145**(1): p. 86-92.

42. Jayuska, A., B. Sitorus, and A. Widyastuti, *Karbon Aktif dari Limbah Cangkang Sawit Sebagai Adsorben Gas dalam Biogas Hasil Fermentasi Anaerobik Sampah Organik [Activated Carbon from Waste Shells Gas Oil As Adsorbent in Biogas Anaerobic Fermentation of Organic Waste]*. Jurnal Kimia Khatulistiwa, 2013. **2**(1): p. 30-33.

43. Mandasari, W., B. Sitorus, and D.R. Jati, *Pembuatan dan Karakterisasi Adsorben Gas H_2S dari Zeolit Alam [Preparation and Characterization of Natural Zeolite as H_2S Adsorbents]*. Jurnal Kimia Khatulistiwa, 2014. **3**(2): p. 56-63.

44. Maleiva, L.T.N., B. Sitorus, and D.R. Jati, *Penurunan Konsentrasi Gas Karbon Monoksida dari Kendaraan Bermotor Menggunakan Adsorben Zeolit Alam [Decreased concentration of Carbon Monoxide Gas Vehicle Using Natural Zeolite Adsorbents]*. Jurnal Kimia Khatulistiwa, 2015. **4**(1): p. 26-33.

45. Weitkamp, J. and L. Puppe, *Catalysis and Zeolites Fundamentals and Applications*. Springer Archives. 1999, Berlin, Heidelberg: Springer Berlin Heidelberg : Imprint: Springer.

46. Han, R., et al., *Ultralow Friction of Carbonate Faults Caused by Thermal Decomposition.* Science, 2007. **316**(5826): p. 878-881.

47. Luo, C., et al., *Wet Mixing Combustion Synthesis of CaO-Based Sorbents for High Temperature Cyclic CO_2 Capture.* Chemical Engineering Journal, 2015. **267**: p. 111-116.

48. Abanades, J.C., *The Maximum Capture Efficiency of CO_2 Using a Carbonation/Calcination Cycle of $CaO/CaCO_3$.* Chemical Engineering Journal, 2002. **90**(3): p. 303-306.

49. Sun, Z., et al., *Density Functional Theory Study on The Thermodynamics and Mechanism of Carbon Dioxide Capture by CaO and CaO Regeneration.* RSC Advances, 2016. **6**(45): p. 39460-39468.

50. Arletti, R., et al., *Evidence for The Formation of Stable CO_2 Hydrates in Zeolite NaY: Structural Characterization by Synchrotron X-Ray Powder Diffraction.* Microporous and Mesoporous Materials, 2016. **228**: p. 248-255.

51. Cobzaru, C., *Modified Zeolites: Modification of Natural Zeolites for Catalytic Applications*, in *Handbook of Natural Zeolites*, V.J. Inglezakis and A.A. Zorpas, Editors. 2012. p. 185-213.

52. Wang, S. and Z.H. Zhu, *Characterisation and Environmental Application of an Australian Natural Zeolite for Basic Dye Removal from Aqueous Solution.* Journal of Hazardous Materials, 2006. **136**(3): p. 946-952.

53. Roque-Malherbe, R., *Applications of Natural Zeolites in Pollution Abatement and Industry*, in *Handbook of Surfaces and Interfaces of Materials*, H.S. Nalwa, Editor. 2001, Academic Press. p. 495-522.

54. Roque-Malherbe, R., et al., *The State of Iron in Natural Zeolites: A Mössbauer Study.* Zeolites, 1990. **10**(7): p. 685-689.

55. Breck, D.W., *Zeolite Molecular Sieves: Structure, Chemistry, and Use*. 1984: R.E. Krieger.

56. Hernandez-Velez, M., et al., *New Materials Obtained from High Temperature Phase Transformations of Natural Zeolites.* Journal of Materials Science Letters, 1995. **14**(23): p. 1653-1656.

57. Arcoya, A., et al., *Role of The Countercations on The Molecular Sieve Properties of a Clinoptilolite.* Microporous Materials, 1996. **7**(1): p. 1-13.

58. Mimura, H. and T. Kanno, *Processing of Radioactive Waste Solution with Zeolites (I): Thermal-Transformations of Na, Cs and Sr Forms of Zeolites.* Science reports of the Research Institutes, Tohoku University. Ser. A, Physics, chemistry and metallurgy, 1980. **29**: p. 102-111.

59. Calleja, G., J. Pau, and J.A. Calles, *Pure and Multicomponent Adsorption Equilibrium of Carbon Dioxide, Ethylene, and Propane on ZSM-5 Zeolites with Different Si/Al Ratios.* Journal of Chemical & Engineering Data, 1998. **43**(6): p. 994-1003.

60. Shirazi, L., E. Jamshidi, and M.R. Ghasemi, *The Effect of Si/Al Ratio of ZSM-5 Zeolite on Its Morphology, Acidity and Crystal Size.* Crystal Research and Technology, 2008. **43**(12): p. 1300-1306.

61. Ramesh, K. and D.D. Reddy, *Chapter Four - Zeolites and Their Potential Uses in Agriculture*, in *Advances in Agronomy*, D.L. Sparks, Editor. 2011, Academic Press. p. 219-241.

62. Singh, G., et al., *Single Step Synthesis of Activated Bio-Carbons with a High Surface Area and Their Excellent CO_2 Adsorption Capacity.* Carbon, 2017. **116**: p. 448-455.

63. Samios, S., et al., *The Structure of Adsorbed CO_2 in Slitlike Micropores at Low and High Temperature and The Resulting Micropore Size Distribution Based on GCMC Simulations.* Journal of Colloid and Interface Science, 2000. **224**(2): p. 272-290.

64. Guan, C., et al., *The temperature Effect on The Methane and CO_2 Adsorption Capacities of Illinois Coal.* Fuel, 2018. **211**: p. 241-250.

65. Younas, M., et al., *Feasibility of CO_2 Adsorption by Solid Adsorbents: A Review on Low-Temperature Systems.* International Journal of Environmental Science and Technology, 2016. **13**(7): p. 1839-1860.

66. Pham, T.-H., B.-K. Lee, and J. Kim, *Novel Improvement of CO_2 Adsorption Capacity and Selectivity by Ethylenediamine-Modified Nano Zeolite.* Journal of the Taiwan Institute of Chemical Engineers, 2016. **66**: p. 239-248.

67. Kongnoo, A., et al., *Surface Characteristics and CO_2 Adsorption Capacities of Acid-Activated Zeolite 13X Prepared from Palm Oil Mill Fly Ash.* Fuel, 2017. **193**: p. 385-394.

68. Yang, H., et al., *Cation-Exchanged Zeolitic Chalcogenides for CO_2 Adsorption.* Inorganic Chemistry, 2017. **56**(24): p. 14999-15005.

69. Villarreal, A., et al., *Adsorption and Separation of CO_2 from N_2-Rich Gas on Zeolites: Na-X Faujasite vs Na-Mordenite.* Journal of CO_2 Utilization, 2017. **19**: p. 266-275.

70. Pham, T.D., et al., *Experimental and Computational Studies on The Adsorption of CO_2 and N_2 on Pure Silica Zeolites.* Microporous and Mesoporous Materials, 2014. **185**: p. 157-166.

71. Katsoulidis, A.P. and M.G. Kanatzidis, *Phloroglucinol Based Microporous Polymeric Organic Frameworks with −OH Functional Groups and High CO_2 Capture Capacity.* Chemistry of Materials, 2011. **23**(7): p. 1818-1824.

72. Lakhi, K.S., et al., *Energy Efficient Synthesis of Highly Ordered Mesoporous Carbon Nitrides with Uniform Rods and Their Superior CO_2 Adsorption Capacity.* Journal of Materials Chemistry A, 2017. **5**(31): p. 16220-16230.

73. Singh, G., et al., *Highly Efficient Method for The Synthesis of Activated Mesoporous Biocarbons with Extremely High Surface Area for High-Pressure CO_2 Adsorption.* ACS Applied Materials & Interfaces, 2017. **9**(35): p. 29782-29793.

74. Lakhi, K.S., et al., *Mesoporous Cu-SBA-15 with Highly Ordered Porous Structure and Its Excellent CO_2 Adsorption Capacity.* Microporous and Mesoporous Materials, 2018. **267**: p. 134-141.

Chapter 5 : Natural Zeolite Transformation by Alkali Impregnation for Improving Carbon Dioxide Adsorption Capacity

Abstract

Basicity enhancement by alkali impregnation with potassium hydroxide (KOH) and sodium hydroxide (NaOH) was successfully applied to natural calcite-rich mordenite-clinoptilolite zeolite to enhance CO_2 adsorption. The results showed the highest CO_2 adsorption capacities of 3.54 and 3.56 mmol/g, corresponding to 6.00×10^{-2} and 7.23×10^{-2} mmol/m^2, were respectively observed upon NaOH and KOH impregnation at 0°C and 30 bar. For CO_2 adsorption at 0°C and low pressure, KOH impregnation led to a better adsorption performance than did NaOH impregnation, consistent with material structure transformation which occurred in tandem with the basicity (Si/Al ratio) enhancement. It also demonstrated that the material's alkali impregnation was more effective than non-alkali treatment particularly for CO_2 adsorption at ambient temperature (25°C), in spite of its lower specific surface area. The structural transformation after alkali impregnation together with temperature and pressure selection provides an opportunity for more optimisation and CO_2 adsorption performance enhancement.

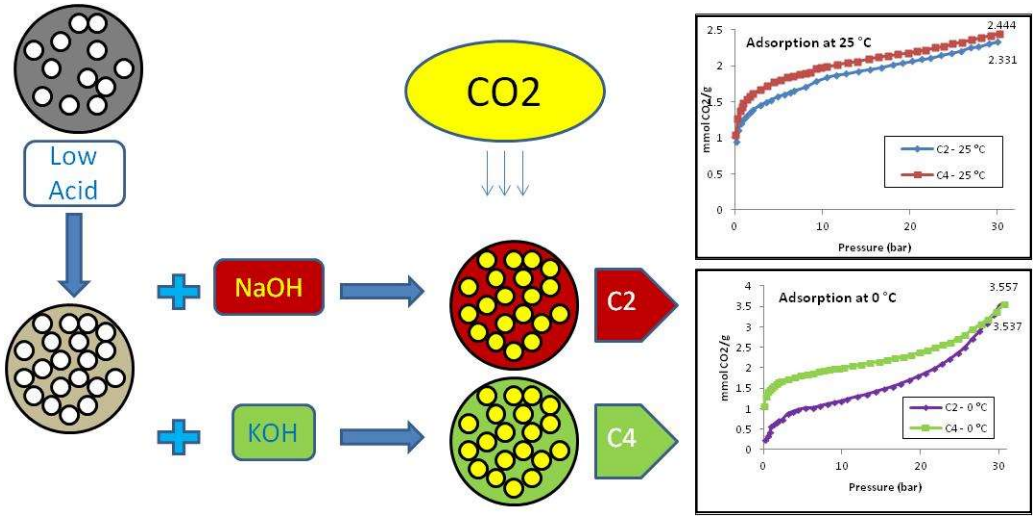

Figure 5.1. Graphical abstract of natural zeolite transformation by alkali impregnation for improving CO_2 adsorption capacity

5.1. Introduction

Biogas is one of the promising renewable energy resources explored in various countries around the world [1]. It is commonly utilised for vehicle fuels, generating heat or electricity but also supplies the gas piping systems and chemical industry [2-4]. Except for heat generation, biogas has to be purified by removing CO_2 which is one of the primary contaminants. Biogas purification provides a range of benefits such as increasing the heating value, reducing corrosion and removing bad odors [5-7].

The use of zeolite adsorbents is one of the conventional techniques for purifying the biogas. Natural zeolites are low-cost resource, available in abundant amounts around the world [8, 9]. Many studies have been reported on utilisation of natural zeolites in removing biogas impurities such as CO_2 [10], water-vapour [11], hydrogen sulphide [12] and others [7, 13-15]. While the adsorption capacities of natural zeolites do not compete with those of synthetic ones [16], their use does not involve the high cost of manufacturing and complex processing challenges and waste production.

The mordenite and clinoptilolite types of natural zeolite are possessed appropriate structures for CO_2 adsorption [17]. Such natural mordenite-clinoptilolite zeolites found in Gunungkidul, Indonesia, in abundance [18-21], have been studied for capturing CO_2. The studies show the capacity of natural zeolite to capture CO_2 when directly used in pristine form [22, 23], or after alkali treatment [24-26] and after dealumination in low acid concentration [27-29]. However, these studies are rather empirical, demonstrating practical applicability. They lack detailed material characterisation, properties' analyses and the in-depth properties-CO_2 adsorption capacity correlation required for achieving optimal results.

Increasing basicity by intercalating an alkali compound in the zeolite structure has been shown to enhance CO_2 adsorption capacity [30-34]. The alkali impregnation generates cation exchange since the alkali metals have the higher priority in ion exchange order [34-37]. However, the alkali impregnation decreases the specific surface area [30, 31, 35], and thus reduce the adsorption capacity. Furthermore, alkali induction also removes Si from the zeolite structure framework and hence, decrease of Si/Al ratio as one of the essential properties of zeolite, particularly for alkali treatment at high temperature [38-41].

Based on the various effects of the alkali impregnation, this modification may create new natural zeolite product characteristics. The optimum conditions for prudent structural modification need to be investigated for producing the best results. Introduction of the right basicity in the pores and channels of the zeolite material is the main thrust, accompanied by structural modification properties such as the porosity, elemental composition, and crystal structure. This transformation is affected by the various effect of alkali impregnation as mentioned in the previous studies. Therefore, this study was carried out to find out the effect of alkali impregnation at ambient temperature on Indonesian natural mordenite-clinoptilolite zeolite, then determined the best impregnation treatment for CO_2 adsorption.

5.2. Results and Discussion

5.2.1. Physicochemical characterisation of modified natural zeolites

The modified natural zeolite was utilised as a base material of non-alkali impregnation on this study (C0 zeolite). This pre-dealumination procedure was conducted to increase specific surface area so that it can minimise or offset the effect of specific surface area reduction after alkali impregnation. The specific surface area (103.82 m^2/g) of C0 zeolite was four times greater than the pristine material (25.95 m^2/g) as shown in Table 5.1.

The SEM images in Figure 5.2(a) show the morphological transformation of base natural zeolite (C0 zeolite) from the pristine natural zeolite (A0). The C0 zeolite crystal was cleaner than the pristine indicated by decreasing the presence of small crystal flakes in the material, attributed to the effect of dealumination and calcination. The XRD analysis of the A0 and C0 zeolites is presented in Figure 5.2(b) which supported by the search-match analysis results in Table 5.2. The A0 zeolite is structured by calcite, mordenite, and clinoptilolite, while the C0 zeolite is structured by anorthite, mordenite, clinoptilolite, and quartz. The spectra show the transformation of calcium structure from calcite (calcium carbonate) into anorthite (calcium silicate) which is indicated by the decreasing peak member and their intensity in the region of 30-60°, which are assignable to calcite. The XRD data is evidence that the treatment purified the zeolite structure from the impurities of

other structures such as quartz. The zeolite crystal did not change in this treatment as mordenite and clinoptilolite were still the primary structures.

The surface elemental composition based on XPS analysis of the A0 and C0 zeolite is shown in Figure 5.2(c) and the Si/Al ratio shown in Table 5.1. The Si/Al ratio based on the XPS analysis was 6.5 $\pm$ 0.1 which indicates more hydrophobic surface since the value was $\geq$ 5 [42-45]. High Si/Al ratio was appropriate for CO_2 adsorption since the low Al content in the structure suits the non-polar molecule of CO_2 [46, 47], but the Si/Al ratio $\geq$ 15 was not selected since it indicates the reduction of CO_2 adsorption capacity [34]. The Si/Al ratio of C0 zeolite suits to the minimum requirement of a hydrophobic surface and still on the range Si/Al ratio between 5 and 15 as suggested.

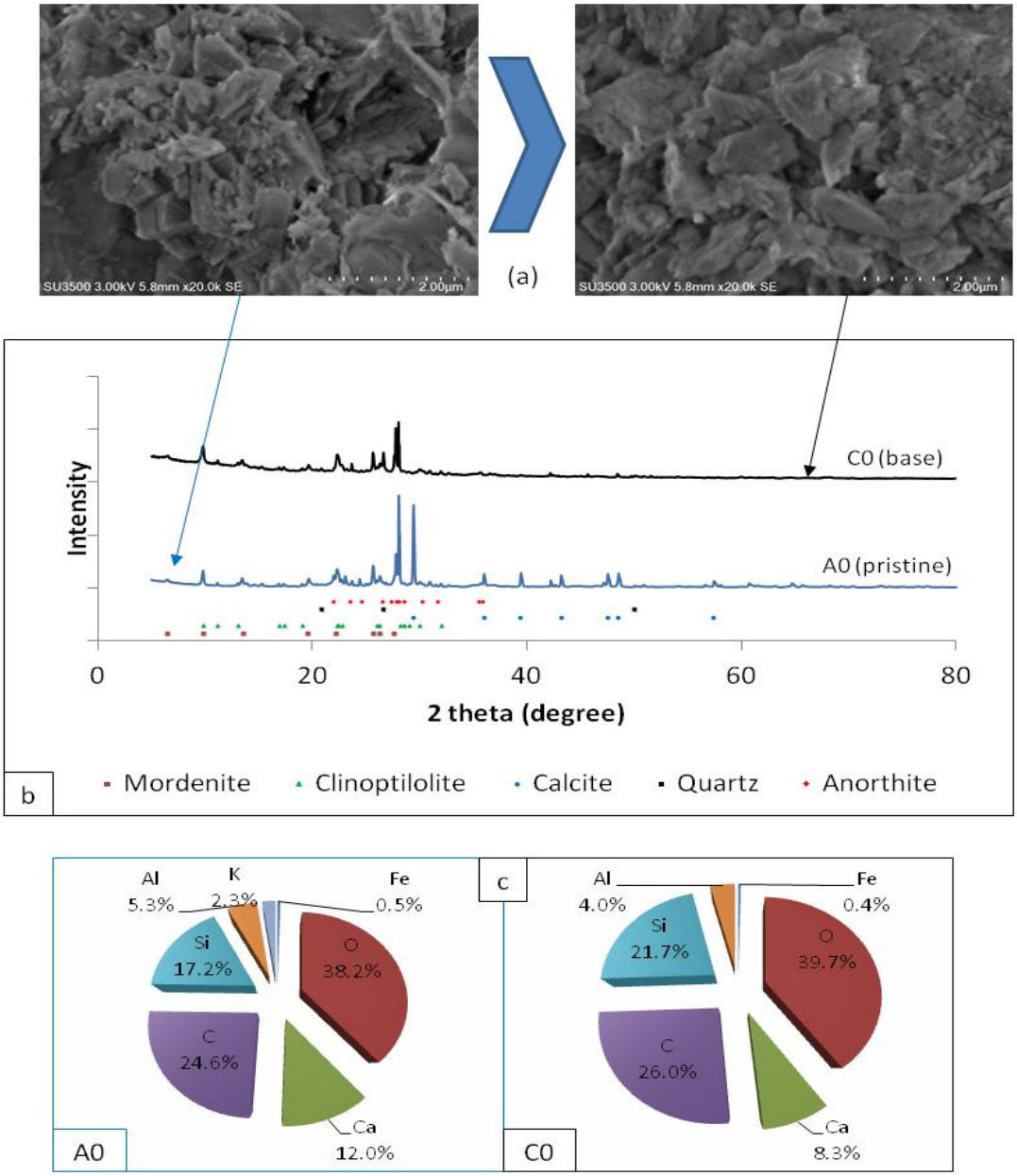

Figure 5.2. Characterisation of A0 and C0 zeolite: (a) SEM photomicrograph, (b) XRD pattern, (c) Atomic percent element composition of XPS

5.2.2. Alkali impregnation

Sodium and potassium were selected as alkali cation because they have higher ion exchangeability with the aluminum ion (Al^{3+}), and thus they can replace aluminum on the channel [35]. Both sodium and potassium are easy to obtain as hydroxide compounds and are highly soluble in water. However, de-silication of the zeolite structure by alkali also occurs in this reaction [38-41], but its impact can be significantly reduced by using low temperature [35].

Table 5.1 shows the Si/Al ratio determined by XPS of C0 zeolites after alkali impregnation in different concentrations of NaOH and KOH. The Si/Al ratio after both treatments modestly increased indicating that dealumination was more dominant than desilication in the low-temperature alkali impregnation. The NaOH treatment did not show any significant effect on the Si/Al ratio which increased slightly from 6.46 to 6.71. KOH provided better results of increasing the Si/Al the ratio to 7.81, which is consistent with published reports and is attributed to the greater cationic exchange potential of potassium [34, 35].

The specific surface area, on the other hand, showed an opposite trend to the Si/Al ratio. Both NaOH and KOH impregnation led to the decrease of the specific surface area of the material by about 50%. This indicates that this type of treatment resulted in the blockage of the channels and pores, an effect that was reported in other studies [30, 31, 35]. KOH impregnation and intercalated in the channels led to a greater decrease in the specific surface area than did NaOH. This is consistent with the fact the potassium ion diameter of 2.7 Å trapped in channels is larger when compared with the sodium ion diameter of 1.9 Å [34, 35].

Table 5.1. Specific surface area and Si/Al ratio of modified natural mordenite-clinoptilolite zeolite after alkali impregnation

Code	Alkali Impregnation (M)	Specific surface area (m^2/g)	Si/Al ratio
A0	0	25.95	3.5
C0	0	103.82	6.5
C1	1.0 NaOH	55.81	6.6
C2	3.0 NaOH	58.91	6.7
C3	5.0 NaOH	42.29	6.7
C4	1.0 KOH	49.21	6.5
C5	3.0 KOH	33.04	7.2
C6	5.0 KOH	37.99	7.8

Crystal structure transformations determined by XRD of NaOH impregnated natural zeolite are shown in Figure 5.3 and supported by the search-match analysis results in Table 5.2. The treated zeolites by NaOH impregnation were constructed by anorthite, mordenite, clinoptilolite, and quartz in different intensity. The NaOH impregnation changes calcite into anorthite as calcium silicate crystal and leaves the zeolite structure dominated by modernite. The transformation was in line with the standard conversion of this natural zeolite from A0 zeolite (the pristine) into C0 zeolite used as the base material in this experiment.

The effects of KOH are shown by XRD analysis in Figure 5.4 which supported by the search-match results in Table 5.2. The treated zeolites by KOH impregnation were constructed by anorthite, mordenite, clinoptilolite, and quartz in different intensity. It indicates the escalating intensity presence of clinoptilolite in the zeolite crystal structure, then obscures anorthite crystal structure; which also shown by increasing the match-score of clinoptilolite from 21 into 40-43. Potassium ion (K^+) has the highest ion exchange power than other common cations (Na^+, Ca^{2+}, Al^{3+}) in zeolite [34, 35] thus substituting other elements, particularly Ca^{2+} for creating a new structure and Al^{3+} for increasing Si/Al ratio. The new clinoptilolite structure is more appropriate for gas capture than mordenite structure [17].

Table 5.2. Match Score of modified natural mordenite-clinoptilolite zeolite crystal structure from XRD analysis for different alkali impregnations

Code	Alkali Impregnation (M)	Match Score of Crystal Structure				
		Calcite	**Mordenite**	**Clinoptilolite**	**Anorthite**	**Quartz**
A0	0	63	48	31	-	-
C0	0	-	52	21	37	51
C1	1.0 NaOH	-	54	29	29	42
C2	3.0 NaOH	-	50	25	22	48
C3	5.0 NaOH	-	52	27	30	59
C4	1.0 KOH	-	52	40	34	44
C5	3.0 KOH	-	52	41	34	52
C6	5,0 KOH	-	52	43	31	54

The SEM images in Figure 5.3 and Figure 5.4 also show the morphology of natural zeolite impregnated alkali, which is C1-C3 as NaOH impregnation and C4-C6 as KOH impregnation. When compared to Figure 5.2 of the base material, the new structure indicates a thick layer on the surface for all type of alkali impregnation. This coat was built by the alkali reacting with the material on the surface. It covered the pores and reduced the specific surface area which is confirmed by the specific surface area reduction reported in Table 5.1.

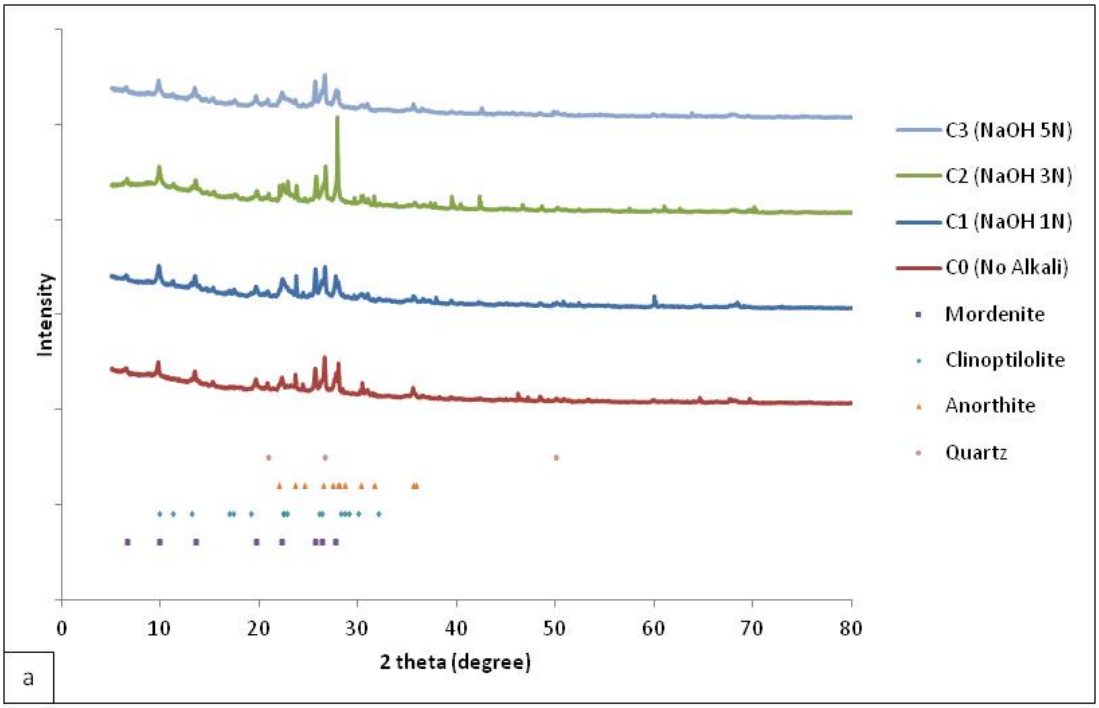

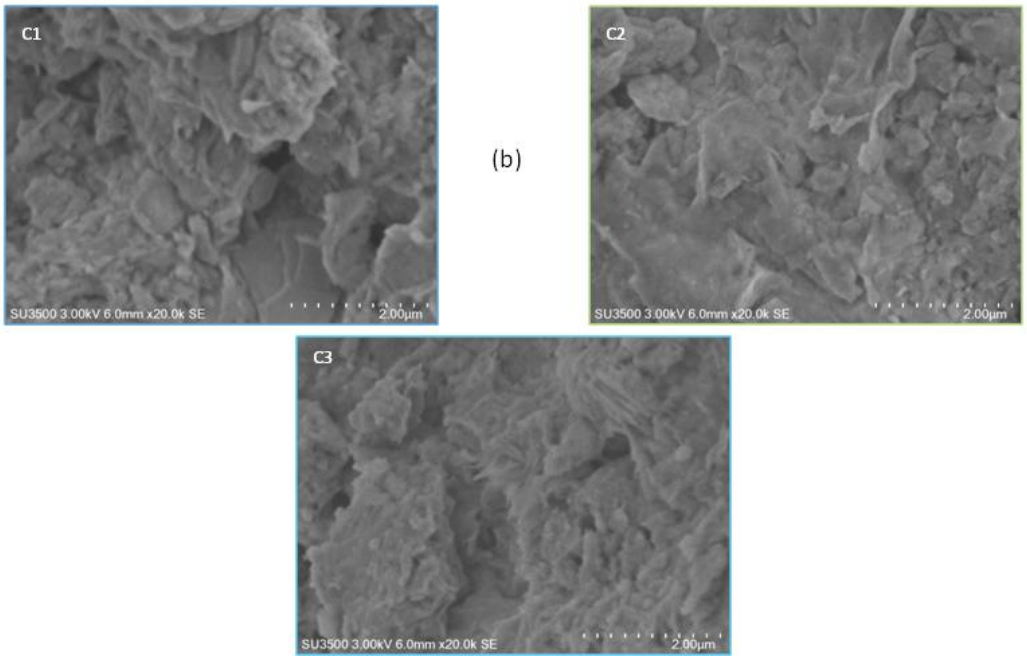

Figure 5.3. Modified natural mordenite-clinoptilolite zeolite after NaOH impregnation: (a) XRD patterns; and (b) SEM photomicrograph.

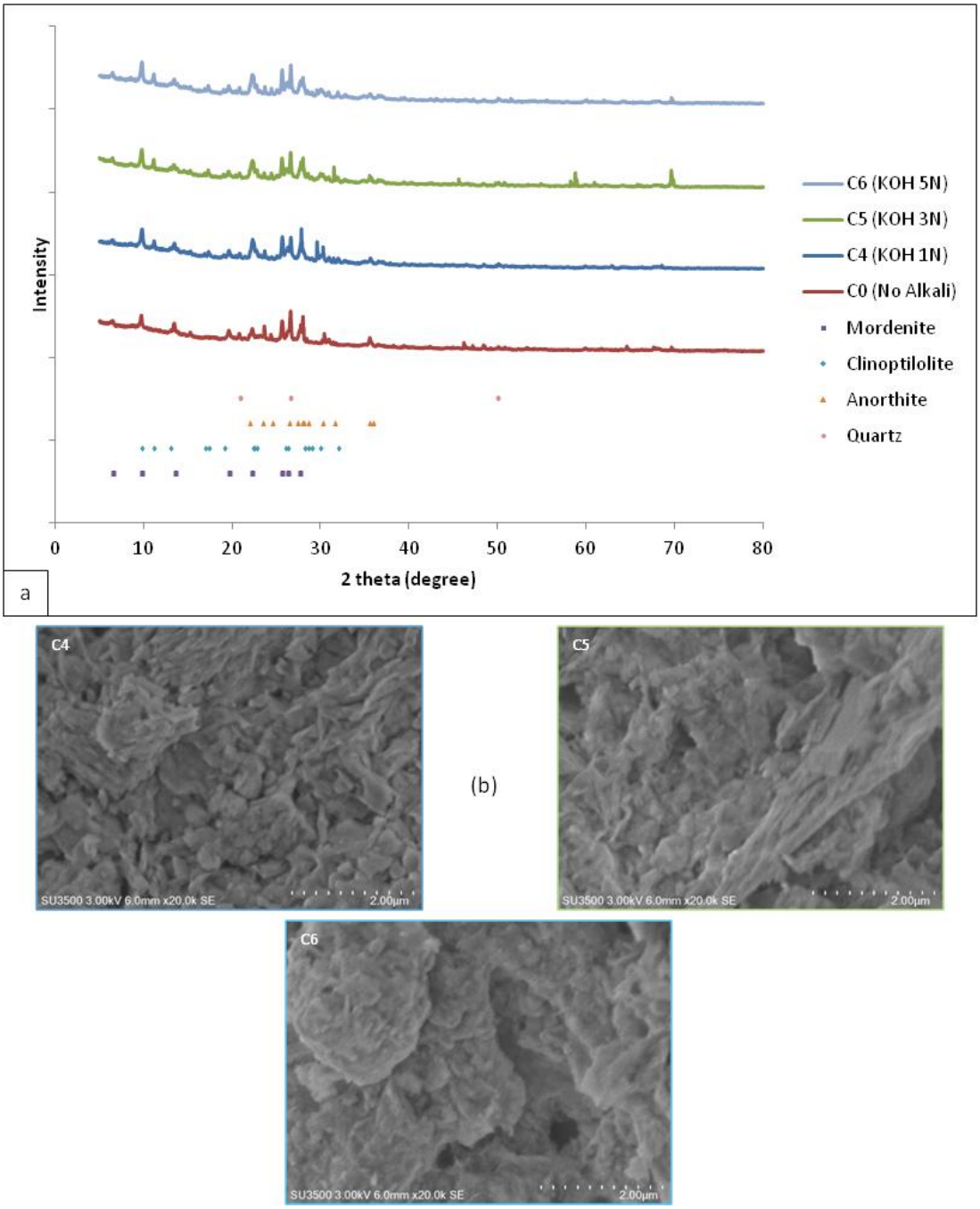

Figure 5.4. Modified natural mordenite-clinoptilolite zeolite after KOH impregnation: (a) XRD patterns; and (b) SEM photomicrograph.

5.2.3. The CO_2 adsorption capacity of the natural zeolite after alkali impregnation

C2 zeolite and C4 zeolite were selected as representative product samples of sodium and potassium impregnation, respectively. The selection considered the highest specific surface area of each alkali impregnation which is regarded as one of the dominant factors influencing CO_2 adsorption capacity [48, 49], mainly for high-pressure adsorption measurement [34, 50]. The adsorption capacity analysis was carried out at three different temperatures (0, 10, and 25°C) and pressure of up to 30 bar in isotherm conditions and are shown in Figure 5.5.

For NaOH treated C2 zeolite, showed interesting temperature dependent behaviour. At the highest temperature of 25°C, this material had high CO_2 adsorption capacity at low pressure which remained nearly constant with just slight increase with pressure. At 0°C, the material had the lowest CO_2 adsorption capacity at low pressure. However, the CO_2 adsorption capacity rapidly increased above the pressure of 15 bar. Intermediate behaviour was observed at 10°C. Overall, the highest CO_2 adsorption capacity was achieved at the highest pressure of 30 bar is 3.54, 2.42, 2.33 mmol/g at 0, 10, and 25°C, respectively. These results indicate that basicity was the dominant factor at low pressure, while the specific surface area was more important at the higher pressure.

These results were also supported by the absolute isosteric heat adsorption value of 83.54 kJ/mol as shown in Figure 5.5(b). Heat adsorption value greater than 50.0 kJ/mol indicates chemisorption as the dominant sorption mechanism [51-54]. Furthermore, the high isosteric heat value indicates the strong interaction between the material surface and CO_2. However, it also indicates the hard regeneration of adsorbent since there was the high energy of chemist reaction involved in this adsorption. Particularly at low pressure, C2 zeolite performs better adsorption in the higher temperature (10 and 25°C) of 0°C. Although the adsorption indicates the exothermic reaction, the warm temperature is needed to facilitate the adsorption reaction.

For KOH treated C4 zeolite, the adsorption was rapid at low pressure, then increased slowly above 15 bar. The highest adsorption capacity was reached at 0°C of 3.56 mmol/g then followed by 10 and 25°C of 2.93 and 2.44 mmol/g, respectively. The data indicates

that in the case of KOH treatment the temperature effect did not impact this adsorption performance at low pressure, in contrast to the NaOH impregnation samples.

The isosteric adsorption heat value for KOH treated zeolite is 4.8576 kJ/mol indicating physisorption [53-55], which is shown the graph in Figure 5.5(d). The low heat value suggests easier desorption, which is beneficial for regeneration of the adsorbent but it also indicates weaker CO_2 attachment to the material surface. The alkali impregnation had a dominant effect on C4 zeolite, particularly influential crystal transformation from anorthite into clinoptilolite.

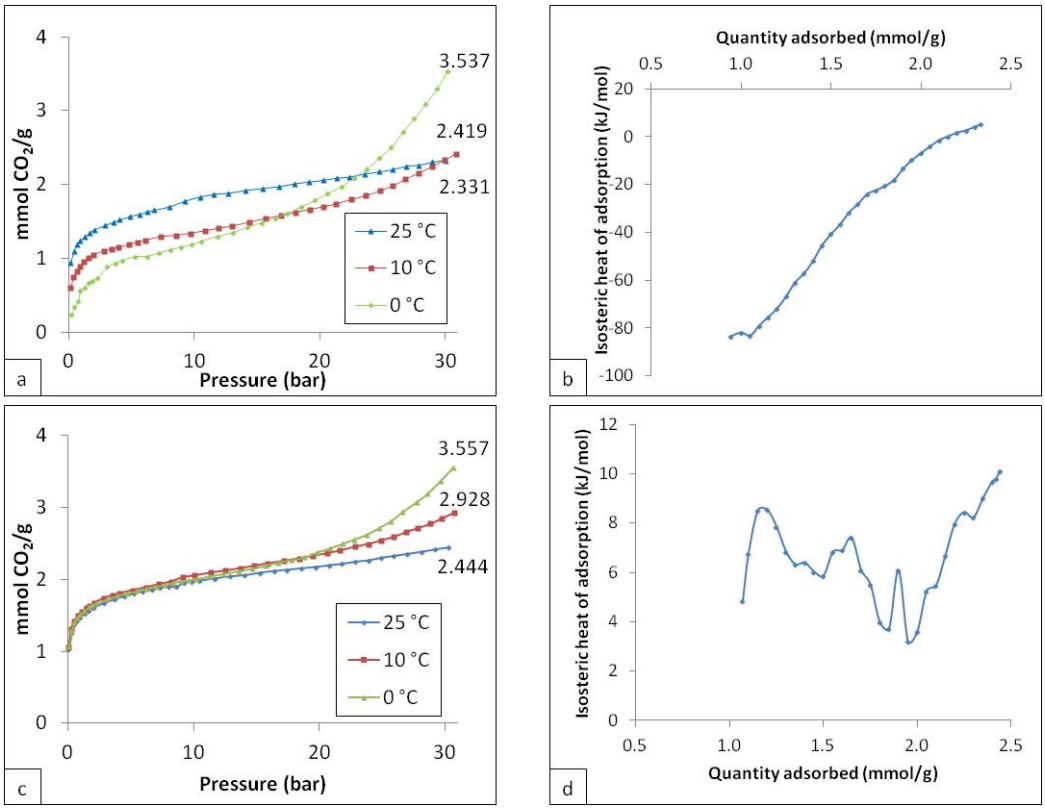

Figure 5.5. The CO_2 adsorption capacity of alkali impregnated modified natural mordenite-clinoptilolite zeolite: (a) NaOH impregnation; (b) NaOH impregnation isosteric heat; (c) KOH impregnation; (d) KOH impregnation isosteric heat

5.2.4. The comparison of alkali impregnation treatment for CO_2 adsorption capacity

The comparison of two types of alkali impregnation of natural zeolite is shown in Figure 5.6 at different temperature of 0 and 25°C. They are C2 and C4 zeolite as representing the NaOH impregnation (58.91 m^2/g) and KOH impregnation (49.21 m^2/g) respectively. At ambient temperature (25°C), both of the alkali impregnations of natural zeolite is shown in Figure 5.6(a). The C4 zeolite provided a higher adsorption capacity than C2 zeolite which demonstrates the crystalline phase transformation impacted the adsorption capacity, besides the basicity impact. This condition also represents in the normalised CO_2 adsorption capacity comparison as shown in Figure 5.6(b).

At 0°C, the C4 zeolite also showed similar behaviour as shown in Figure 5.6(c), even with a higher difference than at 25°C. However, both of alkali treatment zeolite have almost identical adsorption at 30 bar which is in line with their specific surface area. It indicates the specific surface area influenced on the CO_2 adsorption at high-pressure adsorption [34, 50]. The normalised CO_2 adsorption capacity at this temperature is shown in Figure 5.6(d). With a lower specific surface area of C4 zeolite, it provides higher CO_2 adsorption affinity than C2 zeolite. The C4 zeolite has higher normalised CO2 adsorption capacity than C2 Zeolite of 7.23×10^{-2} $mmol/m^2$ and 6.00×10^{-2} $mmol/m^2$ respectively at 0°C and 30 bar.

This phenomenon indicated that the basicity impact is not the single affected factor of the alkali treatment. The reduction of specific surface area and crystallinity transformation are others effect of this alkali impregnation, even these non-basicity factor impacting more to the adsorption performance. The excellent C4 zeolite adsorption ability was supported by the crystallinity transformation into clinoptilolite type, besides the basicity factor of the potassium presence. As the favoured of natural zeolite structure for gas adsorbent, the clinoptilolite provides more appropriate porosity structure and cation composition for capturing gas than mordenite [17].

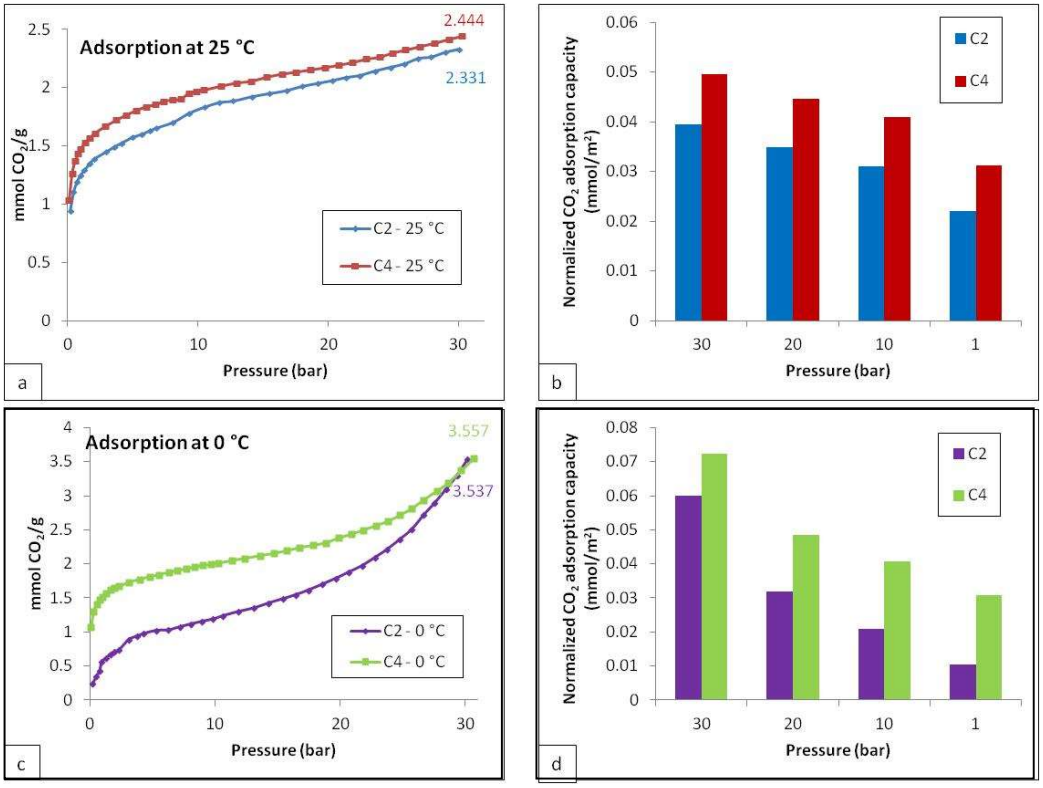

Figure 5.6. CO_2 adsorption comparison of alkali impregnated modified natural mordenite-clinoptilolite zeolite: (a) Capacity (mmol/g) at 25°C; (b) Normalised capacity (mmol/m^2) at 25°C; (c) Capacity (mmol/g) at 0°C; (d) Normalised capacity (mmol/m^2) at 0°C

5.3. Conclusion

KOH and NaOH impregnation into natural calcite-rich mordenite-clinoptilolite zeolite was performed successfully to intercalate alkali ion components into channels which led to the modification of the material properties. The impregnation resulted in increased basicity of the product, suggestive of basicity as one of the essential factors in CO_2 adsorption. The specific surface area of the impregnated product decreased, but the extent of which was greater for KOH than NaOH. Furthermore, a higher Si/Al ratio, reflecting greater basicity, was observed with KOH in contrast to NaOH. The adsorption capacity of alkali impregnation was reached the highest capacity at 0°C and 30 bar for NaOH and KOH of 3.54 and 3.56 mmol/g, corresponding to normalised CO_2 adsorption capacity of 6.00×10^{-2}

and $7.23x10^{-2}$ $mmol/m^2$, respectively. The higher adsorption ability of KOH than NaOH impregnation was supported by crystal structure transformation, which combined with the higher Si/Al ratio. At ambient temperature (25°C) adsorption, the basicity showed the main impact; then the crystallinity transformation provides additional effects. By low specific surface area and some properties transformation, it still has many rooms for further improvement of the natural mordenite-clinoptilolite zeolite to optimise alkali impregnation for CO_2 adsorption performance, even to find other suitable applications.

References

1. Raven, R.P.J.M. and K.H. Gregersen, *Biogas Plants in Denmark: Successes and Setbacks.* Renewable and Sustainable Energy Reviews, 2007. **11**(1): p. 116-132.

2. Kangmin, L. and M.-W. Ho, *Biogas China*. 2006, Institute of Science in Society

3. Weiland, P., *Biogas Production: Current State and Perspectives.* Applied Microbiology and Biotechnology, 2010. **85**(4): p. 849-860.

4. Pöschl, M., S. Ward, and P. Owende, *Evaluation of Energy Efficiency of Various Biogas Production and Utilization Pathways.* Applied Energy, 2010. **87**(11): p. 3305-3321.

5. Ryckebosch, E., M. Drouillon, and H. Vervaeren, *Techniques for Transformation of Biogas to Biomethane.* Biomass and Bioenergy, 2011. **35**(5): p. 1633-1645.

6. Wahono, S.K., H. Julendra, and A. Febrisiantosa, *Peningkatan Performa Biogas Melalui Teknologi Pemurnian Metana di UPT Kapitan Meo, Kabupaten Belu–Nusa Tenggara Timur [Performance Enhancement of Biogas Using Purification Technology of Methane at UPT Kapitan Meo, District Belu-East Nusa Tenggara]*, in *National Seminar on Technology Development Based on Local Materials*. 2009: Yogyakarta–Indonesia. p. 505-508.

7. Wahono, S.K. and W.A. Rizal, *Biogas Filter Based on Local Natural Zeolite Materials.* International Journal of Renewable Energy Development, 2014. **3**(1): p. 1-5.

8. Wang, S. and Y. Peng, *Natural Zeolites as Effective Adsorbents in Water And Wastewater Treatment.* Chemical Engineering Journal, 2010. **156**(1): p. 11-24.

9. Ozaydin, S., G. Kocer, and A. Hepbasli, *Natural Zeolites in Energy Applications.* Energy Sources, Part A: Recovery, Utilization, and Environmental Effects, 2006. **28**(15): p. 1425-1431.

10. Karousos, D.S., et al., *A Study on Natural Clinoptilolite for CO_2/N_2 Gas Separation.* Separation Science and Technology, 2016. **51**(1): p. 83-95.

11. Favvas, E.P., et al., *Clinoptilolite, a Natural Zeolite Material: Structural Characterization and Performance Evaluation on Its Dehydration Properties of Hydrocarbon-Based Fuels.* Microporous and Mesoporous Materials, 2016. **225**(Supplement C): p. 385-391.

12. Yaşyerli, S., et al., *Removal of Hydrogen Sulfide by Clinoptilolite in a Fixed Bed Adsorber.* Chemical Engineering and Processing: Process Intensification, 2002. **41**(9): p. 785-792.

13. Alonso-Vicario, A., et al., *Purification and Upgrading of Biogas by Pressure Swing Adsorption on Synthetic and Natural Zeolites.* Microporous and Mesoporous Materials, 2010. **134**(1–3): p. 100-107.

14. Paolini, V., et al., *Biogas Cleaning and Upgrading with Natural Zeolites from Tuffs.* Environmental Technology, 2016. **37**(11): p. 1418-1427.

15. Sadchikov, A., et al., *Use of Natural Zeolite in Systems for Separation and Purification of Gas Mixtures Containing Methane*, in *Key Engineering Materials*. 2017, Trans Tech Publ. p. 179-182.

16. Misaelides, P., *Application of Natural Zeolites in Environmental Remediation: A Short Review.* Microporous and Mesoporous Materials, 2011. **144**(1–3): p. 15-18.

17. Wang, S., *Utilisation of Natural Zeolites for Air Separation and Pollution Control*, in *Handbook of Natural Zeolites*, V.J. Inglezakis and A.A. Zorpas, Editors. 2012, Bentham Science Publishers. p. 569-587.

18. Marantos, I., G.E. Christidis, and M. Ulmanu, *Zeolite Formation and Deposits*, in *Handbook of Natural Zeolites*, V.J. Inglezakis and A.A. Zorpas, Editors. 2012, Bentham Science Publishers. p. 28-51.

19. Lestari, D.Y., *Kajian Modifikasi dan Karakterisasi Zeolit Alam dari Berbagai Negara [Review of Natural Zeolites Modification and Characterization from Various Countries]*, in *National Seminar of Chemistry and Education of Chemistry*. 2010, Education of Chemistry Department, Yogyakarta State University: Yogyakarta–Indonesia.

20. Kusdarto, K., *Potency of Zeolite in Indonesia.* Jurnal Zeolit Indonesia, 2008. **7**(2): p. 78-87.

21. Kogel, J.E., *Industrial Minerals and Rocks: Commodities, Markets, and Uses*. 2006: SME.

22. Sugiarto, S., et al., *Purifikasi Biogas Sistem Kontinyu Menggunakan Zeolit [Continuing Biogas Purification System Using Zeolite]*. 2013, 2013. **4**(1): p. 10.

23. Yamliha, A., B. Dwiargo, and W.A. Nugroho, *Pengaruh Ukuran Zeolite Terhadap Penyerapan Karbondioksida (CO_2) pada Aliran Biogas [Zeolite Size Effect for Carbon Dioxide Adsorption of Biogas]*. Jurnal Bioproses Komoditas Tropis, 2013. **1**(2): p. 67-72.

24. Dienullah, M., H.S. Tira, and Y.A. Padang, *Pemurnian Biogas dengan Sistem Berlapis Menggunakan Fe_2O_3, Zeolit Sintetik dan Zeolit Alam [Biogas Purification Using Multi-Layer System of Fe_2O_3, Synthetic Zeolite and Natural Zeolite]*. Jurnal Ilmiah Teknik Mesin, 2018. **15**(1): p. 1-8.

25. Hamidi, N., I.N. Gede Wardana, and D. Widhiyanuriyawan, *Peningkatan Kualitas Bahan Bakar Biogas Melalui Proses Pemurnian Dengan Zeolit Alam [Quality*

Improvement of Biogas Fuel by Purification Using Natural Zeolites]. Rekayasa Mesin, 2012. **2**(3): p. 227-231.

26. Widyanuriawan, D. and Sugiarto, *Biogas Purification Using Natural Zeolite and NaOH.* Applied Mechanics and Materials, 2014. **664**: p. 415-418.

27. Wahono, S.K., et al., *Metoda dan Alat untuk Meningkatkan Kadar Methana dalam Biogas [Methods and Tools for Increasing Methane Contents of Biogas]*. Patent, 2010. IDP000038082: Indonesia.

28. Adinurani, P.G., et al., *Carbon Dioxide Capture Efficiency Using Algae Biological Absorbent and Solid Adsorbent for Biogas Purification.* Jurnal Teknologi, 2016. **78**(4-2): p. 175-178.

29. Wahono, S.K., R. Maryana, and M. Kismurtono, *Biogas Purification Process to Increase Gen—Set Efficiency.* AIP Conference Proceedings, 2009. **1169**(1): p. 185-189.

30. Kim, Y.K., G.M. Kim, and J.W. Lee, *Highly Porous N-Doped Carbons Impregnated with Sodium for Efficient CO_2 Capture.* Journal of Materials Chemistry A, 2015. **3**(20): p. 10919-10927.

31. Lee, K.-M., et al., *Adsorption of Low-Level CO_2 Using Modified Zeolites and Activated Carbon.* Industrial & Engineering Chemistry Research, 2012. **51**(3): p. 1355-1363.

32. Iruretagoyena, D., et al., *Influence of Alkali Metals (Na, K, and Cs) on CO_2 Adsorption by Layered Double Oxides Supported on Graphene Oxide.* Industrial & Engineering Chemistry Research, 2015. **54**(46): p. 11610-11618.

33. Liu, X., et al., *Potassium and Zeolitic Structure Modified Ultra-microporous Adsorbent Materials from a Renewable Feedstock with Favorable Surface Chemistry for CO_2 Capture.* ACS Applied Materials & Interfaces, 2017. **9**(32): p. 26826-26839.

34. Bonenfant, D., et al., *Advances in Principal Factors Influencing Carbon Dioxide Adsorption on Zeolites.* Science and Technology of Advanced Materials, 2008. **9**(1): p. 013007.

35. Lin, H., et al., *Physicochemical Properties and Mechanism Study of Clinoptilolite Modified by NaOH.* Microporous and Mesoporous Materials, 2015. **218**: p. 174-179.

36. Arletti, R., et al., *Evidence for The Formation of Stable CO_2 Hydrates in Zeolite NaY: Structural Characterization by Synchrotron X-Ray Powder Diffraction.* Microporous and Mesoporous Materials, 2016. **228**: p. 248-255.

37. Khulbe, K.C., et al., *Recent Development on The Effect of Water/Moisture on The Performance of Zeolite Membrane and MMMs Containing Zeolite for Gas Separation; review.* RSC Advances, 2016. **6**(49): p. 42943-42961.

38. Chen, D.-s., et al., *Desilication from Titanium–Vanadium Slag by Alkaline Leaching.* Transactions of Nonferrous Metals Society of China, 2013. **23**(10): p. 3076-3082.

39. Groen, J.C., et al., *In Situ Monitoring of Desilication of MFI-Type Zeolites in Alkaline Medium.* Physical Chemistry Chemical Physics, 2007. **9**(34): p. 4822-4830.

40. Shen, B., et al., *Desilication by Alkaline Treatment and Increasing The Silica to Alumina Ratio of Zeolite Y.* Chinese Journal of Catalysis, 2012. **33**(1): p. 152-163.

41. Groen, J.C., J.A. Moulijn, and J. Perez-Ramirez, *Desilication: on The Controlled Generation of Mesoporosity in MFI Zeolites.* Journal of Materials Chemistry, 2006. **16**(22): p. 2121-2131.

42. Shirazi, L., E. Jamshidi, and M.R. Ghasemi, *The Effect of Si/Al Ratio of ZSM-5 Zeolite on Its Morphology, Acidity and Crystal Size.* Crystal Research and Technology, 2008. **43**(12): p. 1300-1306.

43. Ramesh, K. and D.D. Reddy, *Chapter Four - Zeolites and Their Potential Uses in Agriculture*, in *Advances in Agronomy*, D.L. Sparks, Editor. 2011, Academic Press. p. 219-241.

44. Sriatun, S. and A. Darmawan, *Dealuminasi Zeolit Alam Cipatujah Melalui Penambahan Asam dan Oksidator [Dealumination of Cipatujah Natural Zeolites by Acid and Oxidants Addition].* Kimia Sains dan Aplikasi, 2005. **8**(2).

45. Mandasari, W., B. Sitorus, and D.R. Jati, *Pembuatan dan Karakterisasi Adsorben Gas H_2S dari Zeolit Alam [Preparation and Characterization of Natural Zeolite as H_2S Adsorbents].* Jurnal Kimia Khatulistiwa, 2014. **3**(2): p. 56-63.

46. Cosoli, P., et al., *Hydrogen Sulphide Removal from Biogas by Zeolite Adsorption: Part I. GCMC Molecular Simulations.* Chemical Engineering Journal, 2008. **145**(1): p. 86-92.

47. Calleja, G., J. Pau, and J.A. Calles, *Pure and Multicomponent Adsorption Equilibrium of Carbon Dioxide, Ethylene, and Propane on ZSM-5 Zeolites with Different Si/Al Ratios.* Journal of Chemical & Engineering Data, 1998. **43**(6): p. 994-1003.

48. Singh, G., et al., *Single Step Synthesis of Activated Bio-Carbons with a High Surface Area and Their Excellent CO_2 Adsorption Capacity.* Carbon, 2017. **116**: p. 448-455.

49. Arefi Pour, A., et al., *Performance Evaluation of Clinoptilolite and 13X Zeolites in CO_2 Separation from CO_2/CH_4 Mixture.* Journal of Natural Gas Science and Engineering, 2015. **26**: p. 1246-1253.

50. Samios, S., et al., *The Structure of Adsorbed CO_2 in Slitlike Micropores at Low and High Temperature and the Resulting Micropore Size Distribution Based on GCMC Simulations.* Journal of Colloid and Interface Science, 2000. **224**(2): p. 272-290.

51. Pham, T.-H., B.-K. Lee, and J. Kim, *Novel Improvement of CO_2 Adsorption Capacity and Selectivity by Ethylenediamine-Modified Nano Zeolite.* Journal of the Taiwan Institute of Chemical Engineers, 2016. **66**: p. 239-248.

52. El-Naas, M.H., A.H. Al-Marzouqi, and O. Chaalal, *A Combined Approach for The Management of Desalination Reject Brine and Capture of CO_2.* Desalination, 2010. **251**(1): p. 70-74.

53. Chowdhury, S., et al., *Adsorption Thermodynamics, Kinetics and Isosteric Heat of Adsorption of Malachite Green onto Chemically Modified Rice Husk.* Desalination, 2011. **265**(1): p. 159-168.

54. Doğan, M. and M. Alkan, *Removal of Methyl Violet from Aqueous Solution by Perlite.* Journal of Colloid and Interface Science, 2003. **267**(1): p. 32-41.

55. Singh, G., et al., *Highly Efficient Method for The Synthesis of Activated Mesoporous Biocarbons with Extremely High Surface Area for High-Pressure CO_2 Adsorption.* ACS Applied Materials & Interfaces, 2017. **9**(35): p. 29782-29793.

Chapter 6 : Combination of Plasma Polymer Allylamine and Natural Zeolite as The Novel Carbon Dioxide Adsorbent

PART 1: Combination of Amine and Natural Zeolite as New Adsorbent Material for Carbon Dioxide Capture

Abstract

CO_2 is the most significant contributor to global warming. It demands the development of technologies which are capable of limiting CO_2 emissions to the atmosphere. One of the ways to achieve this purpose is CO_2 capture from industrial emissions as well as natural gas and landfill/biogas upgrading systems. Molecular sieve utilising natural zeolites as an adsorbent is one of the technologies for capturing CO_2 that has attracted significant attention. Natural zeolite is abundant, accessible and capable of capturing greenhouse gases effectively with an appropriate pre-treatment. Our previous studies demonstrated that natural zeolites, treated with chemical and physical means, reduced CO_2 content from biogas flow. However, the capture efficacy provides a room for improvements. In industry, amine solution absorption technology, which has several weaknesses such as high investment, high corrosive, high risk for human health, is commonly utilised. Solid amine adsorbents are considered as a promising alternative to overcome these drawbacks. This study aims to develop a hybrid technology combining the natural adsorption capacity of zeolites and the specific CO_2 capture properties of amines. To obtain amine-functionalised zeolite adsorbent, it used plasma deposition from amine-rich precursors such as allylamine. The results demonstrated that amine plasma polymers were successfully deposited on natural zeolite (Gunungkidul-Yogyakarta). For further improvement, it suggests conducting plasma on time deposition fewer than 10 s and power of 10 W or 50 W. Currently, studies are underway to evaluate the adsorption properties of these new CO_2 capture materials.

6.1. Introduction

The greenhouse gases, which consist of CO_2 (81%), CH_4 (7%), and N_2O (9%) [1], have become a big issue for the environmental community as a global warming trigger. As the first rank contributor to global warming, CO_2 needs to be reduced from the atmosphere. CO_2 capture, as developed technology, may become a strategy for limiting atmospheric emissions of CO_2 from industrial emissions as well as natural gas and landfill/biogas upgrading systems.

Recently, molecular sieve utilising natural zeolites is widely seen as an effective adsorbent. Zeolites, which are the member of aluminium silicate minerals group, have the microporous structure of crystalline solids and similar basic tetrahedral structure of $Al_XSi_YO_Z$. Based on the pores size, the zeolite is divided into three groups: small, medium and large; and commonly filled with water and cations. Aluminium, silicone and oxygen atoms of zeolites are commonly found in the form of SiO_2 and Al_2O_3 compounds. There are many types of zeolites depending on the formation of the environment and the source of materials [2-7]. The natural zeolite has a similar adsorption ability with synthetic zeolite, but it has lower adsorption capacity based on the characterisation results [8, 9]. The adsorption capacity of natural zeolite (raw or modified) cannot be compared to synthetic materials; however, it can be compensated by their low cost and bulk availability in the world [10].

Zeolite structure can perform adsorption and absorption of the compounds of H_2O, CO_2, SO_2, H_2S [11]; the absorption ability of zeolite to the gas is up to 25% [12]. Furthermore, the zeolite can control greenhouse gases such as CO_2 and N_2O, except CH_4 which is not absorbed [1]. Zeolite has high selectivity to CO_2; so, it can upgrade the quality of natural gas, biogas or others fuel gas [13-15]. Particularly for Gunungkidul-natural zeolite, it has been proved for upgrading biogas quality for electricity generation [16-19].

There are two types of natural zeolites which are commonly found in Indonesia, namely Clinoptilolite and Mordenite [20]. They have high purity and silica concentration of about 60%, commonly found in the following areas: South Lampung, Bajah, Cikembar, Cipatujah, West Java Nangapada, Ende, Nusa Tenggara Timur, Malang and Gunung Kidul Regency [21]. Natural zeolite, particularly Gunungkidul's zeolite, has the potential to be

used as adsorbents for CO_2 Capture. Not only does Gunungkidul's zeolite have fairly large deposits (55,000,000 m^3) [22], it also has the silica content of approximately 60% [21].

On the other hand, the utilisation of amine solution for CO_2 absorption is the most practical one in the industry, such as natural gas treatment, flue gas of food industry, landfill upgrading and flue gas of power plants. It can absorb the most CO_2 content of the gases (85-90%), other impurity gases (NO_x and SO_2), and particles (ashes). Amines compounds which are usually utilised for CO_2 absorption are monoethanolamine (MEA), diethanolamine (DEA), methyl diethanolamine (MDEA), diglycol amine (DGA), 2-Amino-2-methyl propanol (AMP), di-isopropanol amine (DIPA), and Piperazine (PIPA). Amines absorption process has a low operational cost, low energy requirement, low liquid waste, and low amine-releasing to the atmosphere. However, this method has several problems which need to be solved, namely high investment, difficult regeneration, high corrosive potential, gaps in environmental and human health risks [23].

Consequently, research focusing on the alternatives of amines needs to be improved continuously. One of them is by changing the amine solutions into amine solids so that it will develop on dry process absorption. Several studies on solid amine have increased the capacity of CO_2 capture. They used solid materials as amine carriers of the amine group, such as carbon fly ash-silica, polymethylmethacrylate-silica, polyethyleneimine-silica, and magnesium tetraphenyl porphyrin [24-28]. The solid amine has a high capacity to capture CO_2. However, CO_2 hardly penetrates the material because the pores are filled with amine polymers; it is also hard on the regeneration process [29].

One of the collaboration technologies between the solid amine and natural zeolite is plasma polymerisation. Plasma polymerisation is one of surface modification technologies, coating the surface with ultra-thin layers of monomers for various purposes. The plasma is used to transform and activate the monomers so that the monomers are polymerised or deposited on the material surface. This method is conducted in a dry process so that the surface materials react to the monomers. The monomers form an ultrathin layer on the surface, coating the material. The monomers deposition can be controlled by time of plasma polymerisation. When the deposition occurs continuously, it will produce more thickness of monomers coating on materials. However, after few monomer layers are formed on the surface, the next layer becomes independent substrates on the outer surface

which are able to react with another compound around the materials [30]. The independent substrates can be utilised to improve CO_2 adsorption capacity of natural zeolite.

Particularly for porous materials, continuous deposition of monomer clogs the pores so that the pores function will disappear. However, the deposition duration of plasma polymerisation is able to limit the thickness of monomer. So, it will not stop up the pores but reduce the diameter only [31]. Moreover, Cavallaro and Vasilev [32] have conducted successfully the experiment of controlling chemistry and thickness of plasma polymer for coating granule materials under continuous agitation, which is appropriate in the form of zeolite adsorbents. The zeolite adsorbent surface is coated by monomers which easily react with CO_2, such as amine-monomers. It is in line with the research of Vasilev et al. [33] which suggests that plasma polymer can be used for surface modification, particularly amine- monomers.

This study aims to develop a hybrid technology combining the natural adsorption capacity of zeolites and the specific CO_2 capture properties of amines. To obtain amine-functionalised zeolite adsorbent, it used plasma deposition from amine-rich precursors such as allylamine.

6.2. Results and discussions

6.2.1. Characterisation of amine plasma deposition

Amine plasma deposition was conducted by a plasma reactor using allylamine as amine rich precursor. It has been deposited successfully on the cleared silicon wafer surface and natural zeolite surface. The silicon wafer deposition was conducted to determine the thickness and water contact angle of amine which are shown in Figure 6.1(a) and Table 6.1 respectively.

Figure 6.1(a) shows that there was an increasing amine deposition on the surface which was equal to increasing time and power deposition. It could be assumed as the thickness on natural zeolite surface at the same time although it will be lower than the flat surface deposition due to the higher surface area on the material than the flat surface, the time

function deposition would still be utilised [32]. The increasing time deposition phenomena have a similar condition with the previous deposition research [31]. Furthermore, the different power also provides a different composition of group type deposition. So, it is possible to produce a different effect on the surface activity [34-36].

Table 6.1 shows the water contact angle of the allylamine surface deposition on a cleared silicon wafer. The water contact angle value on the surface is under 90° which indicates hydrophilic properties. The hydrophilic properties support the reaction condition between amine and CO_2 running better on water presence [37, 38]. Water presence usually decreases the ability of natural zeolite to capture CO_2 due to the zeolite adsorbs water-vapour earlier than CO_2 which makes saturation faster. Therefore, the presence of the amine, which attracts water on the surface, is expected to react further with water-vapour and to enhance the capability of CO_2 capture.

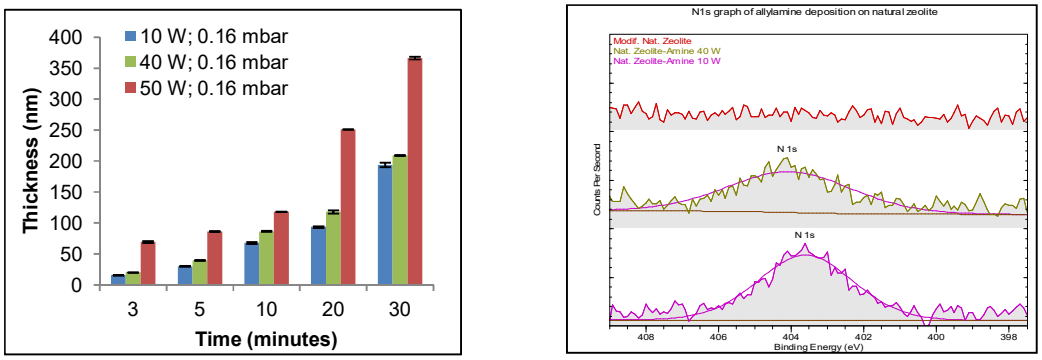

(a) (b)

Figure 6.1. (a) The thickness of allylamine deposition on various power and time; (b) N1s graph of allylamine deposition on natural zeolite

Table 6.1. The contact angle of 50 W allylamine deposition on different time

Time deposition of amine	180 s	300 s	600 s
Drop image			
Contact angle	55°	54°	52°

The amine deposition on the natural zeolite surface has been successfully conducted which is shown by N1s of XPS result in Figure 6.1(b). This graph shows that there is no indication of nitrogen on the natural zeolite surface without the amine coating. Meanwhile, the coated natural zeolites graphs show the peak on N1s for the various power deposition (10 W and 40 W). It means that the allylamine has deposited well on the natural zeolite surface. However, the efficacy of amine groups deposition for capturing CO_2 needs to be proven.

6.2.2. CO_2 capture on natural zeolite and natural zeolite-amine plasma

The CO_2 capture results on the material surface can be determined by XPS analysis, particularly on the C1s graphs. CO_2, which was captured by the adsorbent, was indicated by the carbon elements changing the adsorbent after the process. CO_2 capture result on the C1s graph of modified natural zeolites and natural zeolites coated amine was shown in Figure 6.2(a). On the C1s graph, there is a peak at 289 eV of energy binding which indicates that carbon is bonded to two oxygen (COO-R) or the CO_2 binding on the material surface [39, 40]. However, the natural zeolites without coating amine have a higher peak than zeolites coated amine. The presence of amine coat reduces CO_2 capture capability of natural zeolite. The amine deposition takes too long; so, it covers the natural zeolite pores. The pores volume is one of the important supporting factors for CO_2 capture ability.

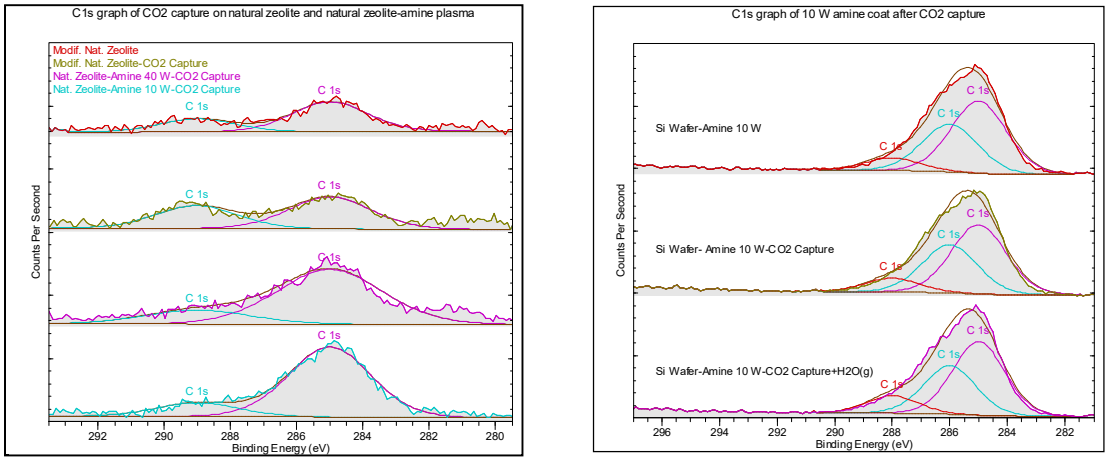

(a) (b)

Figure 6.2. (a) C1s graph of CO_2 capture on natural zeolite and natural zeolite-amine plasma; (b) C1s graph of 10 W amine coat after CO_2 capture

There are two important improvements which need to be conducted in this experiment including the appropriate plasma amine deposition condition and the deposition controlling. The appropriate condition of amine plasma deposition may provide the optimum CO_2 adsorption of amine because plasma reaction was conducted simultaneously and difficult to control. The deposition controlling can reduce the possibility of pores covering so that it can still utilise the pores advantages of natural zeolites.

6.2.3. Power variable of amine plasma deposition for CO_2 capture on Si wafer-amine

Amine plasma deposition was conducted on a flat surface of Si wafer to find appropriate parameter of plasma deposition for capturing CO_2. The power was divided into low power and high power variables because it provides different surface activities. The low power deposition produces more amine groups on the surface, but high power deposition produces more active ion on the surface [34-36].

The C1s graph of low power variable (10 W) amine plasma deposition is shown in Figure 6.2(b). The second peak of the COO-R bond (289 eV) is undetected, but there is an indication of the increase of the C=O bond (288 eV). Therefore, there is a possibility of

CO_2 reaction with the amine on the surface. The C=O bond also increases with the presence of water-vapour which is appropriate with CO_2 capture on solid amine [37, 38].

On the high power variable, there is a qualitative transformation particularly for the power of 50 W. The surface colour changing and the thickness increases, after CO_2 was introduced into the reactor, are shown in Figure 6.3(a) and 6.3(b), respectively. The colour changing shows that it had conducted some reaction on the surface after CO_2 treatment. It only happens to the power of 50 W. So, there is a different preference reaction possibility. It is also supported by the increase in thickness, which shows that some advanced deposition has been applied. The captured CO_2 or others elements by the surface give the possibility to increase the thickness after CO_2 introduction.

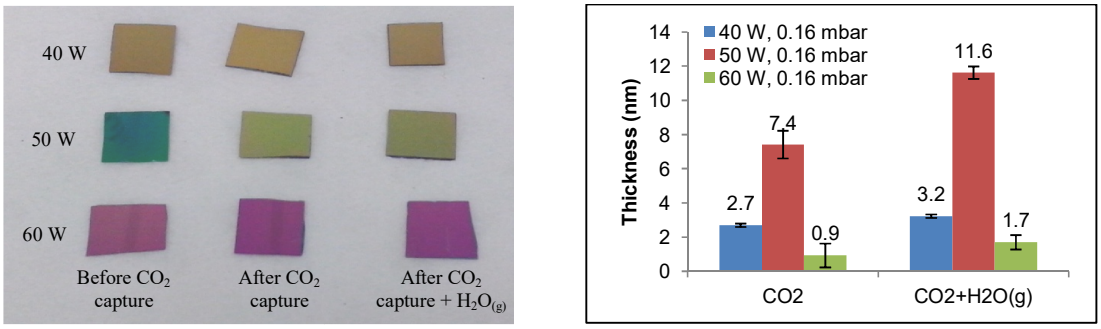

(a) (b)

Figure 6.3. (a) Colour transformation of high power amine coat after CO_2 capture; (b) Coat thickness increase on various condition after CO_2 capture

Another experiment of 50 W power variable has also been conducted; the XPS analysis of C1s and N1s is shown in Figure 6.4. On the C1s graph, the graph shows only one main peak, and it is different from with the previous results on the zeolite-amine which has two peaks on C1s graph. There is an insignificant difference between before and after CO_2 introduction on the surface. The C1s fitting element shows the presence of C-O (286 eV) and C=O (288 eV) bonds, but COO-R bond was undetected. The CO_2 capture indication is weak based on the C1s graph due to the undetected bond of COO-R and an insignificant increase of C=O bond after CO_2 capture. However, there is a strange indication on the N1s graph which brings out a new peak at 407 eV besides the main peak of nitrogen. The new

peak is indicated as nitro (N-O) bond [41], where the resource of oxygen element is possible from the air, water-vapour, and CO_2. The peak also increased significantly in the water-vapour presence of CO_2 introduction. It indicates that the nitro bonding was affected by the oxygen presence of CO_2 and H_2O than oxygen of the fresh air.

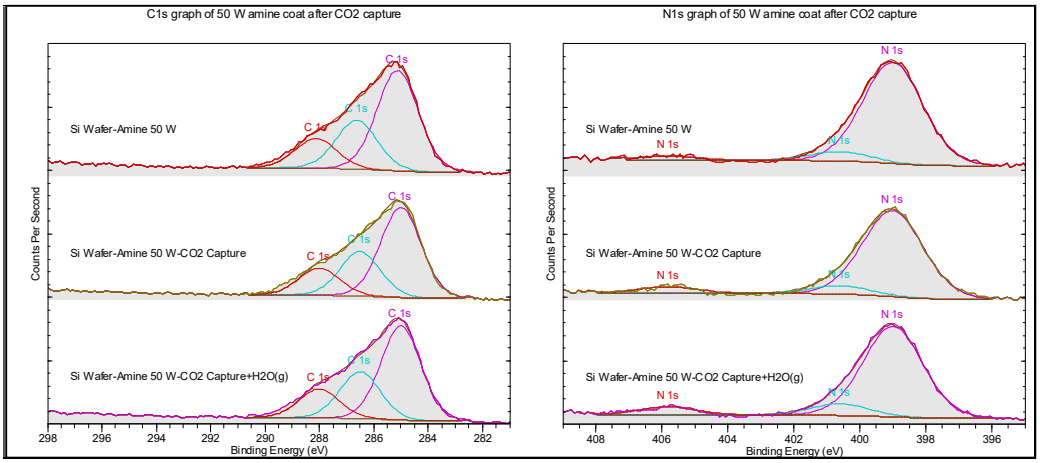

Figure 6.4. C1s and N1s graph of 50 W amine coat after CO_2 capture

The results of low and high power variables can be the preliminary indication that the 10 W and 50 W are potential for advanced improvement of CO_2 capture purpose. They provide different possibilities for capturing or reducing CO_2. The surface can be created as rich solid amine on low power deposition or oxidation catalyst for another power type deposition.

6.2.4. Controlling amine deposition thickness

The results of the CO_2 capture of natural zeolites on Figure 6.2(a) are supported by SEM analysis results which are shown in Figure 6.5. The modified natural zeolite looks like coral reef surface before amine deposition which is shown in Figure 6.5(a). However, on Figure 6.5(b), the zeolites surface is covered by some sandy grain, and it looks like the coral buried the sand after amine deposition. This condition gives a possibility that the pores are also buried by the deposition and closed the entrance of CO_2 so that it reduces the adsorption capability of natural zeolite. Therefore, the short time amine deposition (under

60 s) was also conducted, which is the material performance shown in Figure 6.5(c). The material surface performance was almost similar to the previous material in Figure 6.5(a). More amine deposition on the surface is needed for increasing the chance of capturing CO_2. So, long time amine deposition is a good option. However, natural zeolite as a porous material has the ability to capture CO_2 due to its porosity and compound structure. Thus, the deposition needs to be controlled for taking the best effect of the monomer on the porous surface.

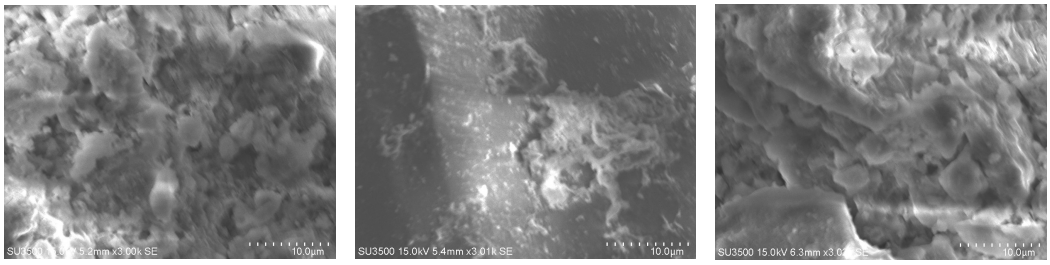

(a) (b) (c)

Figure 6.5. SEM images of modified natural zeolite: (a) before deposition; (b) after long time deposition (300 s); (c) after short time deposition (30 s)

The deposition needs to be reduced until less than 2 nm thickness due to the involvement of natural zeolite on microporous material [11]. The short time deposition was conducted to achieve that thickness purpose, which is shown in Figure 6.6. All types of amine plasma depositions (different power, different pressure, and pulse), which were conducted less than 10 s, were able to deposit thin layer amine. The layer was measured under 2 nm, appropriate with the natural zeolite pore size requirement. Therefore, the deposition of 10 s or under can suit as the base of low thickness amine plasma deposition particularly on natural zeolite as microporous material.

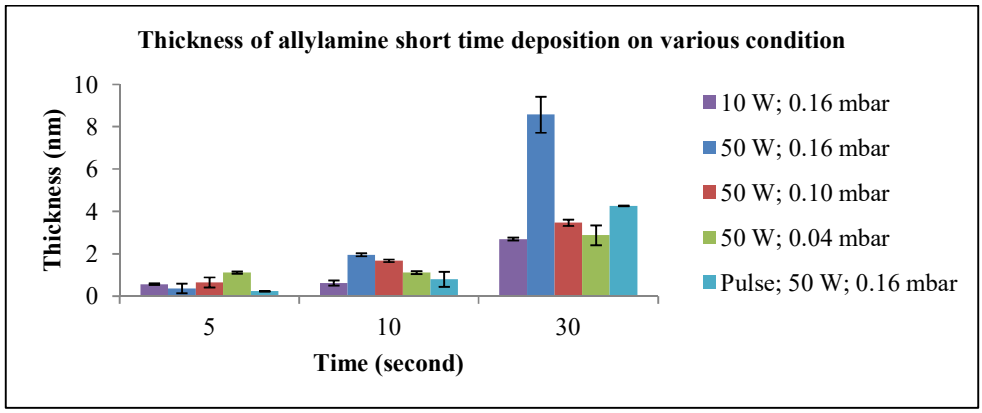

Figure 6.6. Thickness of allylamine short time deposition on various condition

6.3. Conclusions

The results demonstrate that amine plasma polymers can be successfully deposited on natural zeolite (Gunungkidul-Yogyakarta). As preliminary results, there are two recommendations which can be generated from this research, the appropriate plasma amine deposition condition and the deposition controlling. The power variable is the most dominant issue to determine the appropriate condition in this research. 10 W and 50 W power variables were suggested as the base for advanced improvement due to the production of rich solid amine surface or oxidation catalyst as the way of capturing or reducing CO_2. The deposition controlling suggested short deposition time which was conducted in less than 60 s. The appropriate result of deposition time is less than 10 s to avoid pore blocks on natural zeolite surfaces. Currently, studies are underway to evaluate the adsorption properties of these new CO_2 capture materials.

References

1. Delahay, G. and B. Coq, *Pollution Abatement Using Zeolites: State of The Art and Further Needs*, in *Zeolites for Cleaner Technologies*. 2002, Published by imperial college press and distributed by world scientific publishing co. p. 345-374.

2. Fernández, N., et al., *Real Evidence About Zeolite as Microorganisms Immobilizer in Anaerobic Fluidized Bed Reactors.* Process Biochemistry, 2007. **42**(4): p. 721-728.

3. Hansson, A., *Mechanism of Zeolite Activity in Biogas Co-Digestion*, in *Department of Physics, Chemistry and Biology*. 2011, Linköping University: Linköping, Sweden.

4. Hedström, A., *Ion Exchange of Ammonium in Zeolites: A Literature Review.* Journal of Environmental Engineering, 2001. **127**(8): p. 673-681.

5. Mumpton, F.A., *La roca magica: Uses of Natural Zeolites in Agriculture and Industry.* Proceedings of the National Academy of Sciences of the United States of America, 1999. **96**(7): p. 3463-3470.

6. Li, Z., et al., *Long-Term Chemical and Biological Stability of Surfactant-Modified Zeolite.* Environmental Science & Technology, 1998. **32**(17): p. 2628-2632.

7. Venuto, P.B., *Organic Catalysis Over Zeolites: A Perspective on Reaction Paths within Micropores.* Microporous Materials, 1994. **2**(5): p. 297-411.

8. Wahono, S.K., et al., *Characterization and Utilization of Gunungkidul Natural Zeolite for Bioethanol Dehydration.* Energy Procedia, 2014. **47**: p. 263-267.

9. Hernawan, et al., *Modification of Gunungkidul Natural Zeolite as Bioethanol Dehydrating Agents.* Energy Procedia, 2015. **65**: p. 116-120.

10. Misaelides, P., *Application of Natural Zeolites in Environmental Remediation: A Short Review.* Microporous and Mesoporous Materials, 2011. **144**(1–3): p. 15-18.

11. Weitkamp, J. and L. Puppe, *Catalysis and Zeolites Fundamentals and Applications*. Springer Archives. 1999, Berlin, Heidelberg: Springer Berlin Heidelberg : Imprint: Springer.

12. Sutarti, M. and M. Rachmawati, *Zeolit Tinjauan Literatur [Zeolite Literature Review]*. 1994, Scientific Information and Documentation Centre, Indonesian Institute of Sciences: Jakarta.

13. Cavenati, S., C.A. Grande, and A.E. Rodrigues, *Adsorption Equilibrium of Methane, Carbon Dioxide, and Nitrogen on Zeolite 13X at High Pressures.* Journal of Chemical & Engineering Data, 2004. **49**(4): p. 1095-1101.

14. Wahono, S.K., *Kajian: Pemanfaatan Zeolit Lokal Gunungkidul–Yogyakarta untuk Optimasi Sistem Biogas [Review : Utilization of Gunungkidul Local Zeolite for*

Biogas System optimization], in *National Seminar on Chemical Engineering Fundamentals and Applications*. 2008, Chemical Engineering Departement of Institute of Technology Sepuluh November Surabaya: Surabaya–Indonesia. p. E14.

15. Adinurani, P.G., et al., *Carbon Dioxide Capture Efficiency Using Algae Biological Absorbent and Solid Adsorbent for Biogas Purification.* Jurnal Teknologi, 2016. **78**(4-2): p. 175-178.

16. Wahono, S.K. and W.A. Rizal, *Biogas Filter Based on Local Natural Zeolite Materials.* International Journal of Renewable Energy Development, 2014. **3**(1): p. 1-5.

17. Wahono, S.K., R. Maryana, and M. Kismurtono, *Biogas Purification Process to Increase Gen—Set Efficiency.* AIP Conference Proceedings, 2009. **1169**(1): p. 185-189.

18. Wahono, S.K., et al., *Modifikasi Zeolit Lokal Gunungkidul Sebagai Upaya Peningkatan Performa Biogas Untuk Pembangkit Listrik [Modification as An Effort Local Zeolite Gunungkidul Performance Improvement for Biogas Electricity Generation]*, in *National Seminar on Chemical Engineering and Processes*. 2010: Semarang-Indonesia. p. D-11.

19. Wahono, S.K., H. Julendra, and A. Febrisiantosa, *Peningkatan Performa Biogas Melalui Teknologi Pemurnian Metana di UPT Kapitan Meo, Kabupaten Belu–Nusa Tenggara Timur [Performance Enhancement of Biogas Using Purification Technology of Methane at UPT Kapitan Meo, District Belu–East Nusa Tenggara]*, in *National Seminar on Technology Development Based on Local Materials*. 2009: Yogyakarta - Indonesia. p. 505-508.

20. Marantos, I., G.E. Christidis, and M. Ulmanu, *Zeolite Formation and Deposits*, in *Handbook of Natural Zeolites*, V.J. Inglezakis and A.A. Zorpas, Editors. 2012, Bentham Science Publishers. p. 28-51.

21. Widayat, et al., *Pengaruh Konsentrasi HCl dan Jenis Reaktan dalam Pembuatan Katalis Zeolit untuk Proses Dehidrasi dari Zeolit Alam [Effect of HCl Concentration and Reactant Type in The Zeolite Catalysts Production for Dehydration Process of Natural Zeolite]*, in *National Seminar on Chemical Engineering and Processes*. 2008, Chemical Engineering Department, Diponegoro University: Semarang - Indonesia. p. H091 1-9.

22. Idrus, A., et al., *Geology, Characterization, Quality Improvement and Recommended Utilization of Natural Zeolite (Zeolitic Tuff) Deposits from Gunungkidul, Yogyakarta Special Teritory, Indonesia.*, in *"2nd IASME / WSEAS International Conference on Geology and Seismology (GES'08)*. 2008, ISSN 1790-2769; ISBN 978-960-6766-39-8: Cambridge, UK. p. 21-25.

23. Shao, R. and A. Stangeland, *Amines Used in CO_2 Capture*, in *Bellona Report*. 2009, The Bellona Foundation.

24. Govar, A.A., *Development of a Pressure Swing Adsorption Process for CO_2 Capture from Flue Gas Using Solid Amine Sorbents*, in *Chemical Engineering, College of Engineering and Computing*. 2014, University of South Carolina: Columbia.

25. Zhang, Z., et al., *Enhancing Sorption Performance of Solid Amine Sorbents for CO_2 Capture by Additives.* Energy Procedia, 2013. **37**(0): p. 205-210.

26. Veneman, R., et al., *Continuous CO_2 Capture in a Circulating Fluidized Bed Using Supported Amine Sorbents.* Chemical Engineering Journal, 2012. **207–208**(0): p. 18-26.

27. Wang, J., et al., *Surfactant Promoted Solid Amine Sorbents for CO_2 Capture.* Energy & Environmental Science, 2012. **5**(2): p. 5742-5749.

28. Gray, M.L., et al., *Capture of Carbon Dioxide by Solid Amine Sorbents.* International Journal of Environmental Technology and Management, 2004. **4**(1): p. 82-88.

29. Jiang, H., *Amine-Pillared Nanosheet Adsorbents for CO_2 Capture Applications*, in *Department of Chemical Engineering*. 2015, Northeastern University: Boston, Massachusetts.

30. Vasilev, K., et al., *Substrate Influence on The Initial Growth Phase of Plasma-Deposited Polymer Films.* Chemical Communications, 2009(24): p. 3600-3602.

31. Dusan, L., et al., *Surface Modification of Nanoporous Alumina Membranes by Plasma Polymerization.* Nanotechnology, 2008. **19**(24): p. 245704.

32. Cavallaro, A. and K. Vasilev, *Controlled and Sustained Release of Pharmaceuticals via Single Step Solvent-Free Encapsulation.* Chemical Communications, 2015. **51**(10): p. 1838-1841.

33. Vasilev, K., et al., *Early Stages of Growth of Plasma Polymer Coatings Deposited from Nitrogen- and Oxygen- Containing Monomers.* Plasma Processes and Polymers, 2010. **7**(9-10): p. 824-835.

34. Gallino, E., et al., *Plasma Polymerized Allylamine Films Deposited on 316L Stainless Steel for Cardiovascular Stent Coatings.* Surface and Coatings Technology, 2010. **205**(7): p. 2461-2468.

35. Beck, A.J., et al., *The Role of Ions in the Plasma Polymerization of Allylamine.* The Journal of Physical Chemistry B, 2001. **105**(24): p. 5730-5736.

36. Lejeune, M., et al., *Microstructural Evolution of Allylamine Polymerized Plasma Films.* Surface and Coatings Technology, 2006. **200**(20–21): p. 5902-5907.

37. Chen, C., J. Kim, and W.-S. Ahn, *CO_2 Capture by Amine-Functionalized Nanoporous Materials: A Review.* Korean Journal of Chemical Engineering, 2014. **31**(11): p. 1919-1934.

38. Su, F., et al., *Adsorption of CO_2 on Amine-Functionalized Y-Type Zeolites.* Energy & Fuels, 2010. **24**(2): p. 1441-1448.

39. Tian, F., et al., *In Situ Measurement of CO_2 and H_2O Adsorption by ZIF-8 Films.* The Journal of Physical Chemistry C, 2015. **119**(27): p. 15248-15253.

40. Parry, K.L., et al., *ARXPS Characterisation of Plasma Polymerised Surface Chemical Gradients.* Surface and Interface Analysis, 2006. **38**(11): p. 1497-1504.

41. Ershov, S., et al., *Derivatization of Free Radicals in an Isopropanol Plasma Polymer Film: The First Step toward Polymer Grafting.* ACS Applied Materials & Interfaces, 2013. **5**(10): p. 4216-4223.

PART 2: Novel Amine Plasma Polymer Facilitated Carbon Dioxide Adsorbents

Abstract

Solution-based amine absorption technologies have been widely applied for CO_2 capture. However, these technologies have drawbacks associated with investment costs and generation of chemical waste during fabrication, operation, and disposal. One way forward that recently attracted attention are solid state amine adsorbents. In this paper, we report on the production of the first solid-state amine adsorbent prepared by plasma polymerisation and deposition onto physicochemically modified natural mordenite-clinoptilolite zeolite used as a carrier material. The plasma deposition of amine polymer under certain conditions resulted in a significant increase in surface area weighted CO_2 adsorption capacity as the natural zeolite. Furthermore, the CO_2 adsorption bond strength was weaker for the plasma polymer modified zeolite in comparison with the substrate without the plasma polymer coating, which may facilitate regeneration. The markedly enhanced CO_2 adsorption capacity and the indicated regeneration potential (weaker adsorption bond strength) makes the amine plasma polymer based zeolite adsorbent a good candidate for further development to industrial scale applications.

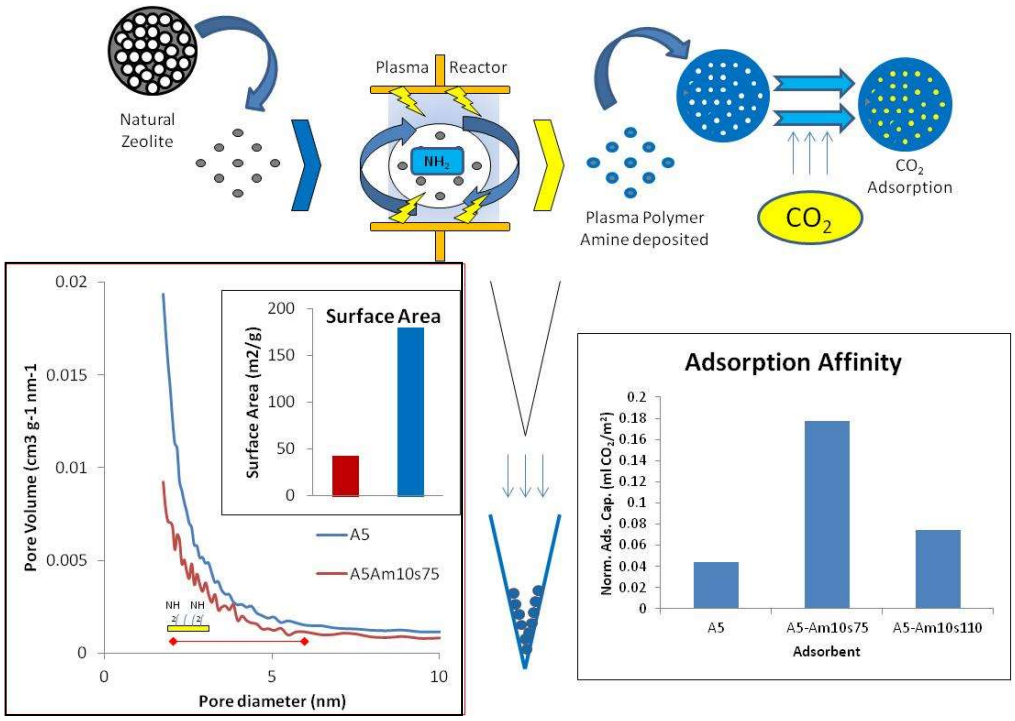

Figure 6.7. Graphical abstract of novel amine plasma polymer facilitated CO_2 adsorbents

6.4. Introduction

CO_2 is ranked highest in the composition of greenhouse gasses released in the atmosphere by many industries, including transportation and electricity generation [1]. The rapid escalation of the CO_2 amount over the last century has triggered intense efforts to create new technologies for CO_2 capture from flue gases before releasing to the atmosphere. Such CO_2 capture technologies are also required in the refinement on natural gas [2-4] and CO_2 conversion into useful products [5, 6].

Various methods for CO_2 capture have been developed involving adsorbents in liquid and solid phases. [7]. Liquid amine-based adsorbents have been commonly used for CO_2 capture in large commercial scale operations over the past 50 years [8]. However, this method has several weaknesses related to investment cost and generation of chemical waste during fabrication, operation, and disposal, which creates environmental and health hazard concerns [9]. On the other hand, solid amine-based adsorbents have become

attractive due to the fact that their use overcomes the drawbacks of the traditionally used liquid-based technologies.

Several solid amine functionalised adsorbents have shown to improve CO_2 adsorption selectivity [7] and have tolerance towards water-vapour presence [10]. They are affected by the formation of carbamate from primary or secondary amines reaction with CO_2 which is accelerated in the water presence [11]. However, the commonly employed technologies of solid amine adsorbent production which utilise wet-chemical processes and complex reactions, are highly substrate dependent and produce toxic waste [12, 13]. Those disadvantages could be overcome by developing a new technique for the incorporation of amine functionalities in the material.

One new technique for amine introduction is plasma polymerisation. The process involves polymer–like material deposition from the vapour phase of an organic precursor [14-16]. This technique overcomes some of the disadvantages of wet-chemical processes as material surface modification can be applied in a single step without using any solvents. In addition, coatings can be deposited on any substrate material [17] and materials of complex shapes, including nano and macroporous platforms [14, 18, 19]. Allylamine (C_3H_7N) is commonly utilised as a precursor for plasma deposition since it yields a coating that has high amine functional groups density. This property has benefited a range of application mainly in the field of biomaterials [17, 20-24].

Zeolites are attractive materials that have already benefited a range of applications including catalysis, water treatment, and gas adsorption. Natural mordenite-clinoptilolite zeolites are a good candidate as an amine carrier substrate because of their abundant availability, porosity and low cost [25-28]. This material has also been demonstrated for its potential as a CO_2 adsorbent in biogas purification [2, 29].

The purpose of this study is to investigate the potential of combining the beneficial properties of amine rich plasma polymers and modified, Indonesian natural zeolites to create a cost-effective solid-state adsorbent material for CO_2 capture.

6.5. Results and Discussions

6.5.1. Modified natural zeolite base material

BET analysis indicated that the specific surface area of A5 was 179.44 m^2/g. The material had contained a high level of micropores and mesopores with specific surface areas of 139.42 and 40.02 m^2/g, respectively. This is in sharp contrast to the specific surface area of A0 (the pristine material) (25.95 m^2/g, with micropores and mesopores specific surface areas of 8.18 and 17.77 m^2/g, respectively). The comparison of specific surface area with micro-mesopores distribution for A0 and A5 zeolites is shown in Figure 6.8(c).

In addition to increase specific surface area, other changes in the material properties also occurred. The XRD, SEM, and XRF analyses are shown in Figure 6.8(a), 6.8(b), and 6.8(d), respectively. The SEM images suggest greater porosity at the mesoscale after modification as well as cleaner structure.

The XRD results determined that the A0 zeolite is structured by calcite, mordenite, and clinoptilolite; while A5 zeolite is structured by anorthite, quartz, mordenite, and clinoptilolite [30]. It indicates changes in the calcite structure, from carbonate type (calcite) in A0 zeolite into silicate type (anorthite) in A5 zeolite which is indicated by the reduction of the two theta peak between 30° to 60°. The search-match analysis showed the transformation of match score between calcite in A0 zeolite and anorthite in the A5 zeolite, while there was no significant change in the match score of the zeolite structure (mordenite-clinoptilolite).

Furthermore, the Si/Al ratio increased from 6.1 in A0 to 11.0 in A5, accompanied by the reduction of some alkaline and metal components such as Ca, Na, Fe, and Al. Published studies point that the increase in Si/Al ratio above 15 reduced the capacity for CO_2 adsorption [31-33]. However, the Si/Al ratio lower than 5 increased the adsorption to water-vapour at the expense of CO_2 [34]. The Si/Al ratio of the A5 zeolite is between 5 and 15, which is in the range appropriate for adsorption of CO_2.

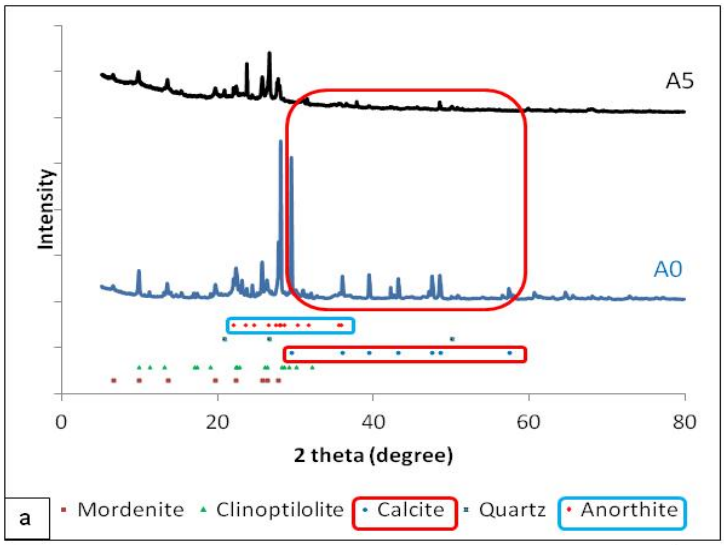

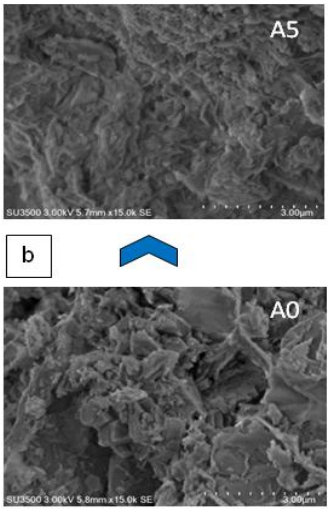

Code	Crystal Structure Match Score				
	Calcite	Mordenite	Clinoptilolite	Anorthite	Quartz
A0	68	49	25	-	-
A5	-	52	21	29	51

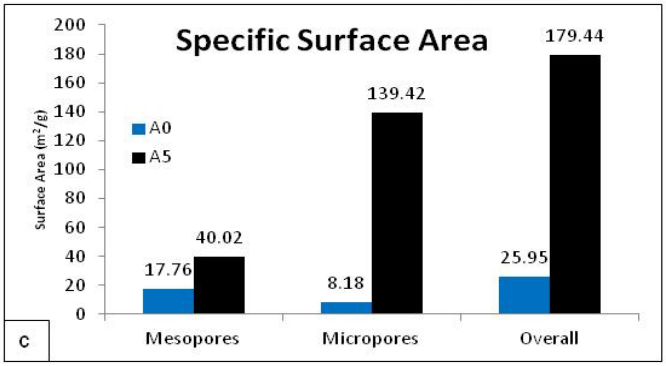

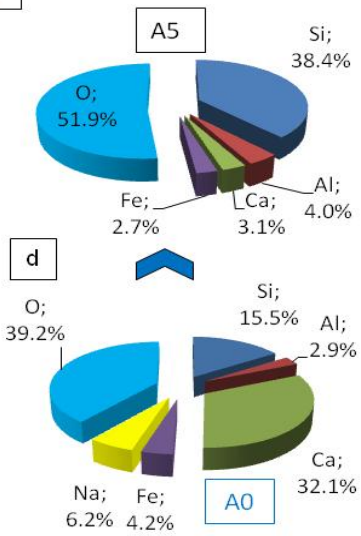

Figure 6.8. Characteristics of mordenite-clinoptilolite natural zeolite A0 and its modified product, A5 zeolite: (a) XRD spectra and crystal structure search-match analysis; (b) Surface morphology by SEM; (c) specific surface area with micro-mesopores distribution; and (d) elemental composition determined by XRF

6.5.2. Optimisation of plasma polymer deposition

Before plasma deposited allylamine film was applied to the zeolite powders, it was important to determine the optimal deposition conditions. This process was carried out using planner silicon wafers since these substrates allowed for film thickness

measurements by ellipsometry. Plasma power, deposition pressure and time of deposition are key parameters that influence the properties of the prepared polymer-like coatings.

Figure 6.9(a) shows the thickness of the allylamine plasma polymer coatings deposited at precursor pressure of 16 Pa, plasma power of 10 W and 50 W and deposition times between 10 – 600 s. The coating thickness increased gradually with increasing time of deposition which suggests that under the selected conditions constructive film growth dominated over the competing process of plasma etching. The deposited coatings were relatively hydrophilic, as recourse to wettability tests showed, consistent with published studies [35-37]. Water droplet spreading with low contact angles on films deposited using the power of 50 W and 600 s is shown in Figure 6.9(b).

To avoid complete blockage the pores in the zeolite, a further focus was placed on deposition times < 30 s that gave thinner films. Coatings were deposited for 10 s and 30 s using powers of 10 and 50 W and lower pressures of 10 and 4 Pa. In addition, the pulsing of the plasma power (on/off: 90 ms/10 ms) was applied. The resulting film thicknesses observed are presented in Figure 6.9(c). In view of retaining high porosity of the structure as much as possible, a deposition time of 10 s appeared as the most appropriate. Other considerations for selecting the conditions of deposition on the zeolite powders were the stability of the films and the retention of amine functionalities [24, 38]. The previous studies demonstrated that films deposited as 50 W are highly stable, but this is at the expense of reduced density of functional amine groups [36, 38]. Pulsing the plasma leads to the greatest retention of functionality, but the mild condition of deposition used may compromise the stability of the films. Based on this rationale, the deposition condition for further use with zeolites was a power of 10 W and 10 s time of deposition which gave a film thickness of about 1 nm and was expected to have satisfactory stability and amine functional group density.

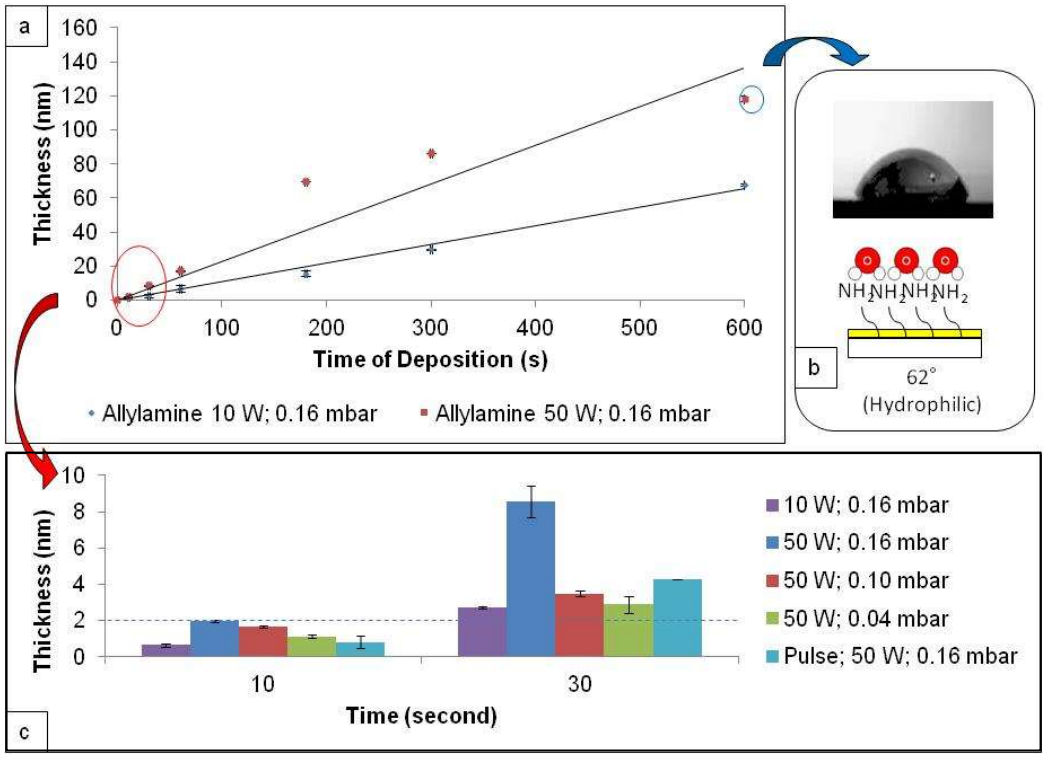

Figure 6.9. Properties of allylamine based plasma polymer films deposited on silicon wafers. (a) Thickness growth as a function of deposition time and power; (b) water droplet spreading (c) thickness of films deposited for 10 s and 30 s at different pressure and power, and upon power pulsing.

6.5.3. Plasma polymer deposition on the A5 zeolite

A5 zeolite modified with plasma deposited allylamine was assigned as A5-Am10W-10s zeolite. Figure 6.10(a) shows the high-resolution N1s spectra measured by XPS of A5 zeolite after modification by plasma of allylamine for time intervals from 0 to 1800 s. The presence of nitrogen can be detected by XPS only after 60 s of deposition. This indicates that the thickness of the plasma deposited coating at 10 s is very thin (consistent with thickness measurements on a planner silicon wafer) and much of the material is deposited within the pores. Another reason for the slow build-up of nitrogen-containing material is that during deposition the particles are continuously agitated leading to some abrasion

forces when particles collide with one another. This effect further slows down the build-up rate of the plasma polymer film.

The evidence that the plasma material is deposited in the pores is presented by the decreasing of specific surface area as shown in Figure 6.10(b) and Table 6.2. The specific surface area was determined after the material degassed at temperature of 50°C, which appropriate with plasma amine degassing temperature of published study [39, 40]. The specific surface area of the A5 zeolite dramatically decreased after plasma deposition. The surface area of micro and mesopores was decreased by over 90% and 40-60% from the base material. The deposition of the plasma polymer within the mesopores reduces their size to the scale of micropores. It is supported by the results of a published study which stated the pores diameter reduction in the mesopores deposition [14, 18, 41].

EDX analysis shown in Figure 6.10(c) also supports the hypothesis of plasma polymer deposition within the pores of the materials. The nitrogen content in the range of 3-4% was detected by EDX analysis for samples after 10, 30 and 60 s of deposition. EDX measurements determine the material composition within 500-2000 nm of the surface and different to what XPS can detect an up to 10 nm deep into the surface and within the pores of the zeolite.

Finally, very sensitive ToF-SIMS analyses were carried out to evaluate the availability of plasma deposited material of the surface of the zeolite. The spectra of A5 and A5-Am10W-10s zeolite are shown in Figure 6.10(d) and 6.10(e), respectively. A significant difference in the spectra of the untreated and plasma polymer modified materials were the ion fragments with masses of 41 and 58 amu, available only in the spectrum of A5-Am10W-10s. These can be assigned to nitrogen-containing fragments of CH_4N (30.035), C_2H_6N (44.050), and C_3H_8N (58.067) [42]. Moreover, the fragments at 58.067 amu (C_3H_8N) can be directly assigned to allylamine (C_3H_7N) which is the actual precursor used for plasma deposition. The XPS, EDX, ToF-SIMS and specific surface area analysis provide convincing evidence that plasma polymer deposition has occurred and that most of the amine-containing material is placed in the pores of the zeolite particles.

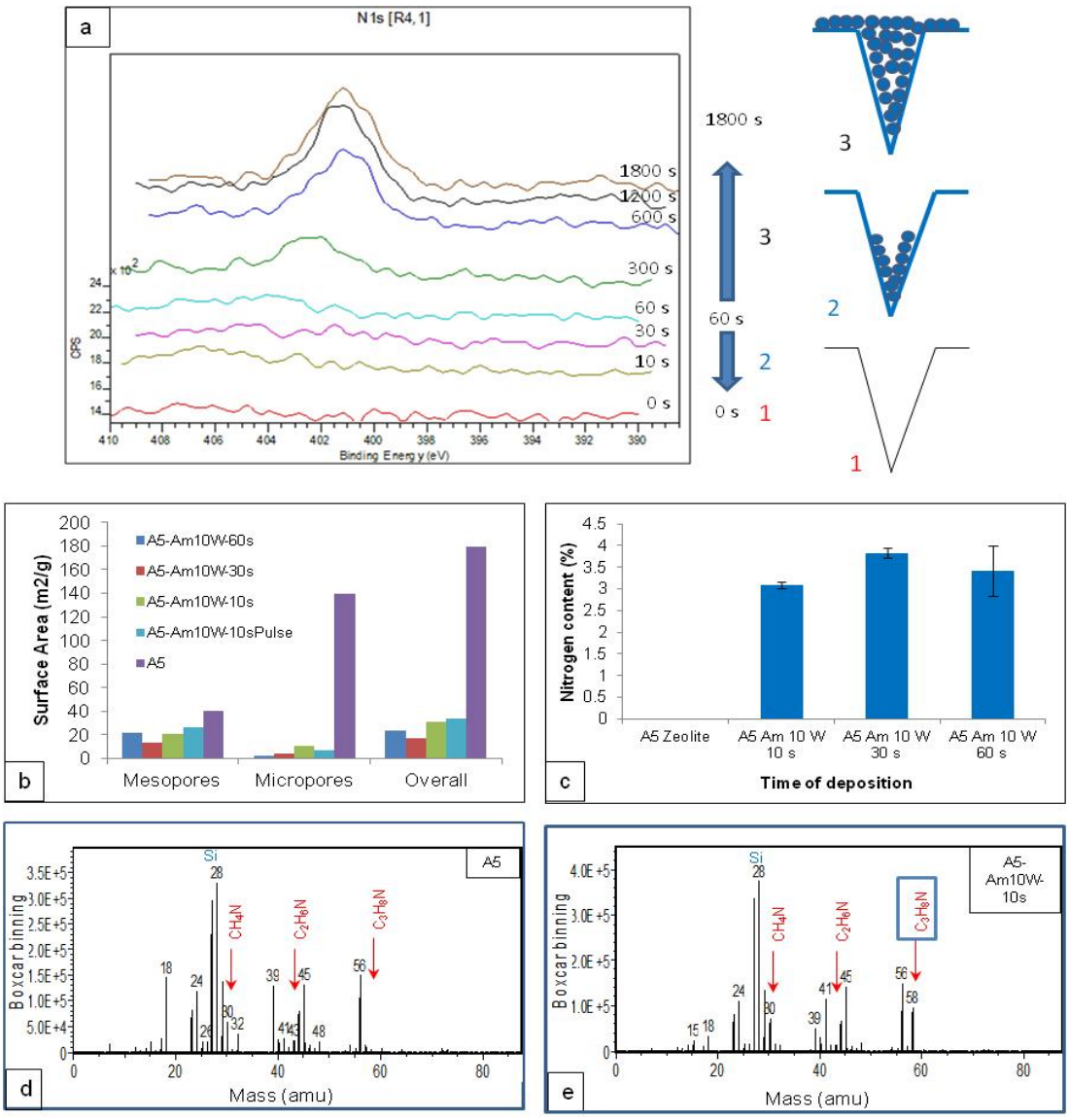

Figure 6.10. (a) N1s high-resolution XPS spectra at various deposition times; (b) specific surface area of A5 zeolite before and after deposition of allylamine plasma polymer; (c) Nitrogen content measured by EDX; ToF-SIMS spectra of (d) A5 zeolite, and (e) A5-Am10W-10s.

Table 6.2. The specific surface area of 10 W plasma polymer amine deposited on A5 zeolite in different duration and pulse.

Code	Plasma Power (W)	Plasma Duration (s)	Specific Surface Area (m^2/g)		
			Micropores	Mesopores	Overall
A5	0	0	139.42	40.02	179.44
A5-Am-10W-60s	10	60	2.35	21.36	23.71
A5-Am-10W-30s		30	3.76	13.34	17.10
A5-Am-10W-10s		10	10.33	20.63	30.96
A5-Am-10W-10sPulse	10 (Pulse)	10	6.82	26.71	33.53

6.5.4. Optimisation of the degassing temperature before CO_2 adsorption measurements

Selection of the appropriate degassing temperature is a critical factor, particularly for temperature-sensitive materials [43]. Although the zeolite as a base material can be heated to 400°C, the plasma deposited amine-containing material can be susceptible to temperature treatment [44, 45]. Therefore, the appropriate degassing temperature has to be determined by consideration of amine functionality retention in the system after degassing. Degassing temperatures of 50, 75, 110, and 250°C were investigated for their influence on the chemistry and structure of the material.

To facilitate XPS analysis of the effect of degassing temperature, the plasma polymer was deposited for 1800 s. The evolution of the N1s peak as a function of temperature is shown in Figure 6.11(a). At the highest temperature of 250°C, the nitrogen nearly completely disappeared from the zeolite which suggests that the plasma polymer has been heavily damaged. However, at temperatures of 110°C and below, the intensity of the nitrogen peak remained the same as in the non-heated material.

Further, we analyzed the specific surface area of the A5-Am10W10s zeolite after degassing at different temperatures which shown in Figure 6.11(b) and Table 6.3. The overall specific surface area increased with greater degassing temperature. The highest

specific surface area was determined at degassing temperature of 250°C. However, this temperature resulted in decomposition of the allylamine plasma polymer coating. At temperatures of 110°C and below there was no significant change in the specific surface area. Pore volume distribution before and after degassing is presented in Figure 6.11(c). As expected, the deposition of plasma polymer reduced the pore volume, most significantly was affected those pores of diameters below 4 nm.

Based on the chemical and structural analysis, we selected degassing temperatures of 75 and 110°C for CO_2 adsorption studies. These materials were assigned as A5-Am10s75 zeolite and A5-Am10s110.

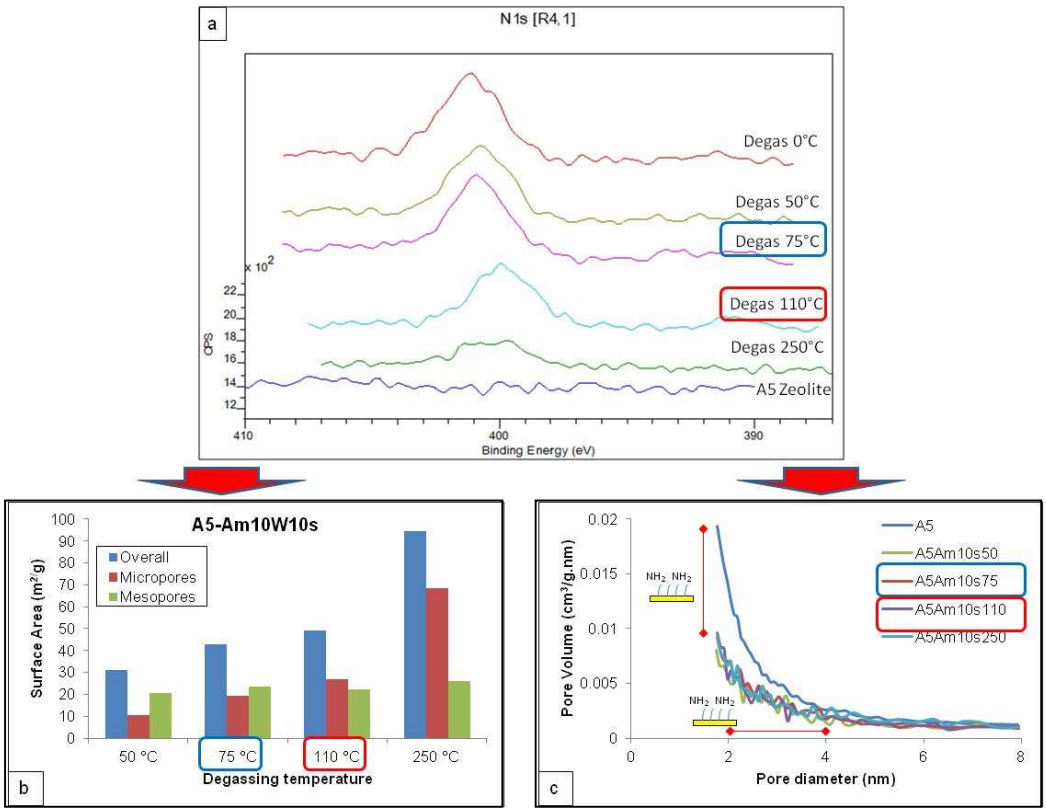

Figure 6.11. Effect of degassing temperature on the chemical and structural properties of the untreated and plasma treated zeolites: (a) Evolution of the N1s high-resolution XPS spectra after degassing at different temperatures; (b) Specific surface area; and (c) Pores size distribution.

Table 6.3. The specific surface area of 10 W plasma polymer amine deposited on A5 zeolite in different degassing temperature

Code	Plasma Power (W)	Plasma Duration (s)	Degas. Temp. (°C)	Specific Surface Area (m^2/g)		
				Micropores	Mesopores	Overall
A5	0	0	350	139.42	40.02	179.44
A5Am10s50	10	10	50	10.33	20.63	30.96
A5Am10s75			75	19.53	23.37	42.90
A5Am10s110			110	26.91	22.22	49.12
A5Am10s250			250	68.34	25.95	94.29

6.5.5. The CO_2 adsorption capacity

A5 zeolite, A5-Am10s75 zeolite, and A5-Am10s110 zeolite were selected to be measured for their CO_2 adsorption capacity. The CO_2 adsorption profiles of the three selected adsorbents are shown in Figure 6.12.

Figure 6.12(a) shows the surface bond adsorption strength of CO_2 to the material. As a general rule, a shift of the peak towards the left side indicates a weak bond during a shift to the right a stronger bond. The A5-Am10s75 zeolite provides a weaker surface adsorption bond compared to A5 zeolite and A5-Am10s110 zeolite. Low strength of the adsorption bond suggests more facile regeneration process. Thus the A5-Am10s75 zeolite could be easier to regenerate than the other two adsorbents. Furthermore, A5-Am10s75 zeolite also showed a sharper peak than the other two materials which indicates more homogeneous adsorption. This could be attributed to the retention of a high level of amine functionalities in the A5-Am10s75 zeolite. In comparison, due to the higher degassing temperature A5-Am10s110 may have undergone chemical changes in the amine functional groups which resulted in more heterogenous CO_2 adsorption.

Figure 6.12(b) shows the CO_2 adsorption capacities of A5, A5-Am10s75 and A5-Am10s110 zeolites to be 0.32, 0.31, and 0.15 mmol CO_2/g, respectively. The highest CO_2 adsorption capacity displayed by A5 zeolite which could be attributed to its highest specific surface area. However, this parameter is not sufficient to explain the determined

adsorption capacities. A5-Am10s75 zeolite has the lowest specific surface area, but its adsorption capacity was close to that of A5 zeolite (highest specific surface area) and greater than A5-Am10s110. This could be attributed to the amine rich plasma polymer layer which has a strong capacity to adsorp CO_2.

Further investigation of the specific surface area normalised adsorption capacity was conducted to determine the adsorption affinity of the material, shown in Figure 6.12(c). The specific surface area normalised of CO_2 adsorption for A5, A5-Am10s75, and A5-Am10s110 zeolite are 0.0018, 0.0072, and 0.0030 mmol CO_2/m^2, respectively. The highest adsorption affinity was obtained for A5-Am10s75 zeolite where the amine groups are retained in highest density. It is evident that the amine present in the pores enhanced the affinity of the plasma modified adsorbent towards CO_2. Our findings are in good agreement with published studies where amine functionalities prepared by wet chemistry displayed increased CO_2 adsorption capacity [46-50] and selectivity [7, 10].

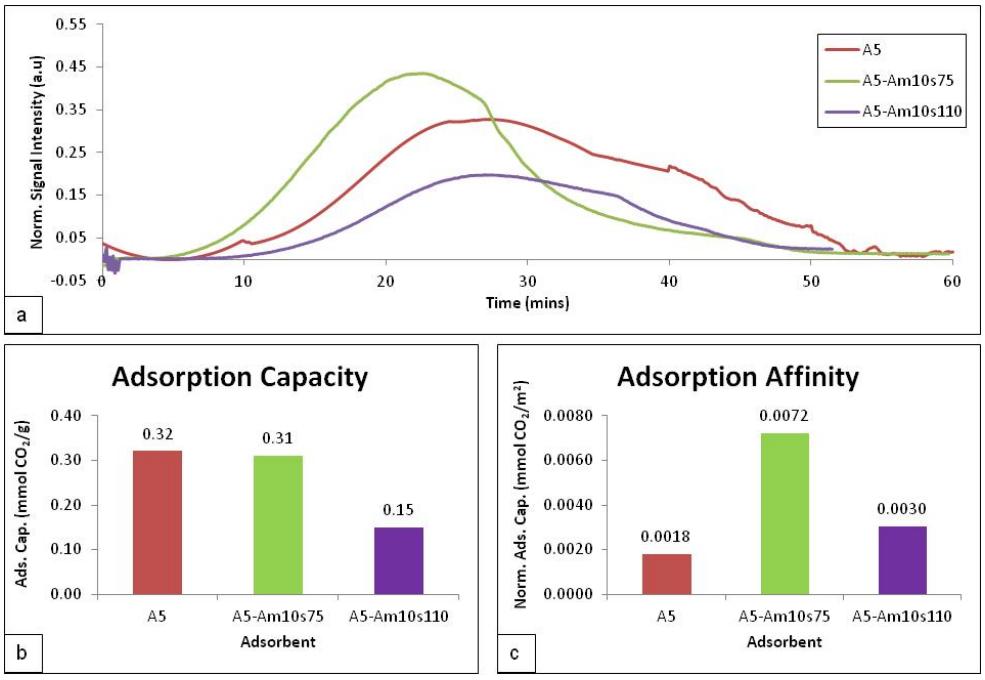

Figure 6.12. CO_2 adsorption of A5, A5-Am10s75, and A5-Am10s110 zeolite: (a) Bond strength profile of adsorbed CO_2; (b) CO_2 adsorption capacity (mmol CO_2/g); CO_2 adsorption affinity based on normalised specific surface area (mmol CO_2/m^2)

6.6. Conclusions

In summary, we demonstrate for the first time the application of amine plasma polymer films on the surface and within the pores of natural zeolites for the fabrication of solid CO_2 adsorbents. First, the mordenite-clinoptilolite natural zeolite was modified by physicochemical means to increase the material specific surface area from 25.95 m^2/g into 179.44 m^2/g; for improving the opportunity of amine deposition in the pores. Plasma polymer deposition was first optimised on planar, non-porous silicon wafers to generate coatings with optimal chemical properties and thickness below 2 nm; for determining the appropriate plasma amine deposition procedure. When plasma polymer was applied to the zeolites, the specific surface area was reduced significantly affecting mostly the microstructure of the original material. The optimum degassing temperature for sample treatment before CO_2 adsorption capacity measurements was determined to be 75 and 110°C. CO_2 adsorption measurements determined nearly identical adsorption capacities for the A5 and A5-Am-10W10s75 zeolite at 0.32 mmol and 0.31 mmol CO_2/g, respectively. However, the highest specific surface area normalised adsorption capacity, which also addressing adsorption affinity, to CO_2 adsorption was obtained for the A5-Am-10W10s75 zeolite of 0.0072 mmol CO_2/m^2. It could be attributed to the high concentration of amine functionality on the surface and within the pores of the material. Importantly, A5-Am-10W10s75 zeolite had the lowest adsorbed CO_2 bond strength which may present an easy pathway to regeneration. The high adsorption affinity and the potential for regeneration make the amine plasma polymerisation facilitated solid adsorbents developed in this paper a candidate material for further development to potential industry scale applications.

References

1. Delahay, G. and B. Coq, *Pollution Abatement Using Zeolites: State of The Art and Further Needs*, in *Zeolites for Cleaner Technologies*. 2002, Published by imperial college press and distributed by world scientific publishing co. p. 345-374.

2. Wahono, S.K. and W.A. Rizal, *Biogas Filter Based on Local Natural Zeolite Materials.* International Journal of Renewable Energy Development, 2014. **3**(1): p. 1-5.

3. First, E.L., M.M.F. Hasan, and C.A. Floudas, *Discovery of Novel Zeolites for Natural Gas Purification Through Combined Material Screening and Process Optimization.* AIChE Journal, 2014. **60**(5): p. 1767-1785.

4. Chen, S.J., et al., *Experimental Investigation of CO_2 Separation by Adsorption Methods in Natural Gas Purification.* Applied Energy, 2016. **179**: p. 329-337.

5. Pan, S.-Y., et al., *An Innovative Approach to Integrated Carbon Mineralization and Waste Utilization: A Review.* Aerosol Air Qual Res, 2015. **15**: p. 1072-1091.

6. Li, P., et al., *Challenges and Perspectives on Carbon Fixation and Utilization Technologies: An Overview.* Aerosol Air Qual. Res, 2016. **16**: p. 1327-1344.

7. Chen, C., J. Kim, and W.-S. Ahn, *CO_2 Capture by Amine-Functionalized Nanoporous Materials: A Review.* Korean Journal of Chemical Engineering, 2014. **31**(11): p. 1919-1934.

8. Rochelle, G.T., *Amine Scrubbing for CO_2 Capture.* Science, 2009. **325**(5948): p. 1652-1654.

9. Shao, R. and A. Stangeland, *Amines Used in CO_2 Capture*, in *Bellona Report*. 2009, The Bellona Foundation.

10. Sayari, A. and Y. Belmabkhout, *Stabilization of Amine-Containing CO_2 Adsorbents: Dramatic Effect of Water Vapor.* Journal of the American Chemical Society, 2010. **132**(18): p. 6312-6314.

11. Ünveren, E.E., et al., *Solid Amine Sorbents for CO_2 Capture by Chemical Adsorption: A Review.* Petroleum, 2017. **3**(1): p. 37-50.

12. Morent, R., et al., *Plasma Surface Modification of Biodegradable Polymers: A Review.* Plasma Processes and Polymers, 2011. **8**(3): p. 171-190.

13. Hernandez-Lopez, J.L., et al., *Functional Polymers as Nanoscopic Building Blocks.* Materials Science and Engineering: C, 2003. **23**(1): p. 267-274.

14. Vasilev, K., *Nanoengineered Plasma Polymer Films for Biomaterial Applications.* Plasma Chemistry and Plasma Processing, 2014. **34**(3): p. 545-558.

15. Yasuda, H. and Y. Matsuzawa, *Economical Advantages of Low-Pressure Plasma Polymerization Coating.* Plasma Processes and Polymers, 2005. **2**(6): p. 507-512.

16. Denes, F.S. and S. Manolache, *Macromolecular Plasma-Chemistry: An Emerging Field of Polymer Science.* Progress in Polymer Science, 2004. **29**(8): p. 815-885.

17. Vasilev, K., et al., *Substrate Influence on The Initial Growth Phase of Plasma-Deposited Polymer Films.* Chemical Communications, 2009(24): p. 3600-3602.

18. Simovic, S., D. Losic, and K. Vasilev, *Controlled Drug Release from Porous Materials by Plasma Polymer Deposition.* Chemical Communications, 2010. **46**(8): p. 1317-1319.

19. Kafshgari, M.H., et al., *Nitric Oxide-Releasing Porous Silicon Nanoparticles.* Nanoscale Research Letters, 2014. **9**(1): p. 333.

20. Siow, K.S., et al., *Plasma Methods for The Generation of Chemically Reactive Surfaces for Biomolecule Immobilization and Cell Colonization - A Review.* Plasma Processes and Polymers, 2006. **3**(6-7): p. 392-418.

21. Liu, X., et al., *Surface Modification by Allylamine Plasma Polymerization Promotes Osteogenic Differentiation of Human Adipose-Derived Stem Cells.* ACS Applied Materials & Interfaces, 2014. **6**(12): p. 9733-9741.

22. Vasilev, K., S.S. Griesser, and H.J. Griesser, *Antibacterial Surfaces and Coatings Produced by Plasma Techniques.* Plasma Processes and Polymers, 2011. **8**(11): p. 1010-1023.

23. Goreham, R.V., et al., *A Substrate Independent Approach for Generation of Surface Gradients.* Thin Solid Films, 2013. **528**: p. 106-110.

24. Ruiz, J.-C., et al., *Approaches to Quantify Amine Groups in the Presence of Hydroxyl Functional Groups in Plasma Polymerized Thin Films.* Plasma Processes and Polymers, 2014. **11**(9): p. 888-896.

25. Marantos, I., G.E. Christidis, and M. Ulmanu, *Zeolite Formation and Deposits*, in *Handbook of Natural Zeolites*, V.J. Inglezakis and A.A. Zorpas, Editors. 2012, Bentham Science Publishers. p. 28-51.

26. Kogel, J.E., *Industrial Minerals and Rocks: Commodities, Markets, and Uses*. 2006: SME.

27. Lestari, D.Y., *Kajian Modifikasi dan Karakterisasi Zeolit Alam dari Berbagai Negara [Review of Natural Zeolites Modification and Characterization from Various Countries]*, in *National Seminar of Chemistry and Education of Chemistry*. 2010, Education of Chemistry Department, Yogyakarta State University: Yogyakarta–Indonesia.

28. Kusdarto, K., *Potency of zeolite in Indonesia.* Jurnal Zeolit Indonesia, 2008. **7**(2): p. 78-87.

29. Wahono, S.K., et al., *Modifikasi Zeolit Lokal Gunungkidul Sebagai Upaya Peningkatan Performa Biogas Untuk Pembangkit Listrik [Modification as An Effort Local Zeolite – Gunungkidul Performance Improvement for Biogas Electricity Generation]*, in *National Seminar on Chemical Engineering and Processes*. 2010: Semarang–Indonesia. p. D-11.

30. Wahono, S.K., et al., *Carbon Dioxide Adsorption Enhancement of Natural Mordenite-Clinoptilolite Zeolite by Physicochemical Treatment*. 2018: Unpublished work.

31. Bonenfant, D., et al., *Advances in Principal Factors Influencing Carbon Dioxide Adsorption on Zeolites.* Science and Technology of Advanced Materials, 2008. **9**(1): p. 013007.

32. Calleja, G., J. Pau, and J.A. Calles, *Pure and Multicomponent Adsorption Equilibrium of Carbon Dioxide, Ethylene, and Propane on ZSM-5 Zeolites with Different Si/Al Ratios.* Journal of Chemical & Engineering Data, 1998. **43**(6): p. 994-1003.

33. Tezel, F., P. Harlick, and A. Sirkecioglu, *Adsorption of Nitrogen and Carbon Dioxide on ZSM-5*, in *Proceedings of the 12th International Zeolite Conference*. 1998. p. 309-316.

34. Ramesh, K. and D.D. Reddy, *Chapter Four - Zeolites and Their Potential Uses in Agriculture*, in *Advances in Agronomy*, D.L. Sparks, Editor. 2011, Academic Press. p. 219-241.

35. Ramiasa-MacGregor, M., et al., *Tuning and Predicting The Wetting of Nanoengineered Material Surface.* Nanoscale, 2016. **8**(8): p. 4635-4642.

36. Wahono, S.K., et al., *Preliminary Study: Combination of Amine and Natural Zeolite as New Adsorbent Material for CO2 Capture*, in *Chemeca 2016: Chemical Engineering-Regeneration, Recovery and Reinvention*. 2016. p. 900-910.

37. Gallino, E., et al., *Plasma Polymerized Allylamine Films Deposited on 316L Stainless Steel for Cardiovascular Stent Coatings.* Surface and Coatings Technology, 2010. **205**(7): p. 2461-2468.

38. Vasilev, K., et al., *Solvent-Induced Porosity in Ultrathin Amine Plasma Polymer Coatings.* The Journal of Physical Chemistry B, 2008. **112**(35): p. 10915-10921.

39. Øye, G., et al., *Plasmachemical Amine Functionalization of Porous Polystyrene Beads: The Importance of Pore Architecture.* Langmuir, 2002. **18**(23): p. 8996-8999.

40. Badyal, J.P., et al., *Comparison of The Effect of Pore Architecture and Bead Size on The Extent of Plasmachemical Amine Functionalisation of Poly(Styrene-Co-Divinylbenzene) Permanently Porous Resins.* Polymer, 2004. **45**(7): p. 2185-2192.

41. Dusan, L., et al., *Surface Modification of Nanoporous Alumina Membranes by Plasma Polymerization.* Nanotechnology, 2008. **19**(24): p. 245704.

42. Lu, D., et al., *Analysis of Amine Contamination on Silicon Oxide Surfaces Using ToF-SIMS.* Applied Surface Science, 2004. **233**(1): p. 352-359.

43. Figini-Albisetti, A., et al., *Effect of Outgassing Temperature on The Performance of Porous Materials.* Applied Surface Science, 2010. **256**(17): p. 5182-5186.

44. Jadhav, P.D., et al., *Monoethanol Amine Modified Zeolite 13X for CO_2 Adsorption at Different Temperatures.* Energy & Fuels, 2007. **21**(6): p. 3555-3559.

45. Chatti, R., et al., *Amine Loaded Zeolites for Carbon Dioxide Capture: Amine Loading and Adsorption Studies.* Microporous and Mesoporous Materials, 2009. **121**(1): p. 84-89.

46. Govar, A.A., *Development of a Pressure Swing Adsorption Process for CO_2 Capture from Flue Gas Using Solid Amine Sorbents*, in *Chemical Engineering, College of Engineering and Computing*. 2014, University of South Carolina: Columbia.

47. Gray, M.L., et al., *Capture of Carbon Dioxide by Solid Amine Sorbents.* International Journal of Environmental Technology and Management, 2004. **4**(1): p. 82-88.

48. Veneman, R., et al., *Continuous CO_2 Capture in a Circulating Fluidized Bed Using Supported Amine Sorbents.* Chemical Engineering Journal, 2012. **207–208**(0): p. 18-26.

49. Wang, D., et al., *Adsorption of Oils from Pure Liquid and Oil–Water Emulsion on Hydrophobic Silica Aerogels.* Separation and Purification Technology, 2012. **99**: p. 28-35.

50. Zhang, Z., et al., *Enhancing Sorption Performance of Solid Amine Sorbents for CO_2 Capture by Additives.* Energy Procedia, 2013. **37**(0): p. 205-210.

Chapter 7 : Plasma Activation on Natural Mordenite-Clinoptilolite Zeolite for Water-vapour Adsorption Enhancement

Abstract

Water-vapour is one of the crucial impurities in biogas which have to be removed for optimal performance. Utilisation of natural zeolites as water-vapour adsorbents is one of the proposed solutions. However, the small specific surface area of natural zeolite needs to be improved to increase the material adsorption capacity, one of the methods being physicochemical treatment. The consequences of the increased specific surface area by physicochemical treatment are the Si/Al ratio and hydrophobicity enhancement which counterbalance the benefits of the increased specific surface area. In this work, plasma activation treatment was applied successfully to increase the water adsorption capacity of natural zeolites after dealumination. The transformations of the chemical and physical properties of the material after plasma treatment are discussed. Our results point that the certain intrinsic properties on the zeolites in terms of Si/Al ratio and specific surface area are prerequisite to benefit from plasma activation. This work offers a new perspective on improving porous silica-based materials water adsorption characteristics which could lead to improved adsorbents in the future.

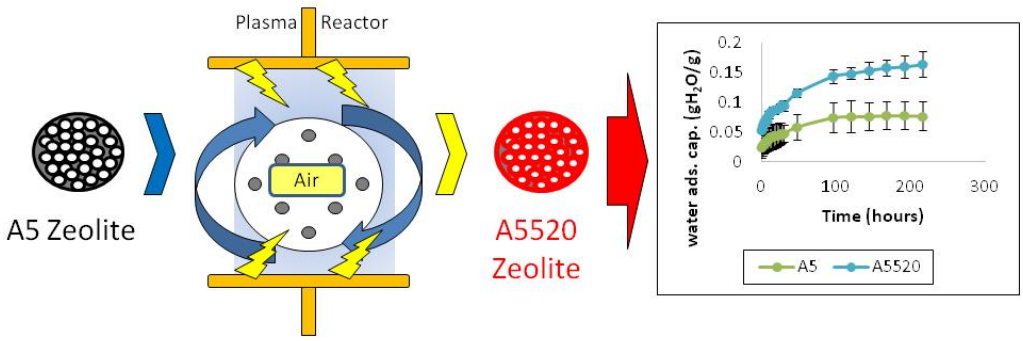

Figure 7.1. Graphical abstract of plasma activation on natural mordenite-clinoptilolite zeolite for water-vapour adsorption enhancement

7.1. Introduction

Biogas is one of the promising renewable energy sources. It can be produced in small or large capacities by processing organic waste. Some studies claim that biogas is the most efficient production of biomass conversion [1-4]. The World Bank announced biogas as a modern fuel for cooking [5]. Biogas contains methane as the fuel gas and various other impurities. These impurities limit biogas utilisation beyond heating source for cooking [6-8].

The methane enrichment of biogas is needed to increase energy level utilisation, particularly for electricity production. One of the gas impurities which need to be removed is water-vapour since it decreases the heating value and accelerates the corrosion of the equipment for electricity generation [8, 9]. Various biogas purification technologies have been utilised to reduce the water-vapour content in biogas, one of these is based on natural zeolites as a molecular sieve. Also, several studies have reported that natural zeolites have an excellent capacity to adsorb water-vapour in various other application such as in agricultural product drying [10], diesel/biodiesel dehydration [11], and bioethanol dehydration [12, 13]. The drawback of natural zeolites is their small specific surface area, typically in the range of 14-30 m^2/g [11, 12, 14, 15].

Increasing natural zeolites specific surface area can substantially improve their adsorption capacity. Physicochemical modification of Gunungkidul natural zeolite has been demonstrated to increase the material surface area significantly [16-18]. However, the treatment led to a decrease in the hydrophilic properties of the zeolite which is in line with the increase in the Si/Al ratio [19-23]. As a consequence, the benefits of the increased surface area is canceled by the increased hydrophobicity and could not positively affect the adsorption of water-vapour.

Plasma treatment offers potential pathways for improvement of the wetting properties of natural zeolites. This hypothesis is substantiated by published studies of plasma activation employed on plane surfaces of silicon, silica oxide, and glass, where the water contact angle was substantially reduced [24, 25]. Other published studies also reported that plasma charging creates a hydrophilic surface which is caused by oxide layer constructions [26, 27], porous surface diffusivity [28], and silanol groups bonding [29, 30]. A technology for

plasma treatment of particulate materials using customised plasma reactor that we reported recently provides opportunities to improve the water adsorption properties of zeolite microparticles [31-36].

The goal of this study is to investigate the potential of air plasma treatment to improve the hydrophilicity of natural zeolites, which had undergone physicochemical treatment for increasing their surface area. Ultimately, this work aims to demonstrate that plasma treatment can be a viable technology the produce high surface area, natural zeolite based water adsorbents.

7.2. Results and Discussions

7.2.1. Characterisation and water-vapour adsorption capacity of physiochemically modified natural zeolites

Three types of natural zeolites were utilised in this experiment assigned as A0, A1, and A5 zeolites. The material was in the form of a powder of identical particles size of under 425 microns, shown in the images in the top right-hand side of Figure 7.2. The Si/Al ratios (Figure 7.2(a)) in A0, A1, and A5 zeolites were 4.5, 6.2, and 11.1 determined by EDX measurement, while XPS resulted in 3.9, 5.4, and 11.9, respectively. As expected, the Si/Al ratio increased with the higher acid concentration used in the preparation process [37]. The Si/Al transformation of the zeolites also resulted in changes in their surface area. The specific surface areas of A0, A1, and A5 zeolites were 25.95, 98.37, and 179.44 m^2/g, respectively (Figure 7.2(b)). This was an increase of nearly four times for A1 zeolite and seven times for A5 zeolite relative to A0 zeolite. However, the increased surface area did not result in greater water-vapour adsorption capacity (Figure 7.2(c)). The water adsorption capacity of A0, A1, and A5 zeolites were 0.148, 0.143, and 0.078 gH_2O/g, respectively. Strikingly, the A5 zeolite had the highest surface area but the lowest water-vapour adsorption capacity. This is consistent with published studies which report that increased Si/Al ratio adversely affects the hydrophilicity of the material and thus its water adsorption properties [19-23].

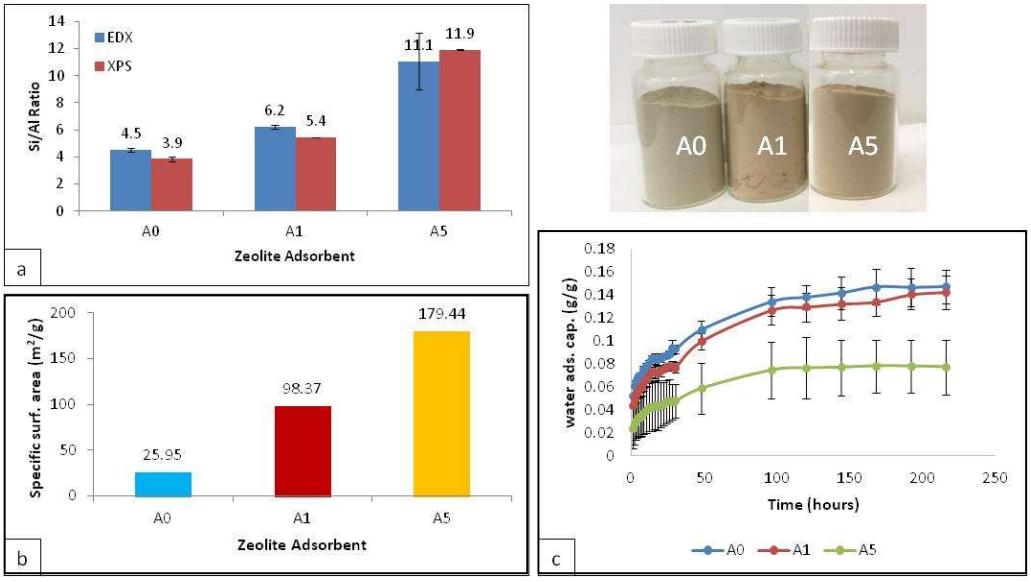

Figure 7.2. Properties of zeolites before and after dealumination: (a) Si/Al ratio determined from EDX and XPS measurements; (b) Specific surface area; (c) water adsorption capacity

7.2.2. Plasma activation

Plasma activation was carried out in a custom build system equipped with a platform for continuous agitation of particles [33-35, 38]. The condition for air plasma treatment was plasma power of 50 W, the pressure of 16 Pa and treatment time of 1200 s which applied on A0, A1 and A5 zeolites. For optimisation purposes, plasma activation was also conducted in different plasma powers and durations on the highest Si/Al ratio natural zeolite (A5 zeolite) with the reference of plasma condition at a pressure of 16 Pa, power of 50 W, and treatment time of 1200 s. The conditions of treatment of the different material used through this study and their assigned codes are shown in Table 7.1.

Table 7.1. Code of the natural zeolites in the various treatment of plasma activation

Natural Zeolite	Plasma Activation Power (W)	Activation Time (s)	Code
A0	0	0	A0
	50	1200	A0520
A1	0	0	A1
	50	1200	A1520
A5	0	0	A5
	50	1200	A5520
		600	A5510
		300	A5505
	30	1200	A5320
	10		A5120

The XPS survey spectra of the A5 zeolite before and after plasma treatment (assigned as A5520) are shown in Figure 7.3(a) and Figure 7.3(b). The spectra show the presence of oxygen (O 1s), silicon (Si 2p) and aluminium (Al 2p) at binding energies of 532 eV, 99 eV, and 73 eV, respectively. Quantification of the oxygen content of all zeolite samples before and after air plasma treatment is shown in Figure 7.3(c). Overall the plasma process increased the oxygen content in all samples. The most significant increase was observed in A1 and A5 zeolites of 1.4% and 3.3%, while the increase in oxygen content in the original A0 zeolite was insignificant and within the measurement error. The increased oxygen concentration suggests that the oxygen from the air that was present during plasma treatment has triggered oxidation reactions on the surface of the zeolites, a phenomenon that has also been observed by others [24].

Table 7.2 presents the O/Si ratio in all three zeolites before and after plasma treatment determined from XPS and EDX measurements. XPS is sensitive to the outermost 10 nm of the material surface while EDX allows probing the entire structure of the zeolites. In the case of A1 and A5 zeolites, which had undergone dealumination, the O/Si ratio increased after plasma treatment. Interestingly, there was no change in the O/Si ratio in the A0 zeolite when measured by XPS and even smaller decrease according to EDX. The changes in surface area after plasma treatment are also shown in Table 7.2. In the case of A0

zeolite, the surface area slightly increased which could be explained by the removal of impurities from the original materials. In contrast, there was a decrease in surface area in the cases of A1 and A5 zeolites which could be attributed to the build-up of an oxide layer of SiO_x in the pores of the zeolites when the Si/Al ratio is high. These results are consistent with published studies on different silica surfaces supporting the build-up of a silica layer by plasma charging [26, 27].

Further studies were conducted by FTIR. The spectra of A5 zeolite before and after air plasma treatment are shown in Figure 7.3(d). The spectra show peaks associated with Al-O / Si-O (500-800 cm^{-1}), Si-O-Si (1000 cm^{-1}), Al-OH / Si-O-Al (1500-1800 cm^{-1}), Si-OH-Al (3500-3600 cm^{-1}), and Si-OH (3700-3900 cm^{-1}) bonds. It is interesting to note the disappearance of the Si–OH bond (3700-3900 cm^{-1}) after plasma activation. This may create dangling bonds important for water-vapour adsorption since the structure will tend to attempt for regenerating [30, 39, 40].

Finally, changes in the morphology of the zeolites were studied by SEM (Figure 7.3(e)). The images of A5 zeolite before and after air plasma treatment do not show any significant morphological changes on the surface of the material. While the measurement of the specific surface area by BET showed a slight decrease in this parameter, the changes do not appear to be significant enough to be detected by SEM.

Table 7.2. O/Si ratio and specific surface area of the natural zeolites before and after plasma activation

Code	Plasma Activation Power (W)	Activation Time (s)	O/Si		Specific Surface Area (m^2/g)
			XPS	EDX	
A0	0	0	1.6	1.5	25.95
A0520	50	1200	1.6	1.4	29.81
A1	0	0	1.6	1.3	98.37
A1520	50	1200	1.7	1.5	48.40
A5	0	0	1.6	1.2	179.44
A5520	50	1200	1.7	1.3	153.15

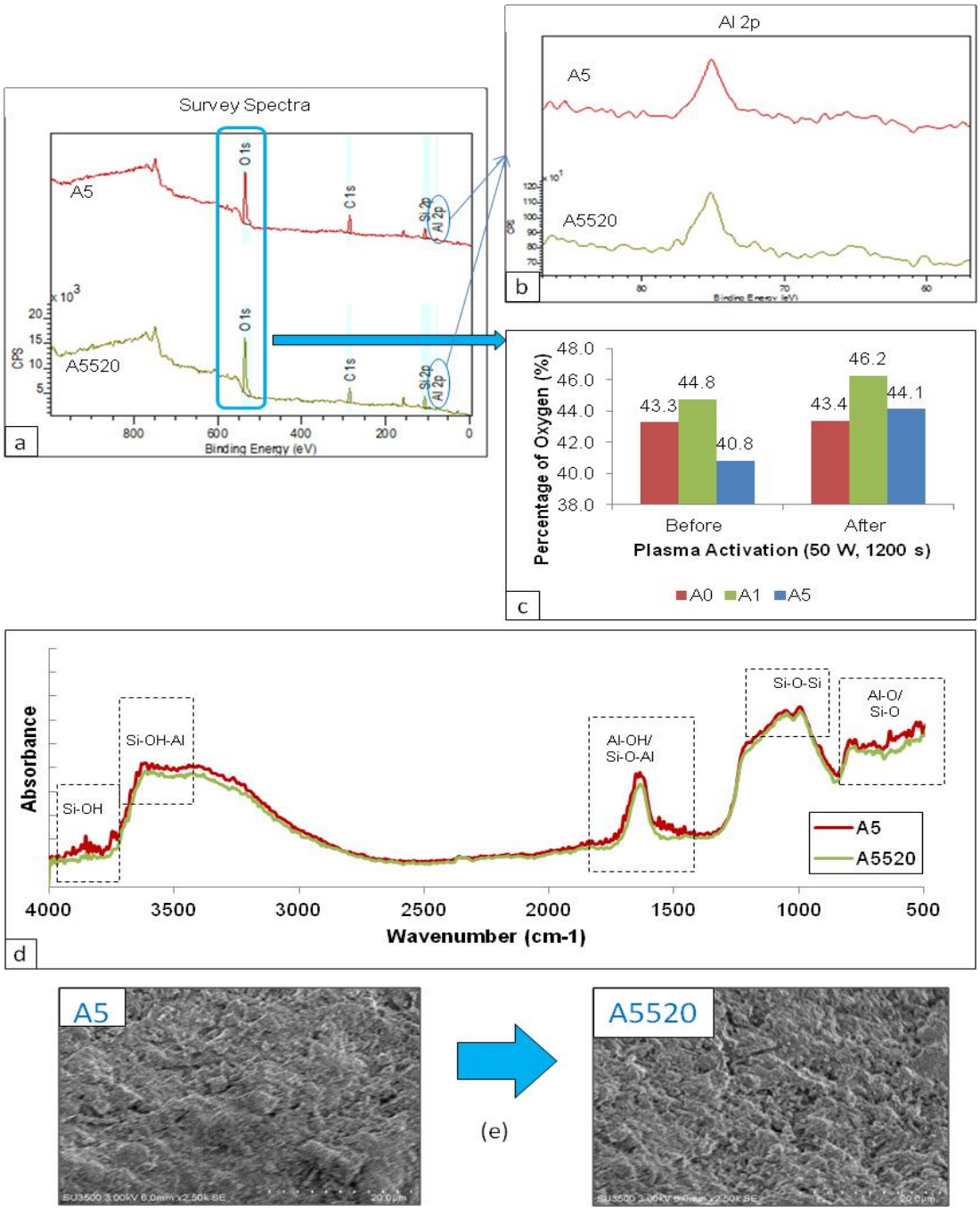

Figure 7.3. (a) XPS Survey spectra of A5 zeolite before and after plasma treatment; (b) Al 2p region zoom; (c) Oxygen percentage of A0, A1 and A5 zeolites as determined by XPS before and after plasma treatment; (d) FTIR spectra of A5 zeolite and; (e) SEM images of A5 zeolite before and after plasma treatment.

7.2.3. The water-vapour adsorption capacity of natural zeolite after plasma activation at 50 W and 1200 s

Plasma activation had only a small impact on the water-vapour adsorption capacity of A0 zeolite as shown in Figure 7.4(a). The adsorption capacity of A0 and A0520 zeolites were 0.148 and 0.142 g H_2O/g, respectively. The low Si/Al and O/Si ratios in this material, combined with its low surface area, do not appear to favour significant water-vapour adsorption even after plasma treatment.

Air plasma treatment adversely affected the A1 zeolite (Figure 7.4(b)). The adsorption capacity of A1 and A1520 zeolites were 0.143 and 0.134 g H_2O/g, respectively. Although the O/Si ratio increased for A1 zeolite treatment, the surface area of this material significantly decreased. The later counterbalanced the increased oxidation of the A1 zeolite caused by plasma treatment. However, the A5 zeolite showed the opposite trend (Figure 7.4(c)). The water adsorption capacity of A5 zeolite increased from 0.078 to 0.165 g H_2O/g. This is a significant increase that exceeded the water adsorption capacity of the other two zeolites being considered in this study. This could be attributed to the high Si content of this material which is oxidised after air plasma treatment. Our finding is supported by published studies showing that plasma activation improves Si surface reactivity and hydrophilicity [30, 39, 41].

Further, in order to determine the affinity to water-vapour, we looked at the normalised specific surface area as a function of the water-vapour adsorption capacity of the material. Two different trends are shown in Figure 7.4(d). The normalised water-vapour adsorption capacity was reduced for the A0 zeolite after plasma activation, while the affinities for water-vapour increased for A1 and A5 zeolites. These trends can be correlated with the increased oxygen content and O/Si ratios for A1 and A5 zeolites, as reported in Table 7.2.

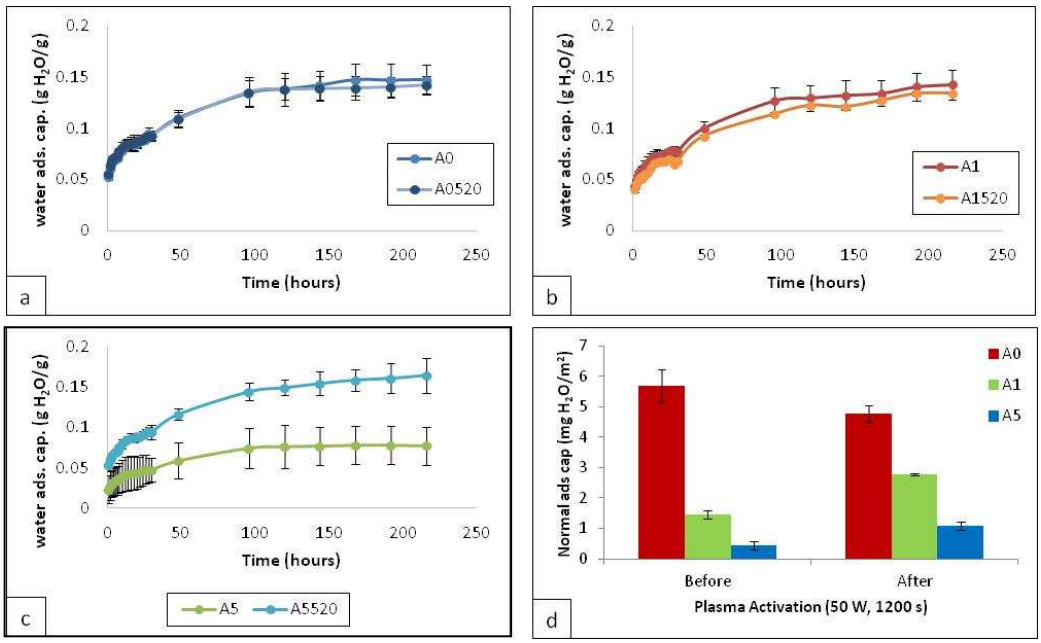

Figure 7.4. Water adsorption capacity before and after plasma activation for (a) A0 zeolite; (b) A1 zeolite; (c) A5 zeolite; and (d) water adsorption capacity normalised to the zeolites specific surface area.

7.2.4. Effect of plasma power and time of treatment on the water adsorption of A5 zeolites

Since A5 zeolite has shown to be most favourably affected by the air plasma treatment process, we carried out further studies to determine the influence of plasma power and time of treatment on the water-vapour adsorption of this material. The studied durations of treatment were 300s (A5505), 600s (A5510) and 1200s (A5520). These times of material activation did not produce significantly different results as a maximum adsorption capacity of 0.167 gH_2O/g was reached even at the shortest time (Figure 7.5(a)). The effect of plasma power used for treatment was also insignificant. Figure 7.5(b) shows that plasma powers of 10, 30, 50 W led to materials with water adsorption capacities of 0.164, 0.160, 0.165 gH_2O/g respectively. The only significant effect of plasma power and time was on the specific surface area which increased with plasma power, as shown in Table 7.3.

However, this effect did not benefit the water adsorption capacity since the affinity to water-vapour remained unchanged when different plasma powers were applied.

The results from the last section indicate the plasma power and time of treatment in the range used in this study had the almost negligible effect of the material water adsorption capacity. However, these findings may have important process design consequences. The lowest power used and the shortest time of treatment was sufficient to obtain optimal outcomes in terms of water adsorption which can be converted into economic and environmental benefits due to time, costs and electrical energy savings.

Table 7.3. O/Si ratio, specific surface area, and adsorption affinity of the A5 zeolites after treatment using different plasma power and duration

Code	Plasma Activation Power (W)	Activation Time (s)	O/Si (XPS)	Specific Surface Area (m^2/g)	Adsorption Affinity (mgH_2O/m^2)
A5	0	0	1.6	179.44	0.43 ± 0.13
A5505	50	300	1.7	148.48	1.11 ± 0.11
A5120	10	1200	1.7	146.87	1.12 ± 0.12
A5520	50	1200	1.7	153.15	1.08 ± 0.14

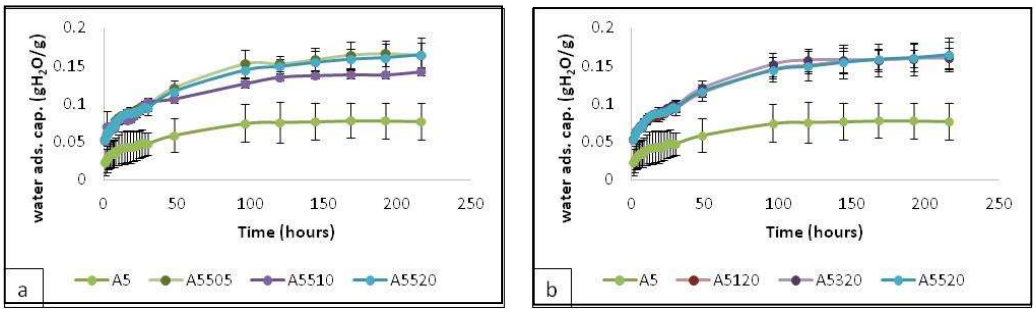

Figure 7.5. The water adsorption capacity of A5 zeolite as a function of the conditions of plasma activation used: (a) duration of plasma activation and (b) plasma power.

7.3. Conclusions

In this work, plasma activation was implemented to improve the water-vapour capacity of natural zeolites. The original material (A0 zeolite) was treated with HCl to investigate the influence of air plasma treatment on zeolites with different specific surface areas and Si/Al ratios. Plasma activation resulted in notable oxidation of the A1 and A5 zeolites which had high Si content. However, the treatment resulted in a significant reduction of the specific surface area of A1 zeolite. Plasma treatment did not affect the water adsorption capacity of A0 and A1 zeolites. This can be explained by the low O/Si ratio in the original A0 zeolite and the reduced specific surface area of A1 zeolite after plasma treatment. However, the activation by plasma had a significant positive effect on A5 zeolite, where a 2.5-time increase in water absorption capacity was observed. Overall, we showed that plasma activation had caused significant transformation of the chemical and physical properties of zeolites. However, careful consideration of the intrinsic properties of the starting material is required to achieve desired benefits in terms of water adsorption capacity. This work offers a new perspective on improving porous silica-based materials water adsorption characteristics which could lead to adsorbents with superior properties in the future.

References

1. Arumugam, S., et al., *Bio-fuels : Technology Status and Future Trends, Technology Assessment and Decision Support*. 2007: International Centre for Science and High Technology, United Nations Industrial Development Organization.

2. Salafudin, et al., *Biological Purification System: Integrated Biogas from Small Anaerobic Digestion and Natural Microalgae.* Procedia Chemistry, 2015. **14**(0): p. 387-393.

3. Pöschl, M., S. Ward, and P. Owende, *Evaluation of Energy Efficiency of Various Biogas Production and Utilization Pathways.* Applied Energy, 2010. **87**(11): p. 3305-3321.

4. Deublein, D. and A. Steinhauser, *Utilization of Gas to Generate Current and Heat*, in *Biogas from Waste and Renewable Resources*. 2010.

5. Burke, P.J., *One Goal, Two Paths: Achieving Universal Access to Modern Energy in East Asia and The Pacific–By World Bank.* Asian-Pacific Economic Literature, 2012. **26**(2): p. 167-168.

6. Ryckebosch, E., M. Drouillon, and H. Vervaeren, *Techniques for Transformation of Biogas to Biomethane.* Biomass and Bioenergy, 2011. **35**(5): p. 1633-1645.

7. Wahono, S.K., H. Julendra, and A. Febrisiantosa, *Peningkatan Performa Biogas Melalui Teknologi Pemurnian Metana di UPT Kapitan Meo, Kabupaten Belu–Nusa Tenggara Timur [Performance Enhancement of Biogas Using Purification Technology of Methane at UPT Kapitan Meo, District Belu–East Nusa Tenggara]*, in *National Seminar on Technology Development Based on Local Materials*. 2009: Yogyakarta–Indonesia. p. 505-508.

8. Wahono, S.K. and W.A. Rizal, *Biogas Filter Based on Local Natural Zeolite Materials.* International Journal of Renewable Energy Development, 2014. **3**(1): p. 1-5.

9. Wahono, S.K., R. Maryana, and M. Kismurtono, *Biogas Purification Process to Increase Gen—Set Efficiency.* AIP Conference Proceedings, 2009. **1169**(1): p. 185-189.

10. Anggoro, D.D., et al., *Pemanfaatan Zeolit Alam dalam Proses Pengeringan Daun Tembakau [Natural Zeolites Utilization for Drying of Tobacco Leaf]*, in *National Seminar on Chemical Engineering Fundamentals and Applications*. 2005, Chemical Engineering Departement of Institute of Technology Sepuluh November Surabaya: Surabaya–Indonesia. p. DP8 1-5.

11. Favvas, E.P., et al., *Clinoptilolite, a Natural Zeolite Material: Structural Characterization and Performance Evaluation on Its Dehydration Properties of*

Hydrocarbon-Based Fuels. Microporous and Mesoporous Materials, 2016. **225**(Supplement C): p. 385-391.

12. Hernawan, et al., *Modification of Gunungkidul Natural Zeolite as Bioethanol Dehydrating Agents.* Energy Procedia, 2015. **65**: p. 116-120.

13. Wahono, S.K., et al., *Characterization and Utilization of Gunungkidul Natural Zeolite for Bioethanol Dehydration.* Energy Procedia, 2014. **47**: p. 263-267.

14. Dziedzicka, A., B. Sulikowski, and M. Ruggiero-Mikołajczyk, *Catalytic and Physicochemical Properties of Modified Natural Clinoptilolite.* Catalysis Today, 2016. **259**: p. 50-58.

15. Korkuna, O., et al., *Structural and Physicochemical Properties of Natural Zeolites: Clinoptilolite and Mordenite.* Microporous and Mesoporous Materials, 2006. **87**(3): p. 243-254.

16. Widayat, A. Roesyadi, and M. Rachimoellah, *The Effect of Time Dealumination and Solvent Concentration in Synthesis of Zeolite Catalyst and Catalytic Test for DiEthyl Ether Production Process.* AIP Conference Proceedings, 2009. **1169**(1): p. 106-112.

17. Ahmed, M.H.M., et al., *Effect of Multi-Step Desilication and Dealumination Treatments on The Performance of Hierarchical EU-1 Zeolite for Converting Methanol to Olefins.* Microporous and Mesoporous Materials, 2017. **241**: p. 79-88.

18. Ban, S., et al., *Insight into the Effect of Dealumination on Mordenite Using Experimentally Validated Simulations.* The Journal of Physical Chemistry C, 2010. **114**(5): p. 2056-2065.

19. Mandasari, W., B. Sitorus, and D.R. Jati, *Pembuatan dan Karakterisasi Adsorben Gas H_2S dari Zeolit Alam [Preparation and Characterization of Natural Zeolite as H_2S Adsorbents]*. Jurnal Kimia Khatulistiwa, 2014. **3**(2): p. 56-63.

20. Shirazi, L., E. Jamshidi, and M.R. Ghasemi, *The Effect of Si/Al Ratio of ZSM-5 Zeolite on Its Morphology, Acidity and Crystal Size.* Crystal Research and Technology, 2008. **43**(12): p. 1300-1306.

21. Sriatun, S. and A. Darmawan, *Dealuminasi Zeolit Alam Cipatujah Melalui Penambahan Asam dan Oksidator [Dealumination of Cipatujah Natural Zeolites by Acid and Oxidants Addition]*. Kimia Sains dan Aplikasi, 2005. **8**(2).

22. Ramesh, K. and D.D. Reddy, *Chapter Four - Zeolites and Their Potential Uses in Agriculture*, in *Advances in Agronomy*, D.L. Sparks, Editor. 2011, Academic Press. p. 219-241.

23. Barrer, R., *Porous Crystals: A Perspective.* Pure and Applied Chemistry, 1986. **58**(10): p. 1317-1322.

24. Alam, A., M. Howlader, and M. Deen, *Oxygen Plasma and Humidity Dependent Surface Analysis of Silicon, Silicon Dioxide and Glass for Direct Wafer Bonding.* ECS Journal of Solid State Science and Technology, 2013. **2**(12): p. P515-P523.

25. Alam, A., M. Howlader, and M. Deen, *The Effects of Oxygen Plasma and Humidity on Surface Roughness, Water Contact Angle and Hardness of Silicon, Silicon Dioxide and Glass.* Journal of Micromechanics and Microengineering, 2014. **24**(3): p. 035010.

26. Farrens, S.N., et al., *Chemical Free Room Temperature Wafer to Wafer Direct Bonding.* Journal of The Electrochemical Society, 1995. **142**(11): p. 3949-3955.

27. Sung, K.T. and S.W. Pang, *Oxidation of Silicon in an Oxygen Plasma Generated by a Multipolar Electron Cyclotron Resonance Source.* Journal of Vacuum Science & Technology B: Microelectronics and Nanometer Structures Processing, Measurement, and Phenomena, 1992. **10**(5): p. 2211-2216.

28. Amirfeiz, P., et al., *Formation of Silicon Structures by Plasma-Activated Wafer Bonding.* Journal of The Electrochemical Society, 2000. **147**(7): p. 2693-2698.

29. Suni, T., et al., *Effects of Plasma Activation on Hydrophilic Bonding of Si and SiO2.* Journal of The Electrochemical Society, 2002. **149**(6): p. G348-G351.

30. Tan, C.M., W. Yu, and J. Wei, *Comparison of Medium-Vacuum and Plasma-Activated Low-Temperature Wafer Bonding.* Applied Physics Letters, 2006. **88**(11): p. 114102.

31. Jarvis, K.L. and P. Majewski, *Plasma Polymerized Allylamine Coated Quartz Particles for Humic Acid Removal.* Journal of Colloid and Interface Science, 2012. **380**(1): p. 150-158.

32. De Vietro, N., R. d'Agostino, and F. Fracassi, *Introduction of Basic Functionalities on The Surface of Granular Adsorbers by Low Pressure Plasma Processes.* Plasma Processes and Polymers, 2012. **9**(9): p. 911-918.

33. Cavallaro, A. and K. Vasilev, *Controlled and Sustained Release of Pharmaceuticals via Single Step Solvent-Free Encapsulation.* Chemical Communications, 2015. **51**(10): p. 1838-1841.

34. Wahono, S.K., et al., *Preliminary Study: Combination of Amine and Natural Zeolite as New Adsorbent Material for CO_2 capture*, in *Chemeca 2016: Chemical Engineering-Regeneration, Recovery and Reinvention*. 2016. p. 900-910.

35. Mierczynska-Vasilev, A., et al., *A Novel Technology for The Rapid, Selective, Magnetic Removal of Pathogenesis-Related Proteins from Wines.* Food Chemistry, 2017. **232**(Supplement C): p. 508-514.

36. Michl, T.D., et al., *Laboratory Scale Systems for The Plasma Treatment and Coating of Particles.* Plasma Processes and Polymers, 2015. **12**(4): p. 305-313.

37. Wahono, S.K., et al., *Carbon Dioxide Adsorption Enhancement of Natural Mordenite-Clinoptilolite Zeolite by Physicochemical Treatment*. 2018: Unpublished work.

38. Wahono, S.K., et al., *Plasma Polymer Facilitated Magnetic Technology for Removal of Oils from Contaminated Waters.* Environmental Pollution, 2018. **240**: p. 725-732.

39. Ma, X., et al., *Study of The Ge Wafer Surface Hydrophilicity After Low-Temperature Plasma Activation.* Journal of The Electrochemical Society, 2009. **156**(5): p. H307-H310.

40. Howlader, M.M.R., F. Zhang, and M.G. Kibria, *Void Nucleation at a Sequentially Plasma-Activated Silicon/Silicon Bonded Interface.* Journal of Micromechanics and Microengineering, 2010. **20**(6): p. 065012.

41. Byun, K.Y., et al., *Comprehensive Investigation of Ge–Si Bonded Interfaces Using Oxygen Radical Activation.* Journal of Applied Physics, 2011. **109**(12): p. 123529.

Chapter 8 : Plasma Polymer Facilitated Magnetic Technology for Removal of Oils from Contaminated Waters

Abstract

Oil pollution of waters is one of the most serious environmental problems globally. The long half-life and persistence within the environment make oil particularly toxic and difficult to remediate. There is a significant need for efficient and cost-effective oil recovery technologies to be brought in to practice. In this study, we developed a facile and efficient magnetic separation method. The surface of 316L stainless steel nanoparticles was modified by plasma deposition of 1,7-octadiene and perfluorooctane, producing relatively hydrophobic coatings having water contact angles of 86 and 100 degrees, respectively. Both coatings had high oil removal efficiency (ORE) of >99%. The captured oil could be easily separated by applying an external magnetic force. The ease of material preparation and separation from the water after the oil is captured, and its high ORE is a compelling argument for further development and optimisation of the technology to possible utilisation into practice. Furthermore, the capacity of plasma polymerisation to deliver desired surface properties can extend the application of the technology to removing other chemical and biological contaminants from polluted waters.

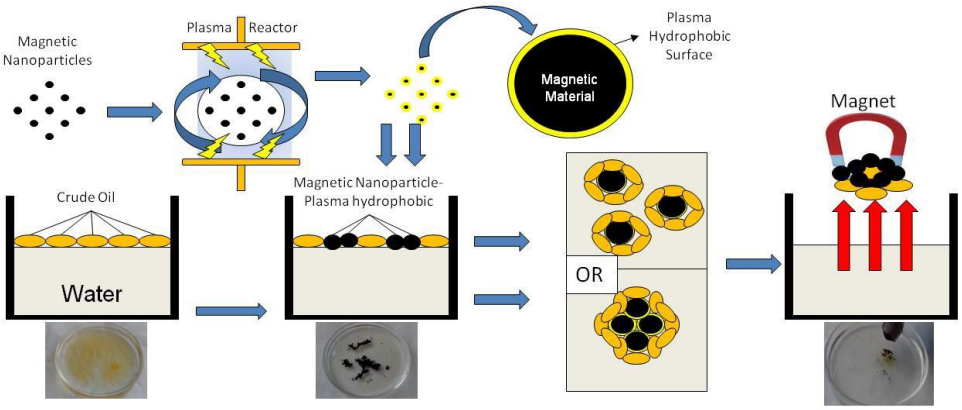

Figure 8.1. Graphical abstract of plasma polymer facilitated magnetic technology for the removal of oils from contaminated waters

8.1. Introduction

With the growth of industrial development and exploration, production, and refining, the possibility for oil pollution of the environment presents a significant risk. Oils are considered particularly dangerous contaminants because of their persistence and extremely long half-lives in the environment [1]. Some sources often causing water pollution by oil contaminants are factories waste, petroleum transport and refinement, transportation leakages and household waste [2-4]. Furthermore, common strategies and technologies implemented for oil removal are gravity separation, physical separation, flotation, evaporation, chemical extraction, membrane separation, and adsorption [5, 6].

The adsorption method is by far the most popular technique because of its efficiency, low cost, simplicity of utilisation and the ease of the application [7]. This process exploits the physical adhesion of the pollutant to a solid physical surface. The essential requirement for adsorbent materials is to be hydrophobic and oleophilic [8]. Such materials have already been applied for water-oil separation, particularly for high viscosity oils [9]. Recently, considerable efforts have been made to develop efficient adsorbents by modifying material surface properties. Typical chemistries used to generate hydrophobic surfaces are hydrocarbon [3, 10, 11], fluorocarbon [12-15], or siloxane [16-18]. These adsorbents have been demonstrated to deliver good outcomes when applied for removing oil spillage, organic solvents and toxic organic compounds [19-23].

One of the current challenges related to the methods for material surface modification is that the procedures are commonly conducted by wet-chemistry and rely on complex reactions, which are highly substrate type dependent and produce an excess of potentially toxic waste products [24, 25]. This complexity leads to limitations in the selection of carrier material and prohibitive costs associated with west solvent treatment. Thus, it is logical to develop methods which can potentially overcome these limitations. An example of such alternatives is a technique called plasma polymerisation. The methods involve the deposition of polymer–like, highly crosslinked coating from the vapour of an organic precursor [26-28].

Plasma polymerisation offers many benefits compared to wet processes. It is substrate independent, which means that identical coatings can be deposited on the surface of

different materials using the same process [29]. The techniques consist of a single step and do not require the use of any solvents. Furthermore, coatings can be deposited on substrates of compact sizes and shapes, including micro and nanoparticles. Finally, there is a substantial body of literature from our group and others pointing that hydrophobic coatings can be prepared in a very facile way using plasma-based techniques [30-34].

Another challenge is to separate the adsorbent material from the contaminated continuum. Processes such as centrifugation and filtration give excellent results in some situations, but they are too expensive or inapplicable in some instances. In this work, we selected to use as hydrophobic coating carrier 316L stainless steel nanoparticles because they can be easily separated by the contaminated medium by an external magnetic field. Nanoparticles also have a very high surface to volume ratio, thus providing a large surface area to which oil contaminants could be concentrated. The surface of magnetic and others particulate can be modified by plasma polymerisation using customised systems developed by our group and others. [35-40]

The hypothesis underpinning this work is that 316L stainless steel nanoparticles modified by hydrophobic plasma polymer layers can be successfully utilised for the removal of oils from aqueous media. To validate this hypothesis, we coated the surface of magnetic nanoparticles using two precursors known to deliver coatings with different levels of hydrophobicity. After characterising the chemical and physical properties of the coatings, we evaluated the capacity of newly developed plasma polymer coated magnetic adsorbents to oils from model aqueous media.

8.2. Results and Discussion

8.2.1. Crude oils characteristics

Crude oil samples appeared black-brownish or amber. Density and viscosity values for both samples are shown in Table 8.1. Crude Oil 1 had a density of 779.1 kg/m^3 and viscosity of 5.22 mPa.s whereas crude Oil 2 has a density of 769.2 kg/m^3 and viscosity of 2.11 mPa.s. These values indicate that the oils can be classified as ‘light’ since their

density and viscosity are under 887.0 kg/m^3 and 300 mPa.s, respectively [41]. The oils flow naturally at room temperature.

Table 8.1. Density and viscosity of crude oil samples

Properties	**Crude Oil 1**	**Crude Oil 2**
Color		
Density (kg/m3)	779.1 + 0.2	769.2 + 1.0
Viscosity (mPa.s)	5.22 + 0.4410	2.11 + 0.4859

8.2.2. Plasma polymer modification

Two different compounds were selected as precursors for the plasma deposition. 1,7-octadiene was chosen because of the high number of non-polar CxHy functionalities in its structure, while perfluorooctane was also selected because of the high fluorocarbon content is known to result in hydrophobic plasma polymers.

The thickness of the deposited plasma polymer layers was determined by ellipsometry. The thicknesses were measured on coatings deposited on silicon wafers and are shown in Table 8.2. When deposited using the power of 50 W and pressure of 16 Pa, the thickness of the octadiene film was 57 nm, 187 nm, and 356 nm after 180 s, 300 s and 600 s of plasma deposition, respectively. Under the same deposition conditions, the perfluoroctane polymer layers were significantly thinner, reaching only 43 nm after 600 s of plasma deposition. The thickness of the plasma polymer layer deposited on particles surface is expected to be significantly lower compared to that placed on flat surface because: 1) the surface area of the particles is significantly greater compared to planar surfaces [37, 38]; 2) the particles continually move exposing only small surface area to the species depositing from the plasma at a given time and; 3) the continuous particle motion may result in abrasion which further delays coating deposition.

Table 8.2. Thickness and surface wettability of plasma polymer films deposited on a silicon wafer

Monomer	Plasma processing conditions		Plasma polymer layer thickness as a function of plasma deposition time (nm)			Surface Wettability
	Power	Pressure	180 s	300 s	600 s	600 s
Octadiene	50 W	16 Pa	58 + 0.3	187 + 2	356 + 5	 86°
Perfluorooctane	50 W	16 Pa	5 + 0.2	31 + 0.1	43 + 0.5	
Perfluorooctane	50 W	23 Pa	92 + 5	141 + 4	239 + 2	 100°

To increase the deposition rate of perfluoroctane and make sure that there is sufficient plasma polymer coverage on the magnetic nano-particles surface, the deposition pressure was increased from 16 Pa to 23 Pa. This resulted in coating thicknesses of 92 nm, 141 nm and 239 nm obtained after 180 s, 300 s, and 600 s, respectively.

To determine the hydrophobicity of the plasma deposited octadiene and perfluorooctane derived coatings the static water contact angles were measured by the sessile drop method. Both precursors delivered hydrophobic surfaces. Perfluorooctane based coatings had a water contact angle of 100° at 600 s deposition while this parameter was slightly lower for octadiene films, i.e., in the range of 86° which also shown in Table 8.2. As it was expected, perfluorooctane resulted in more hydrophobic than octadiene.

8.2.3. Stability of the coatings in water

Since the coatings were intended for use in water, it was important to assess the stability of the coatings when placed in this medium. To do this, we used established procedures which we developed in our group over the last years [42, 43]. Coatings are immersed in water for a predetermined period of time. The coating thickness is then measured and compared with the thickness before immersion. If the coating dissolves or delaminates, this is reflected in a loss of film thickness. Figure 8.2 shows the coating thickness before and after immersion in water. The results show that regardless of the time of deposition the coatings we stable in an aqueous medium, and no loss of thickness was registered.

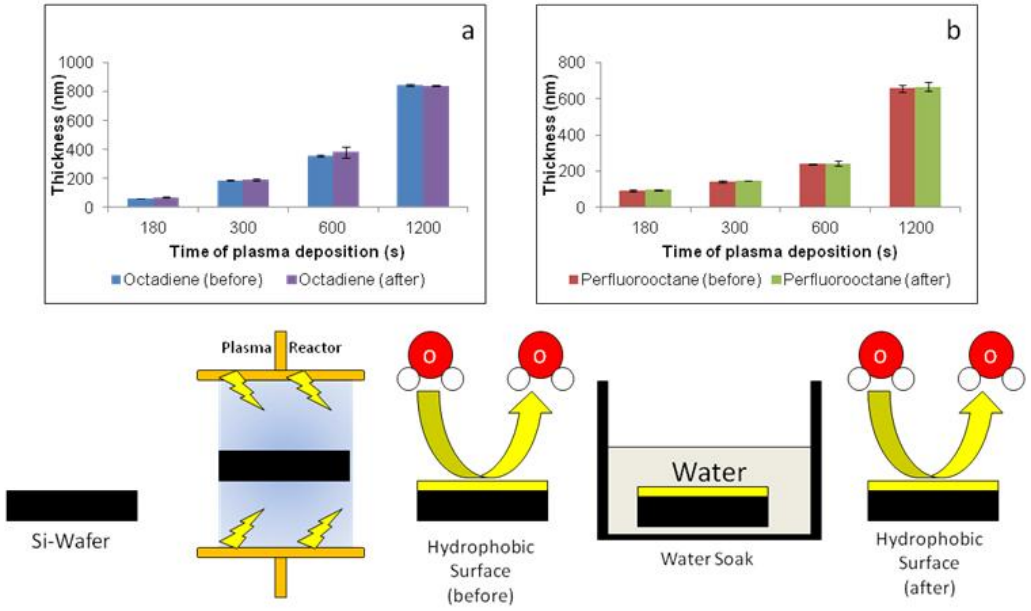

Figure 8.2. Coating thickness at four different deposition times before and after immersion in water: (a) Octadiene and (b) Perfluorooctane

8.2.4. Chemical characterisation of coated magnetic nanoparticles

As discussed above, the thickness of the plasma polymer coating is much lower when deposited on particulates compared to flat surfaces. The chemical composition of the plasma polymer coatings deposited on the surface of the magnetic nanoparticles was characterised by XPS. Knowing the sampling depth of XPS of about 10 nm, these

measurements also allowed us to make estimations for the thickness of the coating deposited on the particles. Figure 8.3 shows the atomic percentage of element available on the nanoparticles surface as a function of plasma deposition time. We should note that the uncoated magnetic nanoparticles had significant hydrocarbon content, i.e., 42.5 At%. This could be attributed to contaminations resultant from the fabrication process and/or exposure to ambient air since no cleaning process was used before nanoparticles surface modification. These contaminations can be different depending on the environment the nanoparticles were exposed. Thus, plasma polymer modification can help define the surface chemical composition of the material. When coatings deposited from the vapour of 1,7-octadiene were placed on the surface of the nanoparticles an apparent increase in the concentration of carbon was observed with a decrease in oxygen and iron content. 1200 s deposition time led to an increase in the atomic surface concentration of carbon to about 63 At%. Further increase in the deposition time did not result in any change in the atomic concentration of carbon, oxygen, and iron, which suggests that the thickness of the coating has exceeded 10 nm.

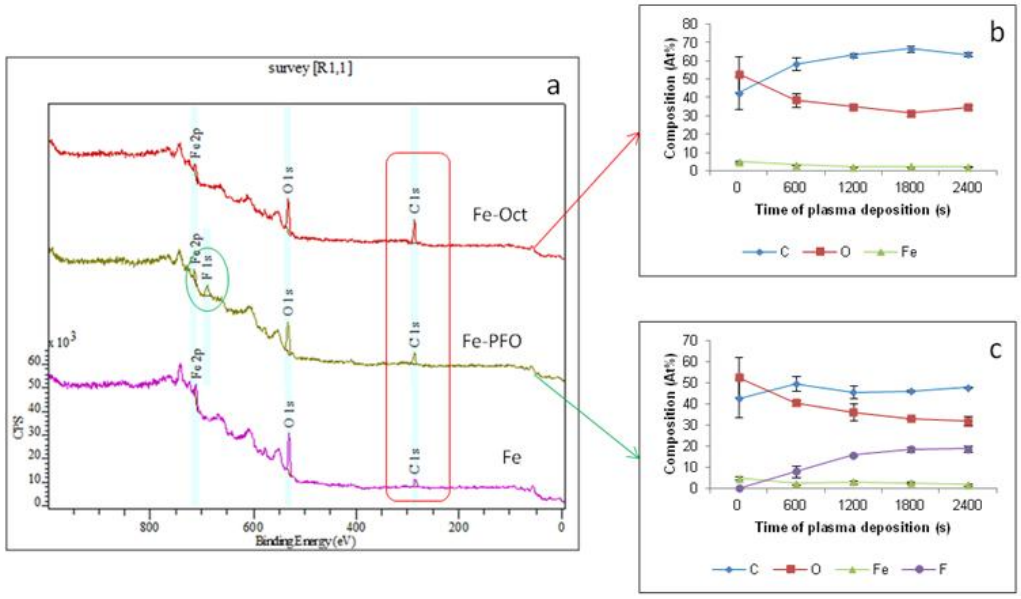

Figure 8.3. The chemical composition of the nanoparticles surfaces determined by XPS before and after modification: (a) XPS survey spectra of Fe-Raw, Fe-Octadiene, and Fe-PFO; (b) Fe-1.7-octadiene; (c) Fe-perfluorooctane

Similar trends were observed when the nanoparticles were modified with coatings deposited from the vapour of perfluorooctane. The presence of fluorine in the molecule of the precursor made it relatively easy to monitor the evolution of the coating with time on deposition. After 600 s of deposition, the particle surface has approximately 7.9 At% of fluorine. The atomic percent of fluorine increased with plasma deposition time. After 1200 s of deposition, the fluorine concentration was 16 At%, increasing to 18 At% at 1800 s of deposition and remaining unchanged at 2400 s. In the same time, the atomic concentration of carbon, oxygen, and iron all decreased and remained constant after 1800 s of plasma polymer deposition. This data suggests that a nearly continuous coating with a thickness above 10 nm was created at 1800 s of plasma deposition.

8.2.5. Oil recovery

The wettability and chemical analysis of the coatings deposited on the magnetic nanoparticles point to relatively hydrophobic coatings rich in non-polar hydrocarbon and fluorocarbon chemistries. The characteristics of the coatings suggest the potential for binding dispersed in water-oil molecules which are also hydrophobic and nonpolar in nature. The magnetic properties of the nanoparticles will facilitate their easy collection together with the oil captured molecules.

Figure 8.4(a) shows the relative ORE for the octadiene, and perfluorooctane plasma polymer coated magnetic nanoparticles. After 600 s of plasma deposition, the octadiene coated particles removed 99.9% of crude oil 1 and 99.2% of crude oil 2. Although the adsorption of crude oil 1 did not seem to change with increasing deposition time, the uptake of crude oil 2 increased to 100% after 20 min plasma deposition. Those results are in agreement with the XPS surface composition analysis where optimum polymer coverage was obtained after 1200 s of plasma deposition. The ORE for the perfluorooctane coating also depends on the time of deposition of the coating. After 600 s of perfluorooctane deposition, the magnetic nanoparticles were able to adsorb 98.6% and 99.3% of crude oil 1 and crude oil 2, respectively. Adsorption of crude oil 1 increased further to 99.2% and 99.8% as deposition time was increased to 1200 s and beyond.

Interestingly, uptake of crude oil 2 plateaued at 99.8% after increasing the deposition time to 1200 s. Ultimately, it appeared that when deposited for short periods, i.e., <1200 s; the octadiene coated magnetic nanoparticles seemed to have a higher oil affinity and removal efficiency. At longer deposition times, such as 1800 and 2400 s, both polymers showed equal performance. This indicates that coatings derived from octadiene plasma form faster a continuous film on the surface of the nanoparticles, a result that was also suggested by the XPS characterisation.

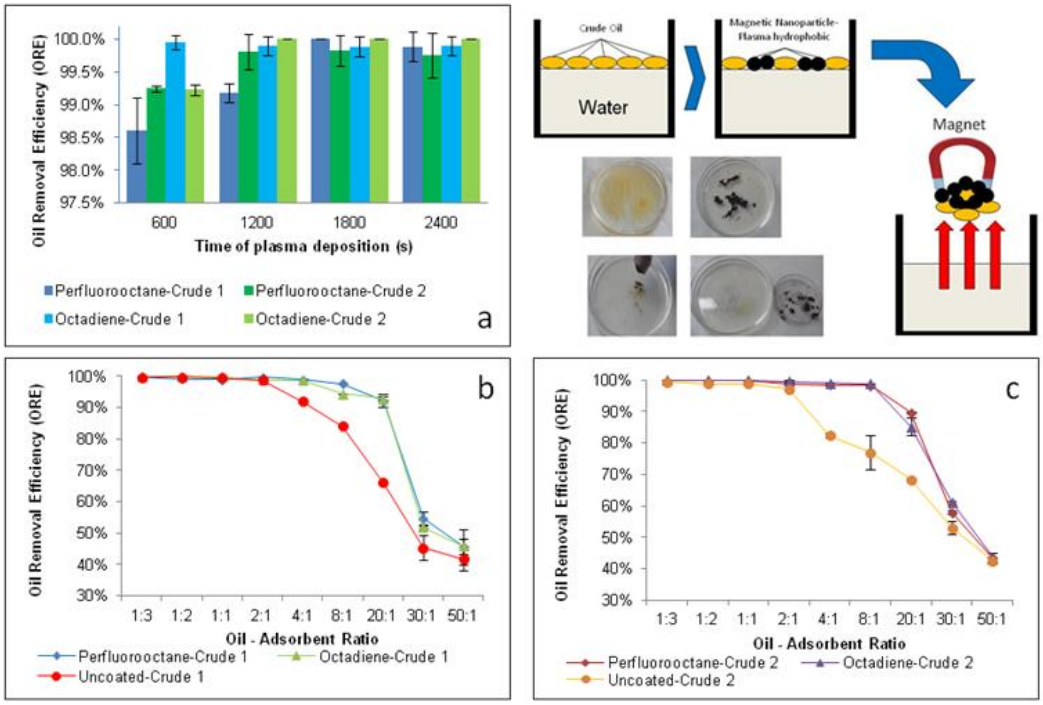

Figure 8.4. ORE of magnetic nanoparticles: (a) coated with octadiene and perfluorooctane plasma polymers for different deposition times (Oil:Adsorbent ratio = 1:2); (b, c) plasma polymer coated and uncoated versus oil:adsorbent ratio for: (b) Crude oil 1; (c) Crude oil 2

8.2.5.1. Effect of Oil-Adsorbent Ratio

ORE of different oil/adsorbent ratios was used to investigate the impact of the adsorbent concentration on oil recovery. Naturally, we expected that the total oil recovery is related to the adsorbent surface area and the hydrophobicity of the coating. An increased amount

of the adsorbent would naturally provide a greater surface area for attachment of oil molecules.

Figure 8.4(b) and 8.4(c) show the total ORE for different oil to adsorbent ratios. When more oil is added to the system, the same quantity of adsorbent material is not able to remove the increased amount of oil. This phenomenon is clearly seen in Figure 8.4(b) and 8.4(c) where ORE decreases as the oil-adsorbent ratio increases. However, higher oil/adsorbent ratio may eventually provide better ORE values per gram of adsorbent as demonstrated in published reports [44].

At low oil/adsorbent ratios, both uncoated and coated magnetic nanoparticles reached ORE of greater than 99%. The result indicates that unmodified magnetic nanoparticles also have the ability to capture oil. This is to be expected if we revisit Figure 8.3 where we noted the high carbon content on the surface of the untreated magnetic nanoparticles. This high amount of carbon is likely a result of the manufacturing process and environmental contamination, which may differ from batch to batch making the utilisation of unmodified material unreliable. Furthermore, unmodified magnetic nanoparticles readily sank and became saturated quicker than the plasma coated identical material. The greater capacity to "float" of plasma polymer modified particles was due to their more hydrophobic nature. The uncoated magnetic adsorbent performed well when the oil/adsorbent ratio was 1:3, 1:2, 1:1 and 2:1 for both types of crude oil samples, which translated to oil-capture capacity of 0.33 g/g, 0.5 g/g, 1 g/g, and 2 g/g, respectively. Above 2:1 ratio, the oil-capture capacity of uncoated magnetic adsorbent dramatically decreases.

A comparison between the two different types of plasma polymer coatings revealed that there is no significant difference between them in terms of ORE. Magnetic nanoparticles modified with octadiene and perfluorooctane maintained a maximum ORE of more than 99% until the oil-adsorbent ratio was higher than 4:1 regardless of the crude oil used. For 8:1 ratio, the modified magnetic material performed better for crude oil 2 samples with ORE of >99%, compared to crude oil 1 where ORE was 94%. The coated magnetic adsorbent had an oil-capture capacity of 8g/g, which is an increase of 400% compared to the uncoated magnetic adsorbent. These results demonstrate that the plasma deposition significantly enhanced the capacity for oil capture of the untreated material.

8.2.5.2. Effect of scale-up

Since the contamination of water with oil commonly occurs in a large water volume, it is essential to investigate the performance of the magnetic adsorbent in greater water volumes. In this experiment, 8:1 and 20:1 of oil:adsorbent ratios were chosen because both of the plasma-coated magnetic nanoparticles have ORE value of above 85%. The resultants ORE value is shown in Figure 8.5 for the 8:1 and 20:1 ratio.

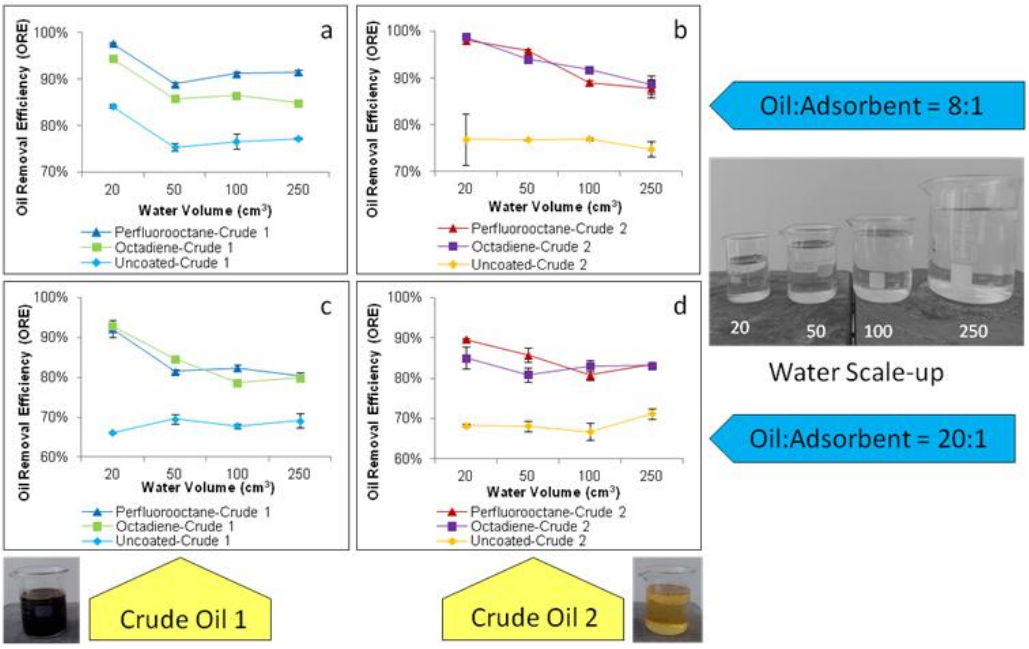

Figure 8.5. The ORE of coated and uncoated magnetic adsorbents as a function of increasing water volume for 8:1 of oil:adsorbent ratio: (a) Crude oil 1; (b) Crude oil 2; and for 20:1 of oil:adsorbent ratio: (c) Crude oil 1; (d) Crude oil 2

As shown in Figure 8.5(a) and 8.5(b) the performance of magnetic adsorbent moderately decreases when the total volume of water is scaled-up as compared to the initial experiment using only 20 cm^3 of suspension. The ORE of crude oil 1 decreased from 97% to 82% when perfluorooctane was used and from >94% to approximately 82% in the case of octadiene when water volume increased to 250 cm^3. The ORE of crude oil 2 was also affected by increasing the volume of water. In this case, the ORE decreased from ~99% to 89% for both plasma-coatings. The uncoated magnetic nanoparticles showed the same

trend, but ORE decreased to a lower value (~75%) compared to the coated magnetic adsorbent.

Figure 8.5(c) and 8.5(d) shows water scale-up of 20:1 ratio for both crude oil samples and both hydrophobic coatings. The ORE decreases to ~80% for the coated magnetic adsorbent and ~68% for the bare magnetic nanoparticles. Since the total ORE is mostly affected by the oil which floats on the water surface, thus greater water oil did not significantly impact the oil recovery. These studies once again demonstrate the benefit of applying plasma polymer modification of the surface of the magnetic nanoparticles.

8.2.6. Comparison of newly developed technology for oil recovery with literature

The technology for oil recovery developed in this work provides high efficacy of oil recovery and high oil adsorption capacity. To illustrate this, we compared with published studies which shown in Table 8.3. Overall, our technology appears to be more efficient than those reported so far. We should also stress that plasma surface modification is a one-step facile and fast process to achieve optimal surface properties of the adsorbent material. Combined with the ease to separate the captured oil via an external magnetic force a compelling argument can be made for further development and optimisation to possible utilisation in practice.

Table 8.3. Adsorption capacity and oil recovery for comparable materials published in the literature.

Adsorbent	Adsorbate	Adsorption capacity (g/g)	Removal Efficiency (%)	Reference
Octadiene/plasma polymer coated magnetic nanoparticles	crude oil	8	80 – 99	Present Work
Perfluorooctane/plasma polymer coated magnetic nanoparticles	crude oil	8	80 – 99	Present Work
Polyvinylpyrrolidone coated magnetic nanoparticles	crude oil	not reported	85 – 95	[45]
Magnetic titania nanotubes	various oil	>1.5	not reported	[46]
Magnetic nanoparticle coated fluorinated carbon fabric membrane	olive oil	not reported	>95	[47]
Modified $FeNi_3$ magnetic nano-chains	lubricating oil	not reported	66.18 – 88.28	[48]
Modified magnetic porous silica submicron particles	lubricating oil	11.51	not reported	[49]
Magnetic cellulose/ TiO2 aerogel	paraffin oil	28	not reported	[50]
Octadiene plasma polymer coated silica particles	crude oil	0.5	70 – 99	[44]
Magnetic macro-porous carbon nanotubes	diesel oil	56	not reported	[51]

8.3. Conclusions

Collectively, we report a facile technology of oil recovery from contaminated waters via a magnetic force. Plasma deposition of 1,7-octadiene and perfluorooctane precursors was implemented to modify the surface of magnetic nanoparticles in order to generate new hydrophobic adsorbents. Both precursors resulted in effective oil recovery with ORE >99% after 1200 s of plasma deposition. The octadiene plasma polymer coated magnetic nanoparticles appeared to perform better after a shorter time of plasma polymer modifications which suggests that this precursor leads to fasted achieving uniform coatings on the surface of the nanoparticles.

On the other hand, perfluorooctane modified nanoparticles worked better when a smaller amount of adsorbent was used. The greater hydrophobicity of the perfluorooctane coating is likely to provide more efficient interaction with oil molecules. The scale-up experiments demonstrated that both types of plasma polymer coated magnetic adsorbents retained 80% ORE when water amount was increased 12 fold. The technology for oil recovery presented here is an attractive alternative to existing methods considering the facile fabrication, efficiency of recovery and ease of separation. Furthermore, the versatility of plasma polymerisation to deliver coatings of tailored properties paves the foundation for developing of derivative separation technologies for other chemical and biological pollutants from waters.

References

1. Guix, M., et al., *Superhydrophobic Alkanethiol-Coated Microsubmarines for Effective Removal of Oil.* ACS Nano, 2012. **6**(5): p. 4445-4451.

2. Jha, M.N., J. Levy, and Y. Gao, *Advances in Remote Sensing for Oil Spill Disaster Management: State-of-The-Art Sensors Technology for Oil Spill Surveillance.* Sensors, 2008. **8**(1): p. 236-255.

3. Wang, D., et al., *Adsorption of Oils from Pure Liquid and Oil–Water Emulsion on Hydrophobic Silica Aerogels.* Separation and Purification Technology, 2012. **99**: p. 28-35.

4. Seifi, L., et al., *Adsorption of Petroleum Monoaromatics from Aqueous Solutions Using Granulated Surface Modified Natural Nanozeolites: Systematic Study of Equilibrium Isotherms.* Water, Air, & Soil Pollution, 2011. **217**(1): p. 611-625.

5. Arthur, J.D., B.G. Langhus, and C. Patel, *Technical Summary of Oil and Gas Produced Water Treatment Technologies*, in *All Consulting, LLC, Tulsa, OK*. 2005. p. 42-50.

6. Fakhru'l-Razi, A., et al., *Review of Technologies for Oil and Gas Produced Water Treatment.* Journal of Hazardous Materials, 2009. **170**(2–3): p. 530-551.

7. Ali, I., M. Asim, and T.A. Khan, *Low Cost Adsorbents for The Removal of Organic Pollutants from Wastewater.* Journal of Environmental Management, 2012. **113**: p. 170-183.

8. Chu, Y. and Q. Pan, *Three-Dimensionally Macroporous Fe/C Nanocomposites as Highly Selective Oil-Absorption Materials.* ACS Applied Materials & Interfaces, 2012. **4**(5): p. 2420-2425.

9. Xue, Z., et al., *A Novel Superhydrophilic and Underwater Superoleophobic Hydrogel-Coated Mesh for Oil/Water Separation.* Advanced Materials, 2011. **23**(37): p. 4270-4273.

10. Venkateswara Rao, A., N.D. Hegde, and H. Hirashima, *Absorption and Desorption of Organic Liquids in Elastic Superhydrophobic Silica Aerogels.* Journal of Colloid and Interface Science, 2007. **305**(1): p. 124-132.

11. Nash, L.D., et al., *Characterization of Plasma Deposited Hydrocarbon Diffusion Barriers for Embolic Foam Devices*, in *2015 9th IEEE International Conference on Nano/Molecular Medicine & Engineering (NANOMED)*. 2015. p. 1-6.

12. Tomina, V.V., et al., *Synthesis of Polysiloxane Xerogels with Fluorine-Containing Groups in The Surface Layer and Their Sorption Properties.* Journal of Fluorine Chemistry, 2011. **132**(12): p. 1146-1151.

13. Zhu, L., et al., *Superhydrophobicity on Two-Tier Rough Surfaces Fabricated by Controlled Growth of Aligned Carbon Nanotube Arrays Coated with Fluorocarbon.* Langmuir, 2005. **21**(24): p. 11208-11212.

14. Kylián, O., et al., *Hydrophobic and Super-Hydrophobic Coatings Based on Nanoparticles Overcoated by Fluorocarbon Plasma Polymer.* Vacuum, 2014. **100**: p. 57-60.

15. Gürsoy, M. and M. Karaman, *Hydrophobic Coating of Expanded Perlite Particles by Plasma Polymerization.* Chemical Engineering Journal, 2016. **284**: p. 343-350.

16. Zhang, B., et al., *A Novel Approach for The Preparation of Organic-Siloxane Oligomers and The Creation of Hydrophobic Surface.* Applied Surface Science, 2007. **254**(2): p. 452-458.

17. Tsoi, S., et al., *Superhydrophobic, High Surface Area, 3-D SiO_2 Nanostructures Through Siloxane-Based Surface Functionalization.* Langmuir, 2004. **20**(24): p. 10771-10774.

18. Ferrara, L. and A. Pattarini, *Siloxanes in Concrete: From Manual Application of Water-Proofing Treatments to Mix-Design Addition for Concrete Hydrophobicity*, in *Key Engineering Materials*. 2016, Trans Tech Publ. p. 263-268.

19. Bi, H., et al., *Spongy Graphene as a Highly Efficient and Recyclable Sorbent for Oils and Organic Solvents.* Advanced Functional Materials, 2012. **22**(21): p. 4421-4425.

20. Dong, X., et al., *Superhydrophobic and Superoleophilic Hybrid Foam of Graphene and Carbon Nanotube for Selective Removal of Oils or Organic Solvents from The Surface of Water.* Chemical Communications, 2012. **48**(86): p. 10660-10662.

21. Zhu, Q., Q. Pan, and F. Liu, *Facile Removal and Collection of Oils from Water Surfaces Through Superhydrophobic and Superoleophilic Sponges.* The Journal of Physical Chemistry C, 2011. **115**(35): p. 17464-17470.

22. Monopoli, M.P., et al., *Physical−Chemical Aspects of Protein Corona: Relevance to in Vitro and in Vivo Biological Impacts of Nanoparticles.* Journal of the American Chemical Society, 2011. **133**(8): p. 2525-2534.

23. Zhang, M., et al., *A Multi-Aromatic Hydrocarbon Unit Induced Hydrophobic Metal-Organic Framework for Efficient C2/C1 Hydrocarbon and Oil/Water Separation.* Journal of Materials Chemistry A, 2017. **5**(3): p. 1168-1175.

24. Morent, R., et al., *Plasma Surface Modification of Biodegradable Polymers: A Review.* Plasma Processes and Polymers, 2011. **8**(3): p. 171-190.

25. Hernandez-Lopez, J.L., et al., *Functional Polymers as Nanoscopic Building Blocks.* Materials Science and Engineering: C, 2003. **23**(1): p. 267-274.

26. Vasilev, K., *Nanoengineered Plasma Polymer Films for Biomaterial Applications.* Plasma Chemistry and Plasma Processing, 2014. **34**(3): p. 545-558.

27. Yasuda, H. and Y. Matsuzawa, *Economical Advantages of Low-Pressure Plasma Polymerization Coating.* Plasma Processes and Polymers, 2005. **2**(6): p. 507-512.

28. Denes, F.S. and S. Manolache, *Macromolecular Plasma-Chemistry: an Emerging Field of Polymer Science.* Progress in Polymer Science, 2004. **29**(8): p. 815-885.

29. Vasilev, K., et al., *Substrate Influence on The Initial Growth Phase of Plasma-Deposited Polymer Films.* Chemical Communications, 2009(24): p. 3600-3602.

30. Michelmore, A., et al., *Role of Positive Ions in Determining The Deposition Rate and Film Chemistry of Continuous Wave Hexamethyl Disiloxane Plasmas.* Langmuir, 2011. **27**(19): p. 11943-11950.

31. Ramiasa-MacGregor, M., et al., *Tuning and Predicting The Wetting of Nanoengineered Material Surface.* Nanoscale, 2016. **8**(8): p. 4635-4642.

32. Akhavan, B., K. Jarvis, and P. Majewski, *Evolution of Hydrophobicity in Plasma Polymerised 1,7-Octadiene Films.* Plasma Processes and Polymers, 2013. **10**(11): p. 1018-1029.

33. Vaswani, S., J. Koskinen, and D.W. Hess, *Surface Modification of Paper and Cellulose by Plasma-Assisted Deposition of Fluorocarbon Films.* Surface and Coatings Technology, 2005. **195**(2–3): p. 121-129.

34. Hegemann, D., H. Brunner, and C. Oehr, *Plasma Treatment of Polymers to Generate Stable, Hydrophobic Surfaces.* Plasmas and Polymers, 2001. **6**(4): p. 221-235.

35. Jarvis, K.L. and P. Majewski, *Plasma Polymerized Allylamine Coated Quartz Particles for Humic Acid Removal.* Journal of Colloid and Interface Science, 2012. **380**(1): p. 150-158.

36. De Vietro, N., R. d'Agostino, and F. Fracassi, *Introduction of Basic Functionalities on The Surface of Granular Adsorbers by Low Pressure Plasma Processes.* Plasma Processes and Polymers, 2012. **9**(9): p. 911-918.

37. Cavallaro, A. and K. Vasilev, *Controlled and Sustained Release of Pharmaceuticals via Single Step Solvent-Free Encapsulation.* Chemical Communications, 2015. **51**(10): p. 1838-1841.

38. Wahono, S.K., et al., *Preliminary Study: Combination of Amine and Natural Zeolite as New Adsorbent Material for CO_2 Capture*, in *Chemeca 2016: Chemical Engineering-Regeneration, Recovery and Reinvention*. 2016. p. 900-910.

39. Mierczynska-Vasilev, A., et al., *A Novel Technology for The Rapid, Selective, Magnetic Removal of Pathogenesis-Related Proteins from Wines.* Food Chemistry, 2017. **232**(Supplement C): p. 508-514.

40. Michl, T.D., et al., *Laboratory Scale Systems for The Plasma Treatment and Coating of Particles.* Plasma Processes and Polymers, 2015. **12**(4): p. 305-313.

41. Ghannam, M.T., et al., *Rheological Properties of Heavy and Light Crude Oil Mixtures for Improving Flowability.* Journal of Petroleum Science and Engineering, 2012. **81**: p. 122-128.

42. Macgregor-Ramiasa, M.N., A.A. Cavallaro, and K. Vasilev, *Properties and Reactivity of Polyoxazoline Plasma Polymer Films.* Journal of Materials Chemistry B, 2015. **3**(30): p. 6327-6337.

43. Vasilev, K., et al., *Solvent-Induced Porosity in Ultrathin Amine Plasma Polymer Coatings.* The Journal of Physical Chemistry B, 2008. **112**(35): p. 10915-10921.

44. Akhavan, B., K. Jarvis, and P. Majewski, *Hydrophobic Plasma Polymer Coated Silica Particles for Petroleum Hydrocarbon Removal.* ACS Applied Materials & Interfaces, 2013. **5**(17): p. 8563-8571.

45. Mirshahghassemi, S., et al., *Application of High Gradient Magnetic Separation for Oil Remediation Using Polymer-Coated Magnetic Nanoparticles.* Separation and Purification Technology, 2017. **179**(Supplement C): p. 328-334.

46. Patowary, M., R. Ananthakrishnan, and K. Pathak, *Effective Oil Removal from Water by Magnetically Driven Superhydrophobic and Oleophilic Magnetic Titania Nanotubes.* Environmental Science and Pollution Research, 2017. **24**(22): p. 18063-18072.

47. Zhang, J., et al., *Synthesis of Magnetic Iron Oxide Nanoparticles onto Fluorinated Carbon Fabrics for Contaminant Removal and Oil-Water Separation.* Separation and Purification Technology, 2017. **174**(Supplement C): p. 312-319.

48. Bhattacharya, K., M. Gogoi, and P. Deb, *Molecular Design of One Dimensional Magnetic FeNi3 Nanochains and Their Application in Oil Removal*, in *AIP Conference Proceedings*. 2016. p. 0501051-0501053.

49. Yu, L., et al., *Fabrication of Magnetic Porous Silica Submicroparticles for Oil Removal from Water.* Industrial & Engineering Chemistry Research, 2015. **54**(38): p. 9440-9449.

50. Chin, S.F., A.N. Binti Romainor, and S.C. Pang, *Fabrication of Hydrophobic and Magnetic Cellulose Aerogel with High Oil Absorption Capacity.* Materials Letters, 2014. **115**(Supplement C): p. 241-243.

51. Gui, X., et al., *Magnetic and Highly Recyclable Macroporous Carbon Nanotubes for Spilled Oil Sorption and Separation.* ACS Applied Materials & Interfaces, 2013. **5**(12): p. 5845-5850.

Chapter 9 : Conclusion and Future Work

9.1. Conclusion

This thesis aimed to improve the Indonesian Gunungkidul natural zeolites capability in advanced combination with plasma surface engineering for innovating advanced adsorbents, particularly in biogas purification. The aim was achieved by applying various modifications of chemical treatments, physical treatments and plasma polymerisation technology to natural zeolite. In this work, five prototype products were developed from the pristine natural zeolite to improve the methane purification of biogas through CO_2 or water-vapour removal. The targeted improvement of the adsorption capability of the modified natural zeolite was demonstrated. The CO_2 adsorbent was fabricated using physicochemical treatment, alkali impregnation and plasma polymer induction allylamine, while the water-vapour adsorbent was developed using air-plasma activation. As additional products, two prototypes of oil adsorbent were also created using hydrophobic surface engineering of plasma polymerisation.

The chemical and physical treatment of natural zeolite and characterisation of the products was conducted to achieve the best condition of preparation for CO_2 adsorption measurement. The best result demonstrated a significant improvement of the specific surface area. The highest CO_2 adsorption capacity of 5.218 mmol/g was achieved at 0°C and 30 bar pressure, corresponding to a normalised specific surface area of CO_2 adsorption capacity of 2.91 x 10^{-2} mmol/m^2. This adsorbent led to good CO_2 adsorption affinity when compared with the more costly synthetic materials. The physisorption mechanism was confirmed in this interaction, which also indicates a reversible adsorption process and provides opportunities for regeneration.

The investigation of alkali impregnation produced a good indication of the presence of new composition and structural transformation. The results showed the most prominent adsorption capacity of NaOH and KOH were reached at 0°C and 30 bar of 3.537 and 3.557 mmol/g, corresponding to normalised CO_2 adsorption capacity of 6.004 x 10^{-2} and 7.228 x 10^{-2} mmol/m^2, respectively. This result demonstrated that the material surface of alkali impregnation works more effectively (has a higher affinity) than non-alkali treatment, although it has a lower specific surface area. There is an indication of a chemisorption mechanism in the interaction of sodium and good adsorption at ambient

temperature. Potassium impregnation indicates physisorption, structure transformation and performs better than the higher surface area of non-alkaline natural zeolite at low-pressure adsorption. A higher surface efficiency of adsorption was obtained for potassium impregnation compared with non-alkali impregnation but a decrease in the material specific surface area also occurred.

The preliminary results using the plasma-deposition method were obtained for controlling thin coat and providing the best possibility of a plasma-deposition operating condition for CO_2 adsorption/reaction. The controlling deposition inside the micro–mesopores of natural zeolite was already confirmed by this research. The degassing optimisation of plasma polymer amine obtained the best condition for cleaning the pores. The CO_2 adsorption capacity of the plasma polymerised allylamine natural zeolite was almost identical to that of the non-coated zeolites, which means the adsorption affinity increased significantly. This adsorbent has a CO_2 adsorption capacity of 0.31 mmol CO_2/g, which addressed to the normalised specific surface area of CO_2 adsorption capacity of 0.0072 mmol CO_2/m^2. The adsorption affinity of new adsorbent escalates approximately four times more than the base adsorbent (0.0018 mmol CO_2/m^2) without the amine functional group. The new material is also more comfortable regenerating after CO_2 adsorption than the non-coated material, which needs the low temperature to desorb CO_2 from the pores.

Another result of a combination between natural zeolite and plasma technology is plasma activation of natural zeolite for enhancement of water-vapour adsorption, which is also related to biogas purification. This activation provided evidence of increasing water-vapour adsorption capacity, particularly with the high Si/Al ratio of modified natural zeolite, while the high Si/Al ratio of zeolite is known as the hydrophobic surface. There was an increase in water-vapour adsorption capacity and affinity of approximately 2.5 times more than the non-plasma activated adsorbent, which means there was an increase of the hydrophilicity of the material surface.

An application of surface engineering by plasma polymerisation also successfully created a hydrophobic surface, while the hydrophilic surface engineering was also applied successfully on the previous products. The hydrophobic plasma polymer was deposited on the nanomagnetic particle, then demonstrated the ability of oil-contaminant removal from water. This material showed excellent increase in performance after surface engineering

and good work efficiency after scaling up the contamination capacity. Further, the captured oil could be easily separated by applying an external magnetic force. The evidence of plasma polymerisation's capacity to engineer the surface properties provides further opportunities for implementing technology to remove other chemical and biological contaminants from polluted waters.

This research was conducted to develop the natural zeolite as a biogas purifier using various physicochemical treatments and plasma technology. All the treatments provide evidence of increased capability of natural zeolite to remove the biogas impurities of CO_2 and water vapour. The material investigation of the physicochemical treatments and alkali impregnation also provided a great deal of valuable information about properties of natural zeolite for further applications. The novel approach of amine induction by allylamine plasma polymerisation creates a new and promising solid amine adsorbent. Transforming the hydrophobic surface of porous material into a hydrophilic surface using plasma activation also offers a new approach of adsorbent treatment. In addition, a further investigation of hydrophobic surface engineering by plasma polymerisation can also be utilised for solving the environmental problem of oil contaminants in water.

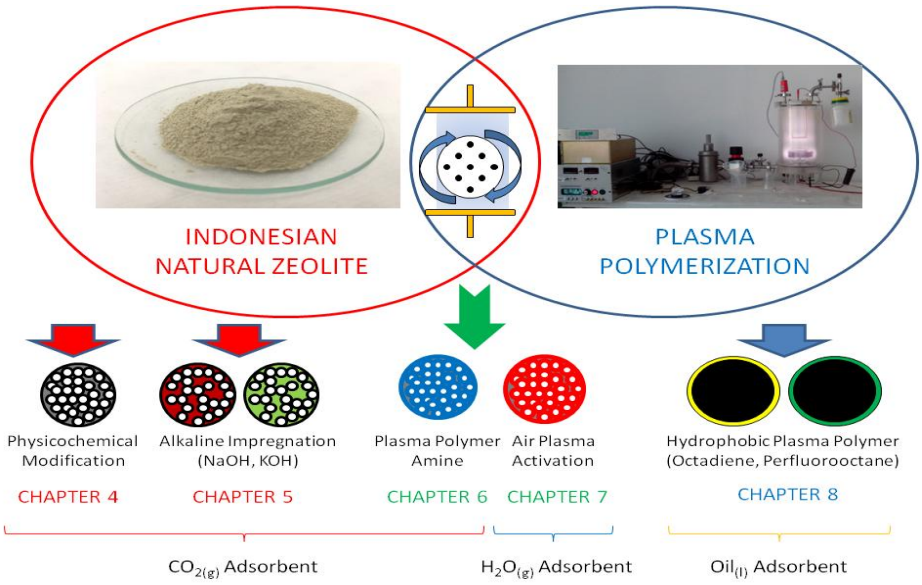

Figure 9.1. Product prototype and application of Indonesian natural zeolite and plasma polymerisation modification

9.2. Future Work

Many challenges and opportunities for improving natural-zeolite modification and application were developed in this research. The use of natural zeolite is particularly attractive due to the low production cost and its abundant availability worldwide. The successful application of a facile operation of plasma technology to improve the performance of the material surface creates further opportunity to combine and apply this technology in various fields. Further investigation is important for developing an understanding of natural zeolite and plasma technology characteristics in future applications.

The wide range of properties of modified natural zeolite provides further opportunity for various applications. Further combinations and modifications such as multilevel dealumination, higher calcination temperatures or different combination steps of dealumination, calcination, alkali impregnation, plasma charging and plasma polymerisation provide room for developing this material in different applications. By adjusting the appropriate properties of modified natural zeolite, the other environmental investigations could be applied to more casual way adsorptions such as removing water pollutants or specific organic compounds, rather than removing air pollutants. Increasing the Si/Al ratio and specific surface area of natural zeolite after physicochemical treatment provides a new opportunity for excellent catalyst for particular chemical reactions. Increasing the surface reactivity of natural zeolite after plasma activation also provides the chance to apply this method to other adsorption activities of gas, liquid and solid pollutants.

Plasma polymerisation offers a facile way to deposit a functional group on the material though an ecofriendly process. Various precursor and deposited surface exploration of plasma polymerisation in this work create a new perspective of the application surface engineering by plasma polymer. The facile induction of the wettability surface and of depositing a functional group on porous and compact spherical material offers furhter possible applications than conventional approaches. The different method used for creating a new catalyst or adsorbent that needs the specific presence of the amine functional group can be conducted by manipulating the operation condition of allylamine plasma polymer. Wettability surface engineering of material also can be executed by plasma polymerisation

using an appropriate precursor or air-plasma activation only. The deposition controlling ability for depositing the nanothick plasma polymer onto the porous material also offers further options for porous material treatment in broad applications.

A great deal of information has been provided by the various treatments of the natural zeolite as an adsorbent and through the exploration of plasma technology as an adsorbent. This information can be applied in further research in many fields related to this study. Currently, another method of plasma polymer surface engineering in my research group project for water-contaminant removal is under investigation and indicates a promising performance. Moreover, some natural-zeolite preparations for other applications were conducted in other my research group projects to expand the utilisation of this material for human life (e.g., catalyst, waste water treatment, food processing, and adsorbent), which is a clear sign of progress.

APPENDIX A: Copyrights and Permissions

MANUSCRIPT 1

Copyright permission Request for Paper Publication of Chemeca 2016

Elena Vvedenskaia <EVvedenskaia@engineersaustralia.org.au>

Tue 5/22/2018 8:49 AM

To:Wahono, Satriyo Krido ; wahsk001 <satriyo.wahono@mymail.unisa.edu.au>;

Dear Satriyo Krido Wahono,

Your enquiry was passed on to me this morning for response.

Permission is granted to reprint your article below in your PhD thesis providing acknowledgement is given that the article was first published in Chemeca 2016 proceedings, @Engineers Australia, also subject to 3 other authors' agreement.

Wahono, Satriyo Krido; Skinner, William; Addai-Mensah, Jonas and Vasilev, Kresimir. Preliminary study: Combination of amine and natural zeolite as new adsorbent material for CO2 capture [online]. In: Chemeca 2016: Chemical Engineering - Regeneration, Recovery and Reinvention. Melbourne, Vic.: Engineers Australia, 2016: 900-910. Availability: <https://search.informit.com.au/documentSummary;dn=641078056124003;res=IELENG> ISBN: 9781922107831

Regards,
Elena Vvedenskaia, FIEAust | Library Manager
Learned Society Business Unit
Professional Standards & Practice Group

Engineers Australia | 11 National Circuit BARTON ACT 2600 Australia
t: (61) 26270 6535 | Ext: 2535
w: www.engineersaustralia.org.au



MANUSCRIPT 2



APPENDIX B: Published Manuscripts

MANUSCRIPT 1

https://search.informit.com.au/documentSummary;dn=411079056124005;res=IELENG

Paper no. 3405749

Chemeca 2016
25 – 28 September 2016, Adelaide, Australia

Preliminary Study: Combination of Amine and Natural Zeolite as New Adsorbent Material for CO_2 Capture

Satriyo Krido Wahono[1,2,3*], William Skinner[1], Jonas Addai-Mensah[1] and Krasimir Vasilev[2]

[1] *Future Industry Institute, University of South Australia, Mawson Lakes 5095, South Australia, Australia*
[2] *School of Engineering, University of South Australia, Mawson Lakes 5095, South Australia, Australia*
[3] *Research Unit for Natural Product Technology, Indonesian Institutes of Sciences, Gunungkidul 55861, Yogyakarta, Indonesia*

*Corresponding author.
Email: wahsk001@mymail.unisa.edu.au; satr002@lipi.go.id; satriyo.krido.wahono@gmail.com

Abstract: Carbon dioxide (CO_2) is the most significant contributor to global warming. It demands the development of technologies which are capable of limiting CO_2 emissions to the atmosphere. One of the ways to achieve this purpose is CO_2 capture from industrial emissions as well as natural gas and landfill/biogas upgrading systems. Molecular sieve utilizing natural zeolites as an adsorbent is one of the technologies for capturing CO_2 that has attracted significant attention. Natural zeolite is abundant, accessible and capable of capturing greenhouse gases effectively with an appropriate pre-treatment. Our previous studies demonstrated that natural zeolites, treated with chemical and physical means, reduced CO2 content from biogas flow. However, the capture efficacy provides a room for improvements. In industry, amine solution absorption technology, which has several weaknesses such as high investment, high corrosive, high risk for human health, is commonly utilized. Solid amine adsorbents are considered as a promising alternative to overcome these drawbacks. This study aims to develop a hybrid technology combining the natural adsorption capacity of zeolites and the specific CO_2 capture properties of amines. To obtain amine-functionalized zeolite adsorbent, it used plasma deposition from amine-rich precursors such as allylamine. The results demonstrated that amine plasma polymers were successfully deposited on natural zeolite (Gunungkidul-Yogyakarta). For further improvement, it suggests conducting plasma on time deposition fewer than 10 seconds and power of 10 Watt or 50 Watt. Currently studies are underway to evaluate the adsorption properties of these new CO_2 capture materials.

Keywords: amine, amine-functionalized zeolite, CO_2 capture, natural zeolite, plasma polymers.

1 Introduction

The greenhouse gases, which consist of CO_2 (61%), CH_4 (7%), and N_2O (9%) [1], have become a big issue for the environmental community as a global warming trigger. As the first rank contributor of global warming, Carbon dioxide (CO_2) needs to be reduced from the atmosphere. CO_2 capture, as a developed technology, may become a strategy for limiting atmospheric emissions of CO_2 from industrial emissions as well as natural gas and landfill/biogas upgrading systems.

Recently, molecular sieve utilizing natural zeolites is widely seen as an effective adsorbent. Zeolites, which are the member of aluminium silicate minerals group, have the microporous structure of crystalline solids and similar basic tetrahedral structure of $Al_xSi_yO_z$. Based on the pores size, the zeolite is divided into three groups: small, medium and large; and commonly filled with water and cations. Aluminium, silicone and oxygen atoms of zeolites are commonly found in the form of SiO_2 and Al_2O_3 compounds. There are many types of zeolites depending on the formation of the environment and the source of materials [2-7]. The natural zeolite has a similar adsorption ability with synthetic zeolite, but it has lower adsorption capacity based on the characterization results [8, 9]. The

adsorption capacity of natural zeolite (raw or modified) cannot be compared to synthetic materials; however, it can be compensated by their low cost and bulk availability in the world [10].

Zeolite structure can perform adsorption and absorption of the compounds of H_2O, CO_2, SO_2, H_2S [11]; the absorption ability of zeolite to the gas is up to 25% [12]. Furthermore, the zeolite can control greenhouse gases such as CO_2 and N_2O, except CH_4 which is not absorbed [1]. Zeolite has high selectivity to carbon dioxide; so, it can upgrade the quality of natural gas, biogas or others fuel gas [13-15]. Particularly for Gunungkidul-natural zeolite, it has been proved for upgrading biogas quality for electricity generation [16-19].

There are two types of natural zeolites which are commonly found in Indonesia, namely Clinoptilolite and Mordenite [20]. They have high purity and silica concentration of about 60%, commonly found in the following areas: South Lampung, Bajah, Cikembar, Cipatujah, West Java Nangapada, Ende, Nusa Tenggara Timur, Malang and Gunung Kidul Regency [21]. Natural zeolite, particularly Gunungkidul's zeolite, has the potential to be used as adsorbents for CO_2 Capture. Not only does Gunungkidul's zeolite have fairly large deposits (55,000,000 m^3) [22], it also has the silica content of approximately 60% [21].

On the other hand, the utilization of amine solution for CO_2 absorption is the most practical one in the industry, such as natural gas treatment, flue gas of food industry, landfill upgrading and flue gas of power plants. It can absorb most CO_2 content of the gases (85-90%), other impurity gases (NO_x and SO_x), and particles (ashes). Amines compounds which are usually utilized for CO_2 absorption are monoethanolamine (MEA), diethanolamine (DEA), methyl diethanolamine (MDEA), diglycol amine (DGA), 2-Amino-2-methyl propanol (AMP), di-isopropanol amine (DIPA), and Piperazine (PIPA). Amines absorption process has a low operational cost, low energy requirement, low liquid waste, and low amine-releasing to the atmosphere. However, this method has several problems which need to be solved, namely high investment, difficult regeneration, high corrosive potential, gaps on environmental and human health risks [23].

Consequently, research focusing on the alternatives of amines needs to be improved continuously. One of them is by changing the amine solutions into amine solids, so that it will develop on dry process absorption. Several studies on solid amine have increased the capacity of CO_2 capture. They used solid materials as amine carriers of the amine group, such as carbon fly ash-silica, polymethylmethacrylate-silica, polyethyleneimine-silica, and magnesium tetraphenyl porphyrin [24-28]. The solid amine has a high capacity to capture CO_2. However, CO_2 hardly penetrates into the material because the pores are filled with amine polymers; it is also hard on regeneration process [29].

One of the collaboration technologies between the solid amine and natural zeolite is plasma polymerization. Plasma polymerization is one of surface modification technologies, coating the surface with ultra-thin layers of monomers for various purposes. The plasma is used to transform and activate the monomers, so that the monomers are polymerized or deposited on the material surface. This method is conducted in a dry process so that the surface materials react to the monomers. The monomers form an ultrathin layer on the surface, coating the material. The monomers deposition can be controlled by time of plasma polymerization. When the deposition occurs continuously, it will produce more thickness of monomers coating on materials. However, after few monomer layers are formed on the surface, the next layer becomes independent substrates on the outer surface which are able to react with another compound around the materials [30]. The independent substrates can be utilized to improve CO_2 adsorption capacity of natural zeolite.

Particularly for porous materials, continuous deposition of monomer clogs the pores, so the pores function will disappear. However, the deposition duration of plasma polymerization is able to limit the

thickness of monomer. So, it will not stop up the pores, but reduce the diameter only [31]. Moreover, Cavallaro and Vasilev [32] have conducted successfully the experiment of controlling chemistry and thickness of plasma polymer for coating granule materials under continuous agitation, which is appropriate in the form of zeolite adsorbents. The zeolite adsorbent surface is coated by monomers which easily react with CO_2, such as amine-monomers. It is in line with the research of Vasilev et al. [33] which suggests that plasma polymer can be used for surface modification, particularly amine-monomers.

This study aims to develop a hybrid technology combining the natural adsorption capacity of zeolites and the specific CO_2 capture properties of amines. To obtain amine-functionalized zeolite adsorbent, it used plasma deposition from amine-rich precursors such as allylamine.

2 Methodology

2.1 Materials

Natural zeolite from Gunungkidul, Yogyakarta-Indonesia was utilized as a porous material having a particle size of under 40 mesh (0.500 mm). It has been activated by dealumination (soaked in HCl 1 N for 24 hours) and calcination (heated at 400°C for 4 hours), called as modified natural zeolites. Allylamine was utilized as an amine resource for coating the porous material by plasma deposition. It was supplied by Sigma-Aldrich with 98% purity which was applied directly without purification.

2.2 Characterization of natural zeolite

Determination of natural zeolite element was analyzed by the quantitative X-Ray Diffraction (XRD), the qualitative X-Ray Fluorescence (XRF) and ICP-MS at Future Industry Institute Laboratory. The quantitative XRD was determined by Search-Match of the PDF-2 Powder diffraction file, the Webmineral database, and the SIROQUANT database. ICP-MS analysis was combined with gravimetry analysis to determine Si element content of the materials as the measurement procedure was unable to determine it. Scanning Electron Microscope (SEM) was employed to show the structure image of natural zeolites powder and its variables treatment results. It was analyzed by Hitachi SU3500 at Natural Product Technology Research Center of Indonesian Institutes of Sciences Laboratory.

2.3 Characterization of amine plasma deposition

The deposition was conducted at a custom built cylindrically designed plasma reactor with a U-shaped upper electrode and a round-shaped bottom electrode which was powered by 13.56 MHz plasma generator. Allylamine deposition as rich amine precursors was executed at a pressure of 0.16 mbar; plasma power of 10 Watt as a low power variable and 40, 50, 60 Watt as high power variables; and deposition time on various variables of 0-30 minutes for different purposes to get the best results. It was implemented on 1 cm square cleared silica wafer for ellipsometry and water contact angle measurement and 40 mesh natural zeolite powder for SEM analysis. Ellipsometry measurement was conducted to get thickness approximation of plasma deposition for allylamine on materials. It was measured by J. A. Woollam Co., Inc. V-VASE Ellipsometer on silica wafer coated allylamine at Future Industry Institute Laboratory. Water contact angle measurement was conducted to find out hydrophilicity or hydrophobicity of monomer deposition. The water dropped image was captured by Logitec digital camera on silica wafer coated allylamine after a second dropping time and angle measurement with ImageJ software.

2.4 CO_2 capture on natural zeolite, natural zeolite-amine plasma, Si wafer-amine

CO2 capture experiment was conducted on a simple reactor which was shown as the scheme on Figure 1. CO_2 which used as simulation gas was supplied by BOC on D size cylinder. Modified natural zeolites, natural zeolites coated amine and silica wafer coated amine were used as the adsorbent materials of CO_2. The adsorbent materials were put in the reactor for two hours with refreshment every hour with new CO_2 to provide high concentration of CO_2 on internal reactor air. For some variables which need water vapour presence, hot water was also provided in the reactor with a similar procedure of CO_2. After all of the processes on the reactor, the CO_2 capture indication was analyzed with XPS of SPECS SAGE spectrometer at Future Industry Institute Laboratory and measured by CasaXPS software.

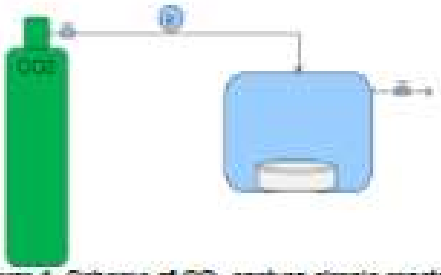

Figure 1. Scheme of CO_2 capture simple reactor

3 Results and discussions

3.1 Characterization of natural zeolite

The element composition (ICP-MS and quantitative XRD), XRD graph and XRF graph of Gunungkidul natural zeolites were shown by Table 1, Figure 2, and Figure 3 respectively. Based on Table 1, the most part of this material was CaO-SiO_2-Al_2O_3 indicated as aluminosilicate minerals with various cations or zeolites. Indonesian natural zeolites (Gunungkidul natural zeolite as part of them), are involved on Clinoptilolite and Mordenite zeolite type [20]. On this natural zeolite, mordenite has been associated with clinoptilolite-Ca due to Ca element which has the biggest portion than sodium and potassium in this material. It was supported by Ca peak at Figure 3 as the highest peak of this material. Based on the quantitative XRD analysis, this natural zeolite is composed of anorthite of 45.1%, labradorite of 29.7%, stellerite of 20.1%, and calcite1 of 5.1%. Structure analysis of these natural zeolites has been conducted by SEM analysis which is shown in Figure 4. The picture shows that the natural zeolite structure may be similar with coral reef surface with many pores for adsorption or for the structure of reaction chamber.

Table 1. Element composition of raw Gunungkidul natural zeolites

Element	XRD Quantitative	ICP-MS	Oxide Element	XRD Quantitative	ICP-MS
Ca	12.30	64.71	CaO	16.79	57.17
C	0.61	-	CO_2	2.24	-
O	48.56	-	-	-	-
Al	15.00	6.87	Al_2O_3	27.99	8.19
Si	22.07	44.97	SiO_2	47.78	28.39
H	0.40	-	H_2O	3.60	-
Na	1.00	2.90	Na_2O	1.61	2.47
Fe	-	2.26	FeO	-	1.85
Mg	-	0.84	MgO	-	0.88
K	-	1.39	K_2O	-	1.05

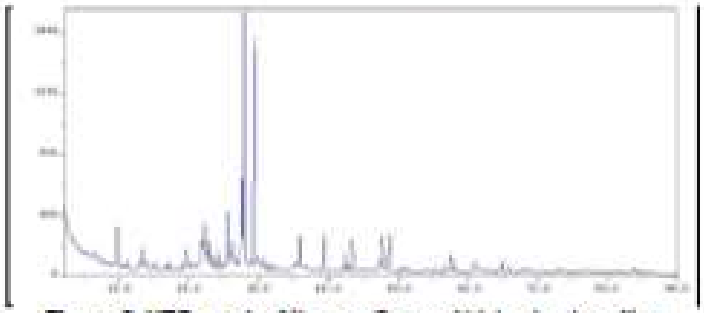

Figure 2. XRD graph of the raw Gunungkidul natural zeolites

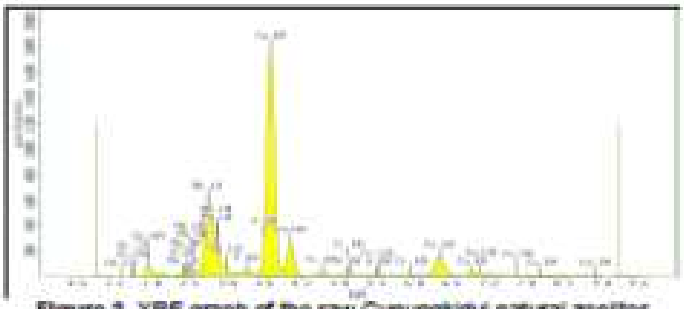

Figure 3. XRF graph of the raw Gunungkidul natural zeolites



Figure 4. SEM image of the raw Gunungkidul natural zeolites

3.2 Characterization of amine plasma deposition

Amine plasma deposition was conducted by plasma reactor using allylamine as amine rich precursor. It has been deposited successfully on the cleared silica wafer surface and natural zeolite surface. The silica wafer deposition was conducted to determine thickness and water contact angle of amine which are shown in Figure 5 and Table 2 respectively.

Figure 5 shows that there was an increasing amine deposition on the surface which was equal to increasing time and power deposition. It could be assummed as the thickness on natural zeolite surface at the same time although it will be lower than the flat surface deposition due to the higher surface area on the material than the flat surface, but the time function deposition would still be utilized [32]. The increasing time deposition phenomena have a similar condition with the previous deposition research [31]. Furthermore, the different power also provides a different composition of group type deposition. So, it is possible to produce a different effect on the surface activity [34–36].

Table 2 shows the water contact angle of the allylamine surface deposition on cleared silica waffer. The water contact angle value on the surface is under 90° which indicates hydrophilic properties. The hydrophilic properties support the reaction condition between amine and CO_2 running better on water presence [37, 38]. Water presence usually decreases the ability of natural zeolite to capture CO_2 due to the zeolite adsorbs water vapour earlier than CO_2 which makes saturation faster. Therefore, the presence of the amine, which attracts water on the surface, is expected to react further with water vapour and to enhance the capability of CO_2 capture.

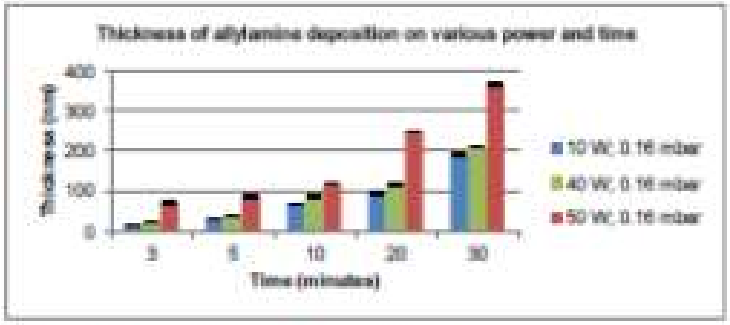

Figure 5. Thickness of allylamine deposition on various power and time

Table 2. Contact angle of 50 W allylamine deposition on various time

Time deposition of amine	3 minutes	5 minutes	10 minutes
Drop image	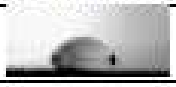		
Contact angle	55°	54°	52°

The amine deposition on the natural zeolite surface has been conducted successfully which is shown by N1s of XPS result on Figure 6. This graph shows that there is no indication of nitrogen on the natural zeolite surface without amine coating. Meanwhile, the coated natural zeolites graphs show the peak on N1s for the various power deposition (10 W and 40 W). It means that the allylamine has deposited well on the natural zeolite surface. However, the efficacy of amine groups deposition for capturing CO_2 needs to be proven.

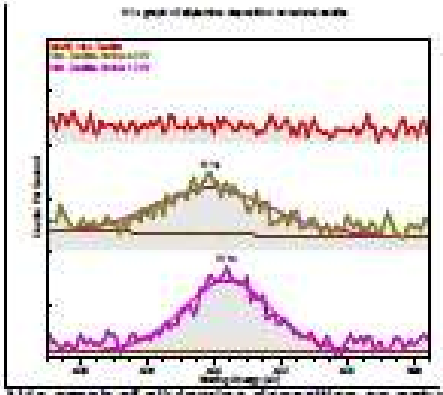

Figure 6. N1s graph of allylamine deposition on natural zeolite

3.3 CO_2 capture on natural zeolite and natural zeolite-amine plasma

The CO_2 capture results on the material surface can be determined by XPS analysis, particularly on the C1s graphs. CO_2, which was captured by the adsorbent, was indicated by the carbon elements changing the adsorbent after the process. CO_2 capture result on the C1s graph of modified natural zeolites and natural zeolites coated amine was shown in Figure 7. On the C1s graph, there is a peak at 289 eV of energy binding which indicates that carbon is bonded to two oxygen (COO-R) or the CO_2 binding on the material surface [39, 40]. However, the natural zeolites without coating amine have a higher peak than zeolites coated amine. The presence of amine coat reduces CO_2 capture capability of natural zeolite. The amine deposition takes too long; so, it covers the natural zeolite pores. The pores volume is one of important supporting factors for CO_2 capture ability.

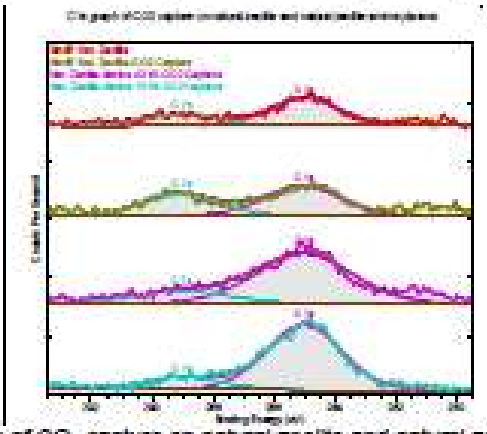

Figure 7. C1s graph of CO_2 capture on natural zeolite and natural zeolite-amine plasma

There are two important improvements which need to be conducted in this experiment including the appropriate plasma amine deposition condition and the deposition controlling. The appropriate condition of amine plasma deposition may provide the optimum CO_2 adsorption of amine because plasma reaction was conducted simultaneously and difficult to control. The deposition controlling can reduce the possibility of pores covering, so that it can still utilize the pores advantages of natural zeolites.

3.4 Power variable of amine plasma deposition for CO_2 capture on Si wafer-amine

Amine plasma deposition was conducted on a flat surface of Si wafer to find appropriate parameter of plasma deposition for capturing CO_2. The power was divided into low power and high power variables because it provides different surface activities. The low power deposition produces more amine groups on the surface, but high power deposition produces more active ion on the surface [34-36].

The C1s graph of low power variable (10 W) amine plasma deposition is shown in Figure 8. The second peak of COO-R bond (289 eV) is undetected, but there is an indication of the increase of C=O bond (286 eV). Therefore, there is a possibility of CO_2 reaction with the amine on the surface. The C=O bond also increases with the presence of water vapour which is appropriate with CO_2 capture on solid amine [37, 38].

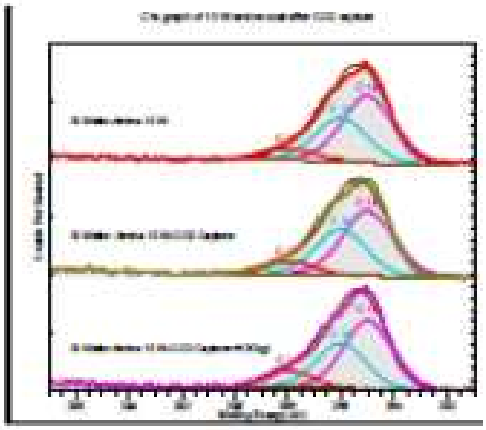

Figure 8. C1s graph of 10 W amine coat after CO_2 capture

On the high power variable, there is a qualitative transformation particularly for the power of 50 W. The surface colour changing and the thickness increasing, after CO_2 was introduced into the reactor, are shown in Figure 9 and Figure 10 respectively. The colour changing shows that it had conducted some reaction on the surface after CO_2 treatment. It only happened to the power of 50 W. So, there is a different preference reaction possibility. It is also supported by the increase of thickness, which shows that some advanced deposition has been applied. The captured CO_2 or others elements by the surface give the possibility to increase the thickness after CO_2 introduction.



Figure 9. Colour transformation of high power amine coat after CO_2 capture

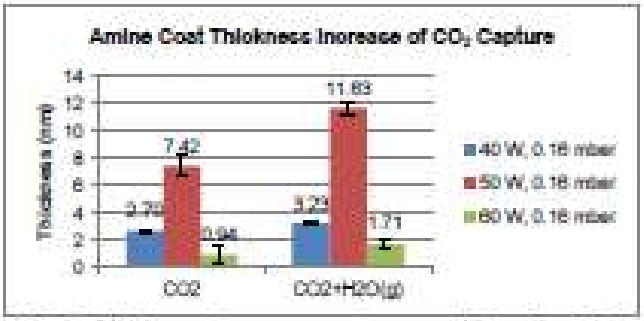

Figure 10. Coat thickness increase on various condition after CO_2 capture

Another experiment of 50 W power variable has also been conducted; the XPS analysis of C1s and N1s is shown in Figure 11. On the C1s graph, the graph shows only one main peak and it is different from with the previous results on the zeolite-amine which has two peaks on C1s graph. There is an insignificant difference between before and after CO2 introduction on the surface. The C1s fitting element shows the presence of C-O (286 eV) and C=O (288 eV) bonds, but COO-R bond was undetected. The CO_2 capture indication is so weak based on the C1s graph due to the undetected bond of COO-R and an insignificant increase of C=O bond after CO_2 capture. However, there is a strange indication on the N1s graph which brings out a new peak on 407 eV besides the main peak of nitrogen. The new peak is indicated as nitro (N-O) bond [41], where the resource of oxygen element is possible from air, water vapour, and CO_2. The peak also increased significantly in the water vapour presence of CO_2 introduction. It indicates that the nitro bonding was affected by the oxygen presence of CO_2 and H_2O than oxygen of the fresh air.

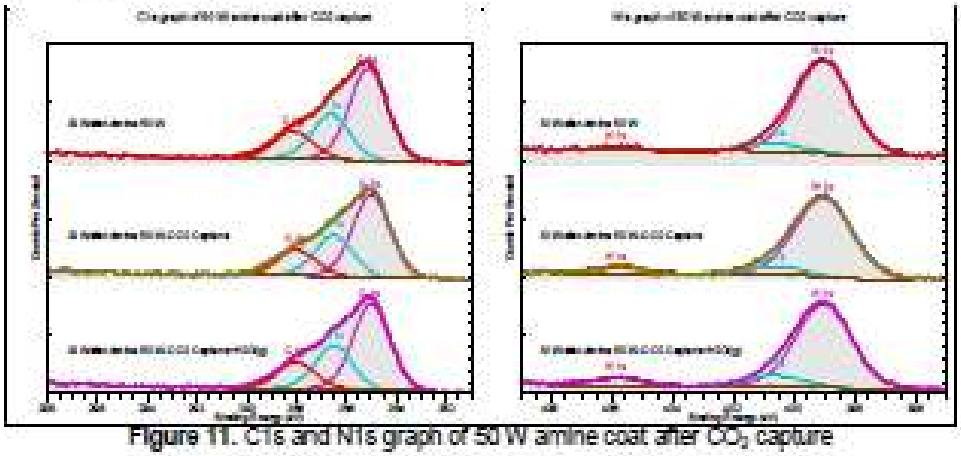

Figure 11. C1s and N1s graph of 50 W amine coat after CO_2 capture

The results of low and high power variables can be the preliminary indication that the 10 W and 50 W are potential for advanced improvement of CO_2 capture purpose. They provide different possibilities for capturing or reducing CO_2. The surface can be created as rich solid amine on low power deposition or oxidation catalyst for another power type deposition.

3.5 Controlling amine deposition thickness

The results of the CO_2 capture of natural zeolites on Figure 7 are supported by SEM analysis results which are shown in Figure 12. The modified natural zeolite looks like coral reef surface before amine deposition which is shown on Figure 12a. However, on Figure 12b, the zeolites surface is covered by some sort of sandy grain and it looks like the coral buried the sand after amine deposition. This condition gives a possibility that the pores are also buried by the deposition and closed the entrance of CO_2, so that it reduces the adsorption capability of natural zeolite. Therefore, the short time amine deposition (under a minute) was also conducted, which is the material performance shown on Figure 12c. The material surface performance was almost similar to the previous material on Figure 12a. More amine deposition on the surface is needed for increasing the chance of capturing CO_2. So, long

time amine deposition is a good option. However, natural zeolite as a porous material has the ability to capture CO_2 due to its porosity and compound structure. Thus, the deposition needs to be controlled for taking the best effect of the monomer on the porous surface.

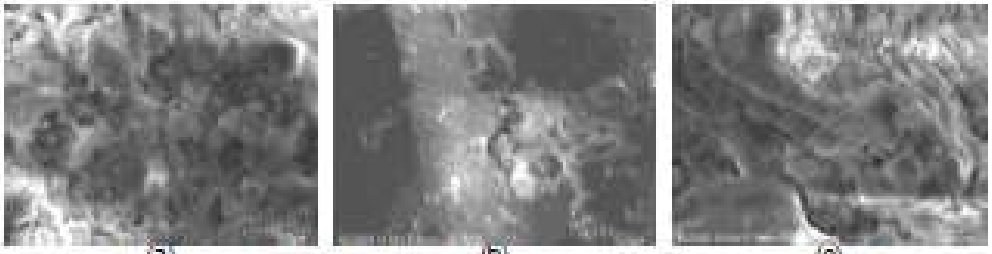

(a) (b) (c)

Figure 12. SEM images of modified natural zeolite: (a) before deposition; (b) after long time deposition (5 minutes); (c) after short time deposition (30 seconds)

The deposition needs to be reduced until less than 2 nm thickness due the involvement of natural zeolite on microporous material [11]. The short time deposition was conducted to achieve that thickness purpose, which is shown in Figure 13. All types of amine plasma depositions (different power, different pressure, and pulse), which were conducted less than 10 seconds, were able to deposit thin layer amine. The layer was measured under 2 nm, appropriate with the natural zeolite pore size requirement. Therefore, the deposition of 10 seconds or under can suit as the base of low thickness amine plasma deposition particularly on natural zeolite as microporous material.

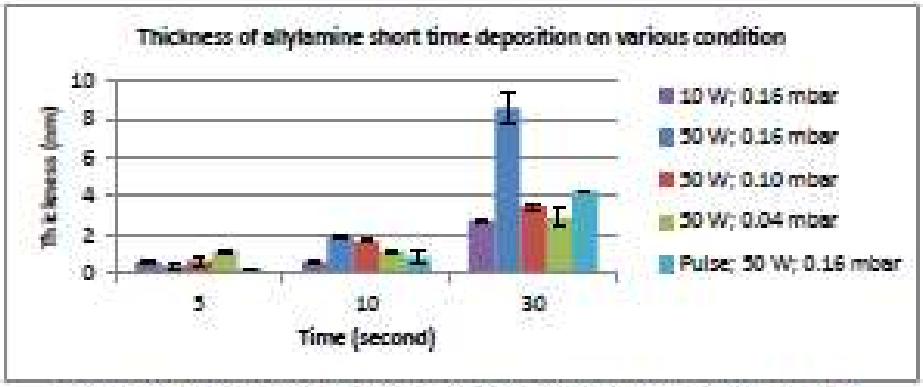

Figure 13. Thickness of allylamine short time deposition on various condition

3 Conclusions and recommendations

The results demonstrate that amine plasma polymers can be successfully deposited on natural zeolite (Gunungkidul-Yogyakarta). As preliminary results, there are two recommendations which can be generated from this research, the appropriate plasma amine deposition condition and the deposition controlling. The power variable is the most dominant issue to determine the appropriate condition in this research. 10 W and 50 W power variables were suggested as the base for advanced improvement due to the production of rich solid amine surface or oxidation catalyst as the way of capturing or reducing CO_2. The deposition controlling suggested short deposition time which was conducted in less than one minute. The appropriate result of deposition time is less than 10 seconds to avoid pore blocks on natural zeolite surfaces. Currently, studies are underway to evaluate the adsorption properties of these new CO_2 capture materials.

Acknowledgements

The authors would like to acknowledge the scholarship support from RISET-PRO Project, Ministry of Research, Technology and Higher Education, Republic of Indonesia and the research facilities support from Vasiev Group Laboratory, Future Industry Institute-School of Engineering, Div. ITEE, University of South Australia.

References

1. Delahay, G. and B. Coq. (2002), *Pollution abatement using zeolites: State of the art and further needs*, In *Zeolites for Cleaner Technologies*, Published by imperial college press and distributed by world scientific publishing co., p. 345-374.
2. Fernández, N., et al. (2007), *Real evidence about zeolite as microorganisms immobilizer in anaerobic fluidized bed reactors*, Process Biochemistry, 42(4): p. 721-728.
3. Hansson, A. (2011), *Mechanism of zeolite activity in biogas co-digestion*, In *Department of Physics, Chemistry, and Biology*, Linköping University: Linköping, Sweden.
4. Hedström, A. (2001), *Ion Exchange of Ammonium in Zeolites: A Literature Review*, Journal of Environmental Engineering, 127(8): p. 673-681.
5. Mumpton, F.A. (1999), *La Roca Magica: Uses of natural zeolites in agriculture and industry*, Proceedings of the National Academy of Sciences of the United States of America, 96(7): p. 3463-3470.
6. Li, Z., et al. (1998), *Long-Term Chemical and Biological Stability of Surfactant-Modified Zeolite*, Environmental Science & Technology, 32(17): p. 2628-2632.
7. Venuto, P.B. (1994), *Organic catalysis over zeolites: A perspective on reaction paths within micropores*, Microporous Materials, 2(5): p. 297-411.
8. Wahono, S.K. (2014), et al., *Characterization and Utilization of Gunungkidul Natural Zeolite for Bioethanol Dehydration*, Energy Procedia, 47: p. 263-267.
9. Hernawan, et al. (2015), *Modification of Gunungkidul Natural Zeolite as Bioethanol Dehydrating Agents*, Energy Procedia, 65: p. 116-120.
10. Misaelides, P. (2011), *Application of natural zeolites in environmental remediation: A short review*, Microporous and Mesoporous Materials, 144(1–3): p. 15-18.
11. Weitkamp, J. and L. Puppe (1999), *Catalysis and Zeolites Fundamentals and Applications*, Springer Archives, Berlin, Heidelberg: Springer Berlin Heidelberg : Imprint: Springer.
12. Sutarti, M. and M. Rachmawati (1994), *Zeolit Tinjauan Literatur [Zeolite Literature Review]*, Scientific Information and Documentation Centre, Indonesian Institute of Sciences: Jakarta.
13. Cavenati, S., C.A. Grande, and A.E. Rodrigues (2004), *Adsorption Equilibrium of Methane, Carbon Dioxide, and Nitrogen on Zeolite 13X at High Pressures*, Journal of Chemical & Engineering Data, 49(4): p. 1095-1101.
14. Wahono, S.K. (2008), *Kajian: Pemanfaatan Zeolit Lokal Gunungkidul–Yogyakarta untuk Optimasi Sistem Biogas [Review : Utilization of Gunungkidul Local Zeolite for Biogas System optimization]*, Proceedings of National Seminar on Chemical Engineering Fundamentals and Applications, Chemical Engineering Departement of Institute of Technology Sepuluh November Surabaya: Surabaya – Indonesia, ISSN : 1410-9867, p. E14.
15. Adinurani, P.G., et al. (2016), *Carbon Dioxide Capture Efficiency Using Algae Biological Absorbent and Solid Adsorbent for Biogas Purification*, Jurnal Teknologi, 78(4-2).
16. Wahono, S.K., R. Maryana, and M. Kismurtono. (2009), *Biogas Purification Process to Increase Gen—Set Efficiency*, AIP Conference Proceedings, 1169(1): p. 185-189.
17. Wahono, S.K., H. Julendra, and A. Febrisiantosa (2009), *Peningkatan Performa Biogas Melalui Teknologi Pemurnian Metana di UPT Kapitan Meo, Kabupaten Belu – Nusa Tenggara Timur [Performance Enhancement of Biogas Using Purification Technology of Methane at UPT Kapitan Meo, District Belu - East Nusa Tenggara]*, Proceedings of National Seminar on Technology Development Based on Local Materials, Yogyakarta – Indonesia, ISBN: 979-1519-62-8.
18. Wahono, S.K., et al. (2010), *Modifikasi Zeolit Lokal Gunungkidul Sebagai Upaya Peningkatan Performa Biogas Untuk Pembangkit Listrik [Modification as An Effort Local Zeolite – Gunungkidul Performance Improvement for Biogas Electricity Generation]*, Proceedings of National Seminar on Chemical Engineering and Processes, Diponegoro University: Semarang-Indonesia, ISSN : 1411-4216.
19. Wahono, S.K. and W.A. Rizal (2014), Biogas Filter Based on Local Natural Zeolite Materials, International Journal of Renewable Energy Development, 3(1): p. 1-5.
20. Marantos, I., G.E. Christidis, and M. Ulmanu. (2012), *Zeolite Formation and Deposits*, In *Handbook of Natural Zeolites*, V.J. Inglezakis and A.A. Zorpas, Editors, Bentham Science Publishers. p. 29-51.
21. Widayat, et al. (2008), *Pengaruh Konsentrasi HCl dan Jenis Reaktan dalam Pembuatan Katalis Zeolit untuk Proses Dehidrasi dari Zeolit Alam [Effect of HCl Concentration and Reactant Type in The Zeolite Catalysts*

Production for Dehydration Process of Natural Zeolite], Proceedings of National Seminar on Chemical Engineering and Processes, Diponegoro University: Semarang – Indonesia, ISSN : 1411-4216.

22. Anonimous (2012). *Potensi [Potency]*, [cited 2015 17 April 2015]; Available from: http://www.gunungkidulkab.go.id/home.php?mode=content&id=307.
23. Shao, R. and A. Stangeland (2009), *Amines Used in CO2 Capture*, In *Bellona Report*, The Bellona Foundation.
24. Gowar, A.A. (2014), *Development of a Pressure Swing Adsorption Process for CO2 Capture from Flue Gas Using Solid Amine Sorbents*, In *Chemical Engineering, College of Engineering and Computing*, University of South Carolina: Columbia.
25. Zhang, Z., et al. (2013), *Enhancing Sorption Performance of Solid Amine Sorbents for CO2 Capture by Additives*, Energy Procedia, 37(0): p. 205-210.
26. Veneman, R., et al. (2012), *Continuous CO2 capture in a circulating fluidized bed using supported amine sorbents*, Chemical Engineering Journal, 207–208(0): p. 18-26.
27. Wang, J., et al. (2012), *Surfactant promoted solid amine sorbents for CO2 capture*, Energy & Environmental Science, 5(2): p. 5742-5749.
28. Gray, M.L., et al. (2004), *Capture of carbon dioxide by solid amine sorbents*, International Journal of Environmental Technology and Management, 4(1): p. 62-88.
29. Jiang, H. (2015), *Amine-pillared nanosheet adsorbents for CO2 capture applications*, In *Department of Chemical Engineering*, Northeastern University: Boston, Massachusetts.
30. Vasilev, K., et al. (2009), *Substrate influence on the initial growth phase of plasma-deposited polymer films*, Chemical Communications, (24): p. 3600-3602.
31. Dusan, L., et al. (2006), *Surface modification of nanoporous alumina membranes by plasma polymerization*, Nanotechnology, 19(24): p. 245704.
32. Cavallaro, A. and K. Vasilev (2015), *Controlled and sustained release of pharmaceuticals via single step solvent-free encapsulation*, Chemical Communications, 51(10): p. 1838-1841.
33. Vasilev, K., et al. (2010), *Early Stages of Growth of Plasma Polymer Coatings Deposited from Nitrogen- and Oxygen-Containing Monomers*, Plasma Processes and Polymers, 7(9-10): p. 824-836.
34. Gallino, E., et al. (2010), *Plasma polymerized allylamine films deposited on 316L stainless steel for cardiovascular stent coatings*, Surface and Coatings Technology, 205(7): p. 2461-2468.
35. Beck, A.J., et al. (2001), *The Role of Ions in the Plasma Polymerization of Allylamine*, The Journal of Physical Chemistry B, 105(24): p. 5730-5736.
36. Lejeune, M., et al. (2006), *Microstructural evolution of allylamine polymerized plasma films*, Surface and Coatings Technology, 200(20–21): p. 5902-5907.
37. Chen, C., J. Kim, and W.-S. Ahn (2014), *CO2 capture by amine-functionalized nanoporous materials: A review*, Korean Journal of Chemical Engineering, 31(11): p. 1919-1934.
38. Su, F., et al. (2010), *Adsorption of CO2 on Amine-Functionalized Y-Type Zeolites*, Energy & Fuels, 24(2): p. 1441-1448.
39. Tian, F., et al. (2015), *In Situ Measurement of CO2 and H2O Adsorption by ZIF-8 Films*, The Journal of Physical Chemistry C, 119(27): p. 15248-15253.
40. Parry, K.L., et al. (2006), *ARXPS characterisation of plasma polymerised surface chemical gradients*, Surface and Interface Analysis, 38(11): p. 1497-1504.
41. Ershov, S., et al. (2013), *Derivatization of Free Radicals in an Isopropanol Plasma Polymer Film: The First Step toward Polymer Grafting*, ACS Applied Materials & Interfaces, 5(10): p. 4216-4223.

Presenting author biography

I am a chemical engineer and researcher from Indonesia. I obtained a bachelor degree from Diponegoro University on 2004. Since 2005, I have worked as a researcher for Indonesian Institute of Sciences. I am a researcher at Environment, Renewable Energy, and Natural Resources Laboratory and my specialties are separation technology, waste utilization, renewable energy development (biogas and bioethanol) and environment issues. I am also involved in The Institution of Engineers Indonesia as a board member. Since 2015, I have been a Ph.D. Candidate at the School of Engineering and Future Industry Institute, University of South Australia.

Chemeca 2016 - full paper review results and conference programme 3405749

Shocklogic Online Systems Mailer on behalf of 'conference team'

Reply all

Mon 8/1/2016, 3:29 PM

Wahono, Satriyo Krido - wahsk001



Dear Satriyo Wahono,

On behalf of the Chemeca 2016 technical committee, we are delighted to announce the conference progra again for your valuable contribution to this programme. You will find all of the information relating to your fi

User ID: 3405749

Password: OIDBX

Abstract title: Preliminary Study: Combination Of Amine And Natural Zeolite As New Adsorbent Material

Reviewer comments:

This is an interesting paper on the preparation of CO2 adsorbent on allylamine surface functionalised nati 'Figure' and 'Table' 2. Explain how the thickness of allamine deposited on zeolite was measured.

(If blank, then no comments have been made)

Guidelines for final full papers

Before submitting your final full paper, please read and adhere to the requirements below:

- all abstracts and full papers must be original work
- the final full paper should take into consideration any comments from the review
- full papers must be prepared according to the appropriate template and guidelines
  Download, read and use the full paper template and guidelines
- your unique user ID becomes your full paper number and must be included on your final full paper
- the title of the full paper must be identical to the title used for your abstract
- the overall length of a full paper, including abstract, all illustrations, tables, and references is limited
- all full papers to be saved as a PDF only and named - full paper number_presenting author surnam e.g 38123456_Smith, John
- all other style guide requirements are within the full paper template and guidelines

MANUSCRIPT 2

https://doi.org/10.1016/j.envpol.2018.05.023

Environmental Pollution 240 (2018) 725–733

Contents lists available at ScienceDirect

Environmental Pollution

journal homepage: www.elsevier.com/locate/envpol

Plasma polymer facilitated magnetic technology for removal of oils from contaminated waters*

Satriyo Krido Wahono [a, b, c], Alex Cavallaro [a], Krasimir Vasilev [a, b, *], Agnieszka Mierczynska [d]

[a] Future Industries Institute, University of South Australia, Mawson Lakes 5095, South Australia, Australia
[b] School of Engineering, University of South Australia, Mawson Lakes 5095, South Australia, Australia
[c] Research Unit for Natural Product Technology, Indonesian Institute of Sciences, Gunungkidul 55861, Yogyakarta, Indonesia
[d] The Australian Wine Research Institute, Glen Osmond 5064, South Australia, Australia

ARTICLE INFO

Article history:
Received 9 March 2018
Received in revised form
7 May 2018
Accepted 7 May 2018

Keywords:
Plasma polymers
Hydrophobic adsorbent
Magnetic separation
Nanomaterials
Oil removal
1,7-Octadiene
Perfluorooctane

ABSTRACT

Oil pollution of waters is one of the most serious environmental problems globally. The long half-life and persistence within the environment makes oil particularly toxic and difficult to remediate. There is a significant need for efficient and cost-effective oil recovery technologies to be brought in to practice. In this study, we developed a facile and efficient magnetic separation method. The surface of 316L stainless steel nanoparticles was modified by plasma deposition of 1,7-octadiene and perfluorooctane, producing relatively hydrophobic coatings having water contact angles of 88 and 102°, respectively. Both coatings had high oil removal efficiency (ORE) of >99%. The captured oil could be easily separated by applying an external magnetic force. The ease of material preparation and separation from the water after the oil is captured, and its high ORE is a compelling argument for further development and optimization of the technology to possible utilization into practice. Furthermore, the capacity of plasma polymerization to deliver desired surface properties can extend the application of the technology to removing other chemical and biological contaminants from polluted waters.

© 2018 Elsevier Ltd. All rights reserved.

1. Introduction

With the growth of industrial development and exploration, production, and refining, the possibility for oil pollution of the environment presents a significant risk. Oils are considered particularly dangerous contaminants because of their persistence and extremely long half-lives in the environment (Gaix et al., 2012). Some sources often causing water pollution by oil contaminants are factories waste, petroleum transport and refinement, transportation leakages and household waste (Jha et al., 2008; Seiffert et al., 2011; Wang et al., 2012). Furthermore, common strategies and technologies implemented for oil removal are gravity separation, physical separation, flotation, evaporation, chemical extraction, membrane separation, and adsorption (Arthur et al., 2005; Fakhru'l-Razi et al., 2009).

The adsorption method is by far the most popular technique because of its efficiency, low cost, simplicity of utilization and the ease of the application (Ali et al., 2012). This process exploits the physical adhesion of the pollutant to a solid physical surface. The essential requirement for adsorbent materials is to be hydrophobic and oleophilic (Chu and Pan, 2012). Such materials have already been applied for water-oil separation, particularly for high viscosity oils (Xue et al., 2011). Recently, considerable efforts have been made to develop efficient adsorbents by modifying material surface properties. Typical chemistries used to generate hydrophobic surfaces are hydrocarbon (Nash et al., 2015; Venkateswara Rao et al., 2007; Wang et al., 2012), fluorocarbon (Gürsoy and Karaman, 2016; Kyllán et al., 2014; Tomina et al., 2011; Zhu et al., 2005), or siloxane (Ferrara and Pattarini, 2016; Tsai et al., 2004; Zhang et al., 2007). These adsorbents have been demonstrated to deliver good outcomes when applied for removing oil spillage, organic solvents and toxic organic compounds (Bi et al., 2012; Dong et al., 2012; Monopoli et al., 2011; Zhang et al., 2007b; Zhu et al., 2011).

* This paper has been recommended for acceptance by Dr. Harrison Sarah Michele.

+ Corresponding author. School of Engineering, University of South Australia, Mawson Lakes 5095, South Australia, Australia.
E-mail address: krasimir.vasilev@unisa.edu.au (K. Vasilev).

https://doi.org/10.1016/j.envpol.2018.05.023
0269-7491/© 2018 Elsevier Ltd. All rights reserved.

One of the current challenges related to the methods for material surface modification is that the procedures are commonly conducted by wet-chemistry and rely on complex reactions, which are highly substrate type dependent and produce an excess of potentially toxic waste products (Hernandez-Lopez et al., 2003; Morent et al., 2011). This complexity leads to limitations in the selection of carrier material and prohibitive costs associated with wet solvent treatment. Thus, it is logical to develop methods which can potentially overcome these limitations. An example of such alternatives is a technique called plasma polymerization. The methods involve the deposition of polymer-like, highly cross-linked coating from the vapor of an organic precursor (Denes and Manolache, 2004; Vasilev, 2014; Yasuda and Matsuzawa, 2005).

Plasma polymerization offers many benefits compared to wet processes. It is substrate independent, which means that identical coatings can be deposited on the surface of different materials using the same process (Vasilev et al., 2009). The techniques consist of a single step and do not require the use of any solvents. Furthermore, coatings can be deposited on substrates of compact sizes and shapes, including micro and nanoparticles. Finally, there is substantial body of literature from our group and others pointing that hydrophobic coatings can be prepared in a very facile way using plasma-based techniques (Al Mawari et al., 2018a; Hegemann et al., 2003; Michelmore et al., 2013; Ramsua-MacGregor et al., 2016; Vaswani et al., 2005).

Another challenge is to separate the absorbent material from the contaminated continuum. Processes such as centrifugation and filtration give excellent results in some situations, but they are too expensive or inapplicable in some instances. In this work, we selected to use as hydrophobic coating carrier 316L stainless steel nanoparticles because they can be easily separated by the contaminated medium by an external magnetic field. Nanoparticles also have a very high surface to volume ratio, thus providing a large surface area to which oil contaminants could be concentrated. The surface of magnetic and others particulate can be modified by plasma polymerization using customized systems developed by our group and others (Cavallaro and Vasilev, 2015; De Vietro et al., 2012; Jarvis and Majewski, 2012; Michl et al., 2015; Mieszynska-Vasilev et al., 2017; Wahono et al., 2016).

The hypothesis underpinning this work is that 316L stainless steel nanoparticles modified by hydrophobic plasma polymer layers can be successfully utilized for the removal of oils from aqueous media. To validate this hypothesis, we coated the surface of magnetic nanoparticles using two precursors known to deliver coatings with different levels of hydrophobicity. After characterizing the chemical and physical properties of the coatings, we evaluated the capacity of newly developed plasma polymer coated magnetic adsorbents to oils from model aqueous media.

2. Materials and methods

2.1. Materials

For plasma precursor, 1,7-octadiene and perfluorooctane (octadecafluorooctane) were purchased from Sigma-Aldrich and used as received. Two types of crude oil samples from the waste-store of the University of South Australia were used as model oils. Density and viscosity of the oil samples were measured. The density measurements were conducted using 25 cm^3 pycnometer and the JF3004 ProfiCiTech, whereas the viscosity measurements were conducted using the LVT-93405 Brookfield Viscometer with spindle number LV 1, LV 2 and 4D, 30 rpm. All measurements were performed at 23.0 ± 0.5 °C. 316L stainless steel nanoparticles (Hongwu International Group, Guangzhou, China) were chosen as the base for the adsorbent material due to their magnetic properties and size. This material is a black powder with a purity of 99.9% and size of 70 nm.

2.2. Plasma deposition

The nanoparticles were coated with hydrophobic polymers using 1,7-octadiene and perfluorooctane (octadecafluorooctane). The coating process utilized a cylindrical custom built plasma reactor, which is supported by the U-shaped upper electrode, round-shaped bottom electrode, and powered by RF plasma generator of 13.56 MHz. The reactor was equipped with agitation platform for coating of powder or particulate material (Cavallaro and Vasilev, 2015; Wahono et al., 2016). Octadiene and perfluorooctane were coated using the pressure of 16 Pa and 23 Pa, respectively. In both cases, deposition was carried out using RF power of 50 W. Total deposition times varied between 600 and 2400 s.

2.3. Characterization

SEM analysis was conducted to determine the morphology of the magnetic nanoparticles and possible changes of the plasma polymerization treatment. SEM was performed on the Hitachi SU3500 at the Indonesian Institute of Sciences. The sample was dried in the oven at 110 °C for an hour to remove water. A small quantity of powder sample was splashed on carbon tape surface as preparation before analysis. The results of this analysis show in Supplementary Information part.

To investigate the coatings thickness, wettability, and stability, 1 cm^2 silicon wafers were also coated with the same polymers. Ellipsometry was used to determine the thickness of the coatings. All measurements were conducted using J. A. Woollam Co., Inc. V-VASE Ellipsometer with the plasma polymers deposited on silicon wafers and data collected and analyzed using the WVASE32 software. Surface wettability was used to investigate the hydrophobicity of surface coatings. A sessile drop method was employed, and all images were captured by Logitec digital camera and contact angles determined by ImageJ software. The thickness changes caused by polymer loss were measured to determine the relative stability of the coatings in aqueous environments. The stability test was conducted by soaking silicon wafers coated with the hydrophobic polymers in ultra-pure water for an hour and measuring the thickness by ellipsometry (as above).

XPS analysis was used to determine the surface composition of bare and plasma coated magnetic nanoparticles. XPS spectra were recorded on a Specs SAGE XPS spectrometer. The results were processed and fitted using CasaXPS software. The XPS was operated with Mg Kα radiation source (hν = 1253.6 eV) at 10 kV and 20 mA. It used a Phoibos 150 with MCD-9 detector as the hemispherical analyzer. The atomic composition was calculated from the survey spectra in the energy range 0–1000 eV at the pass energy of 30 eV and resolution of 0.5 eV. The C1s neutral carbon peak of 285 eV was used a reference for all the binding energies to compensate the surface charging effect.

2.4. Oil capture experiments

A mixture of water (20 cm^3) and crude oil (400 mm^3 = 20,000 ppm) was prepared. The coated magnetic nanoparticles as adsorbent were used in various oil-to-adsorbent-weight ratios (between 8 mg and 1200 mg of adsorbent). The adsorbent was added to the oil/water samples then agitated for 30 s and allowed to rest for 600 s. A magnet was then used to collect the adsorbent after capturing oil from the oil/water solution which shown in Video 1. The rest of the solution was mixed with n-hexane to determine oil residue within the samples. The oil residue content

Table 2
Thickness and surface wettability of plasma polymer films deposited on silicon wafer.

Monomer	Plasma processing conditions		Plasma polymer layer thickness as a function of plasma deposition time (nm)			Surface Wettability
	Power	Pressure	180 s	300 s	600 s	600 s
Octadiene	50 W	10 Pa	59 ± 0.3	187 ± 2	356 ± 5	 80°
Perfluorooctane	50 W	10 Pa	5 ± 0.2	31 ± 0.1	45 ± 0.5	
Perfluorooctane	50 W	25 Pa	90 ± 5	141 ± 4	239 ± 2	 130°

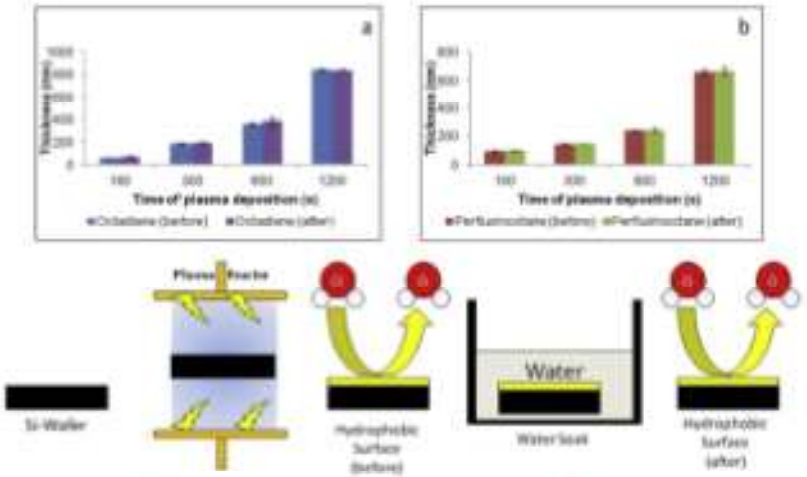

Fig. 1. Coating thickness at four different deposition times before and after immersion in water: (a) Octadiene and (b) Perfluorooctane.

different depending on the environment the nanoparticles were exposed to, thus, plasma polymer modification can help define the surface chemical composition of the material. When coatings deposited from the vapor of 1,7-octadiene were placed on the surface of the nanoparticles an apparent increase in the concentration of carbon was observed with decrease in oxygen and iron content. 1200 s deposition time led to an increase the atomic surface concentration of carbon to almost 63 At%. Further increase in the deposition time did not result in any change in the atomic concentration of carbon, oxygen, and iron, which suggests that the thickness of the coating has exceeded 10 nm.

Similar trends were observed when the nanoparticles were modified with coatings deposited from the vapor of perfluorooctane. The presence of fluorine in the molecule of the precursor made it relatively easy to monitor the evolution of the coating with time on deposition. After 600 s of deposition, the particle surface has approximately 7.9 At% of fluorine. The atomic percent of fluorine increased with plasma deposition time. After 1200 s of deposition, the fluorine concentration was 16 At%, increasing to 18 At% at 1800 s of deposition and remaining unchanged at 2400 s. In the same time, the atomic concentration of carbon, oxygen, and iron all decreased and remained constant after 1800 s of plasma polymer deposition. This data suggests that a nearly continuous coating with a thickness above 10 nm was created at 1800 s of plasma deposition.

3.5. Oil recovery

The wettability and chemical analysis of the coatings deposited on the magnetic nanoparticles point to relatively hydrophobic coatings rich in non-polar hydrocarbon and fluorocarbon chemistries. The characteristics of the coatings suggest the potential for binding dispersed in water-oil molecules which are also hydrophobic and nonpolar in nature. The magnetic properties of the nanoparticles will facilitate their easy collection together with the oil captured molecules.

Fig. 1a shows the relative OBR for the octadiene and perfluorooctane plasma polymer coated magnetic nanoparticles. After 600 s of plasma deposition, the octadiene coated particles removed 99.9% of crude oil 1 and 99.2% of crude oil 2. Although the

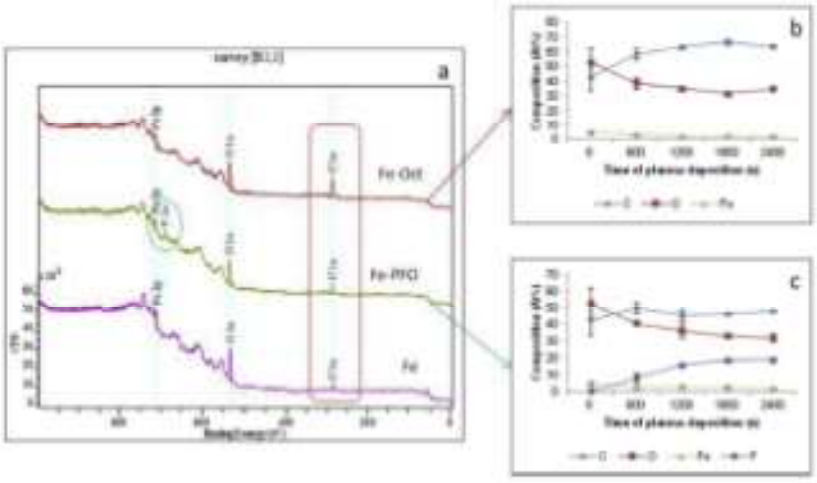

Fig. 2. The chemical composition of the nanoparticle surface determined by XPS before and after modifications: (a) XPS survey spectra of Fe-Raw, Fe-Octadiene and Fe-PFO; (b) Fe-1,7-octadiene; (c) Fe-perfluorooctane.

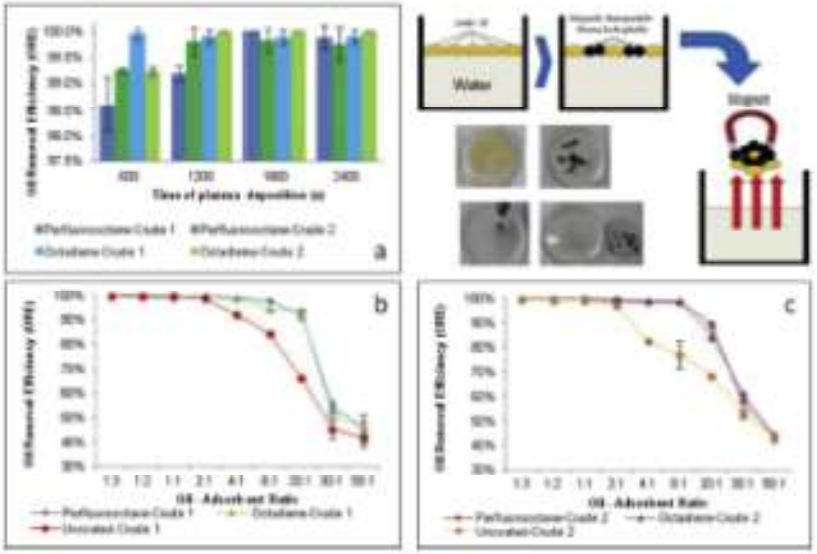

Fig. 3. ORE of magnetic nanoparticles: (a) coated with octadiene and perfluorooctane plasma polymers for different deposition times (Oil:Adsorbent ratio = 1:2); (b, c) plasma polymer coated and uncoated vortex oil:adsorbent ratio for: (b) Crude oil 1; (c) Crude oil 2.

adsorption of crude oil 1 did not seem to change with increasing deposition time, the uptake of crude oil 2 increased to 100% after 20 min plasma deposition. These results are in agreement with the XPS surface composition analysis where optimum polymer coverage was obtained after 1200 s of plasma deposition. The ORE for the perfluorooctane coating also depends on the time of deposition of the coating. After 600 s of perfluorooctane deposition, the magnetic nanoparticles were able to adsorb 98.6% and 99.3% of crude oil 1 and crude oil 2, respectively. Adsorption of crude oil 1 increased further to 99.2% and 99.8% as deposition time was increased to 1200 s and beyond. Interestingly, uptake of crude oil 2 plateaued at 99.8% after increasing the deposition time to 1200 s. Ultimately, it appeared that when deposited for short periods, i.e. <1200 s, the octadiene coated magnetic nanoparticles seemed to have a higher oil affinity and removal efficiency. At longer deposition times, such as 1800 and 2400 s, both polymers showed equal

performance. This indicates that coatings derived from octadiene plasma form faster a continuous film on the surface of the nanoparticles, a result that was also suggested by the XPS characterization.

3.5.1. Effect of oil-adsorbent ratio

ORE of different oil/adsorbent ratios was used to investigate the impact of the adsorbent concentration on oil recovery. Naturally, we expected that the total oil recovery is related to the adsorbent surface area and the hydrophobicity of the coating. An increased amount of the adsorbent would naturally provide a greater surface area for attachment of oil molecules.

Fig. 3b and c shows the total ORE for different oil to adsorbent ratios. When more oil is added to the system, the same quantity of adsorbent material is not able to remove the increased amount of oil. This phenomenon is clearly seen in Fig. 3b and c where ORE decreases as the oil-adsorbent ratio increases. However, higher oil/adsorbent ratio may eventually provide better ORE values per gram of adsorbent as demonstrated in published reports (Alhawari et al., 2018a).

At low oil/adsorbent ratios, both uncoated and coated magnetic nanoparticles reached ORE of greater than 98%. The result indicates that unmodified magnetic nanoparticles also have the ability to capture oil. This is to be expected if we revisit Fig. 2 where we noted the high carbon content on the surface of the untreated magnetic nanoparticles. This high amount of carbon is likely a result of the manufacturing process and environmental contamination, which may differ from batch to batch making the utilization of unmodified material unreliable. Furthermore, unmodified magnetic nanoparticles readily sank and became saturated quicker than the plasma coated identical material. The greater capacity to "float" of plasma polymer modified particles was due to their more hydrophobic nature. The uncoated magnetic adsorbent performed well when the oil/adsorbent ratio was 1:3, 1:2, 1:1 and 2:1 for both types of crude oil samples, which translated to oil-capture capacity of 0.33 g/g, 0.5 g/g, 1 g/g, and 2 g/g, respectively. Above 2:1 ratio, the oil-capture capacity of uncoated magnetic adsorbent dramatically decreases.

A comparison between the two different types of plasma polymer coatings revealed that there is no significant difference between them in terms of ORE. Magnetic nanoparticles modified with octadiene and perfluorooctane maintained a maximum ORE of more than 98% until the oil-adsorbent ratio was higher than 4:1 regardless of the crude oil used. For 8:1 ratio, the modified magnetic material performed better for crude oil 2 samples with ORE of ~98%, compared to crude oil 1 where ORE was 94%. The coated magnetic adsorbent had an oil-capture capacity of 8 g/g which is an increase of 400% compared to the uncoated magnetic adsorbent. These results demonstrate that the plasma deposition significantly enhanced the capacity for oil capture of the untreated material.

3.5.2. Effect of scale-up

Since contamination of water with oil commonly occurs in a large water volume, it is essential to investigate the performance of the magnetic adsorbent in greater water volumes. In this experiment, 8:1 and 20:1 of oil:adsorbent ratios were chosen because both of the plasma-coated magnetic nanoparticles have ORE value of above 85%. The resultant ORE value is shown in Fig. 4 for the 8:1 and 20:1 ratios.

As shown in Fig. 4a and b the performance of magnetic adsorbent moderately decreases when the total volume of water is scaled-up as compared to the initial experiment using only 20 cm^3 of suspension. The ORE of crude oil 1 decreased from 97% to 82% when perfluorooctane was used and from ~94% to approximately 82% in the case of octadiene when water volume increased to 250 cm^3. The ORE of crude oil 2 was also affected by increasing the volume of water. In this case, the ORE decreased from ~99% to 89% for both plasma coatings. The uncoated magnetic nanoparticles showed the same trend but ORE decreased to a lower value (~75%) compared to the coated magnetic adsorbent.

Fig. 4c and d shows water scale-up of 20:1 ratio for both crude oil samples and both hydrophobic coatings. The ORE decreases to

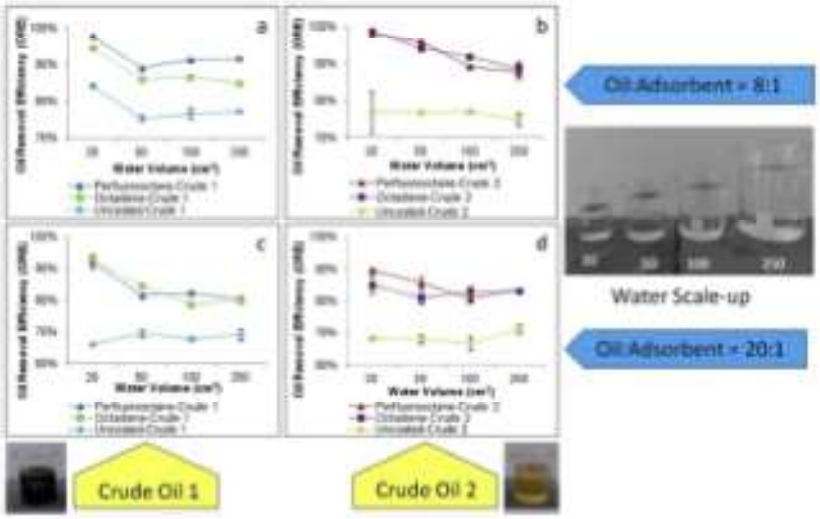

Fig. 4. The ORE of coated and uncoated magnetic adsorbents as a function of increasing water volume for 8:1 of oil adsorbent ratio: (a) Crude oil 1; (b) Crude oil 2; and for 20:1 of oil adsorbent ratio: (c) Crude oil 1; (d) Crude oil 2.

Table 3
Adsorption capacity and oil recovery for comparable materials published in the literature.

Adsorbent	Adsorbate	Adsorption capacity (g/g)	Removal Efficiency (%)	Reference
Octadiene/plasma polymer coated magnetic nanoparticles	crude oil	8	80–90	Present Work
Perfluorooctane/plasma polymer coated magnetic nanoparticles	crude oil	8	80–90	Present Work
Polyvinylpyrrolidone coated magnetic nanoparticles	crude oil	not reported	85–95	(Mirbagheri et al., 2017)
Magnetic titania nanotubes	various oil	>15	not reported	(Parowary et al., 2017)
Magnetic nanoparticle coated fluorinated carbon fabric membrane	olive oil	not reported	>95	(Zhang et al., 2017a)
Modified $FeNi_3$ magnetic nano-chains	lubricating oil	not reported	90.18–98.28	(Bhabatcharya et al., 2016)
Modified magnetic porous silica submicron particles	lubricating oil	11.51	not reported	(Yuan et al., 2015)
Magnetic cellulose/TEO aerogel	paraffin oil	28	not reported	(Chen et al., 2014)
Octadiene plasma polymer coated silica particles	crude oil	0.5	70–90	(Akhavan et al., 2013b)
Magnetic macroporous carbon nanotubes	diesel oil	50	not reported	(Gui et al., 2013)

~80% for the coated magnetic adsorbent and ~68% for the bare magnetic nanoparticles. Since the total ORE is mostly affected by the oil which floats on the water surface, thus greater water oil did not significantly impact the oil recovery. These studies once again demonstrate the benefit of applying plasma polymer modification of the surface of the magnetic nanoparticles.

3.6. Comparison of newly developed technology for oil recovery with literature

The technology for oil recovery developed in this work provides high efficacy of oil recovery and high oil adsorption capacity. To illustrate this, we compared with published studies which shown in Table 3. Overall, our technology appears to be more efficient than those reported so far. We should also stress that plasma surface modification is a one-step facile and fast process to achieve optimal surface properties of the adsorbent material. Combined with the ease to separate the captured oil via an external magnetic force a compelling argument can be made for further development and optimization to possible utilization in practice.

4. Conclusions

Collectively, we report a facile technology of oil recovery from contaminated waters via a magnetic force. Plasma deposition of 1,7-octadiene and perfluorooctane precursors was implemented to modify the surface of magnetic nanoparticles in order to generate new hydrophobic adsorbents. Both precursors resulted in effective oil recovery with ORE >80% after 1200 s of plasma deposition. The octadiene plasma polymer coated magnetic nanoparticles appeared to perform better after a shorter time of plasma polymer modifications which suggests that this precursor leads to faster achieving uniform coatings on the surface of the nanoparticles. On the other hand, perfluorooctane modified nanoparticles worked better when a smaller amount of adsorbent was used. The greater hydrophobicity of the perfluorooctane coating is likely to provide more efficient interaction with oil molecules. The scale-up experiments demonstrated that both types of plasma polymer coated magnetic adsorbents retained 80% ORE when water amount was increased 12 fold. The technology for oil recovery presented here is an attractive alternative to existing methods considering the facile fabrication, efficiency of recovery and ease of separation. Furthermore, the versatility of plasma polymerization to deliver coatings of tailored properties paves the foundation for developing of derivative separation technologies for other chemical and biological pollutants from waters.

Acknowledgements

The authors would like to acknowledge the scholarship support from RISET-PRO Project, Ministry of Research, Technology and Higher Education, Republic of Indonesia. Kradimir Vasilev thanks ARC for DP150104212, NHMRC for Fellowship APP1122825 and Project grant APP1032738, and the Alexander von Humboldt Foundation for Fellowship for Experienced Researchers.

Appendix A. Supplementary data

Supplementary data related to this article can be found at https://doi.org/10.1016/j.envpol.2018.05.023.

References

Akhavan, B., Jarvis, K., Majewski, P., 2013a. Evolution of hydrophobicity in plasma polymerized 1,7-octadiene films. Plasma Process. Polym. 10, 1018–1028.
Akhavan, B., Jarvis, K., Majewski, P., 2013b. Hydrophobic plasma polymer coated silica particles for petroleum hydrocarbon removal. ACS Appl. Mater. Interfaces 5, 8520–8531.
Ali, I., Asim, M., Khan, T.A., 2012. Low cost adsorbents for the removal of organic pollutants from wastewater. J. Environ. Manag. 113, 170–183.
Arthur, J.D., Langhus, B.G., Patel, C., 2005. Technical Summary of Oil & Gas Produced Water Treatment Technologies. All Consulting, LLC, Tulsa, OK, pp. 42–53.
Bhabatcharya, K., Gogoi, M., Deb, P., 2016. Molecular design of one dimensional magnetic $FeNi_3$ nanochains and their application in oil removal. In: AIP Conference Proceedings, pp. 050005-1–050005-3.
Bi, H., Xie, X., Yin, K., Zhou, Y., Wan, S., He, L., Xu, F., Banhart, F., Sun, L., Ruoff, R.S., 2012. Spongy graphene as a highly efficient and recyclable sorbent for oils and organic solvents. Adv. Funct. Mater. 22, 4421–4425.
Bush, V.E., Barringer, S.A., 2007. Comparison of hexane and petroleum ether to measure surface oil content. J. AOAC Int. 90, 1729–1736.
Casalboni, A., Vasilev, K., 2017. Controlled and sustained release of pharmaceuticals via single-step solvent-free encapsulation. Chem. Commun. 53, 1838–1841.
Chen, S.F., Bee Abdullah, A.H., Pang, S.C., 2014. Fabrication of hydrophobic and

magnetic cellulose aerogel with high oil absorption capacity. Mater. Lett. 115, 246–249.
Cao, Y., Feng, Q., 2013. Three-dimensionally macroporous PdC nanocomposites as highly selective oil-absorption materials. ACS Appl. Mater. Interfaces 5, 2400–2405.
De Vrieze, M., d'Agostino, R., Faussurier, N., 2002. Introduction of hard functionalities on the surface of granular adsorbers by low pressure plasma processes. Plasma Process. Polym. 9, 911–919.
Denes, F.S., Manolache, S., 2004. Macromolecular plasma-chemistry: an emerging field of polymer science. Prog. Polym. Sci. 29, 815–885.
Dong, X., Chen, J., Ma, Y., Wang, J., Chan-Park, M.B., Liu, X., Wang, L., Huang, W., Chen, P., 2012. Superhydrophobic and superoleophilic hybrid foam of graphene and carbon nanotube for selective removal of oils or organic solvents from the surface of water. Chem. Commun. 48, 10660–10662.
Fakhru'l-Razi, A., Pendashteh, A., Abdullah, L.C., Biak, D.R.A., Madaeni, S.S., Abidin, Z.Z., 2009. Review of technologies for oil and gas produced water treatment. J. Hazard. Mater. 170, 530–551.
Ferrara, L., Ferrante, A., 2016. Silanes in concrete: from manual application of water-proofing treatments to mix-design addition for concrete hydrophobizing/self-healing materials. Trans Tech Publ 283–288.
Ghannam, M.T., Nasr, N.W., Abu-Jdayil, B., Esmail, N., 2012. Rheological properties of heavy & light crude oil mixtures for improving flowability. J. Petrol. Sci. Eng. 81, 122–128.
Gui, X., Zeng, Z., Lin, Z., Gan, Q., Wang, R., Zhu, Y., Cao, A., Yang, Z., 2013. Magnetic and highly recyclable macroporous carbon nanotube for actual oil sorption and separation. ACS Appl. Mater. Interfaces 5, 5848–5855.
Guo, M., Cheung, J., Garcia, M., Gao, W., Sattayasamitsathit, S., Mishra, A., Balasa, A., Wang, J., 2013. Superhydrophobic diatomite-based micromotors for efficient removal of oil. ACS Nano 8, 4447–4451.
Güney, M., Karaman, M., 2010. Hydrophobic coating of expanded perlite particles by plasma polymerization. Chem. Eng. J. 264, 343–350.
Hegemann, D., Brunner, H., Oehr, C., 2003. Plasma treatment of polymers to generate stable, hydrophilic surfaces. Plasma Polym. 8, 239–255.
Hernandez-Sosa, J.L., Baier, R.E., Chang, W.S., Cleaver, C., Cortez-Klaiber, D., Cappay, M., Kinlen, M., Lentzos, J., Majors, J.E., Müller, S., Millon, K., Vanlen, K., Wall, T., Wu, J., Zhu, T., Weil, W., 2013. Functional polymers as nanoscale building blocks. Mater. Sci. Eng. C 33, 267–274.
Jones, K.L., Majewski, P., 2013. Plasma polymerised allylamine coated quartz particles for humic acid removal. J. Colloid Interface Sci. 393, 151–158.
Jha, M.N., Levy, J., Gao, Y., 2008. Advances in remote sensing for oil spill disaster management: state-of-the-art sensor technology for oil spill surveillance. Sensors 8, 236–255.
Kylian, O., Petr, M., Serov, A., Solar, P., Polonskyi, O., Hanuš, J., Choukourov, A., Biederman, H., 2014. Hydrophilic and superhydrophobic coatings based on nanoparticles overcoated by fluorocarbon plasma polymer. Vacuum 100, 57–60.
Macgregor-Ramiasa, M.N., Cavallaro, A.A., Vasilev, K., 2015. Properties and reactivity of polyoxazoline plasma polymer films. J. Mater. Chem. B 3, 6307–6317.
Mahdavian, A., Bryant, P.M., Steele, D.A., Vasilev, K., Bradley, J.W., Short, R.D., 2013. Role of positive ions in determining the deposition rate and film chemistry of continuous wave hexamethyldisiloxane plasma. Langmuir 27, 13940–13950.
Mohr, T.D., Ewalt, B.R., Hanan, A., Vasilev, K., Graham, N.J., 2015. Laboratory-scale systems for the plasma treatment and coating of particles. Plasma Process Polym. 12, 305–313.
Mrozynska-Vasilev, A., Bajer, P., Vasilev, K., Smith, P.A., 2017. A novel technology for the rapid, selective, magnetic removal of pathogenic-related proteins from whole Food Chem. 233, 508–514.
Mirshaghavand, S., Ehsani, A.D., Cai, B., Lead, J.R., 2017. Application of high gradient magnetic separation for oil remediation using polymer-coated magnetic nanoparticles. Separ. Purif. Technol. 179, 328–334.
Monopoli, M.P., Walczyk, D., Campbell, A., Elia, G., Lynch, I., Baldelli Bombelli, F., Dawson, K.A., 2011. Physical–Chemical aspects of protein corona: relevance to in vitro and in vivo biological impacts of nanoparticles. J. Am. Chem. Soc. 133, 2525–2534.
Morent, R., De Geyter, N., Desmet, T., Dubruel, P., Leys, C., 2011. Plasma surface modification of biodegradable polymers: a review. Plasma Process. Polym. 8, 171–190.
Nash, I.D., Ewalt, K.P., Hasan, S.M., Mahmud, D.J., 2015. Characterization of plasma deposited hydrocarbon diffusion barriers for enterosthesis devices. In: 2015 9th IEEE International Conference on Nano/Molecular Medicine & Engineering (NANOMED), Pp. 1–6.
Patowary, M., Arunbalakrishnan, K., Patowary, R., 2017. Effective oil removal from water by magnetically driven superhydrophobic and oleophilic magnetic nitinol nanotube. Environ. Sci. Pollut. Control Ser. 24, 18003–18007.
Ramiasa-MacGregor, M., Mierczynska, A., Sedev, R., Vasilev, K., 2016. Tuning and predicting the wetting of nanoengineered material surfaces. Nanoscale 8, 4035–4042.
Seth, L., Pendleton, A., Kuperman, H., Rothwell, G.N., Aaron, A.A., Charlet, A., 2011. Adsorption of petroleum nonaromatics from aqueous solutions using granulated surface modified natural nanocrystalline cyclosilicate: systematic study of equilibrium isotherms. Water, Air, Soil. Pollut. 217, 611–625.
Sharma, V.V., Yurchenko, O.E., Maksimkin, A.K., Zuh, Yu., Kozak, A., Ignatiik, A., 2013. Synthesis of polysiloxane aerogels with fluorine-containing groups in the cubic layer and their sorption properties. J. Fluorine Chem. 152, 1146–1151.
Tiraz, S., Bak, E., Sit, J.C., Veinot, J.G.C., 2004. Superhydrophobic, high surface area, 3-d SiO2 nanostructures through siloxane-based surface functionalization. Langmuir 20, 10771–10774.
Vasilev, K., 2014. Nanoengineered plasma polymer films for biomaterial applications. Plasma Chem. Plasma Process. 34, 545–558.
Vasilev, K., Britcher, L., Casalis, A., Griesser, H.J., 2008. Solvent-induced porosity in ultrathin amine plasma polymer coatings. J. Phys. Chem. B 112, 10825–10831.
Vasilev, K., Michelmore, A., Griesser, H.J., Short, R.D., 2009. Substrate influence on the initial growth phase of plasma-deposited polymer films. Chem. Commun. 3010–3012.
Vesaratchanon, S., Kiatkamjornwong, S., Hoven, D.W., 2005. Surface modification of paper and cellulose by plasma-assisted deposition of fluorocarbon films. Surf. Coating. Technol. 195, 121–129.
Venkateswara Rao, A., Hegde, N.D., Hirashima, H., 2007. Absorption and desorption of organic liquids in elastic superhydrophobic silica aerogels. J. Colloid Interface Sci. 305, 124–132.
Wahono, S.K., Scheers, W., Addai-Mensah, J., Vasilev, K., 2016. Preliminary study: combination of amine and natural zeolite as new adsorbent material for CO2 capture. Chemeca 2016: chemical Engineering-Regeneration, Recovery and Reinvention 800–810.
Wang, D., Mikaelyan, K., Rhodes, K., Lin, Y.S., 2013. Adsorption of oils from pure liquid and oil–water emulsion on hydrophobic silica aerogels. Separ. Purif. Technol. 99, 28–33.
Wei, Z., Wang, C., Liu, L., Chen, L., Liu, M., Feng, L., Jiang, L., 2012. A novel superhydrophilic and underwater superoleophobic hydrogel-coated mesh for oil/water separation. Adv. Mater. 23, 4270–4273.
Yasuda, H., Matsuzawa, Y., 2005. Economical advantages of low-pressure plasma polymerization coating. Plasma Process. Polym. 2, 507–512.
Yu, L., Han, C., Liang, Q., Jiang, W., 2015. Fabrication of magnetic porous silica submicrosphere for oil removal from water. Ind. Eng. Chem. Res. 54, 9440–9448.
Zhang, X., Liu, B., Deng, K., Cao, S., Hou, W., Chen, H., 2007. A novel approach for the preparation of organic-inorganic aerogels and the creation of hydrophobic surface. Appl. Surf. Sci. 254, 453–459.
Zhang, J., Shen, Y., Meek, C.-E., Chen, Y.-E., Su, T.-C., Hsu, J.-P., Jiang, B.-C., 2017a. Synthesis of magnetic iron oxide nanoparticles coated fluorinated carbon fabrics for contaminant removal and oil-water separation. Separ. Purif. Technol. 179, 313–319.
Zhang, M., Xin, X., Xiao, Z., Wang, R., Zhang, L., Sun, G., 2017b. A multi-antenna hydrocarbon and haloalkyl hydrophobic metal-organic framework for efficient C2/C1 hydrocarbon and oil/water separation. J. Mater. Chem. A 5, 1058–1065.
Zhu, L., Xiu, Y., Xu, J., Tamirisa, P.A., Hess, D.W., Wong, C.-P., 2005. Superhydrophobicity on two-tier rough surfaces fabricated by controlled growth of aligned carbon nanotube arrays coated with fluorocarbon. Langmuir 21, 11208–11212.
Zhu, Q., Pan, Q., Liu, F., 2011. Facile removal and collection of oils from water surfaces through superhydrophobic and superoleophilic sponges. J. Phys. Chem. C 115, 17464–17470.

APPENDIX C: Supporting Information

MANUSCRIPT 2

Supplementary Information

Plasma polymer facilitated magnetic technology for removal of oils from contaminated waters

Satriyo Krido Wahono[1,2,3], Alex Cavallaro[1], Krasimir Vasilev[1,2*] and Agnieszka Mierczynska[4],

[1] Future Industries Institute, University of South Australia, Mawson Lakes 5095, South Australia, Australia
[2] School of Engineering, University of South Australia, Mawson Lakes 5095, South Australia, Australia
[3] Research Unit for Natural Product Technology, Indonesian Institutes of Sciences, Gunungkidul 55861, Yogyakarta, Indonesia
[4] The Australian Wine Research Institute, Glen Osmond 5064, South Australia, Australia
***Author for correspondence**: krasimir.vasilev@unisa.edu.au

This supplementary information consists of a page about results and discussions of morphological studies of bare and coated magnetic nanoparticles (3.7), including a complete set figure (Figure S1).

3.1.Morphological studies of bare and coated magnetic nanoparticles

SEM was employed to determine the morphology of the plasma coated magnetic nanoparticles before and after oil recovery. Figure S1a shows the morphology of the uncoated magnetic nanoparticles. There are no significant visual differences between uncoated and octadiene or perfluorooctane plasma coated nanoparticles as shown in Figure S1a, S1b, and S1d, respectively. The plasma coated layer on the magnetic nanoparticle surface was quite thin and did not affect material cohesively in a dry state. After contact with oil, the material strongly agglomerated as shown in Figure S1c and S1e for octadiene and perfluorooctane coating, respectively. The agglomeration is a result of hydrophobic interaction between oil molecules, and a plasma polymer coated magnetic nanoparticle surface.

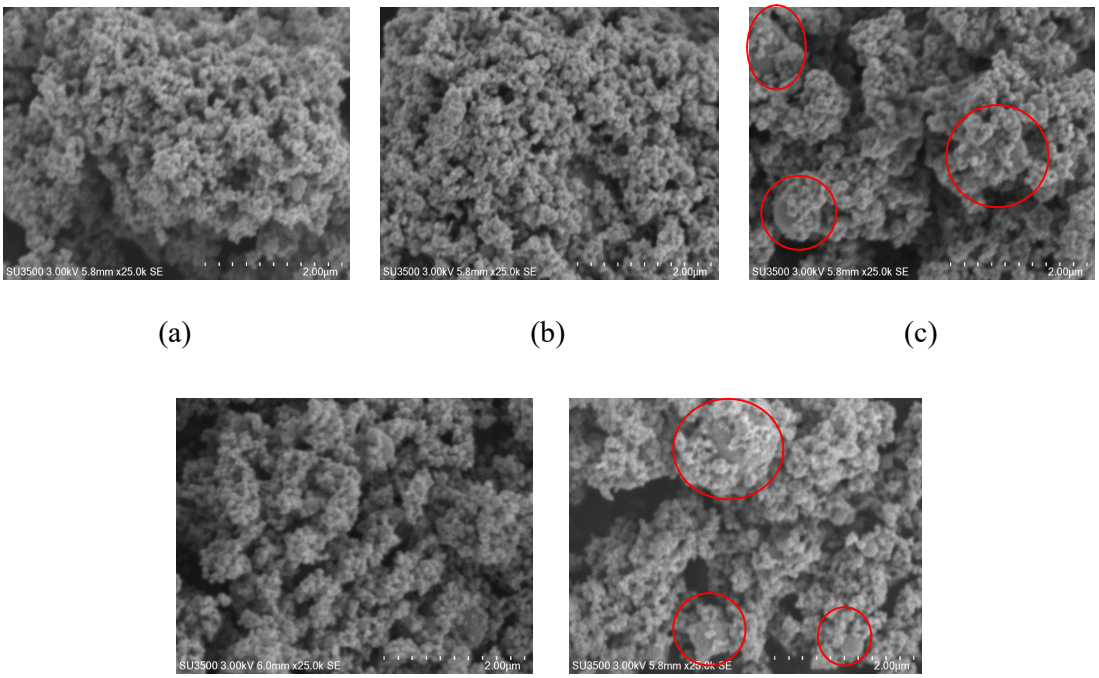

(a) (b) (c)

(d) (e)

Figure S1. The morphology of oil molecules captured by the plasma coated-magnetic nanoparticles: (a) bare magnetic nanoparticles; (b) octadiene-coated magnetic nanoparticles; (c) post capturing oil on octadiene-coated magnetic nanoparticles; (d) perfluorooctane-coated magnetic nanoparticles; (e) post capturing oil on perfluorooctane-coated magnetic nanoparticles